

# ***Investigations of Dual-Purpose Canister Direct Disposal Feasibility (FY14)***

## **Fuel Cycle Research & Development**

*Prepared for:  
U.S. Department of Energy  
Office of Used Nuclear Fuel Disposition*

*E. Hardin, C. Bryan, A. Ilgen, E. Kalinina and S. Teich-McGoldrick,  
Sandia National Laboratories*

*K. Banerjee, J. Clarity, R. Howard, R. Jubin and J. Scaglione,  
Oak Ridge National Laboratory*

*F. Perry, Los Alamos National Laboratory*

*L. Zheng, J. Rutqvist and J. Birkholzer,  
Lawrence Berkeley National Laboratory*

*H. Greenberg, Lawrence Livermore National Laboratory*

*J. Carter and T. Severynse,  
Savannah River National Laboratory*

*October, 2014*

**FCRD-UFD-2014-000069 Rev. 1**



**Revision History**

| <b>Revision</b>             | <b>Description</b>   |
|-----------------------------|--|
| FCRD-UFD-2014-000069 Rev. 0 | Sandia programmatic review (for DOE/NE-53 policy review; SNL tracking number 143790)                                 |
| FCRD-UFD-2014-000069 Rev. 1 | Incorporate DOE/NE-53 approval, and Sandia Review & Approval for Unclassified, Unlimited Release (SAND2014-18271 R). |

**CONTEXT FOR THIS STUDY**

This is a technical presentation that does not take into account the contractual limitations under the Standard Contract. Under the provisions of the Standard Contract, DOE does not consider spent fuel in canisters to be an acceptable waste form, absent a mutually agreed to contract modification.

**DISCLAIMER**

This information was prepared as an account of work sponsored by an agency of the U.S. Government. Neither the U.S. Government nor any agency thereof, nor any of their employees, makes any warranty, expressed or implied, or assumes any legal liability or responsibility for the accuracy, completeness, or usefulness, of any information, apparatus, product, or process disclosed, or represents that its use would not infringe privately owned rights. References herein to any specific commercial product, process, or service by trade name, trade mark, manufacturer, or otherwise, does not necessarily constitute or imply its endorsement, recommendation, or favoring by the U.S. Government or any agency thereof. The views and opinions of authors expressed herein do not necessarily state or reflect those of the U.S. Government or any agency thereof.



Sandia National Laboratories is a multi-program laboratory managed and operated by Sandia Corporation, a wholly owned subsidiary of Lockheed Martin Corporation, for the U.S. Department of Energy’s National Nuclear Security Administration under contract DE-AC04-94AL85000.

Sandia Review and Approval Number: SAND2014-18271 R. Approved for Unclassified Unlimited Release.

## Table of Contents

|   |            |
|---|------------|
| <b>Executive Summary .....</b>  | <b>1-1</b> |
| <b>1. Introduction.....</b>   | <b>1-5</b> |
| 1.1 Purpose and Scope .....   | 1-6        |
| 1.2 Assumptions.....  | 1-7        |
| 1.3 Focus on Clay/Shale Media .....   | 1-9        |
| References for Section 1 .....  | 1-9        |
| <b>2. Engineering of Repository Openings in Clay/Shale Media.....</b>                   | <b>2-1</b> |
| 2.1 Discussion of Excavation and Liner Types .....                                      | 2-2        |
| 2.2 Selected Case Studies .....   | 2-10       |
| 2.3 Discussion, Summary and Repository Construction Scenario .....                      | 2-22       |
| References for Section 2 .....  | 2-24       |
| <b>3. System-Level Logistics Modeling of DPC Direct Disposal.....</b>                   | <b>3-1</b> |
| <b>4. Criticality Investigations .....</b>  | <b>4-1</b> |
| 4.1 Review of Literature .....  | 4-2        |
| 4.2 Methodology .....   | 4-2        |
| 4.3 Effects from Aqueous Species in Ground Water.....                                   | 4-7        |
| 4.4 High-Reactivity Configuration .....   | 4-16       |
| 4.5 Analysis with Canister-Specific Loading .....                                       | 4-17       |
| 4.6 Component Credit Analysis.....  | 4-33       |
| 4.7 Summary and Conclusions .....   | 4-34       |
| References for Section 4 .....  | 4-37       |
| <b>5. Survey of Ground Water Compositions in Representative Geologic Settings .....</b> | <b>5-1</b> |
| 5.1 Overview of Chloride and Total Dissolved Solids .....                               | 5-1        |
| 5.2 Chloride Data for Crystalline and Shale Formation Waters .....                      | 5-2        |
| 5.3 Geologic Environments and the Origins of Saline Pore Waters.....                    | 5-4        |
| 5.4 Conclusions.....  | 5-7        |
| References for Section 5 .....  | 5-8        |
| <b>6. Thermally-Driven Coupled Processes in Clay/Shale Media .....</b>                  | <b>6-1</b> |
| 6.1 TOUGH2 Model for Desaturation of the Host Rock.....                                 | 6-2        |
| 6.2 TOUGH2 Initial Scoping Results .....  | 6-3        |
| 6.3 Thermal-Hydrologic-Mechanical Model .....   | 6-10       |
| 6.4 Summary and Conclusions .....   | 6-19       |
| References for Section 6 .....  | 6-20       |

|            |   |             |
|------------|---|-------------|
| <b>7.</b>  | <b>Potential for Vertical Movement of Waste Packages in a Salt Repository.....</b>                                | <b>7-1</b>  |
|            | References for Section 7 .....  | 7-6         |
| <b>8.</b>  | <b>DPC Materials and Corrosion Environments.....</b>  | <b>8-1</b>  |
| 8.1        | Materials Used in DPCs.....   | 8-1         |
| 8.2        | Factors Controlling Material Corrosion Rates in Disposal Environments .....                                       | 8-2         |
| 8.3        | Survey of Corrosion Rates and Mechanisms, and Corrosion Products for<br>Stainless Steels AISI 304L and 316L ..... | 8-7         |
| 8.4        | Research Needs for Predicting Stability of DPC Materials in Disposal<br>Environments .....                        | 8-12        |
| 8.5        | Prospective Overpack Materials .....  | 8-13        |
| 8.6        | Summary and Application to DPC Inventory .....  | 8-16        |
|            | References for Section 8 .....  | 8-23        |
| <b>9.</b>  | <b>Potential DPC Filler Materials .....</b>   | <b>9-1</b>  |
| 9.1        | Filler Material Requirements .....  | 9-3         |
| 9.2        | Canister Filling Requirements .....   | 9-3         |
| 9.3        | Candidate Filler Materials.....   | 9-6         |
| 9.4        | Criticality Analysis of Filled DPCs .....   | 9-13        |
| 9.5        | Filling Methods.....  | 9-20        |
| 9.6        | Conclusions and Recommendations .....   | 9-22        |
|            | References for Section 9 .....  | 9-23        |
| <b>10.</b> | <b>R&amp;D Needs for Technical Feasibility Evaluation.....</b>  | <b>10-1</b> |
| 10.1       | DPC Characteristics and Loading.....  | 10-1        |
| 10.2       | DPC Disposal Concept Development.....   | 10-3        |
| 10.3       | Thermal Analysis.....   | 10-4        |
| 10.4       | Waste Package/DPC Chemical and Physical Environment After Breach.....   | 10-5        |
| 10.5       | DPC and Disposal Overpack Corrosion .....   | 10-5        |
| 10.6       | Postclosure Criticality Analysis.....   | 10-6        |
| 10.7       | Analysis of Key Features, Events and Processes.....   | 10-7        |
| 10.8       | Performance Assessment for DPC Direct Disposal.....   | 10-9        |
| 10.9       | System Logistics .....  | 10-10       |
| 10.10      | Canister Fillers .....  | 10-10       |
| 10.11      | Preclosure Operations and Safety .....  | 10-10       |
| 10.12      | Decision Support.....   | 10-11       |
| 10.13      | Closeout .....  | 10-11       |
|            | References for Section 10 .....   | 10-12       |

|  |            |
|--|------------|
| 11. Summary of FY14 Investigations .....   | 11-1       |
| References for Section 11 .....  | 11-7       |
| <b>Appendix A. Trip Report: Symposium on Rock Mechanics and Rock Engineering<br/>of Geological Repositories in Opalinus Clay and Similar Claystones.....</b> | <b>A-1</b> |
| A.1 Laboratory and In Situ Experiments, and Models .....   | A-1        |
| A.2 Underground Construction Experience.....   | A-2        |
| A.3 Proposed Repository Layouts and Construction Methods.....  | A-4        |
| Reference for Appendix A .....   | A-6        |
| <b>Appendix B. Peer Review Plan and Approvals .....</b>  | <b>B-1</b> |
| <b>Appendix C. System-Level Logistical Calculations for DPC Direct Disposal .....</b>  | <b>C-1</b> |
| C.1 Results of Logistical Simulations .....  | C-4        |
| C.2 Comparison with Re-Packaging .....   | C-14       |
| C.3 Fuel Age at Emplacement.....   | C-17       |
| C.4 Summary.....   | C-27       |
| References for Appendix C .....  | C-28       |

## Tables

|             |  |      |
|-------------|--|------|
| Table 2-1.  | Comparison metrics for tunneling projects discussed in this report.....  | 2-11 |
| Table 2-2.  | Properties of well-characterized clay/shale media (after Hansen et al. 2010).....  | 2-12 |
| Table 2-3.  | Summary data for San Juan–Chama Project tunnels.....   | 2-18 |
| Table 4-1.  | Burnup analysis isotope set including actinides and 16 fission products.....   | 4-4  |
| Table 4-2.  | Representative loading map.....  | 4-18 |
| Table 4-3.  | Calculated $k_{eff}$ for the Site A DPCs with design basis fuel and loss of absorbers.....   | 4-19 |
| Table 4-4.  | Final Site A DPC statistics in the year 9999.....  | 4-19 |
| Table 4-5.  | Type and number of DPCs in the Site B ISFSI.....   | 4-21 |
| Table 4-6.  | Calculated $k_{eff}$ for the Site B DPCs with design basis fuel and loss of absorbers.....   | 4-23 |
| Table 4-7.  | Final Site B DPC statistics in the year 9999.....  | 4-23 |
| Table 4-8.  | Calculated $k_{eff}$ for the Site C DPCs with loss-of-absorber and basket degradation scenarios, and design basis fuel.....                  | 4-26 |
| Table 4-9.  | Final Site C statistics in the year 9999.....  | 4-26 |
| Table 4-10. | Calculated $k_{eff}$ for the Site D DPCs with design basis fuel and loss of absorbers.....   | 4-29 |
| Table 4-11. | Final Site D statistics in the year 9999.....  | 4-30 |
| Table 4-12. | Calculated $k_{eff}$ for the Site E DPCs with design basis fuel and loss of absorbers.....   | 4-31 |
| Table 4-13. | Final Site E statistics in the year 9999.....  | 4-32 |
| Table 4-14. | Reactivity reduction from non-fuel assembly components for Site E DPCs with loss of neutron absorber.....                                    | 4-34 |
| Table 4-15. | Summary of DPC criticality analyses.....   | 4-37 |
| Table 6-1.  | Thermal and hydrodynamic parameters for host rock and bentonite buffer.....  | 6-3  |
| Table 6-2.  | Thermal, mechanical and hydrodynamic parameters for concrete liner.....  | 6-13 |
| Table 8-1.  | DPC materials summary (data from Greene et al. 2013).....  | 8-2  |
| Table 8-2.  | Range of geochemical conditions in three main geologic repository types (concentration values in mg/L, temperature in degrees Celsius).....  | 8-6  |
| Table 8-3.  | Pit initiation in stainless steels 304/304L and 316/316L exposed to 0.1N NaCl at 25°C (from Streicher and Grubb 2011).....                   | 8-12 |
| Table 8-4.  | Domestic inventory of UNF in dry storage, by canister type, transportability, and susceptibility to degradation in disposal environments.... | 8-20 |

|             |   |      |
|-------------|---|------|
| Table 8-5.  | Summary of the distribution of canisters and fuel types, by canister type and material susceptibility ..... | 8-22 |
| Table 9-1.  | Comparison of DPC filler metrics relevant to transportation and postclosure criticality control.....        | 9-4  |
| Table 9-2.  | Criticality control criteria.....   | 9-5  |
| Table 9-3.  | General performance criteria .....  | 9-5  |
| Table 9-4.  | Filler materials emplaced as liquids.....   | 9-7  |
| Table 9-5.  | Filler materials emplaced as solids .....   | 9-7  |
| Table 9-6.  | Melting points of potential liquid fill materials .....   | 9-9  |
| Table 9-7.  | Characteristics of CANDU and PWR SNF (Forsberg 1997).....   | 9-11 |
| Table 10-1. | R&D activities for technical feasibility evaluation, and status.....  | 10-2 |
| Table 11-1. | Summary of R&D activity status.....   | 11-7 |
| Table C-1.  | Summary of alternative cases used for logistical analysis.....  | C-3  |
| Table C-2.  | Summary of CSF peak storage inventory and CSF operating times for the 18 alternative cases .....            | C-15 |

## Figures

|             |  |       |
|-------------|--|-------|
| Figure 2-1. | Open-type double-shield TBM with trailing gear, during assembly, Yucca Mountain, Nevada (diameter 7.6 m) .....   | 2-3   |
| Figure 2-2. | Schematics of an EPB tunnel boring machine showing shield, segmented liner, muck removal system, and other features .....  | 2-4   |
| Figure 2-3. | Viscoplastic solution to stress distribution in the Pierre Shale, around a 3-m (finished) diameter circular tunnel at 700 m depth, showing load transfer to a 0.75-m thick concrete liner (with permission, Figure 4-12 from Nopola 2013)..... | 2-9   |
| Figure 2-4. | Concrete liner stress after 20 years of load transfer, for a 3-m (finished) diameter tunnel in the Pierre Shale, at the depths indicated (liner thicknesses of 0.25, 0.50 and 0.75 m; with permission, Figure 4-8 from Nopola 2013) .....      | 2-9   |
| Figure 2-5. | Yielding initial support (wire fabric, shotcrete and long rock bolts) just after installation in the Lower Cretaceous clay at the Konrad repository site (depth ~1,000 m) .....  | 2-16  |
| Figure 2-6. | Mill Creek Tunnel Phase 2 showing steel ribs and lagging support (upper) and final cast-in-place concrete liner (lower) (with permission, HMM 2010) .....  | 2-20  |
| Figure 2-7. | In-drift disposal after emplacement and during repository ventilation, prior to installation of backfill then repository closure .....   | 2-24  |
| Figure 4-1. | Axial burnup profiles for PWR assemblies, with normalized distribution and 18 nodes, with 1 being the bottom of the assembly .....   | 4-4   |
| Figure 4-2. | Reactivity impact of <sup>10</sup> B areal density variation .....   | 4-7   |
| Figure 4-3. | Graphical depiction of the center plane of the MPC-32 KENO-VI model used for ground water composition studies with varying <sup>10</sup> B areal density in the neutron absorber panels .....  | 4-8   |
| Figure 4-4. | KENO-VI depiction of the MPC-32 basket degradation scenario.....   | 4-9   |
| Figure 4-5. | Correlation of ppm-chlorine units used in neutronics calculations (nominal) with NaCl concentration .....  | 4-110 |
| Figure 4-6. | Impact on reactivity from chlorine concentration in ground water: (a) for different levels of neutron absorber; and (b) for degraded basket configuration .....  | 4-11  |
| Figure 4-7. | Impact on reactivity from lithium concentration in ground water: (a) for different levels of neutron absorber; and (b) for degraded basket configuration .....   | 4-12  |
| Figure 4-8. | Impact on reactivity from boron concentration in ground water: (a) for different levels of neutron absorber; and (b) for degraded basket configuration .....   | 4-13  |

|              |   |      |
|--------------|---|------|
| Figure 4-9.  | Impact on reactivity from Br and Mn concentration in ground water: (a) for complete loss of neutron absorber; and (b) for degraded basket configuration .....   | 4-14 |
| Figure 4-10. | Impact on reactivity from other elements in ground water: (a) for complete loss of neutron absorber; and (b) for degraded basket configuration .....  | 4-15 |
| Figure 4-11. | High-reactivity configuration as modeled in KENO-VI.....  | 4-16 |
| Figure 4-12. | Reactivity effect from chlorine concentration in flooding ground water, for high-reactivity configuration .....   | 4-17 |
| Figure 4-13. | NAC UMS 24-assembly basket without neutron absorbers as modeled in SCALE.....   | 4-20 |
| Figure 4-14. | Calculated maximum neutron multiplication factor ( $k_{eff}$ ) vs. calendar year, for as-loaded Site A 24-assembly DPCs with loss-of-absorber configuration .....   | 4-20 |
| Figure 4-15. | Radial layout of the Site B 26-assembly basket without neutron absorbers as modeled in SCALE.....   | 4-21 |
| Figure 4-16. | Radial layout of the Site B 24-assembly basket without neutron absorbers as modeled in SCALE.....   | 4-22 |
| Figure 4-17. | Calculated maximum neutron multiplication factor ( $k_{eff}$ ) vs. calendar year, for as-loaded Site B DPCs with loss of neutron absorber.....  | 4-24 |
| Figure 4-18. | Isometric view of the Site C DPC as modeled in SCALE.....   | 4-26 |
| Figure 4-19. | Calculated maximum neutron multiplication factor ( $k_{eff}$ ) for Site C DPCs: (a) loss of absorber configuration as modeled in KENO-VI; and (b) $k_{eff}$ vs. calendar year, based on actual loading .....      | 4-27 |
| Figure 4-20. | Calculated maximum neutron multiplication factor ( $k_{eff}$ ) for Site C DPCs: (a) degraded spacer disks configuration as modeled in KENO-VI; and (b) $k_{eff}$ vs. calendar year, based on actual loading ..... | 4-28 |
| Figure 4-21. | Radial layout of the MPC-24E/EF without neutron absorbers as modeled in SCALE.....  | 4-29 |
| Figure 4-22. | Calculated maximum neutron multiplication factor ( $k_{eff}$ ) vs. calendar year, for as-loaded Site D DPCs with loss of neutron absorber .....   | 4-30 |
| Figure 4-23. | Radial layout of the MPC-32 without neutron absorbers as modeled in SCALE.....  | 4-31 |
| Figure 4-24. | Calculated maximum neutron multiplication factor ( $k_{eff}$ ) vs. calendar year, for as-loaded Site E DPCs with loss of neutron absorber.....  | 4-32 |
| Figure 4-25. | Radial view of WABAs in guide tubes as modeled in SCALE for Site E DPCs .....   | 4-34 |
| Figure 5-1.  | Salinity vs. depth for sedimentary basins in North America (from Kharaka and Hanor 2003) .....  | 5-2  |
| Figure 5-2.  | Chloride concentration vs. depth for various crystalline terranes.....  | 5-3  |

Figure 5-3. Depth vs. chloride concentrations vs. depth for selected shale formations in North America and Europe ..... 5-5

Figure 5-4. Stratigraphic cross-section of the Michigan Basin beneath Michigan and southern Ontario (from Clark et al. 2013) ..... 5-6

Figure 5-5. Distribution and depth of salt formations in the US (from Perry et al. 2014) ..... 5-6

Figure 6-1. Repository layout for modeling drift at 500 m below ground surface..... 6-2

Figure 6-2. Temperature evolution at several locations for backfill and non-backfill operation modes for the 40-year ventilation case ..... 6-4

Figure 6-3. Gas saturation evolution at several locations for the 40-year ventilation case..... 6-5

Figure 6-4. Temperature evolution at several locations for the 350-year ventilation case..... 6-5

Figure 6-5. Gas saturation evolution at several locations for the 350-year ventilation case..... 6-6

Figure 6-6. Temperature evolution for the 350-year ventilation scenario ( $K_{wet} = 1.75$  W/m·K and  $K_{dry} = 1.48$  W/m·K) ..... 6-7

Figure 6-7. Thickness of the desaturated zone for the 40-year ventilation case, with doubled permeability ..... 6-8

Figure 6-8. Thickness of the desaturated zone for the 350-year ventilation case, with doubled permeability ..... 6-8

Figure 6-9. Gas saturation evolution at several points for the 40-year ventilation scenario: with DRZ (sensitivity) and without DRZ (base) ..... 6-9

Figure 6-10. Gas saturation evolution at several points for the 350-year ventilation scenario: with DRZ (sensitivity) and without DRZ (base) ..... 6-9

Figure 6-11. Geometry of a cross section of a drift for DPC disposal ..... 6-11

Figure 6-12. Mesh used in THM model for the configuration shown in Figure 6-11 ..... 6-11

Figure 6-13. Heat load for the 2D THM model..... 6-12

Figure 6-14. Temperature evolution at several locations, solid lines represent the temperature at locations above of the waste package and dashed lines are the temperature at locations below the waste package. .... 6-14

Figure 6-15. Temperature evolution at canister surface and in the backfill ..... 6-14

Figure 6-16. Gas saturation evolution at several locations. Solid lines represent locations above the waste package, and dashed lines indicate locations below the waste package..... 6-15

Figure 6-17. Gas saturation evolution at two points in the backfill..... 6-15

|              |  |      |
|--------------|--|------|
| Figure 6-18. | Pore pressure evolution at several locations. Solid lines represent the pressure at locations above the waste package, and dashed lines indicate the pressure at locations below the waste package .....   | 6-16 |
| Figure 6-19. | Minimum and maximum compressive principal stress within the backfill near the canister .....   | 6-17 |
| Figure 6-20. | Minimum and maximum compressive principal stress within the concrete liner at the bottom .....   | 6-17 |
| Figure 6-21. | Minimum and maximum compressive principal stress at the drift wall.....  | 6-18 |
| Figure 6-22. | Minimum and maximum compressive principal stress in the host rock 10 m away from the drift wall.....   | 6-18 |
| Figure 7-1.  | Strain vs. time and strain-rate vs. time, for a core of Etrez salt, unconfined and axially dead-loaded at the levels shown.....  | 7-2  |
| Figure 7-2.  | Modeling details: (a) spliced Norton and Newtonian constitutive laws, and (b) FLAC model grid used in comparative analysis. ....   | 7-4  |
| Figure 7-3.  | Time dependent crown and invert displacements for a rectangular waste emplacement opening in salt, for 100 years, using: (a) a Norton-type constitutive power law, and (b) a Norton-type power law spliced to a Newtonian LS-LSR at stresses less than 8.1 MPa. .... | 7-5  |
| Figure 8-1.  | Critical pitting temperature for stainless steel alloys as a function of chloride concentration (from Jassen 2011) .....   | 8-4  |
| Figure 8-2.  | General disposal environments and geochemical conditions .....   | 8-5  |
| Figure 8-3.  | Time-dependent chemical corrosion drivers for Fe-based materials (carbon steel and stainless steel) .....  | 8-8  |
| Figure 8-4.  | Nomogram relating soil resistivity, pH, and corrosion rate for steel pipe in soil (from Jack and Wilmott 2011; original source King 1977) .....  | 8-9  |
| Figure 8-5.  | Schematic cutaway of the FO/FC-DSC manufactured by Transnuclear, an example of tube-and-disk basket design.....  | 8-18 |
| Figure 8-6.  | Schematic cutaway of the DSC-32PTH manufactured by Transnuclear, an example of egg-crate basket design .....   | 8-18 |
| Figure 8-7.  | Fractional representation of the total number of DPCs and bare fuel casks by canister type and material susceptibility .....   | 8-21 |
| Figure 8-8.  | Fractional representation of PWR fuel assemblies by canister type and material susceptibility .....  | 8-21 |
| Figure 8-9.  | Fractional representation of BWR fuel assemblies by canister type and material susceptibility .....  | 8-22 |
| Figure 9-1.  | Surrogate waste package with bead filler .....   | 9-2  |
| Figure 9-2.  | Comparison of void space and pin arrangement for CANDU and PWR fuel assemblies.....  | 9-11 |

|              |   |      |
|--------------|---|------|
| Figure 9-3.  | Graphical depiction of the center plane of the MPC-32 KENO-VI model with complete loss of neutron absorber used for filler materials study .....                                  | 9-16 |
| Figure 9-4.  | KENO-VI depiction of the MPC-32 basket degradation scenario with filler material .....  | 9-16 |
| Figure 9-5.  | Reactivity reduction ( $\Delta k_{eff}$ ) as a function of aluminum powder volume fraction for: (a) complete loss of neutron absorber; and (b) basket degradation scenario .....  | 9-17 |
| Figure 9-6.  | Reactivity reduction ( $\Delta k_{eff}$ ) as a function of B <sub>4</sub> C volume fraction for: (a) complete loss of neutron absorber, and (b) basket degradation scenario ..... | 9-19 |
| Figure 9-7.  | Reactivity reduction ( $\Delta k_{eff}$ ) as a function of gibbsite volume fraction for complete loss of neutron absorber .....   | 9-20 |
| Figure 9-8.  | Vent port details .....   | 9-21 |
| Figure 9-9.  | Canadian waste package filler and vibrator compactor concept.....   | 9-21 |
| Figure C-1.  | Reference re-packaging case for ranges of throughput and repository start date, showing history of CSF inventory .....  | C-4  |
| Figure C-2.  | SNF inventory that has cooled to a 6 kW emplacement power limit .....   | C-6  |
| Figure C-3.  | SNF inventory that has cooled to a 10 kW emplacement power limit .....  | C-7  |
| Figure C-4.  | Repository throughput with (a) 6 kW, and (b) 10 kW emplacement power limits, maximum throughput of 3,000 MTHM per year and repository start date of 2036.....                     | C-9  |
| Figure C-5.  | Repository throughput with (a) 6 kW and (b) 10 kW emplacement power limits, maximum throughput of 3,000 MTHM per year and repository start date of 2048.....                      | C-10 |
| Figure C-6.  | Repository throughput with (a) 6 kW and (b) 10 kW emplacement power limits, maximum throughput of 4,500 MTHM per year and repository start date of 2036.....                      | C-12 |
| Figure C-7.  | Repository throughput with (a) 6 kW and (b) 10 kW emplacement power limits, maximum throughput of 4,500 MTHM per year and repository start date of 2048.....                      | C-13 |
| Figure C-8.  | Inventory age at emplacement (a) and cumulative inventory as a function of age at emplacement (b) with a 6 kW emplacement limit and 2036 repository start date.....               | C-18 |
| Figure C-9.  | Inventory age at emplacement (a) and cumulative inventory as a function of age at emplacement (b) with a 10 kW emplacement limit and 2036 repository start date.....              | C-19 |
| Figure C-10. | Inventory age at emplacement (a) and cumulative inventory as a function of age at emplacement (b) with a 6 kW emplacement limit and 2048 repository start date.....               | C-20 |

Figure C-11. Inventory age at emplacement (a) and cumulative inventory as a function of age at emplacement (b) with a 10 kW emplacement limit and 2048 repository start date..... C-21

Figure C-12. Fuel age at emplacement with a 10 kW emplacement limit and 2036 repository start date: (a) DPCs-only, and (b) DPCs with transition to MPCs in 2031 ..... C-23

Figure C-13. Average age at emplacement as a function of repository start date and emplacement thermal power limit: (a) DPCs-only and (b) DPCs with transition to MPCs at 5 years before the repository start date ..... C-24

Figure C-14. Age of fuel at emplacement in DPCs and MPCs, with the 6 kW power limit and repository start in 2036, expressed as histograms (upper) and cumulative distributions (lower)..... C-25

Figure C-15. Burnup of fuel in DPCs and MPCs, expressed as histograms (upper) and cumulative distributions (lower) for the 6 kW power limit and repository start in 2036..... C-26

## Acronyms

|        |   |
|--------|---|
| 2D     | 2-Dimensional   |
| 3D     | 3-Dimensional   |
| AECL   | Atomic Energy of Canada, Ltd.                             |
| ANDRA  | National Agency for Radioactive Waste Management (France) |
| BPRA   | Burnable Poison Rod Assembly                              |
| BRC    | Blue Ribbon Commission on America's Nuclear Future        |
| BSC    | Bechtel-SAIC Co.  |
| BWR    | Boiling Water Reactor                                     |
| CALVIN | CRWMS Analysis and Logistics Visually INteractive model   |
| CANDU  | CANadian Deuterium-Uranium reactor type                   |
| CFR    | Code of Federal Regulations                               |
| cm     | centimeter  |
| COX    | Callovo-Oxfordian argillite formation                     |
| CRA    | Control Rod Assembly                                      |
| CRWMS  | Civilian Radioactive Waste Management System              |
| CS     | Carbon Steel  |
| CSF    | Centralized Storage Facility                              |
| CSO    | Combined Sewerage Overflow                                |
| DFC    | Damaged Fuel Can  |
| DOE    | U.S. Department of Energy                                 |
| DPC    | Dual-Purpose Canister                                     |
| DRZ    | Disturbed Rock Zone                                       |
| DU     | Depleted Uranium  |
| DUS    | DU Silicate glass   |
| EBS    | Engineered Barrier System                                 |
| ECT    | Euclid Creek Tunnel                                       |
| EDZ    | Excavation Damage Zone                                    |
| EPA    | U.S. Environmental Protection Agency                      |
| EPB    | Earth Pressure Balance TBM                                |
| EPRI   | Electric Power Research Institute                         |
| ETH    | Swiss Federal Institute of Technology                     |
| FEPs   | Features, Events, and Processes                           |
| FLAC   | Fast Lagrangian Analysis of Continua                      |
| FSAR   | Final Safety Analysis Report                              |
| FY     | Fiscal Year   |
| GPa    | Gigapascal  |
| GW     | Gigawatt  |
| GW-d   | Gigawatt-day  |

|               |   |
|---------------|---|
| HAZ           | Heat Affected Zones (e.g., around welds in metal)   |
| Hi-Storm      | Trade name for vertical dry storage systems (Holtec International)  |
| HLW           | High-Level Waste  |
| ISFSI         | Independent Spent Fuel Storage Installation   |
| ISO           | International Standards Organization  |
| K             | Kelvin degrees  |
| KENO          | Criticality modeling framework  |
| $k_{eff}$     | Effective reactivity coefficient  |
| $K_{th}$      | Thermal Conductivity  |
| kW            | kilowatt  |
| L             | Liter   |
| LS-LSR        | Low-Stress, Low Strain-Rate   |
| m             | meters  |
| $\mu\text{m}$ | microns   |
| Ma            | Millions of years   |
| mg            | milligrams  |
| Mgal          | Million gallons   |
| MMC           | Metal-Matrix Composite  |
| MPa           | Megapascal  |
| MPC           | Multi-Purpose Canister (used here and internationally for storage-transport canisters that are also disposable, but also used for certain DPCs from Holtec International and other vendors) |
| MT            | Metric Tons   |
| MTHM          | Metric Tons Heavy Metal   |
| MTU           | Metric Tons Uranium   |
| MW            | Megawatt  |
| NAGRA         | National Cooperative for the Disposal of Radioactive Waste (Switzerland)  |
| NAS/NRC       | National Academy of Science/National Research Council   |
| NRC           | U.S. Nuclear Regulatory Commission  |
| NUHOMS        | Trade name for vault –type dry storage system (TransNuclear)  |
| OCRWM         | U.S. Department of Energy, Office of Civilian Radioactive Waste Management  |
| OFA           | Optimized Fuel Assembly   |
| ORP           | Oxidation-Reduction Potential   |
| Pa            | Pascal  |
| ppm           | parts per million   |
| PWR           | Pressurized Water Reactor   |
| R&D           | Research and Development  |

|                  |  |
|------------------|--|
| SJCP             | San Juan-Chama Project                                     |
| SNF              | Spent Nuclear Fuel   |
| SNL              | Sandia National Laboratories                               |
| SS               | Stainless Steel (also Slurry-Shield, a type of TBM)        |
| STAD             | Storage-Transport-Aging-Disposal canister concept          |
| STD              | Standard Fuel Assembly                                     |
| TARP             | Tunnel and Reservoir Project (Chicago)                     |
| TBM              | Tunnel Boring Machine                                      |
| TDS              | Total Dissolved Solids                                     |
| THM              | Thermal-Hydrologic-Mechanical                              |
| TOUGH2           | Thermal-hydrology simulation code                          |
| TSL-CALVIN       | Transportation-Storage Logistics version of CALVIN model   |
| TSPA             | Total System Performance Assessment                        |
| UCS              | Unconfined Compressive Strength                            |
| UFD              | Used Fuel Disposition                                      |
| UNF              | Used Nuclear Fuel  |
| USBR             | U.S. Bureau of Reclamation                                 |
| UNF-<br>ST&DARDS | Library of DPC fuel characteristics with calculation tools |
| URL              | Underground Research Laboratory                            |
| WABA             | Wet Annular Burnable Absorber                              |
| W                | watts  |
| yr               | years  |

## **Investigations of Dual-Purpose Canister Direct Disposal Feasibility (FY14)**

**Milestone Deliverable: M2FT-14SN0816031**

**Work Package: FT-14SN081603**

Ernest Hardin, Charles Bryan, Anastasia Ilgen, Elena Kalinina and Stephanie Teich-McGoldrick,  
Sandia National Laboratories

Kaushik Banerjee, Justin Clarity, Rob Howard, Robert Jubin and John Scaglione  
Oak Ridge National Laboratory

Frank Perry, Los Alamos National Laboratory

Liange Zheng, Jonny Rutqvist and Jens Birkholzer, Lawrence Berkeley National Laboratory

Harris Greenberg, Lawrence Livermore National Laboratory

Joe Carter and Thomas Severynse, Savannah River National Laboratory

### **Executive Summary**

Results reported here continue to support the FY13 conclusion that direct disposal of DPCs is technically feasible, at least for some DPCs, and for some disposal concepts (geologic host media). Much of the work performed has reached a point where site-specific information would be needed for further resolution.

Several activities in FY14 have focused on clay/shale media because of potential complications resulting from low thermal conductivity, limited temperature tolerance, and the need to construct hundreds of kilometers of emplacement drifts that will remain stable for at least 50 years. Technologies for rapid excavation and liner installation have significantly advanced in the past 20 years. Tunnel boring machines are the clear choice for large-scale excavation. The first TBM excavations, including some constructed in clay or shale media, are now approaching 50 years of service. Open-type TBMs are a good choice but the repository host formation would need to have sufficient compressive strength for the excavation face to be self-supporting. One way to improve the strength-stress relationship is to reduce the repository depth in soft formations (e.g., 300 m depth). The fastest construction appears to be possible using TBMs with a single-pass liner made of pre-fabricated concrete segments. Major projects have been constructed with pre-fabricated segmented liner systems, and with cast-in-place concrete liners. Cost comparisons show that differences in project management and financing may be larger cost factors than the choice of liner systems. Costs for large-scale excavation and construction in clay/shale media vary widely but can probably be limited to \$10,000 per linear meter, which is similar to previous estimates for repository construction.

Concepts for disposal of DPC-based waste packages in clay/shale media are associated with thermal management challenges because of the relatively low thermal conductivity and limited temperature tolerance. Peak temperature limits of 100°C or lower for clay-rich materials have been selected by some international programs, but a limit above 100°C could help to shorten the duration of surface decay storage and repository ventilation. The effects of locally higher peak temperatures on repository performance need to be evaluated (in addition to the effects at lower temperatures). This report describes a modeling approach that couples the TOUGH2 and FLAC3D codes to represent thermally driven THM processes, as a demonstration of the types of models needed. The model shows that repository ventilation leads to a desaturated zone (partial desiccation) in the host rock, limited mostly to a few meters with diminishing influence out to

more than 10 m. Longer ventilation duration, greater host rock permeability, and the existence of a DRZ tend to increase the extent of desaturation. After ventilation ceases and backfill is installed, resaturation (moisture migrating from the far field) takes place over a period tens to a few hundred years. Transient increases in stress are calculated in the host rock and backfill due to thermally and mechanically induced increases in pore pressure, and thermal expansion of the solid framework. With a thick concrete liner and swelling-clay backfill, stability is predicted for emplacement drift openings at a depth of 500 m, using properties for the Opalinus Clay. The models used in this work are 2D and therefore tend to underestimate peak temperatures and associated coupled processes, however, regions between waste packages are known to be cooler, with peak temperatures potentially much less than 100°C.

A new set of neutronics calculations evaluates DPC criticality when flooded with ground water containing a range of neutron absorbing elements, at different concentrations. The configuration has no basket or neutron absorbers, only fuel rods arrayed with generous, uniform spacing so that the fuel rods entirely fill the canister (increasing reactivity). Of the elements commonly found in ground water, only chlorine could contribute significant neutron absorption at concentrations likely to occur in a repository. The chloride content of seawater may be enough to ensure subcriticality of some DPCs, while more saturated salt brines could ensure subcriticality for all DPCs (fresh fuel at 4% enrichment, or some burnup with 5% enrichment).

Another set of neutronics evaluates the reactivity of DPCs in as-loaded configurations, flooded with fresh or saline ground water, and using “uncredited margin.” The licensing basis for existing DPCs involves criticality analysis for flooding associated with a transportation accident. Fuel characteristics assumed for that analysis may be conservative compared to fuel that is actually loaded, and the difference is uncredited reactivity margin. Uncredited margin is evaluated using burnup credit analysis with 28 actinide and fission product nuclides, and accounting for radionuclide decay. Criticality analyses are presented for actual, as-loaded DPCs flooded with fresh water, for two canister degradation scenarios: loss-of-absorber and complete basket degradation. Uncredited margin offsets the increases in reactivity associated with degradation scenarios. Five types of DPCs presently located at five dry storage sites, are analyzed. For four of these the loss-of-absorber scenario is analyzed, but not the basket degradation scenario because the baskets are made from stainless steel which could last much longer than other basket materials used in DPCs. For the fifth DPC type both scenarios are analyzed. Of the 179 DPCs analyzed all would exceed the subcritical limit ( $k_{eff} > 0.98$ ) when flooded with fresh water, with loss of neutron absorbers, if loaded with the design-basis fuel used for licensing. Using uncredited margin only 23 of the 179 would exceed the subcritical limit for the loss-of-absorber scenario, unless the chlorine concentration of flooding ground water is at least 13,500 ppm (seawater is 19,400 ppm). For the fifth site, 18 of the 20 DPCs would exceed the subcritical limit with the basket degradation scenario, unless the chlorine concentration is at least 32,500 ppm. These results may be typical of some early DPC designs, but other, more recent designs could have less uncredited margin with as-loaded fuel characteristics.

High-chloride waters occur at depth in both crystalline rock and clay/shale media under certain geologic conditions. Pore waters with chloride content sufficient to significantly reduce the likelihood of criticality in many flooded DPCs, are common in geologically ancient crystalline basement formations at depths greater than 500 m. The origin of highly saline waters in clay/shale media generally involves more complex processes. Shales with sufficient chloride concentrations are found in contact with bedded salt deposits or as marine shales in which waters

are concentrated from evaporation or water-rock interaction. In both crystalline and sedimentary environments, highly saline waters tend to be old and stagnant. The correlation with age suggests that high-chloride waters may not be common in geologically young granites, or those in tectonically active settings. High-chloride shales have been documented in the Michigan Basin and they probably occur in the Appalachian and Williston Basins, although the extent is not well documented. By analogy, high-chloride shales could be expected in the Permian Basin, but no data have been identified to support this conjecture.

Recently published salt creep test data suggest that heavy DPC-based waste packages could sink in a salt repository, on the order of 1 m or more in 10,000 years. A salt creep constitutive model was developed to highlight the differences between salt creep by solid-dislocation processes, and low-stress low-strain rate creep as published recently by European and U.S. investigators. A Newtonian flow law is spliced together with a widely used power law for dislocation creep in Permian Basin salt, and the resulting model is used to simulate closure of a repository emplacement drift backfilled with crushed salt, with and without low-stress, low strain-rate creep. The results with the spliced function show rapid creep deformation in the near field because of additional load transferred from the far field, where there is confinement but low deviatoric stress. This modeling situation is inconsistent with observed behavior of underground openings, and leads to questions about the role of the mean stress in constitutive models that include low-stress, low strain-rate behavior. A semi-mechanistic, literature-based pressure solution approach is proposed as an alternative to the Newtonian law, whereby confinement slows down the creep rate. Additional testing is needed to better understand low-stress, low strain-rate creep behavior over a wider range of loading conditions in different salt media, and to confirm the role of moisture.

DPCs are constructed from stainless steel alloys and other materials (neutron absorbers are mostly aluminum-based and would corrode readily on exposure to moisture in virtually any disposal environment). Review of corrosion literature shows that stainless steel corrosion may be slow enough to sustain DPC basket structural integrity for a performance period of 10,000 years, especially in reducing conditions. Uncertainties include basket component design, environmental conditions, and effects from radiolysis. Published data also show that prospective disposal overpack materials exist for most disposal environments, including both corrosion allowance and corrosion resistant materials.

Not all DPCs have stainless steel basket structures, so a preliminary screening is presented of the existing inventory of DPCs and other types of canisters, according to the type of closure, whether they can be readily transported, and what types of materials are used in basket construction. DPCs and other types of canisters are grouped according to whether they: 1) are licensed for transport; 2) have any non-stainless basket structural materials that are susceptible to degradation on long-term exposure to ground water; and 3) are bolted casks. The results show that approximately 2/3 of the overall inventory of storage casks and canisters are considered transportable with basket structural components made from stainless steel, while 6% are transportable but with non-stainless components. The remaining 25% consists of storage-only canisters and bolted casks. These screening results are based on assumptions, in particular that stainless steel construction denotes disposability, and that even thin stainless-steel components (e.g., guide sleeves) have sufficient thickness to sustain structural integrity.

A proposal for remediating loaded DPCs to make them more suitable for direct disposal, is to open them and inject a filler material that would mainly help to control postclosure criticality but

could also improve heat transfer and mechanical stability, then re-seal them. The most promising filler materials are: 1) low-melting-point metals such as Pb-Sn, Sn-Ag-Cu or Sn-Zn; and 2) small solid particles such as glass beads, including glass beads that contain DU or UO<sub>2</sub>. In the case of low-melting-point metals, provisions would be needed to pre-heat the entire DPC and its contents to temperatures of 225 to 250°C. Two filling methods are possible: 1) using the drain and vent ports accessed by removing the welded covers; and 2) removal of the entire lid from each DPC. For solid particulate fillers some provision for vibrating the entire DPC may be needed. Cutting off canister lids could be done using a method such as lathing (skiving). Depending on the approach, a separate hot cell facility could be needed for receipt, opening, filling, closure and testing. In any case, containment will be required to control potential radiological releases when DPCs are opened and during filling and subsequent closure operations. Criticality analysis shows that a filler material, irrespective of whether it is a neutron absorber or simply displaces water as a moderator, should occupy most if not all of the DPC free volume. Also, the eventual corrosion product of a filler material and its effect on reactivity should be considered in filler selection.

Logistical simulations were conducted to better understand the relationship between the needed DPC decay storage time for disposal, and future changes in the SNF management system in the U.S. such as repository opening date, and transition to loading smaller multi-purpose canisters. The study is described in Appendix C.

This report contains an annotated a list of 41 R&D topics, consolidated from lists developed in FY13 and FY14. Completed activities are described here and in the FY13 summary report. Partly completed activities are those that depend on data collection from the nuclear utilities (e.g., GC-859 survey in FY15). Many activities are relevant to DPC direct disposal, but are being conducted in other areas of the UFD R&D program (e.g., corrosion testing, performance assessment, investigation of clay-based and cementitious materials, brine migration in salt, etc.). A small number of activities is planned for FY15, and there is an additional group of possible future activities. The most important gaps that could be addressed by future activities include validation of criticality modeling tools (e.g., boiling water reactor fuel burnup analysis), and DPC basket corrosion modeling and testing (stainless steel).

## 1. Introduction

Current used nuclear fuel management practices in the U.S. include heavy reliance on dry storage. Nuclear-electric utility companies are meeting interim storage needs on an individual basis with the use of large-capacity dry storage casks. The design and implementation of dry storage systems is focused on meeting storage and transportation requirements, in part because disposal requirements are not available. Direct disposal of these dual-purpose canisters (DPCs, for storage and transport) instead of re-packaging the spent nuclear fuel (SNF) for disposal, is attractive because it could reduce complexity of the waste management system, reduce cost, reduce waste, and possibly reduce worker dose (Howard et al. 2014).

This report presents interim results from investigation of the technical feasibility of direct disposal of commercial SNF in DPCs of existing design. It follows an earlier report of preliminary feasibility results (Hardin et al. 2013) issued in August, 2013, posted to the [www.doe.gov](http://www.doe.gov) website in December, 2013, and summarized in the Spring, 2014, issue of *RadWaste Solutions* (Hardin et al. 2014).

The 2013 report concluded that direct disposal of existing DPCs could be technically feasible, at least for some part of the inventory as could be determined mainly from consideration of postclosure criticality (these results are summarized in Section 4 along with new calculations for additional DPCs). Packaging and handling of DPCs in waste packages were found to be within the present state of practice. Transport and emplacement of large waste packages underground were found to be technically feasible, although engineering R&D would likely be needed, and some of the possible conveyance systems could be the largest of their kind. Thermal management was found to be feasible given: 1) open emplacement modes with active repository ventilation; 2) sufficient time for cooling before repository closure; and 3) repository host media and engineered materials that can isolate waste even after exposure to elevated temperatures. Further resolution of thermal management and repository waste isolation performance (e.g., performance assessment) will depend on site-specific information such as host rock thermal conductivity.

The 2013 report also identified important topics for additional R&D to support feasibility evaluation. Some of the more promising of these were investigated in FY14, and are documented in this report.

There are now more than 1,900 DPCs and storage-only canisters in service in the U.S., and deployment of new DPCs continues at a rate of approximately 160 per year. A general description of DPC design was provided in the 2013 report along with projections of DPC accumulation through the 21<sup>st</sup> century if current practices are continued and no new nuclear power reactors are built (Hardin et al. 2013). By approximately 2035, half of the total SNF inventory in the U.S. will be stored in approximately 5,000 DPCs. From then on DPCs could continue to accumulate (if new types of SNF canisters are not implemented) until they are used to store the entire U.S. SNF inventory, projected to be approximately 139,000 MTHM by 2055.

The authors of this report have assumed that the reader is familiar with DPC construction and deployment (for example, the survey of Greene et al. 2013). DPCs have thin-walled outer shells, typically of stainless steel, with welded closures. Construction and materials used for the internal baskets vary by manufacturer, and designs have changed over time since the mid-1990's when DPCs came into wide use.

The existing canister inventory includes some storage-only designs (not licensed for transport) which are similar to DPCs but lack neutron absorbing features that would control criticality in the event of a transportation accident that causes flooding. Storage-only designs include the MSB (24 PWR fuel assembly capacity; Energy Solutions), and various NUHOMS canisters (mainly with 24 PWR/52 BWR fuel assembly capacity; Transnuclear, Inc.). These canisters currently exist at the Idaho National Laboratory and several nuclear power plants. For evaluation of direct disposal, these welded storage-only canisters can be treated in the same manner as DPCs. However, they would need to be transported to a repository and the options for doing so are beyond the scope of this study.

The earliest dry storage systems in the U.S. were self-shielded cask systems with bolted closures, which are not considered here. Bolted canisters can be readily opened for unloading or modification, and may be reused. Welded canisters, including all DPCs, must be cut open (if not disposed of as loaded) and canister hulls become low-level nuclear waste.

### 1.1 Purpose and Scope

The purpose of R&D investigations and technical feasibility evaluation is to support future decisions whether to include DPC disposal criteria in site selection and repository development, and what kinds of canister modifications could facilitate disposal as well as storage and transportation. The timing of such decisions and modifications has not been determined, but they could be implemented under the current waste management strategy over the next 10 to 20 years (DOE 2013).

Technical feasibility of DPC direct disposal depends on satisfying four broad objectives, which are described with current status summarized below:

- **Safety of Workers and the Public** – This paramount objective is closely related to those listed above. Preclosure safety of repository operations at the surface and underground would be analyzed as has been done previously (DOE 2008), and appropriate active and passive safety features and redundancy would be built into the design. Detailed safety analysis is beyond the scope of this study and would depend on site-specific information. Safety could be important for first-of-a-kind systems such as a heavy hoist for a waste handling shaft. For postclosure waste isolation safety, generic, qualitative aspects were addressed in the 2013 report including likely effects from additional heating and more waste in packages. Quantitative expressions of waste isolation performance are generated using performance assessment (Bonano et al. 1989), which also depends on site-specific information. Generic (non-site specific) assessments may be strongly influenced by assumptions made in lieu of site-specific data, such as groundwater velocity and radionuclide sorption parameters. The needs for additional information on preclosure safety and postclosure waste isolation are discussed later in this report.
- **Thermal Management** – The heat output of DPCs is due to the large capacity (up to 37 PWR fuel assemblies, or as many as 89 BWR assemblies) and the increasingly higher burnup levels achieved in commercial plants. Peak temperature limits for geologic host media, and for clay-based engineered materials (buffer and backfill), are generally used to limit impacts to waste isolation. These temperature limits constrain waste package heat output after repository closure, and thus, the fuel characteristics and required decay storage duration. Previous studies found that temperature limits on geologic host media could be met, but that engineered backfill materials could sustain peak temperatures in

the range 150 to 200°C. Thermal analyses are described in the 2013 report, and in other previous studies (Hardin et al. 2012, 2013).

- **Postclosure Criticality Control** – Nuclear fuel is designed to achieve criticality in reactors, but it becomes less reactive after burnup, and DPCs are designed with additional features that control neutron multiplication in the event of flooding. However, neutron absorbing materials commonly used in DPCs are aluminum-based, and therefore subject to degradation if exposed to ground water. In a repository with multiple engineered and natural barriers, as projected in previous performance assessments (DOE 2008) a small number of waste packages could become breached and flood due to corrosion, future human interference, etc. Analysis of reactivity without the neutron absorbing materials has shown that criticality may not occur if the ground water is chloride-rich brine, or if there is sufficient fuel burnup for certain DPCs. Initial evaluations of burnup credit and chloride brine effects were described in the 2013 report and further evaluations are described here.
- **Engineering Feasibility** – DPCs are currently handled and stored in heavy, shielded casks at nuclear power plants. For direct disposal the engineering feasibility questions pertain to similar systems for transporting large, heavy packages underground (e.g., ramp or shaft conveyance), and transporting and emplacing them in a repository. Also, in most potential geologic host media (except salt) the emplacement openings would need to stay open for ventilation, with little or no maintenance for at least 50 years. Backfill would need to be installed remotely prior to repository closure, in a thermal and radiological environment. Some proposed engineering solutions would be first-of-a-kind, and development costs could be significant although a small fraction of total disposal cost. Overall, previous studies have found that engineering feasibility would not be a barrier to implementing DPC direct disposal. Engineering feasibility is discussed in the 2013 report (Hardin et al. 2013) and aspects related specifically to construction in clay/shale media are discussed here.

The scope of this study includes disposal of existing DPCs and storage-only canisters, and also modifications to existing DPCs or DPC designs that would facilitate direct disposal. Hence, this report includes discussion of possible filler materials that could be injected into existing canisters. Other possible modifications have been identified (Hardin 2013) and some of these are addressed in this report as information needs.

## 1.2 Assumptions

Evaluation of technical feasibility will be based on targeted technical analyses, conducted over several years (Howard et al. 2014). Assumptions are needed to control this process because: 1) the analyses are generic; 2) it is recognized that statutory and regulatory changes or clarifications would be required (BRC 2012); and 3) the timing of disposal is uncertain so that the future state of the overall fuel management system in the U.S. must be assumed. Assumptions developed for DPC direct disposal evaluation are documented in a separate report (Hardin and Howard 2013). They are categorized into three areas:

- **Engineering and Technology Assumptions** – These describe certain DPC characteristics used for analysis, major aspects of geologic disposal, principles of postclosure criticality analysis, and certain attributes of the repository surface facilities.

- **Statutory and Regulatory Framework for Disposal** – These assumptions describe generally what changes in legislation such as the *Nuclear Waste Policy Act*, would be enacted to allow DPC disposal (e.g., repository capacity and schedule of operations). In addition, they clarify which parts of the current regulatory framework would be applied to licensing such a repository.
- **Assumptions for Storage and Transportation** – These assumptions state that storage and transportation would be regulated the same as they are currently, and movement from storage to the repository could be done with flexibility to accommodate thermal management and other repository constraints.

If and when further design or engineering activities are directed to proceed for DPC direct disposal, assumptions will be reevaluated, and any impacts on the analyses or conclusions of this report will be assessed.

Specific changes from the 2013 report to this report, include the following:

- **Horizontal vs. Vertical** – Whereas it was previously assumed that DPCs designed for vertical storage can be readily adapted for horizontal disposal, a further assumption conversely allows that DPCs designed for horizontal storage can be readily transferred to disposal overpacks in either vertical or horizontal orientation, for disposal.
- **Regulatory Assumption Clarification** – The National Academies/National Research Council recommendations for standards specific to a repository in unsaturated tuff developed pursuant to the *Energy Policy Act of 1992* (NAS/NRC 1995) may be applicable to other repositories for SNF and high-level waste (HLW) even though this act only addresses standards for a repository at Yucca Mountain. If so, then licensing of future repositories will require demonstration of compliance with a peak dose standard, for a period of geologic stability ( $\sim 10^6$  yr was recommended by the NAS/NRC).

Any changes to the EPA standards for repositories in media other than at Yucca Mountain would likely change 40 CFR 191, and would be reflected in corresponding changes to NRC regulation 10 CFR 60. The 10 CFR 60 rule is still applicable to any geologic repository other than at Yucca Mountain, and was not revised when fundamental changes were made to performance assessment requirements in the promulgation of 10 CFR Part 63. In particular, NRC has evolved from disposal subsystem requirements (e.g., engineered barrier system containment) to rely on mean annual dose computed from total system performance assessment (TSPA). Consequently, the NRC stated when promulgating 10 CFR 63 that the “generic Part 60 requirements will need updating” (Rubenstone 2012). Furthermore, NRC has suggested that regulations for future repositories would likely look similar to 10 CFR 63, in presentations to the Blue Ribbon Commission on America’s Nuclear Future (BRC) and the Nuclear Waste Technical Review Board (McCartin 2010; 2012).

- **Nuclear Waste Policy Act Amendment or Replacement Assumption** – The *Nuclear Waste Policy Act* (as amended) will be further amended or replaced with legislation that permits developing one or more geologic repositories for U.S. commercial SNF at sites other than Yucca Mountain, and doing so on a schedule consistent with the DOE strategy for SNF waste management (DOE 2013).
- **SNF Shipments to a Repository** – The preferred disposition pathway is assumed to be transport to a repository directly from a conjunctively operated centralized storage

facility. In logistical simulations, SNF can be transported from dry storage at power plants, directly to the repository, if the fuel is cool enough for disposal and no other fuel suitable for disposal is available at a centralized storage facility.

### 1.3 Focus on Clay/Shale Media

Previous investigations determined that for disposal of the projected inventory of SNF in DPCs, in clay-rich (argillaceous) media including shales, a large repository layout would be needed (Hardin et al. 2013). At least 300 km of emplacement drifts, plus access and service drifts, would need to remain open for at least 50 years to support active, forced ventilation for heat removal. The feasibility and cost of constructing tunnels on this scale in clay/shale, so that they would require little or no maintenance for the 50-year service life, were identified as important issues. Accordingly, this report includes a summary of modern excavation and ground support methods used in clay/shale media, and the associated cost.

Heat dissipation in clay/shale media is less efficient than in salt or crystalline rock, because of lower thermal conductivity. Previous studies identified the possibility of allowing clay/shale host media to exceed the maximum temperature adopted by European repository programs (e.g., 100°C) in the immediate vicinity of waste packages. Such a modified temperature limit could allow less decay storage and repository ventilation, smaller repository layout, and/or earlier repository closure (Hardin et al. 2012, 2013). The impact of heating on clay/shale media is therefore described in this report, with simulations representing the state-of-the-art in thermally driven coupled process modeling.

In addition, previous investigation confirmed the benefit of chloride-rich ground water in controlling criticality in the event of waste package breach and flooding. Some clay/shale formations are known to produce saline ground water, and this report also summarizes a survey of selected ground water composition data from the U.S., that includes clay/shale media.

### References for Section 1

Bonano, E.J., P.A. Davis, L.R. Shippers, K.F. Brinster, W.E. Beyeler, C.D. Updegraff, E.R. Shepherd, L.M. Tilton, K.K. Wahi 1989. *Demonstration of a Performance Assessment Methodology for High-Level Radioactive Waste Disposal in Basalt Formations*. U.S. Nuclear Regulatory Commission, NUREG/CR-4759.

BRC (Blue Ribbon Commission on America's Nuclear Future) 2012. *Report to the Secretary of Energy*. January, 2012. ([www.brc.gov](http://www.brc.gov))

DOE (U.S. Department of Energy) 2008. *Yucca Mountain Repository License Application for Construction Authorization*. DOE/RW-0573. Washington, D.C.: U.S. Department of Energy.

DOE (U.S. Department of Energy) 2013. *Strategy for the Management and Disposal of Used Nuclear Fuel and High-Level Radioactive Waste*. January, 2013.

Greene, S.R., J.S. Medford and S.A. Macy 2013. *Storage and Transport Cask Data for Used Commercial Nuclear Fuel – 2013 U.S. Edition*. ATI-TR-13047. Energx, Oak Ridge, TN, and Advanced Technology Insights, LLC, Knoxville, TN.

Hardin, E. and R. Howard 2013. *Assumptions for Evaluating Feasibility of Direct Geologic Disposal of Existing Dual Purpose Canisters*. FCRD-UFD-2012-000352 Rev. 1. U.S. Department of Energy, Office of Used Nuclear Fuel Disposition. November, 2013.

Hardin, E.L. 2014. *Spent Fuel Canister Disposability Baseline Report*. FCRD-UFD-2013-000330 Rev. 0. U.S. Department of Energy, Office of Used Nuclear Fuel Disposition. December, 2013.

Hardin, E., T. Hadgu, D. Clayton, R. Howard, H. Greenberg, J. Blink, M. Sharma, M. Sutton, J. Carter, M. Dupont and P. Rodwell 2012. *Repository Reference Disposal Concepts and Thermal Management Analysis*. FCRD-USED-2012-000219 Rev. 2. U.S. Department of Energy, Office of Used Nuclear Fuel Disposition. November, 2012.

Hardin, E., D. Clayton., R. Howard, J. Scaglione, E. Pierce, K. Banerjee, M. Voegelé, J. Wen, T. Buscheck , J. Carter, and T. Severynse 2013. *Preliminary Report on Dual-Purpose Canister Disposal Alternatives (FY13) Revision 1* . FCRD-USED-2013-000171 Rev. 1. U.S. Department of Energy, Office of Used Nuclear Fuel Disposition. November, 2013.

Hardin, E.L., D.J. Clayton, R.L. Howard, J. Clarity, J.M. Scaglione, J.T. Carter, W.M. Nutt and R.W. Clark 2014. "Evaluation of Direct Disposal of Spent Fuel in Existing Dual-Purpose Canisters." American Nuclear Society, La Grange Park, IL. *RadWaste Solutions*. V.21, N.1, pp. 26-39.

Howard, R., J. Scaglione, E. Pierce and B. van den Akker and E. Hardin 2014. *Feasibility Evaluation for Direct Disposal of Dual Purpose Canisters: Study Plan*. FCRD-UFD-2014-000518. U.S. Department of Energy, Office of Used Nuclear Fuel Disposition. April, 2014.

McCartin, T. 2010. "Summary Statement: regulations for Geological Disposal of High-Level Radioactive Waste." Blue Ribbon Commission on America's Nuclear Future, Disposal Subcommittee. September 1, 2010. ([www.brc.gov](http://www.brc.gov))

McCartin, T. 2012. United States Nuclear Waste Technical Review Board, Spring Board Meeting. Transcript from March 7,2012. ([www.nwtrb.gov](http://www.nwtrb.gov))

NAS/NRC (National Academy of Sciences/National Research Council) 1995. *Technical Bases for Yucca Mountain Standards*. National Academy Press, Washington, D.C.

Rubenstein, J. 2012. "Emerging regulatory challenges in the management of spent nuclear fuel and high-level radioactive waste." *The Bridge*. National Academy of Engineering. 42(2):32-9.

## 2. Engineering of Repository Openings in Clay/Shale Media

This section reviews worldwide examples of large-scale excavations in clay/shale media, the methods used for excavation and construction, and the costs. This information is intended to support evaluation of the feasibility of construction of a deep geologic repository for ~10,000 large DPC-based waste packages containing approximately 140,000 MT of SNF (Hardin 2014).

Earlier studies compared reference concepts for disposal of SNF and HLW in various media (clay/shale, crystalline and salt) with one result being that construction and maintenance costs for openings in clay/shale were considered to be relatively high (Hardin et al. 2012). A later study adopted in-drift emplacement instead of large-diameter emplacement boreholes, for DPC-based waste packages. This change increased by several-fold the length of emplacement drifts needed to dispose of all the commercial SNF projected to be produced in the U.S. (Hardin et al. 2013). This in turn raised questions of engineering feasibility: whether ~300 km of emplacement drifts could be efficiently constructed, then remain stable with little or no maintenance for at least 50 years, during which the waste packages would be ventilated. This section affirmatively answers these questions based on experience with similar tunnels in service for highways, railroads, and water conveyance for durations approaching 50 years or longer, in the U.S. and Europe.

**Clay/Shale Terminology** – The clay/shale terminology used in this report is intended to include a spectrum of rock types including plastic clay, claystone, mudstone, siltstone, argillites and shales. Hansen et al. (2010) provided working definitions for terms including detrital clay, clay minerals, claystone, siltstone, mudstone, shale, argillite, and argillaceous rock.

Clay/shale rock types considered for repository construction typically would be rich in clay minerals (mainly smectites and illites). Suitable clay/shale rock types may be collectively referred to as argillaceous, specifically addressing those rich in clay minerals (the term can also be used for very fine grain detrital rocks with lower clay mineral content). Hansen et al. (2010) described the ideal clay/shale host medium as fine grained, lightly indurated (too much induration will eliminate plasticity, e.g., as in slate), detrital sediment (weathering products deposited in water) with approximately 50% or greater clay mineral content and low permeability (on the order of  $10^{-19}$  to  $10^{-16}$  m<sup>2</sup>).

**Repository Depth** – The typical depth for a repository in clay/shale media would be 300 to 900 m (Shurr 1977). A shallower repository might be considered to accommodate local stratigraphy, or to simplify construction if the desired characteristics of stability and waste isolation can be achieved. For example, the plastic Boom Clay is a candidate host medium for construction of a repository at a depth of approximately 250 m (ONDRAF/NIRAS 2001). Were it to occur at much greater depths, excavations in this clay could be significantly less stable.

**Groundwater Effects** – Clay/shale media are hydrologically saturated, in that all interstices (macropores, nanopores and inter-layer spaces) are fully occupied by water, but much of the water apparently does not behave as mobile, free water. There currently is scientific debate about the importance of coupling between rock framework stress and pore pressure, at least in some clay/shale media (Appendix A). Clay minerals are water sensitive, and loss of water can be destabilizing, but low permeability media may be very slow to produce groundwater into excavated openings. For excavation and ground support this means that pore pressure coupling varies widely for different media, and water inflow and hydraulic loading are secondary concerns for time scales on the order of years. Whereas water inflow is observed in a few boreholes at the Bure underground research laboratory (URL) and the Mont Terri URL, these are isolated

occurrences representing channelized flow that can have only local impact on repository construction and operation.

The following discussion begins with brief description of excavation methods (drill-and-blast, road headers, and TBMs) and ground support systems (metallic liners, shotcrete, steel sets, rock bolts, cast-in-place concrete, and segmented pre-fabricated concrete) that have been used in clay/shale media. It then describes processes specific to clay/shale geologic settings that are important to long-term tunnel stability and maintenance (response to excavation, shrinkage/swelling, squeezing, ground support interactions, creep, fault deformations, effects from groundwater). This is followed by selected case studies of tunnels in Switzerland, France, Germany, and the U.S. Finally, the discussion and summary section includes a construction/operation scenario description for a repository in an idealized clay/shale medium, for large, heavy DPC-based waste packages.

## **2.1 Discussion of Excavation and Liner Types**

### **2.1.1 Excavation Methods**

Tunnel boring machines (TBMs) are favored for extensive excavation (hundreds of kilometers) because of speed, cost, and minimal rock damage. Modern TBMs have advanced significantly in the past 20 years, including cutters designed for specific rock types, pressurized face machines, improved shields and integrated ground support for soft rock, improvements in waste rock handling, better control and steering, etc. TBMs have also grown larger with 10-m diameter now common, and highway tunnels up to 15 meters across excavated in a single pass. The diameter of openings in a repository could vary from 4.5 to 7 m for emplacement drifts, to 10 m or larger for access drifts, ramps, etc. (Hardin and Voegelé 2013).

The different types of TBMs can be characterized as single-shield or double-shield, with or without grippers, and open- or pressurized-face designs. The open designs (Figure 2-1) have no excavation chamber or pressure bulkhead, and they remove waste rock directly by scooping it onto a conveyor, without slurry. They are used in competent rock with sufficient strength for the excavation face to stand indefinitely without support. Open TBMs may be single- or double-shield designs, with or without hydraulic grippers. Shields stabilize the opening and can serve as anchors propelling the TBM forward. The single-shield and/or gripper configurations advance either by pushing against a liner that is erected immediately behind the machine, or pushing against grippers set against the wall rock. Double-shield TBMs typically advance by two-anchor (inchworm) locomotion, but may also have grippers for simpler operation in hard rock.

Pressurized face machines are used for soft rock, and are either of the slurry shield (SS) or earth-pressure balance (EPB) type. Pressurized-face machines have a pressure bulkhead behind the cutter head, defining an excavation chamber ahead in which the rock is fully exposed. A substantial shield presses against the full circumference of the wall behind this bulkhead, and may also seal against the outer surface of the installed liner behind the shield, to limit groundwater inflow. EPB and SS machines may have single or double shields, and other dual-mode features that support use of a single machine for tunneling in variable ground conditions.



Figure 2-1. Open-type double-shield TBM with trailing gear, during assembly, Yucca Mountain, Nevada (diameter 7.6 m)

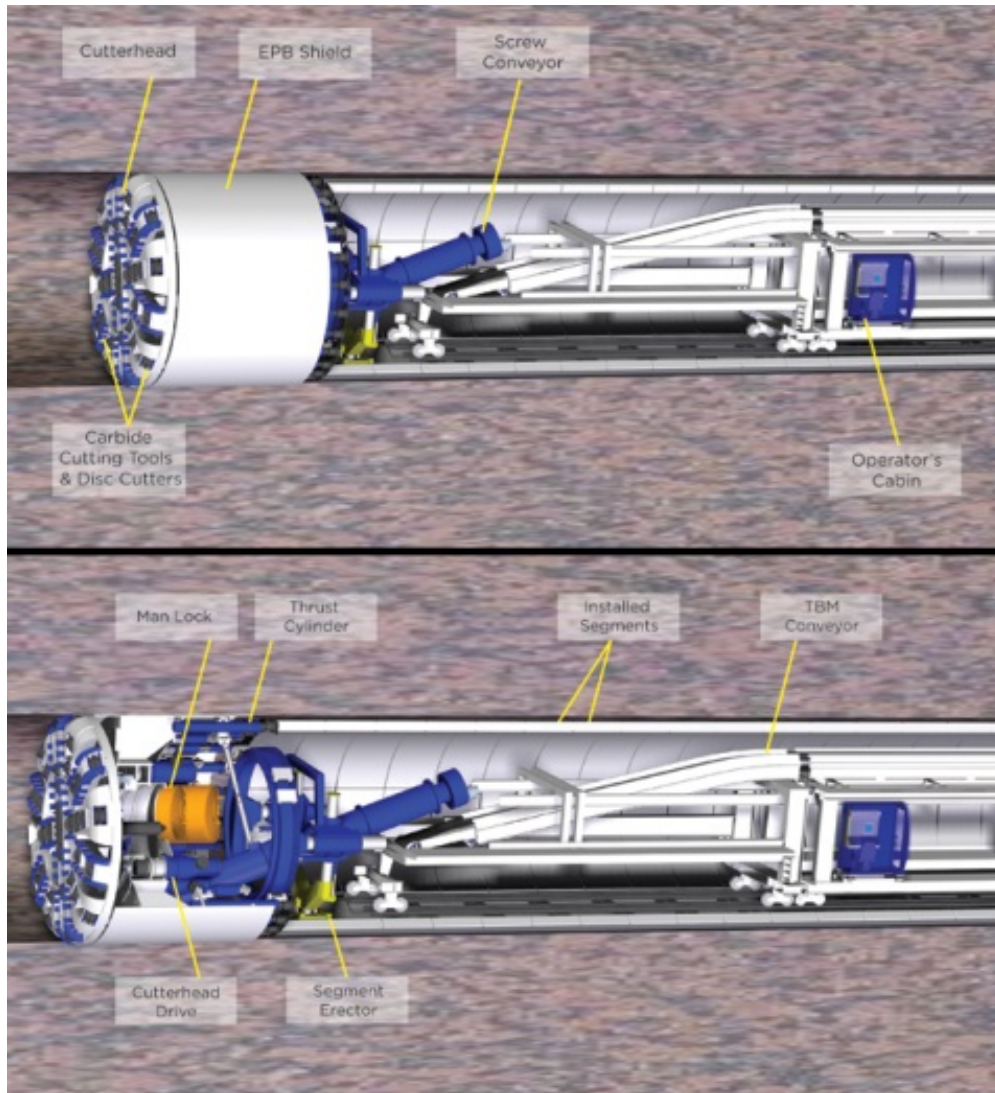


Figure 2-2. Schematics of an EPB tunnel boring machine showing shield, segmented liner, muck removal system, and other features

In a slurry shield design, a clay slurry is injected at pressure into the excavation chamber and removed with the cuttings via a pipeline. Slurry plants at the surface separate cuttings material and recycle the slurry.

Earth-pressure balanced machines (Figure 2-2) are especially effective in shallow settings where the host medium is unconsolidated, or excessive plastic deformation is encountered. They create a clay-bearing muck from the excavated material, and remove it by a screw conveyor which also controls the pressure. Additives such as clay slurry may also be injected into the excavation chamber. EPB machines minimize deformation but are limited to pressures up to approximately 1 MPa. Limits on excavation chamber pressures could preclude their use at repository depths (300 to 900 m). Concerns with EPB machines at higher pressures are: 1) pushing the TBM forward against the chamber pressure; and 2) the excessive air pressure to which workers would be exposed when they enter the excavation chamber for maintenance.

If very soft ground conditions were encountered in repository construction, the less efficient but accepted practice of pre-excitation grouting in boreholes drilled ahead of the excavation face would likely be used, possibly with an open-face TBM. Pre-excitation grouting may be planned in advance based on mechanical and hydraulic testing in exploration boreholes. Repository excavation could be much simpler if the excavation face is self-supporting during drilling, grouting, and maintenance activities. This requires rock compressive strength on the order of 7 to 10 MPa (overburden plus water pressure) depending on excavation depth and *in situ* stress conditions. Such strength is available in clay/shale media except for soft, plastic clay (e.g., the Boom Clay; see Table 2-2).

TBM trailing or “backup” gear consists of equipment linked to the boring machine, arranged on deck structures that typically roll on temporary rails. This equipment may serve the functions of muck handling or pumping, liner segment handling and installation, liner grouting, installation of the invert and rail, installation of electrical power and lighting, and dust control. Trailing gear may extend for 100 m or further behind the face. TBMs can advance up or down at grades of 5% or greater, but use of conventional rail for trailing gear limits grades to approximately 3%.

Waste rock from open TBMs is typically removed on belt conveyors. These are staged for conveyance all the way to the surface especially if ramp access is available. Conveyor belts are configurable for curves and ramps, and are also available for vertical transport in shafts. Shaft conveyors are typically used in shallower applications (less than 300 m) but could be staged to handle greater depths.

Repository drift layouts can be designed for TBM excavation by using appropriate turn radii at intersections (“turnouts”). Examples of proposed TBM layouts for different repository concepts are given by Hardin et al. (2012). The goals of layout design are to limit any need for disassembly and relocation of the TBM and trailing gear, either for maintenance or by design. Instead, optimized layouts have loops that allow the TBM to break through to a previously excavated opening, and to move forward to the location of the next heading to be mined.

This is a brief summary of excavation technologies with emphasis on major types of TBMs. Much more information can be obtained from TBM contractor-vendors, tunneling journals (e.g., *Tunnelling and Underground Space Technology*) and manuals developed by agencies and industry associations (see Section 2.4).

So-called roadheaders constitute another class of smaller, more flexible mining machines. They consist of cutting wheels or bits, faced with hard teeth (e.g., tungsten carbide) spun at the end of a boom. The boom is mounted to a heavy truck and is swept vertically and horizontally across the excavation face. Rubble accumulates below the cutting face until there is enough to remove with front-loading equipment (which requires moving the roadheader out of the way). Roadheaders would likely be used in any repository for alcoves and platforms, TBM launch chambers, small rooms, etc., even if the most tunneling were done with TBMs.

Finally, blasting methods were used for early industrial-age tunnels in clay/shale media, some of which are still in service, but they are not a practical solution for extensive excavation. The reasons include speed, cost, rock damage, and worker safety. Drill-and-blast methods are typically used in hard-rock especially where the volume to be excavated is too small, or opening shape too complex, to justify mechanized mining.

### 2.1.2 Liner Types and Degradation Modes

Liner longevity is a key issue in long-term performance or repository drifts in clay/shale media. Liner materials and dimensions must be selected to bear the applied loads for at least 50 years in the operational repository environment (oxidizing where accessible to air, and ranging from wet to dry at elevated temperatures up to 100°C). In clay/shale media that have the potential for swelling, the liner provides an isolation barrier to moisture movement. As discussed below, the liner may be applied in stages over several months for isolation and confinement during initial deformation, then for long-term performance.

The earliest liners for tunnels in clay/shale media were masonry, typically for rail and canal tunnels. Minimal mechanization was required for construction, and repair or rework was straightforward. However, construction was slow and thicker masonry was needed as opening spans increased. Other methods and materials were eventually adopted, but it is interesting to note that many older masonry-supported tunnels are still open in the U.S. and elsewhere, in shale and other soft sedimentary media. Many older tunnels are located in Pennsylvania and other mountainous areas of the Eastern U.S. (e.g., Staple Bend and Big Savage; NPS 2007).

The design lifetimes of modern liner systems may range from a few years for underground exploration and research, to more than 50 years for highway, railway and water conveyance projects. The range of design solutions varies accordingly, and includes the following:

- **Shotcrete** – Generally Portland cement mixed with sand, with water introduced at the spray nozzle. Plasticizers are used to decrease the water:cement ratio and thus increase strength. Glass or metal fibers may also be introduced for reinforcement. Often used over a layer of wire mesh or fabric bolted to the rock surface. Layers of 5 to 10 cm thickness are typically applied, and may be repeated to achieve 30 to 50 cm total thickness.

A wide variety of shotcrete materials and reinforcing fibers, with ranges of strength, adhesion, mechanical resistance, etc., and applied at different thicknesses for various applications, is reported in the literature (Franzen et al. 2001). It is possible that repository construction would make extensive use of shotcrete because of its low cost compared to steel and cast-in-place forming. Shotcrete could also be significantly cheaper than pre-fabricated liner segments, and suitable if greater strength is not needed.

- **Steel or cast iron** – Used for immediate ground support in potentially unstable (e.g., squeezing) ground. For small openings pipe or tubing may be used, while for larger openings the liner may be assembled in segments bolted together. Used for initial construction at the underground laboratory in the Boom Clay at Mol (ONDRAF/NIRAS 2001; later construction used pre-fabricated concrete segments).
- **Steel ribs or sets** – Often used for extra support of weaker sections. Steel ribs are blocked against the wall and roof using shotcrete, steel, wood, etc. Lagging consisting of wood or steel panels may be laid between steel arches, which are typically flanged. Ribs may be bolted to the walls for additional support, particularly at the tunnel springline (mid-height). Backfilling with additional lagging or shotcrete can be used to fill gaps between support elements and host rock. Steel ribs can be fully circumferential, or partially circumferential and anchored in concrete or steel invert elements. Ribs may be used in conjunction with wire fabric, with shotcrete applied between ribs (e.g., for the underground research laboratory at Bure). They may be used with lattice girders to

support larger spans at intersections, and may also be used with cast-in-place concrete to provide initial support that is later encapsulated (e.g., for the Azotea Tunnel).

- **Segmented pre-fabricated concrete** - This support method is commonly used for TBM-excavated tunnels. Liner segments may be 1 to 2 m high (circumferential), 2 to 3 m long (axial), and 0.3 to 0.75 m in thickness (radial). They generally contain reinforcing steel in some form, and may be fabricated from very high strength concrete (e.g., 70 MPa or greater). Segments may have hollow form or uniform thickness. Their shape and size are amenable to automated handling and installation. A ring of segments may be completed using a wedge segment that can be expanded to generate arch loading. Segmented liners are typically backfilled with grout by pumping through ports in the segments. The grout may be compliant (e.g., with aggregate of plastic beads or foam particles) to accommodate large, localized deformations of the rock wall while maintaining compressive loading in the liner.
- **Cast-in-place concrete** – Unreinforced concrete was used extensively in 20<sup>th</sup> century tunneling, and is still commonly used for shafts. Design thickness of the concrete may range from 0.2 to 0.75 m depending on rock characteristics and *in situ* stresses. Cast-in-place concrete is relatively expensive because of the costs of form setup, mixing or transporting uncured concrete underground, and delay of construction during initial cure.

Assuming that liner elements are correctly specified to meet short- and long-term loading conditions, and that the liner is sufficiently impervious to prevent shrinkage or swelling of the host medium, then maintenance issues could be limited to degradation of liner materials. Concrete can have a lifetime of 50 years especially if unreinforced (e.g., San-Juan Chama Project tunnels) while performance of shotcrete in thinner layers depends on stability of the underlying rock, and bonding strength (see discussion of the Mont Terri URL tunnels).

### 2.1.3 Host Rock Response to Excavation

The initial response to excavation is redistribution of stress from the excavated volume into the surrounding medium. This concentrates stress near the walls, roof and floor of the opening. Whereas the initial *in situ* stress condition in clay/shale media may be nearly lithostatic, the immediate stress condition adjacent to mined openings is strongly deviatoric (i.e., large stress differences depending on direction). Deviatoric stresses can produce large deformations, dilatancy and fracturing especially in media with low strength compared to the overburden stress. For example, a soft shale unit with unconfined compressive strength of 5 MPa will undergo these effects when excavated at a depth of 300 m (7 MPa overburden stress). Strength increases with confinement, which occurs with increasing distance from the opening and after liner installation.

Much of the immediate deformation associated with excavation occurs in the region ahead of, or close to the active excavation face. Thus, stress redistribution is inherently three-dimensional and produces three dimensional deformation features, where concentrated stress magnitudes exceed strength criteria. Fractures form along surfaces of low normal stress and high shear, and parallel arrays of *en echelon* fractures form near the face as the tunnel is excavated. These excavation-induced fractures may be evident as “chevron-like” shear fractures where they intercept the roof or walls of the tunnel (Delay et al. 2010). In laminar, anisotropic media these processes interact with pre-existing planes of weakness. The resulting fractures that form near the working face determine the extent of the excavation damage zone (EDZ) around every underground opening.

Clay-rich media can be sensitive to moistening or drying which causes swelling and shrinkage, respectively. This potentially destabilizing behavior has been understood for many years in soft-rock mining (“slaking”). It can be serious when ground water flows into mined openings and interacts with exposed rock surfaces. Equivalent behavior may also occur with exposure to changes in humidity. Formation of shrinkage cracks during the winter, and closure of the cracks when humidity increases in summer, has been observed and monitored at the Tournemiere URL (Appendix A). In repository drifts heated by SNF waste, severe drying conditions will occur which could produce penetrating shrinkage cracks that destabilize exposed surfaces of the host rock. Also, repeated shrinkage and swelling due to fluctuations in ventilation conditions could cause fatigue. Therefore, an important function of the liner in clay/shale media is to isolate the host rock from open air spaces, especially heated and/or ventilated spaces.

Squeezing behavior is progressive deformation that starts immediately after excavation and can produce large opening closure within days to months. Squeezing depends on rock composition and fabric, and stress conditions. Where it occurs, it commonly causes invert heave (Hung et al. 2009, Sections 8.2.5 and 8.3.4). Squeezing is rate-limited and a form of creep. In mining applications it may be ignored if it does not interfere with the completion of extractive activities. In repository applications squeezing is potentially beneficial as it could eventually close and re-seal repository openings. However, it must be controlled during excavation, construction, and preclosure repository operations. One approach to managing squeezing ground and creep is to use yielding supports, designed to crush or collapse while providing constant support (Hung et al. 2009, Section 8.3.3; also see Section 3). Squeezing and creep may also be controlled by installing a liner robust enough to assume enough of the deviatoric loading in the host rock, to slow or stop the deformation. This process is illustrated by calculations for the Pierre Shale (Figures 2-3 and 2-4) which show how deviatoric stress around a circular opening could relax over 10 to 20 years, as creep occurs and load is transferred to a robust liner of high-strength concrete (Nopola 2013).

Ground water can impact opening stability by causing water inflow, and by hydraulic loading of the liner. In potential clay/shale host media these processes are not expected to be important because: 1) although the host rock may be nominally saturated, bulk permeability will be low; and 2) water-bearing faults can be sealed by grouting or other means, and isolated from repository openings. Ground water could be important in excavations that must penetrate non-host stratigraphic units such as aquifers that overly the host rock. However, the measures needed to mitigate such an occurrence would be site specific, and are beyond the scope of this review.

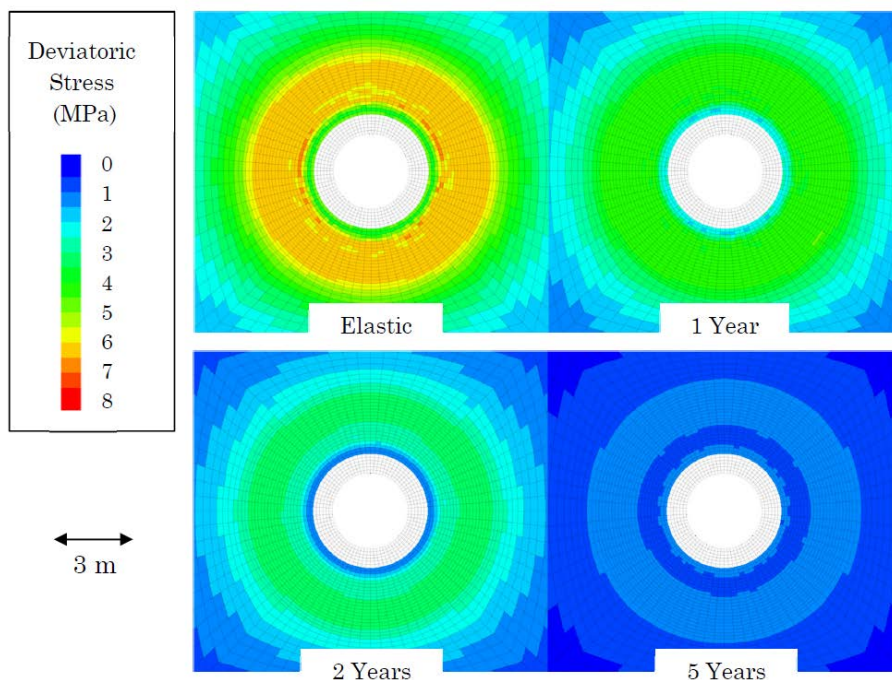


Figure 2-3. Viscoplastic solution to stress distribution in the Pierre Shale, around a 3-m (finished) diameter circular tunnel at 700 m depth, showing load transfer to a 0.75-m thick concrete liner (with permission, Figure 4-12 from Nopola 2013)

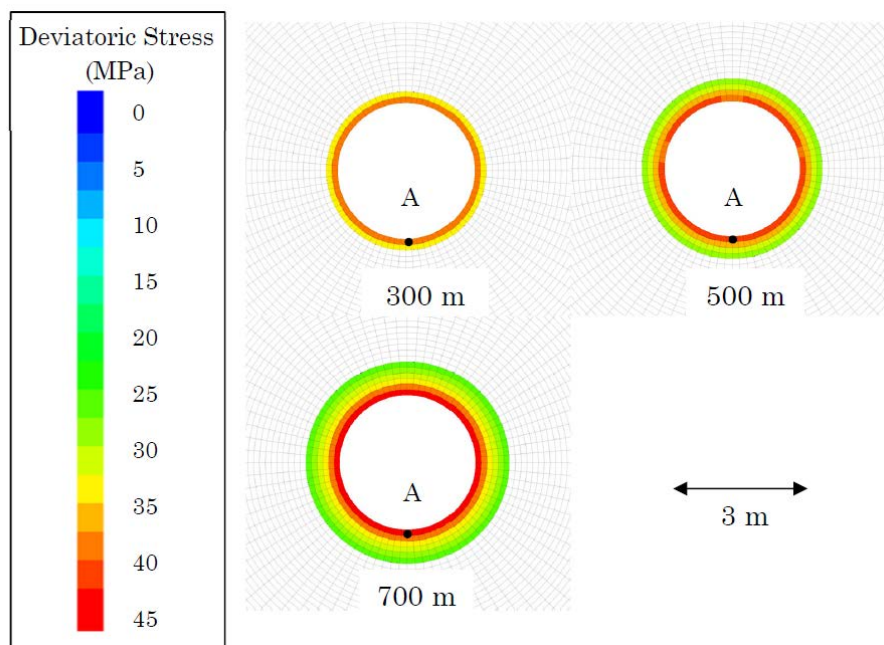


Figure 2-4. Concrete liner stress after 20 years of load transfer, for a 3-m (finished) diameter tunnel in the Pierre Shale, at the depths indicated (liner thicknesses of 0.25, 0.50 and 0.75 m; with permission, Figure 4-8 from Nopola 2013)

Most sedimentary basins contain faults, which may be active or remnants of previous tectonic or glacial activity. Fault zones are fractured, sheared, chemically altered, and may be pathways for groundwater flow. Faults that offset the host rock strata may cause mixed geologic conditions at the excavation face, which complicates mining and construction. In general, repository tunnels could intercept faults with unfavorable geometry (e.g., with parallel strike, or hanging blocks in the walls or roof). Faults are routinely intercepted by tunnels such as those described in the case studies below, so moderate faulting is not an acute concern for repository construction. Pre-excavation borehole grouting is commonly used to remediate faulted ground for tunneling. However, fault characterization is needed and the repository layout and concept of operations should accommodate fault characteristics. To support this goal a minor fault (“Main Fault”) at the Mont Terri URL is being investigated by the PS-Experiment and the planned water injection characterization experiment (Appendix A).

#### **2.1.4 Rail and Highway Tunnel Design Guidelines**

Compendia describing technologies for underground tunneling and construction are available from government and other sources. A recent contribution is the Federal Highway Administration’s *Design and Construction Manual for Road Tunnels* (Hung et al. 2009). This manual summarizes conceptual cost analysis, groundwater control, maximum grades, and geotechnical investigations. It provides a guide to TBM selection, and describes ground support options for adverse rock conditions, seismic design, geotechnical instrumentation, and project management methods.

#### **2.2 Selected Case Studies**

The bulk of this section is devoted to case studies of modern, large-scale tunneling projects in clay/shale media, including some with overburden depth in the range 300 to 900 m. Additional case studies from other media have been compiled (Hardin 2014), including large and/or famous projects that provide context for discussion of engineering feasibility and costs. Metrics for this larger set are summarized in Table 2-1.

Tunneling activities in the Opalinus Clay, Callovo-Oxfordian argillite, Boom Clay, and the Pierre Shale are of special interest because these formations are being studied as potential repository host media, or have been in the past. These rock types were described by Hansen et al. (2010) and a summary of properties is provided in Table 2-2.

Table 2-1. Comparison metrics for tunneling projects discussed in this report

| Project <sup>A</sup>                           | Country        | Lithology                              | Depth (m) | Excavation Method           | Ground Support  | Diameter (m) | Length (km) | Cost           | Escalated Cost/meter <sup>B</sup> |
|--|----------------|--|-----------|-----------------------------|---|--------------|-------------|----------------|-----------------------------------|
| <b>St. Martin La Porte access adit</b>         | France         | Various (Carboniferous)                | <2,500    | Drill/blast and road header | Rock bolts+steel ribs+shotcrete+deformable elements           | 6 to 9       | 2.3         | NA             | NA                                |
| <b>Channel Tunnel</b>                          | France-Britain | Chalk                                  | ≤100      | TBM                         | Pre-fab. segmented concrete liner                             | 5.3 to 8.3   | 50 (×3)     | \$7B (1988)    | \$100k                            |
| <b>SJCP Azotea Tunnel – New Mexico</b>         | USA            | Mancos & Lewis Shales/ other sediments | ≤488      | TBM                         | Rock bolts+steel ribs+cast-in-place concrete liner            | 4.3          | 20.6        | \$17.1M (1989) | \$1.7k                            |
| <b>SJCP Blanco Tunnel – New Mexico</b>         | USA            | Lewis Shale                            | ≤600      | TBM                         | Rock bolts+steel ribs+cast-in-place concrete liner            | 3.1          | 13.9        | \$9.8M (1989)  | \$1.5k                            |
| <b>SJCP Oso Tunnel – New Mexico</b>            | USA            | Shale/glacial debris                   | ≤232      | TBM                         | Rock bolts+cast-in-place concrete liner                       | 3.1          | 8.1         | \$5.8M (1989)  | \$1.5k                            |
| <b>Phase 1 TARP – Chicago</b>                  | USA            | Niagara Dolomite                       | <100      | TBM                         | Rock bolts+cast-in-place concrete liner                       | 10.8         | 176         | \$4B (2006)    | \$29k                             |
| <b>Euclid Creek Storage Tunnel – Cleveland</b> | USA            | Chagrin Shale                          | ~60       | TBM                         | Pre-fab. segmented reinforced concrete liner                  | 8.2          | 5.5         | \$200M (2014)  | \$36k                             |
| <b>Mill Creek Phase 2 – Cleveland</b>          | USA            | Chagrin Shale                          | 49 to 79  | TBM                         | Steel ribs+lagging+cast-in-place concrete liner               | 6            | 4           | \$57M (1999)   | \$22k                             |
| <b>Mill Creek Phase 3 – Cleveland</b>          | USA            | Chagrin Shale                          | 63 to 93  | TBM                         | Steel ribs+lagging+cast-in-place concrete liner               | 6            | 4           | \$73M (2002)   | \$26k                             |
| <b>Oahe Dam tunnels – South Dakota</b>         | USA            | Pierre Shale                           | ~100      | TBM                         | Pre-fab. segmented concrete liner                             | 9            | 14 (total)  | NA             | NA                                |
| <b>Flathead Tunnel – Montana</b>               | USA            | Quartzite/argillite                    | ≤200      | Drill/blast                 | Steel ribs+lagging  | ~7           | 11.3        | \$37.9M (1969) | \$13k                             |
| <b>Niagara Tunnel #3 – Ontario</b>             | Canada         | Queenston Shale                        | ≤140      | TBM                         | Rock bolts+wire fabric+shotcrete+cast-in-place concrete liner | 14.4         | 10.4        | \$3.4B (1999)  | \$500k                            |
| <b>Park River Tunnel – Connecticut</b>         | USA            | Shale/sandstone                        | 60        | TBM                         | Pre-fab. segmented concrete liner                             | ~7           | 2.8         | \$23.3M (1978) | \$24k                             |
| <b>Plateau Creek Tunnels – Colorado</b>        | USA            | Sandstone/shale/ siltstone             | ?         | TBM                         | Rock bolts+wire fabric+shotcrete                              | 3.3          | 4.1         | \$14.1M (2001) | \$5k                              |

Notes: <sup>A</sup> For sources see references in text of Section 3. <sup>B</sup> Escalation factor 3% per year to 2014.

Table 2-2. Properties of well-characterized clay/shale media (after Hansen et al. 2010)

| Shale Formation             | Reference Location | Approximate Geologic Age (Ma) | Typical Thickness (m) | Top Burial Depth Present/Past (m) | Clay Content (wt. %) | Classification <sup>A</sup> | Mineralogy <sup>B</sup>            | Carbonate Content (wt. %) | Hydraulic Conductivity (m/sec)                  | Compressive Strength <sup>C</sup> (MPa) | Organic Content (wt. %) | <i>In situ</i> Water Content (vol. %) |
|-----------------------------|--------------------|-------------------------------|-----------------------|-----------------------------------|----------------------|-----------------------------|------------------------------------|---------------------------|---|---|-------------------------|---------------------------------------|
| <b>Europe:</b>              |                    |                               |                       |                                   |                      |                             |                                    |                           |   |   |                         |                                       |
| Opalinus Clay               | Mont Terri, CH     | 180                           | 160                   | 250/1350                          | 50 to 65             | Claystone                   | Kaolinite, illite, illite/smectite | 10 to 50                  | Est. $5 \times 10^{-13}$ to $6 \times 10^{-14}$ | 12                                      | 0.5                     | 4 to 6                                |
| Callovo-Oxfordian Argillite | Bure, France       | 155                           | 130                   | 400/NA                            | 45                   | Mudstone                    | Illite/smectite                    | 20 to 30                  | Est. $3 \times 10^{-14}$                        | 25                                      | < 3                     | 5 to 8                                |
| Boom Clay                   | Mol, Belgium       | 30                            | 100                   | 220/NA                            | 55                   | Bedded mud                  | Smectite/illite                    | 1 to 5                    | Est. $6 \times 10^{-12}$                        | 2                                       | 1 to 5                  | 22 to 27                              |
| <b>North America:</b>       |                    |                               |                       |                                   |                      |                             |                                    |                           |   |   |                         |                                       |
| Pierre Shale                | Pierre, SD         | 70                            | 400                   | 150/NA                            | 50                   | Mudstone                    | Illite/smectite                    | 0 to 50                   | $10^{-13}$ to $10^{-14.6}$                      | 7                                       | 0.5 to 13               | ~16 (variable)                        |

Sources: ANDRA (2005); Hansen and Vogt (1987); NAGRA (2002); OECD/NEA (2003); Neuzil (2000); Volckaert et al. (2005).

Notes: <sup>A</sup> Use clay-mud-claystone-mudstone-argillite classification from OECD/NEA (1996, p. 4). <sup>B</sup> Predominant assemblage or combination: smectite, illite, kaolinite, chlorite, carbonate, etc. <sup>C</sup> Unconfined, typical laboratory values for fresh samples. NA = not applicable (past burial depth not significant).

### 2.2.1 Switzerland

Highway and rail tunnels are especially abundant in Switzerland because of the populated mountainous terrain, and the practice of high technology. The construction of long, deep rail tunnels began in the mid-1800's (as in the U.S.) and some of these tunnels have been in service for more than 100 years. A summary of early Swiss tunnels in the Opalinus Clay is provided by Einstein (2000). The focus of the present review is modern, TBM-excavated rail and highway tunnels in the Jura region of northwestern Switzerland, and the Mont Terri URL in the Opalinus Clay.

Tunnels in the mountainous Folded Jura tend to be deep, with clay/shale excavation at depths of 300 m or more. In the flat-lying Tabular Jura to the northwest there are far fewer existing tunnels, but this is an area being considered for siting of a repository in the Opalinus at a depth of roughly 800 m. Construction of stable openings in clay/shale media at this depth is an important technical issue for the Swiss repository program. A Swiss national symposium on tunneling in claystone was held on February 14, 2014 at the Swiss Federal Institute of Technology (ETH). A summary of presentations given at that event is included as Appendix A.

**Highway and Rail Tunnels in Northwestern Switzerland** – Early-modern tunneling methods in Switzerland were distinguished by use of movable excavation shields to stabilize the rock before liner installation (Appendix A). The earliest methods used drill-and-blast excavation with a shield, and a segmented liner (e.g., pre-fabricated concrete or cast-iron). For example, the Baregg Tunnel (A1 motorway, tubes 1 and 2) completed in 1970, was constructed by drill-and-blast with a horseshoe-shaped shield. Non-circular shields were found to be unworkable because they have a tendency to roll and cannot be readily corrected or steered.

The Heitersberg Tunnel (single-track rail) was constructed in 1970 using a Robbins open-face TBM (10.8 m diameter). Ground support consisted of an outer liner of shotcrete sprayed by a robot attached to the TBM, with wire fabric and rock bolts, and steel supports where needed (24% of total length). The Gubrist Tunnel (motorway tubes 1 and 2), completed in 1985, was excavated using a similar arrangement and the same shield, and the liner was mated with the shield to improve the stability of the interval between them. The Rosenberg Tunnel, another early-modern highway tunnel, was excavated using a shield with four road headers.

Soft-rock tunneling in Switzerland advanced after the 1970's, accelerated by extensive and rapid tunneling using TBMs, for the A16 and other motorway routes (Appendix A). For example, the Mont Russelin highway tunnel completed in 1998 is 3.5 km long, with more than 300 m of maximum overburden. The Bözberg twin tubes (A3 motorway) were completed in 1994, and are 4.3 km long with more than 200 m maximum overburden. The Adler rail tunnel was completed in 2000, is 5.2 km long, and was excavated to a diameter of 12.5 m (then a TBM record). The Bure highway tunnel was completed in 2011, is 3.1 km long, and has a diameter of 12.6 m. The Mont Terri highway tunnel was completed in 1998, is 4 km long, and replaced the tunnel now used to access the Mont Terri URL.

Tunneling in the Opalinus Clay has achieved good results with single-shield TBMs, with a continuous segmented liner installed immediately to prevent swelling. Stability problems close to the face may be encountered, especially in fault zones, and where there is strong water inflow. Rock instability in the crown can be mitigated by installing deformable filler material (e.g., pea gravel) behind or above the segmented liner, while support can be increased by injecting grout

into the filler (30% to 50% porosity). With application of these methods since the 1970's, advance rates have improved and excavated opening diameters have increased.

Einstein (2000) described a series of experimental and analytical studies sponsored in the 1990's by the Swiss Federal Office for Road Construction, and the Swiss Federal Railroads. These studies comprised laboratory measurements to support constitutive models for anisotropic, elastoplastic deformation with poroelastic coupling. From these results a general prescription for stable tunnel design in the Opalinus emerged (from Einstein 2000):

- Circular tunnel with circular liner of uniform thickness;
- TBM or other mechanized excavation methods, to minimize rock damage and produce smooth-wall openings;
- Initial liner consisting of pre-fabricated, high-strength concrete segments, produced and installed with high quality control;
- Protection of the tunnel invert by liner installation at a relatively short distance behind the face, so that construction water and groundwater inflow do not contact exposed rock; and
- The final liner (grout-backfilled segments, possibly with cast-in-place concrete inner liner) is watertight.

Analyses showed that immediate installation of support causes the greatest tangential normal stress in the liner but that delayed liner installation decreases support loads by more than half (Einstein 2000). The study found that significant anisotropy of the Opalinus should be factored into support design, analysis and testing. Higher permeability allows more drainage after excavation, which increases the magnitude of deformations during the delay before liner installation. Conversely, lower permeability can increase support loads significantly. Analysis showed that unsupported Opalinus Clay may fail as it is being excavated, as excavation stress paths tend to approach modeled strength limits.

Another survey (Appendix A) identified four excavations from which tunneling experience in clay/shale media can be drawn: the historic Grenchenberg tunnel in Switzerland, the Mont Terri URL, excavations at the Konrad repository in Germany, and the Bure URL. Survey of Swiss tunnels would not be complete without mention of the Gotthard Base Tunnel, currently in the final stages of construction. The project consists of twin single-track rail tunnels, with excavated diameter of 8.8 to 9.5 m, and 57 km long, making it the longest in the world (AlpTransit 2010). The tunnel is constructed in metamorphic and igneous rock, and the overburden depth varies up to 2,500 m, with nearly 100% of the tunnel under at least 1,000 m. Drill-and-blast methods were used for approximately 44% of the excavation, while open gripper-type TBMs were used for the other 56%. Tunneling began in 2003 and was completed in 2011. The greatest difficulty, and the reason for so much conventional drill-and-blast excavation, was highly stressed squeezing ground encountered along several sections. Also, strong water inflow in certain sections required extensive borehole grouting (Ehrbar 2008). A similar twin-tunnel project is under construction in Italy, called the Ceneri Tunnel, which will link with the Gotthard line to extend from Zurich to Milan.

**Mont Terri** – The Mont Terri tunnels are designed for R&D, with a lifetime on the order of 20 years with only local repairs needed (Appendix A). Immediately after excavation a thin layer (5 cm) of shotcrete is applied to prevent slaking. All shotcrete is formulated for early strength and low pH (balanced portlandite, excess soluble silica, and super-plasticizer). Wire fabric (e.g., coarse “welded wire cloth”) is then installed with short bolts. Long rock bolts may then be

installed for larger openings, or where dictated by performance requirements (e.g., to minimize maintenance in certain parts of the URL). Rock bolt length is typically 100% to 150% of opening diameter, and they are installed using a full 270° pattern. Bolts may be metal or fiberglass, and may use point anchors or full grouting. Alternatively, steel sets have been installed for additional support at some locations.

After a delay of several months to allow convergence, a final layer of shotcrete is applied (15 cm). As much as 5% convergence has been observed where stress is concentrated by nearby excavations (e.g., the “FE” test alcove). The floor is shotcreted from wall to wall, and the surface of the shotcrete is worked to provide a running surface for water. Drift convergence tends to continue until the floor is shotcreted. Rock damage at Mont Terri is dominated by bedding-induced breakouts. Stress-induced breakouts are uncommon at the 250 to 400 m overburden depth. The EDZ at Mont Terri typically exhibits characteristic *en echelon* fractures (“plumose hackles” of Martin and Lanyon 2002) and the mechanism may be related to pore pressure excursions. Hydraulic conductivity of the EDZ at Mont Terri is on the order of  $10^{-8}$  m/sec, and gradual decrease is observed. For a deeper repository in the Opalinus (e.g., up to 800 m) the intensity and extent of the EDZ could be significantly greater.

### **2.2.2 Germany - Konrad**

The Konrad repository is under construction at a former iron mine in central Germany, and is expected by 2019 to begin accepting nominally non-heat generating wastes from medical and research sites, power plant operations and decommissioning, and nuclear fuel cycle activities. The construction at Konrad is included in this review because supporting underground facilities are being constructed in the Lower Cretaceous clay/shale layer that provides hydrogeologic isolation to the host rock below. The repository depth is approximately 1,000 m, and openings in the clay are being constructed just above.

Repository service openings in the clay/shale layer will have design life of 50 years with minimal maintenance. Excavation is being performed using road headers, starting with a top heading then cutting the floors deeper in successive passes, so that roof support and overhead services such as lighting can be installed first. Initial ground support consists of welded wire fabric bolted to the rock, then 8 to 10 cm of shotcrete applied using masks to produce linear gaps in the shotcrete every few meters (Figure 2-5). This is followed by long rock bolts of (up to 18 m length, fully grouted, and 50 to 70 cm apart). The initial shotcrete forms yielding supports, and the openings (8 m span) are expected to close 30 cm in six months. After that time the closure rate will slow down, and the ground support will be completed with 30 to 50 cm additional shotcrete.

### **2.2.3 France**

Eastern France shares much of the same geologic history as northwestern Switzerland, including the occurrence of sedimentary basins of Mesozoic age containing thick argillaceous intervals. The following examples include the URL at Bure, where conditions for the Cigéo repository project are being evaluated, and two modern large-scale rail tunnel projects.



Figure 2-5. Yielding initial support (wire fabric, shotcrete and long rock bolts) just after installation in the Lower Cretaceous clay at the Konrad repository site (depth ~1,000 m)

**Bure Underground Research Laboratory** – Design of tunnels for the Cigéo repository will be similar to the URL at Bure. The French repository is required to facilitate retrieval for at least 100 years, which means operational areas must remain stable for up to 150 years (Appendix A). The disposal concept for HLW will emplace the glass-waste pour canisters directly into long, horizontal borings excavated using a remotely operated mini-boring machine, and lined with continuous steel casing.

Vault-type rooms for low- and intermediate-level waste will be 9 to 11 m wide and up to 400 m long (ANDRA 2005). Disposal rooms and access tunnels will likely be excavated using road headers because of the many different configurations planned, and limits on the scale of tunneling required. Several support options have been identified: 1) yielding support, with 3-m rock bolts and 8 cm of fiber-reinforced shotcrete; 2) resistant support, combining the yielding elements with an additional 27 cm of cast-in-place, unreinforced concrete; and 3) maximum support, combining the yielding elements with 45 cm of fiber-reinforced concrete applied in four layers. Access drifts designed for long-term service could also be supported in a manner similar to tunnels in the URL, which are lined with steel ribs and lagging, with shotcrete emplaced between the ribs.

**St. Martin La Porte Access Adit** – The Lyon-Turin Base Tunnel is a direct rail link crossing the Southern Alps between France and Italy. When completed, the main tunnels will be approximately 50 km long, with a maximum overburden depth of 2,500 m. Three adits are being driven to intersect the tunnel alignment, for access during construction and for services after the rail tunnel is put into operation. The Saint Martin La Porte access adit was begun in 2003 and completed in 2010, to a final length of 2.3 km. This project has provided important information on tunneling conditions which has been applied for the main tunnels. It is included here because the adit traverses a complex sedimentary geologic section where severe squeezing conditions were encountered, for which novel support methods were developed (Bonini and Barla 2012).

Construction started using stiff supports that included steel ribs and heavy shotcrete, which became overstressed and failed by cracking and buckling. Steel ribs with sliding joints were not effective because of uneven deformation. After about 1.5 km of tunneling, cracking of the shotcrete, failure of the steel ribs, overbreak, and large convergence (up to 2 m) forced construction to stop. A new staged, yielding support system was introduced (Bonini and Barla 2012). This system excavated the tunnel in three stages: 1) installation of grouted fiberglass rods around the tunnel perimeter ahead of the face; 2) mechanical excavation 1 m at a time, with installation of grouted bolts, yielding steel ribs, and 10 cm of shotcrete; and 3) about 30 m back from the face, the tunnel was widened to full size, with support consisting of yielding steel ribs and 20 cm of reinforced shotcrete, and slots cut in the shotcrete and filled with deformable elements (plastic foam aggregate concrete). Up to 60 cm of tunnel closure was accommodated by the initial support, and up to 40 cm after the final support installation. The most important features of this system are staged construction, and control of deformation and stress in the lining using deformable elements (Bonini and Barla 2012).

#### **2.2.4 United States**

For many years tunneling projects in the U.S. were dominated by the U.S. Bureau of Reclamation and the U.S. Army Corps of Engineers, performed for flood control, hydroelectric power, and water conveyance. Several examples are discussed below. More recently, extensive tunneling has been performed to control environmental damage from combined-sewer-overflow (CSO), and examples of these projects are also discussed. Some of these tunnels are shallow compared to a geologic repository, for example the penstock tunnels at Oahe, and the CSO control tunnels near Cleveland. The value of these examples is that they provide cost benchmarks and engineering solutions similar to what could be implemented for repository construction (Table 2-1).

**San Juan-Chama Project** – The San Juan–Chama Project (SJCP) is a series of channels, tunnels, diversion dams, storage dams, and reservoirs that conveys water from the San Juan River in southern Colorado, across the Continental Divide to Azotea Creek, and eventually to the Rio Grande River in northern New Mexico. The project was constructed by the U.S. Bureau of Reclamation in the 1960s and 1970s, and now provides much of the municipal water for the city of Albuquerque and smaller communities upstream along the Rio Grande River.

The SJCP features of interest are three water conveyance tunnels: the Blanco, Azotea, and Oso tunnels (Table 2-3). Each of these is circular in cross-section and lined with unreinforced concrete (USBR 1989). Test borings and geophysical surveys (surface and airborne) were performed during design. During construction, borehole grouting was often used for stabilization and to control groundwater inflow during construction. The SJCP tunnels were excavated mostly

with TBMs, with drill-and-blast excavation used for setup and contingencies (USBR 1989). Unconsolidated glacial deposits were difficult to mine through because of instability and water inflow, but were mitigated with steel ribs and timber lagging (Glaser 2010). Advance rates averaged roughly 1,000 meters per month, depending on rock type (Cannon 1967). Methane intrusion at potentially explosive concentration (1%) was encountered in the Azotea and Blanco tunnels.

Tunnel construction cost averaged less than \$1,000 per lineal meter, fully lined (1989 dollars). Importantly, these tunnels have already provided more than 40 years of service to a critical water supply mission, with little or no maintenance (K. Atwater/USBR, 2014 personal communication). The low maintenance needs may be partly because parts of the SJCP tunnel system are above the water table so that swelling due to moisture intrusion could be avoided during construction. However, cover depth exceeds typical water table depth in many tunnel sections, and significant water inflow (80 to 400 liters per minute) was observed in all three tunnels.

Table 2-3. Summary data for San Juan–Chama Project tunnels

| SJCP Tunnel   | Excavated Dia. (m) | Finished Dia. (m) | Length (km) | Max. Depth (m) | Complete (Cost 1989\$) | Geology/Remarks (USBR 1989)   |
|---------------|--------------------|-------------------|-------------|----------------|------------------------|---|
| <b>Azotea</b> | 4.3                | 3.3               | 20.6        | 488            | 1964-70<br>(\$17.1M)   | Mancos and Lewis Shales, sandstone, siltstone, glacial debris; numerous faults; steel ribs over 36% of length   |
| <b>Blanco</b> | 3.1                | 2.6               | 13.9        | 600            | 1965-69<br>(\$9.8M)    | Lewis Shale, sand, gravel; squeezing encountered; rock bolts; liner plate over 9% of length                     |
| <b>Oso</b>    | 3.1                | 2.6               | 8.1         | 232            | 1966-70<br>(\$5.8M)    | Shale, glacial debris, clay; ~100 m <sup>3</sup> raveling encountered; rock bolts; steel ribs over 3% of length |

**Euclid Creek Project** – The Euclid Creek Storage Tunnel (ECT) is a storage tunnel designed to protect Euclid Creek and Lake Erie from CSO during rainfall events. A 160 Mgal/day pumping station will discharge stored wastewater between storm events, to an existing treatment plant. The ECT has a 7.2-m (finished) diameter and will be 5.5 km in length. A similar effort is underway in Indianapolis, IN with the Deep Rock Connector Project (Van Hampton 2013). The largest CSO project is the TARP (Tunnel and Reservoir Plan) in suburban Chicago (Table 2-1).

The ECT was excavated in the Chagrin Shale member of the Devonian Ohio Shale formation, at depth ranging from 57 to 66 m (HMM 2010). This shale is horizontally bedded, weak to medium strength, with thin interbeds of shaly, calcareous siltstone and sandstone. Sparse fracturing and unconfined compressive strength of 65 MPa make this a robust, indurated lithology compared to claystones, mudstones, and soft shales that could be considered for repository development. The Chagrin Shale has significant slaking potential. Northeastern Ohio is known for high horizontal stresses, and a horizontal:vertical stress ratio of 2.0 to 2.5 was observed and applied in stability analyses. The Chagrin Shale is known for “horizontal slabbing” behavior in excavations (Robbins 2014a), however, over-stress conditions (exceeding compressive strength) did not

occur in the ECT because of the shallow depth. Over-stress conditions at repository depth could require changes in the excavation method and more robust ground support.

The ECT project is expected to be complete in 2015. Tunneling was performed with a Herrenknecht double-shield hard rock TBM, with disc cutters, to a rough diameter of 8.2 m. An Alpine® roadheader was used for the 37-m TBM launch chamber and the 90-m tail tunnel. Waste rock was removed through a 12-m (finished) diameter mining shaft. The one-pass tunnel liner consists of pre-fabricated segments made from steel-fiber reinforced concrete. Liner grouting was performed through the tail of the TBM using a fast-setting two-component grout (TBM 2013). The fast-setting grout quickly established a barrier to natural gas inflow, controlled swelling, and also limited grout intrusion into the TBM area forward of the liner. The one-pass liner design accelerated the schedule (compared to the predecessor Mill Creek tunnels discussed below). A total of five shafts were constructed, ranging in size from 4.9 m to 15 m in diameter, and four will have baffle structures to convey stormflows into the tunnel. Total project cost is estimated to be approximately \$200M (current dollars), or about \$35k per meter of completed tunnel, or \$800 per cubic meter of wastewater storage capacity. This total cost includes lining, shafts, and intake structures.

**Mill Creek Tunnels** – The Mill Creek Tunnels, Phases 1, 2 and 3 were completed prior to the ECT, for CSO storage. The Phase 2 and Phase 3 tunnels are closely comparable to the ECT. The Phase 2 tunnel has a finished diameter of 6 m and is 4 km long. It was also constructed in the horizontally bedded Chagrin Shale, at depth ranging from 49 to 79 m, and a final 1999 cost of \$57M (\$14k per meter). The Phase 3 tunnel is similar, again constructed in the Chagrin Shale, with a length of 4.5 km and depth ranging from 63 to 93 m. Both the Phase 2 and 3 tunnels were constructed with a double-shield Robbins TBM, with disc cutters. Ground support consisted of steel ribs with steel mat lagging and some timber lagging where excessive rock breakage (i.e., overbreak) occurred in the tunnel crown. Overbreak of up to about 0.65 m was attributed to loosening and over-stress fracturing, mostly in the Phase 3 tunnel. It occurred over about 55% of the tunnel length (HMM 2010). Stresses in the rock around the openings were generally much less than the compressive strength discussed previously, suggesting that bedding separation or “slabbing” occurred during excavation. Final construction included a cast-in-place, unreinforced concrete liner with minimum thickness 0.3 m, using 34-MPa (5,000 psi) concrete (Figure 2-6). The original construction contract for \$58M was overrun numerous times resulting in a final 2002 cost of \$85M (\$19k per meter).

**Pierre Shale** – The Pierre Shale was considered for possible repository development in the 1970’s and 1980’s (Gonzales and Johnson 1984; Hansen et al. 2010). The Pierre and correlative Cretaceous facies (e.g., Lewis Shale, Mancos Shale) are well known and widespread across the northern Great Plains and Rocky Mountain regions. The Pierre Shale is thick, “reasonably uniform” (Shurr 1977) and highly deformable, with low permeability (Tourtelot 1962; Neuzil 1986, 2013). It is classified as a mudstone with abundant clay mineral content, and has lower strength than the Opalinus Clay or COX argillite (Table 2-2).

Like other fine-grained clay-rich rock types it would likely exhibit viscoplastic response (i.e., creep) to repository loading conditions (Nopola 2013). It is included here because of ongoing interest (Roggenthen et al. 2013) and because it represents the challenges that would likely be associated with large-scale underground construction in a soft, poorly indurated smectite-rich rock. This discussion could apply also to other strata such as the Lewis and Mancos Formations.



Figure 2-6. Mill Creek Tunnel Phase 2 showing steel ribs and lagging support (upper) and final cast-in-place concrete liner (lower) (with permission, HMM 2010)

There are few TBM excavations in the Pierre Shale, and perhaps the most relevant are the penstock and outlet tunnels of the Oahe Dam in north-central South Dakota. Excavation began in 1955 using a first-generation TBM (Robbins 2012). The dam has seven steel penstocks 7.3 m in diameter, 1,000 to 1,221 m long, which are embedded in tunnels mined in the Pierre Shale. Another six tubes for release of high flows are 6.0 m in diameter, 1,066 to 1,116 m long, and similarly embedded (ACoE 2014). Thus, there are approximately 14 km of large-diameter, TBM-excavated tunnels at the Oahe Dam. The project also marked the first large-scale use of pre-fabricated reinforced concrete liner segments. The penstock and outlet works tunnels at Oahe were mined at grades of a few percent, starting at intake structures constructed in the reservoir and passing underneath the dam abutments. These are early examples of TBM-constructed ramps such as that which could be built for waste handling at a repository.

Nopola (2013) performed ground support performance calculations for a circular tunnel in Pierre Shale, at depth of 300, 500 or 700 m (Figures 2-3 and 2-4). The rock was assigned viscoplastic creep properties estimated by analogy to published test data for the COX argillite and the Kanawha Formation siltstone and shale. Concrete liner properties (compressive strength 60 MPa) and thickness (0.25, 0.5 and 0.75 m) were selected to bear the load transferred over 20 years, from creep deformation of the host rock. Finished tunnel diameter was assumed to be 3 m. *In situ* stress conditions were assumed to be lithostatic. In the simulations, the liner was emplaced after elastic deformations had occurred in response to excavation. These results are a useful starting point for further design analyses and site specific evaluations for the Pierre or other similar shale units.

**Other Large-Scale Tunnels in Argillaceous Rock in North America** – The Flathead Tunnel in Montana is a single-track rail tunnel constructed between 1966 and 1969, in quartzite and argillite, generally medium to hard (Skinner 1974). The tunnel is 11.3 km long, constructed by drill-and-blast methods, with a horseshoe cross-section. It remains the second-longest rail or highway tunnel in the U.S. (first is the Cascade Tunnel). It cost \$37.9M to construct, inclusive of lining, track, utilities and ventilation (\$3,363 per meter; 1969 dollars).

Niagara Tunnel #3 is a hydroelectric tunnel bored under the city of Niagara Falls, Ontario, and completed in 2013 (OPG/Strabag 2014). It runs parallel to twin 13.7-m diameter (finished) tunnels completed in 1955, that divert flow from the Niagara River around the Niagara Falls, to a hydroelectric power station downstream. Tunnel #3 has a 12.5-m finished diameter (14.4 m excavated), and is 10.4 km long, with a maximum depth of 140 m. Much of the tunnel was excavated in the Ordovician Queenston Shale (mudstone facies) which exhibited fracturing and roof breakout throughout the excavation. An open-type TBM was used, of a single-shield hard-rock design with grippers, possibly the largest TBM ever built and used at the time. Initial ground support consisted of rock bolts, wire fabric, and shotcrete. An impervious membrane was then installed, and the final cast-in-place concrete liner. Because this is a pressure tunnel, the entire liner assemblage was pre-stressed by high-pressure grouting. Tunnel #3 was designed for a life of at least 90 years, and cost approximately \$1.5B (2009 dollars) inclusive.

The Boston Harbor Project included a wastewater outfall tunnel from Deer Island to Massachusetts Bay, beneath Boston Harbor, constructed from 1992 to 1996 (Robbins 2014b). The tunnel diameter is 8.0 m (finished), and it is 15.2 km long. The predominant rock type is Cambridge Argillite in beds 1 mm to 8 cm thick, also volcanic flows, tuffs, igneous dikes and sills, etc. A double-shield TBM was selected to handle variable rock conditions and water inflow. A pre-fabricated segmented concrete liner was installed during excavation. The multiple TBM operation modes permitted pushing against the liner, or grippers, for advance depending on rock conditions. Borehole grouting was used extensively where hard, fractured rock and high water inflow were encountered. Total cost of the tunnel and associated outfall management facilities was \$3.4B, or approximately \$224k per meter (Holmstrom 1999).

The Park River Tunnel was completed in 1979 to transfer a portion of the Park River flow to the Connecticut River (Bieniawski 1990). It has a diameter of 6.6 m (finished), is 2.8 km long, and has a maximum depth of 60 m. The geology consisted of dipping Triassic sand red shales and siltstones, interrupted by basalt flows. Fractured rock and fault zones were also encountered. A TBM was used for the excavation and installation of a pre-fabricated segmented concrete liner 0.23 m thick. Ground support was increased in fractured rock, or where close to the surface. Steel rib supports were used in fault zones. The segmented liner was pressure-grouted to pre-

stress it for service. The tunnel was completed at the bid price of \$23.3M (\$8.3k per meter, 1978 dollars).

The Plateau Creek water conveyance project in Colorado involved 21 km of pipelines and tunnels, including two tunnel sections totaling 4.1 km. The tunnels were 3.3 m in diameter (excavated). They were constructed in well-indurated sandstone, shale and siltstone, using an open-face, hard-rock TBM (Robbins 2014c). Tunneling was started mid-2000 and completed in March, 2001. Ground support consisted of rock bolts, wire fabric and shotcrete. The tunnels were completed at the contract cost of \$14.1M (\$3.4k per meter; Tunnelbuilder 2014).

### **2.3 Discussion, Summary and Repository Construction Scenario**

The 50- to 100-year opening stability required for many repository openings can be achieved in clay/shale media, by analogy to rail, highway, water conveyance and hydroelectric tunnels. Selection of host rock that is self-supporting at repository depth, with low-permeability, will significantly lower costs by allowing use of open-type TBMs with dry operations. Methane may be encountered. Creep response may impact cost also, since tunnels in more viscoplastic media like the Pierre Shale may require heavier ground support than less creep-prone media like the Opalinus Clay and COX argillite. A shallower repository could significantly reduce excavation and construction costs in clay/shale media, and improve long-term stability (e.g., 200 to 300 m depth, instead of 500 m). Whereas repository depth of at least 300 m may be considered favorable in a regulatory context (e.g., 10CFR60.122), the repository depth at a specific site would be determined based on system-wide assessment of multiple factors.

Fastest construction is achieved using TBMs with a single-pass, pre-fabricated, segmented concrete liner. Liner segment properties (thickness, strength, reinforcement) can be adjusted to provide needed strength for a range of conditions. A segmented liner can be backfilled with grout after installation to improve mechanical coupling and minimize groundwater inflow. Use of compliant materials for backfilling such as pea gravel (uncemented) or concrete with plastic-foam aggregate, has proven useful to accommodate large deformations of the host rock without liner failure. For host media containing clay minerals the liner may need to be emplaced and sealed immediately to prevent moisture intrusion and swelling.

Cost data only for excavation and ground support are difficult to obtain for historical projects. Published cost data typically lump together tunnels with a wide range of other project features such as portals, shafts, pump houses, underground stations, pressure chambers, rail or roadbed, finance costs, etc. Also, cost data presented here are for tunnels that range from 3 m to 17 m in diameter. The tunnels were completed over a period of approximately 50 years, so cost data must be escalated for comparison. Nevertheless, the summary in Table 2-1 suggests that construction cost on the order of \$10,000 per meter or less may be possible for most repository drifts. This figure is comparable to previous repository cost estimates (Hardin et al. 2012, Section 5.1). For a large repository with 300 km of emplacement drifts, this equates to a total tunneling/lining cost of \$3B (not including ventilation, backfilling, plugging and sealing). The wide range of cost data, even considering excavated volume and ancillary facilities, suggests that experienced management is essential for controlling costs.

**Repository Excavation/Construction Scenario in Clay/Shale Media** – This scenario describes how a repository could be constructed for disposal of large waste packages containing up to 17 MT of spent fuel (equivalent to 37 pressurized water reactor fuel assemblies).

A thick, soft, flat-lying clay/shale host formation is selected that extends to a depth of 500 m (the Pierre Shale is a close example presented in this report). The repository horizon is identified and characterized at a depth of 300 m. A ramp is then constructed from the surface to repository depth, to be used for initial access and eventually for waste transport underground. A TBM is selected based on rock properties, *in situ* stress and hydrogeologic conditions. Rubber-tire equipment can operate at grades up to 10% (Fairhurst 2012) but for TBM excavation and to mitigate operational hazards, a grade of 5% is used resulting in a ramp that is 6 km long. The diameter of the ramp and access drifts is 8 m (finished). Permanent ground support is installed consisting of pre-fabricated, reinforced concrete segments. Larger, heavier invert segments with extra reinforcement serve as the ramp running surface. The liner and invert are fully grouted to prevent groundwater inflow or swelling, to stabilize the liner, and to transfer running loads from the invert to the host rock.

Main drifts at the repository horizon are then constructed using the same TBM, liner and invert specifications. The drift layout will support underground testing activities for characterization, repository design, and licensing. It will then support initial construction of repository emplacement drifts. A simple drift layout is used that will later facilitate construction of disposal panels. This layout is large enough to tie together the minimum number of shafts that will be needed for repository construction (men-and-materials, ventilation, etc.). These shafts are constructed by raise-boring and lined with concrete, as the main drifts are being excavated. More shafts may be constructed later to service additional disposal areas.

Once the underground infrastructure is established and repository construction can begin, another, smaller TBM with a diameter of 5 m or less is assembled underground. This TBM will excavate and install ground support in the emplacement drifts. The diameter is reduced to control the amount of backfill needed at repository closure, and the peak backfill temperature. Ground support consists of a pre-fabricated, segmented, concrete liner backfilled with low-permeability grout. Before waste emplacement, radiation shielding and ventilation regulators are installed. Emplacement drift seals and plugs are pre-constructed to prepare for repository closure after 50 years.

In-drift disposal (Figure 2-7) is used with packages placed on low pedestals or directly on the invert, approximately 30 m apart (Hardin et al. 2013). Emplacement drifts are parallel and arranged in panels for access and to control ventilation. Cementitious materials are used extensively in construction and will have been thoroughly characterized so the possible impacts on longevity of the waste form and packaging, and on radionuclide transport in the host medium, are well understood.

At closure, all the repository drifts are backfilled with granular, swelling clay-based material in a dehydrated form. The functions of the backfill are to prevent large-scale movement of groundwater along the repository openings, and to provide mechanical support when the tunnels eventually collapse. Backfilling is done remotely in the emplacement drifts, and is a process that will have been analyzed and tested to support the original licensing process. Construction of plugs and seals is completed, and the repository is closed. Monitoring continues as long as needed to ensure that system performance is safe and complies with licensing requirements.



Figure 2-7. In-drift disposal after emplacement and during repository ventilation, prior to installation of backfill then repository closure

## References for Section 2

- ACoE (U.S. Army Corps of Engineers, Omaha District) 2014. *Oahe Project Statistics*. (<http://www.nwo.usace.army.mil/Media/FactSheets/FactSheetArticleView/tabid/2034/Article/2960/oahe-project-statistics.aspx>) Downloaded 21May2014.
- AlpTransit (AlpTransit Gotthard Ltd.) 2010. *Project data – raw construction Gotthard Base Tunnel*. LZ01-223480-v1. ([http://www.alptransit.ch/fileadmin/dateien/medien/zahlen/gbt\\_e.pdf](http://www.alptransit.ch/fileadmin/dateien/medien/zahlen/gbt_e.pdf))
- ANDRA (Agence nationale pour la gestion des déchets radioactifs) 2005. *Dossier 2005 Argile: Evaluation of the feasibility of a geological repository in an argillaceous formation - Meuse/Haute-Marne site*. (<http://www.ANDRA.fr>).
- Bieniawski, Z.T. 1990. *Tunnel Design by Rock Mass Classifications*. U.S. Army Corps of Engineers, Waterways Experiment Station, Vicksburg, MS. Update of Technical Report GL-79-19.
- Bonini, M. and G. Barla 2012. “The Saint Martin La Porte access adit (Lyon–Turin Base Tunnel) revisited.” *Tunnelling and Underground Space Technology*. V.30. pp. 38–54.
- Cannon, D.E. 1967. “Record Tunnel Excavation with Boring Machines.” *Civil Engineering*. V.37, N.8. pp. 45-48.
- Delay, J., P. Lebon and H. Rebours 2010. “Meuse/Haute-Marne centre: next steps toward a deep disposal facility.” *J. of Rock Mech. and Geotech. Engr.* 2(1). pp. 52-70.
- Ehrbar, H. 2008. “Gotthard Base Tunnel Switzerland: Experiences with Different Tunnelling Methods.” *2<sup>nd</sup> Brazilian Conference on Tunneling and Underground Construction (2<sup>o</sup> Congresso Brasileiro de Túneis e Estruturas Subterrâneas Seminário Internacional “South American Tunnelling”)*. ([www.alptransit.ch/fileadmin/dateien/medien/artikel/Heinz\\_Ehrbar-Gotthard\\_Base\\_Tunnel\\_Experiences\\_with\\_different\\_tunnelling\\_methods\\_paper\\_Sao\\_Paolo\\_pdf.pdf](http://www.alptransit.ch/fileadmin/dateien/medien/artikel/Heinz_Ehrbar-Gotthard_Base_Tunnel_Experiences_with_different_tunnelling_methods_paper_Sao_Paolo_pdf.pdf))

- Einstein, H.H. 2000. "Tunnels in, Opalinus Clayshale A Review of Case Histories and New Developments." *Tunnelling and Underground Space Technology*. V.15, N.1. pp. 13-29.
- Fairhurst, C. 2012. *Current Approaches to Surface-Underground Transfer of High-Level Nuclear Waste*. Itasca Consulting Group, Minneapolis, MN.
- Franzen, T., K.F. Garshol and N. Tomisawa 2001. "Sprayed concrete for final linings: ITA working group report." *Tunnelling and Underground Space Technology*. V16. pp. 295-309.
- Glaser, L.S. 2010. *San Juan-Chama Project History*. U.S. Department of Interior, Bureau of Reclamation. ([http://www.usbr.gov/projects/ImageServer?imgName=Doc\\_1305641466592.pdf](http://www.usbr.gov/projects/ImageServer?imgName=Doc_1305641466592.pdf))
- Gonzales, S. and K.S. Johnson 1984. *Shale and other argillaceous strata in the United States*. ORNL/Sub/84-64794/1. Oak Ridge National Laboratory. Oak Ridge, TN.
- Hansen, F.D., E.L. Hardin, R.P. Rechard, G.A. Freeze, D.C. Sassani, P.V. Brady, C.M. Stone, M.J. Martinez, J.F. Holland, T. Dewers, K.N. Gaither, S.R. Sobolik, and R.T. Cygan 2010. *Shale Disposal of U.S. High-Level Radioactive Waste*. SAND2010-2843. Sandia National Laboratories. Albuquerque, NM. May, 2010.
- Hansen, F.D. and T.J. Vogt 1987. *Thermomechanical properties of selected shales*. ORNL/Sub/85-97343/2. Oak Ridge National Laboratory, Oak Ridge, TN.
- Hardin, E. 2014. *Review of Underground Construction Methods and Opening Stability for Repositories in Clay/Shale Media*. FCRD-UFD-2014-000330 Rev. 0. U.S. Department of Energy, Office of Used Nuclear Fuel Disposition. May, 2014.
- Hardin, E.L., D.J. Clayton, R.L. Howard, J.M. Scaglione, E. Pierce, K. Banerjee, M.D. Voegele, H.R. Greenberg, J. Wen, T.A. Buscheck, J.T. Carter, T. Severynse and W.M. Nutt 2013. *Preliminary Report on Dual-Purpose Canister Disposal Alternatives (FY13)*. FCRD-UFD-2012-000170 Rev. 0. U.S. Department of Energy, Office of Used Nuclear Fuel Disposition. August, 2013.
- Hardin, E. and M.D. Voegele 2013. *Alternative Concepts for Direct Disposal of Dual-Purpose Canisters*. FCRD-UFD-2013-000102. U.S. Department of Energy, Office of Used Nuclear Fuel Disposition. February, 2013
- Hardin, E., T. Hadgu, D. Clayton, R. Howard, H. Greenberg, J. Blink, M. Sharma, M. Sutton, J. Carter, M. Dupont and P. Rodwell 2012. *Repository Reference Disposal Concepts and Thermal Load Management Analysis*. FCRD-UFD-2012-00219 Rev. 2. U.S. Department of Energy, Office of Used Nuclear Fuel Disposition. November, 2012.
- HMM (Hatch Mott MacDonald LLC) 2010. *Geotechnical Baseline Report for Euclid Creek Tunnel*. Northeast Ohio Regional Sewer District, Cleveland, OH.
- Holmstrom, D. 1999. "Pulling the Plug." *Christian Science Monitor*. " September 9, 1999. (<http://www.csmonitor.com/1999/0909/p15s1.html>)
- Hung, C.J., J. Monsees, N. Munfah and J. Wisniewski 2009. *Technical Manual for Design and Construction of Road Tunnels – Civil Elements*. FHWA-NHI-10-034. U.S. Department of Transportation, Federal Highway Administration, National Highway Institute. December, 2009.
- Martin, D.C. and G.W. Lanyon 2002. *EDZ in clay-shale: Mont Terri Rock Laboratory*. Mont Terri Project Technical Report TR2001-01. Swisstopo.

NAGRA (National Cooperative for the Disposal of Radioactive Waste) 2002. *Project Opalinus Clay: Safety report demonstration of disposal feasibility for spent fuel, vitrified high-level waste and long-lived intermediate-level waste (Entsorgungsnachweis)*. Technical Report 02-05.

Neuzil, C.E. 1986. "Groundwater Flow in Low-Permeability Environments." *Water Resources Research*. V.22, N.8. pp.1163-1195.

Neuzil, C.E. 2000. "Osmotic generation of 'anomalous' fluid pressures in geologic environments." *Nature*. V.403. pp. 182-184.

Neuzil, C.E. 2013. "Can Shale Safely Host U.S. Nuclear Waste?" *Eos*. V.94, N.30. pp. 261-268.

Nopola, J. 2013. *Preliminary Evaluation of the Pierre Shale as a Nuclear Waste Repository*. Thesis submitted in Geological Engineering, South Dakota School of Mines and Technology. Rapid City, South Dakota.

NPS (National Park Service) 2007. *National Register of Historic Places*. U.S. National Park Service. January 23, 2007. ([http://nrhp.focus.nps.gov/natreg/docs/All\\_Data.html](http://nrhp.focus.nps.gov/natreg/docs/All_Data.html))

OECD/NEA (Organization for Economic Co-operation and Development/Nuclear Energy Agency) 1996. *Water, gas and solute movement through argillaceous media*. (Prepared by S.T. Horseman, J.J.W. Higgo, J. Alexander and J. F. Harrington). Report CC-96/1.

OECD NEA (Organization for Economic Co-operation and Development/Nuclear Energy Agency) 2003. *Features, Events and Processes Evaluation Catalogue for Argillaceous Media*. (Prepared by M. Mazurek, F.J. Pearson, G. Volckaert and H. Bock). Report NEA4437.

ONDRAF/NIRAS (Belgian Agency for Radioactive Waste and Enriched Fissile Materials) 2001. *SAFIR 2: Safety Assessment and Feasibility Interim Report 2*. NIROND 2001-06 E, December, 2001.

OPG/Strabag (Ontario Power Generation/Strabag Inc.) 2014. *Niagara Tunnel Project: 2005-2013*. ([www.niagarafrontier.com/tunnel.html](http://www.niagarafrontier.com/tunnel.html))

Roggenthen, W., L. Stetler, J. Nopola, B. Cetin and L. Roberts 2013. *Geological Distribution of Potentially Suitable Shale in the U.S.: Concepts and Literature*. FCRD-UFD-2013-000224. U.S. Department of Energy, Office of Used Nuclear Fuel Disposition.

Robbins (The Robbins Co.) 2012. "Accolades and Awards: Robbins celebrates 60 years of achievement." (<http://tunneltalk.com/Accolades-Awards-Oct12-Robbins-celebrates-60-years-of-TBM-achievement.php>)

Robbins (The Robbins Co.) 2014a. "The Mill Creek II Sanitary Sewer Storage Tunnel." ([www.therobbinscompany.com/en/case-study/the-mill-creek-ii-sanitary-sewer-storage-tunnel/](http://www.therobbinscompany.com/en/case-study/the-mill-creek-ii-sanitary-sewer-storage-tunnel/)).

Robbins (The Robbins Co.) 2014b. "Boston Harbor Project." ([www.therobbinscompany.com/en/case-study/boston-harbor-project/](http://www.therobbinscompany.com/en/case-study/boston-harbor-project/)).

Robbins (The Robbins Co.) 2014c. "Plateau Creek: Long-running TBM sets world records on its fourth project in Colorado." ([www.therobbinscompany.com/en/case-study/plateau-creek/](http://www.therobbinscompany.com/en/case-study/plateau-creek/)).

Shurr, G.W. 1977. *The Pierre Shale, Northern Great Plains; A Potential Isolation Medium for Radioactive Waste*. United States Geological Survey Open File Report 77-776.

Skinner, E.H. 1974. *The Flathead Tunnel: A Geologic, Operations, and Ground Support Study, Burlington Northern Railroad, Salish Mountains, Montana*. U.S. Bureau of Mines, Information Circular 8662.

TBM (Tunnel Business Magazine) 2013. "Euclid Creek Tunnel Mining Completed in Cleveland." ([www.tunnelingonline.com](http://www.tunnelingonline.com))

Tourtlot, H.A. 1962. *Preliminary Investigation of the Geologic Setting and Chemical Composition of the Pierre Shale, Great Plains Region*. U.S. Geological Survey Professional Paper 390.

Tunnelbuilder 2014. "United States – Colorado US/40: Plateau Creek Water Transmission." ([www.tunnelbuilder.com/Archive/Projects.aspx/?&country=United-States&page=8](http://www.tunnelbuilder.com/Archive/Projects.aspx/?&country=United-States&page=8))

USBR (U.S. Bureau of Reclamation) 1989. *Water Conveyance Tunnels: Gravity and Pressure (2<sup>nd</sup> Edition)*. Construction and Engineering Data. USBR, Department of the Interior. August, 1989. (<http://www.ntis.gov/search/product.aspx?ABBR=PB95145538>)

Van Hampton, T. 2013. "Deep Below Indianapolis, Tunnelers Race to Control Waste." *Engineering News Record*. Issue July 29, 2013. ([www.midwest.construction.com/midwest\\_construction\\_projects/2013/0729-deep-below-indianapolis-a-race-to-control-waste.asp](http://www.midwest.construction.com/midwest_construction_projects/2013/0729-deep-below-indianapolis-a-race-to-control-waste.asp))

Volckaert, F., X. Bernier, X. Sillen, M. Van Geet, J.-C. Mayor, I. Göbel, P. Blümling, B. Frieg and K. Su 2005. "Similarities and Differences in the Behaviour of Plastic and Indurated Clays." In: *Proceedings, Euradwaste'04. Radioactive waste management community policy and research initiatives*. EUR-21027. pp. 281-291.

THIS PAGE INTENTIONALLY LEFT BLANK

### 3. System-Level Logistics Modeling of DPC Direct Disposal

Logistical simulations were conducted to better understand the relationship between the needed DPC decay storage time for disposal, and future changes in the SNF management system in the U.S. such as repository opening date, and transition to loading smaller multi-purpose canisters (MPCs) at the nuclear power plants. The study methods, assumptions, and results are described in Appendix C.

The study uses metrics of: 1) maximum system-wide storage capacity required; 2) decay storage time prior to emplacement in a repository; and 3) the profile of fuel age at emplacement, over the duration of repository operations. Results show that the greatest benefit from implementing MPCs, with respect to shortening the required cooling time for all SNF (including that in DPCs), requires a small MPC canister combined with an early repository start date. The small MPC canister can achieve any emplacement power limit sooner, while an early repository start date means earlier transition from DPCs to MPCs. As time passes without a transition to MPCs, more of the total SNF inventory will be in DPCs so the logistical value of a transition to MPCs will decline (without re-packaging which introduces other costs and complications).

At higher emplacement thermal power limits (e.g., 10 kW or greater) there would be little difference in cooling time regardless of transition to MPCs, or the repository start date. Depending on whether and when MPCs are implemented, and the repository emplacement thermal power limit, projected repository closing dates varies from calendar 2067 to 2162. More flexible solutions that require less decay storage, particularly for younger, higher burnup fuel, can be closed sooner.

The projected statistics of SNF age at emplacement are of interest to evaluate the potential risk from future changes in fuel or DPC condition that limit storage time. The minimum fuel age at emplacement is obtained by re-packaging all DPCs into smaller canisters, thus drastically decreasing the required surface decay storage time for disposal. If the industry transitions from DPCs to smaller MPCs without re-packaging, the fuel age at emplacement is comparable to re-packaging if the emplacement power limit is high enough (10 kW or greater). For the lower 6 kW power limit two changes would be needed: both a transition to MPCs, and an early repository start, to achieve fuel age at emplacement that is comparable to the re-packaging case at the same power limit.

THIS PAGE INTENTIONALLY LEFT BLANK

#### 4. Criticality Investigations

Direct disposal of SNF currently stored in DPCs, would involve a disposal overpack designed to provide support and containment in the specific disposal environment. Poor fabrication and handling process control such as improper base material or weld filler selection, improper heat or surface treatment, or mishandling of the waste package might cause one or more waste packages to fail within the regulatory period (SNL 2007, Sections 6.2.3 through 6.2.3.7). Appropriate quality controls can significantly reduce the likelihood of failure. However, there is a small probability that one or more of these overpacks could fail within the regulatory performance period for disposal, e.g., within 10,000 years.(SNL 2007 Sections 6.4 and 6.5) This could then expose the DPC and its contents to ground water for thousands of years, with the possibility of flooding. Neutron absorber materials used in current DPC designs are typically aluminum based, and would readily degrade under long-term exposure to ground water. Further, some DPCs have internal structural components made from materials such as aluminum or low-alloy steel, which would also degrade. This section describes analysis of the potential for criticality, following on preliminary work published previously (Clarity and Scaglione 2013). Note that if ground water can be excluded from waste packages, there is virtually no potential for criticality.

The earlier studies concluded that demonstrating subcriticality for some fraction of the existing DPC inventory could be possible (BSC 2003; EPRI 2008). Previous analysis (Clarity and Scaglione 2013) demonstrated subcriticality for a set of DPCs representing those stored at two nuclear power plants. That analysis included the effects from flooding with ground water, degradation of neutron absorbing materials, and degradation of the structural basket holding the SNF. This section describes similar analysis of additional existing DPCs, and presents more general analysis of the effects of groundwater chemical constituents on the reactivity of flooded and internally degraded DPCs.

Licensed DPCs are loaded using well-defined assembly-loading criteria (i.e., specifications for “approved contents” in the Certificate of Compliance). These criteria define limiting (bounding) loading conditions and fuel characteristics. In practice, because of the diversity in the discharged used nuclear fuel (UNF) available for loading (e.g., variations in fuel assembly burnup, initial enrichment, and age since discharge) it is not possible to load a DPC with fuel that corresponds exactly to the limiting license conditions. Hence, DPCs are typically loaded with some amount of unquantified, uncredited criticality safety margin. By obtaining detailed information on each fuel assembly and how the DPCs are loaded, this uncredited margin can be applied to analysis of postclosure criticality. (The term UNF is used in this discussion of criticality, which in principle includes fuel that may not have been committed to disposal and is therefore not SNF.)

The performance of the neutron absorber material as a function of time inside the canister is a key factor to demonstrating subcriticality. The material used in the majority of currently loaded DPCs is Boral®, composed of boron carbide (B<sub>4</sub>C) particles and aluminum Alloy 1100, hot-rolled together to form a neutron absorbing core which is then bonded to two outer layers of Alloy 1100. Various corrosion tests have been performed on this material because it is used in existing canisters and in spent fuel pool racks. Corrosion tests conducted under pool chemistry conditions have shown a 0.28 mil-per-year rate of cladding material loss, which equates to 40-year service life (in the presence of water) before degradation of the neutron-absorbing core (EPRI 2008). Other tests of Boral® under simulated vacuum drying conditions have shown formation of blisters (EPRI 2009). Considering that the analyzed repository performance period is expected to be at least 10,000 years, and there could be a small probability of waste package

failure at any time during that period, the loss of neutron absorber material is a potentially important condition to evaluate for DPC direct disposal.

This report examines: 1) the uncredited margins associated with actual fuel loading for a sample of existing DPCs; and 2) the increased reactivity because of canister flooding and the associated material and structural changes that can occur in the disposal environment. As-loaded criticality analyses are performed for DPCs loaded at four decommissioned sites and one nuclear power plant, referred to here as Sites A, B, C, D and E. This effort is an extension of work performed previously (Clarity and Scaglione 2013) which analyzed postclosure criticality of as-loaded configurations corresponding to DPCs at Sites A and B. Additionally, this section describes investigation of criticality effects from various dissolved aqueous species that could be present in ground water within a repository. The results indicate that DPC disposal criticality safety demonstration could benefit from credit for neutron absorbers present in ground water.

#### 4.1 Review of Literature

A previous study by the Electric Power Research Institute (EPRI) examined the feasibility of direct disposal of DPCs in a repository in unsaturated, volcanic tuff (EPRI 2008). That study randomly selected two existing, loaded MPC-32 canisters (from Site E discussed below), with average assembly burnup ranging from approximately 30 to 43 GW-d/MTU, and analyzed reactivity under the assumption of fully degraded neutron absorbers but with the canisters otherwise intact. The study used three different sets of burnup credit isotopes containing the five, six, and 16 most important fission products with respect to fuel reactivity. Reactivity was evaluated after 5 years of cooling time. In addition to examining the as-loaded reactivity of the canisters, the study also looked at the potential reactivity suppression effects from adding used burnable poison rod assemblies (BPRAs), surrogate control rods, and alternate loading patterns for use in future canister loadings.

The EPRI study concluded that crediting the 5 most important fission products with respect to fuel reactivity was insufficient to show that the two canisters in question were subcritical, however, it showed that the canisters were marginally acceptable for disposal conditions by including 6 most important fission products ( $k_{eff} \sim 0.995$ ). The study also showed that there is significant uncredited margin even when accounting for the 16 fission products when compared with the full inventory of fission products in the lattice code used in the study. Additionally, the EPRI study showed a 2%  $\Delta k_{eff}$  decrease from modeling the used BPRAs in the canister.

#### 4.2 Methodology

Burnup credit criticality safety analysis for UNF in storage systems requires the determination of isotopic number densities for fuel assemblies by applying assembly-specific irradiation histories, commonly known as depletion calculations. A depletion calculation is followed by a canister criticality evaluation, which uses the isotopic number densities from the depletion step to determine the neutron multiplication factor,  $k_{eff}$  (also referred to as reactivity in this report). Both of these calculations—depletion and criticality—require different tools and methods.

Various modules of the SCALE code system (ORNL 2011) are employed for the criticality analyses presented here. The TRITON two-dimensional (2D) depletion sequence is used to perform depletion calculations that generate cross-section libraries for generic assembly/reactor-specific classes and a range of fuel operating conditions. This information can subsequently be used by ORIGEN-ARP for rapid processing of problem-dependent cross-sections. The TRITON

2D depletion calculation sequence employs CENTRM for multigroup cross-section processing, NEWT for 2D discrete-ordinates transport calculations, and ORIGEN-S for depletion and decay calculations. The resulting nuclide concentrations are passed to the criticality analysis codes. The SCALE CSAS6 criticality analysis sequence is used to perform criticality calculations for a loaded fuel cask using the KENO-VI Monte Carlo code with the continuous-energy ENDF/B-VII cross-section library to determine the effective neutron multiplication factor,  $k_{eff}$ . Note that a pre-released version of SCALE 6.2 which is still under final development, was used for decay and continuous-energy criticality calculations.

Computational analyses of existing, as-loaded DPCs is facilitated by a comprehensive and integrated data and analysis tool: the UNF-Storage, Transportation & Disposal Analysis Resource and Data System (UNF-ST&DARDS) (Scaglione et al. 2013). UNF-ST&DARDS runs the depletion, decay, and criticality analysis modules discussed previously (Smith et al. 2012). Note that bounding irradiation parameters, which are intended to estimate the upper limit of the neutron multiplication after discharge, were used (Smith et al. 2012).

Criticality calculations are performed applying 18-node bounding axial burnup profiles for assemblies. Additionally, 12 actinides and 16 fission products are credited in the criticality analyses as described below. Major assumptions applied to the criticality evaluation are:

- **Depletion** – Conservative depletion conditions are employed for the used fuel isotopic composition determination including burnable poison rod to be inserted in the fuel assembly guide tubes throughout the irradiation time.
- **Criticality** – Discharged control components (like control rod assemblies, BPRAs, etc.) are not considered in the criticality calculations except for Site E. A conservative approach is used for the as-loaded, Site E DPCs to account for water displacement by the control components.
- **Damaged Fuel** – Burnup is not credited for damaged fuel in the damaged fuel cans (DFCs). Instead, the canister design basis or bounding assembly for the DFC, as determined in the Final Safety Analysis Report (FSAR), is modeled for damaged fuel. However, some canned fuels that are not damaged, such as high burnup (>45 GW-d/MTU) assemblies in a DFC are modeled as intact with accumulated burnup.
- **Assembly Axial Burnup Profiles** – Bounding profiles are used for the criticality calculations as discussed below.

Each of these assumptions tends to increase reactivity, therefore, the criticality analyses documented here are expected to be reasonably conservative.

#### 4.2.1 Axial Burnup Profiles

The axial burnup distribution is an important factor in determining the reactivity of fuel at a given average burnup. For example, two fuel assemblies with the same initial enrichment and average burnup could yield different reactivity results depending on the axial burnup profiles of the assemblies at discharge. This work used a set of bounding profiles based on analysis of 3,169 axial profiles taken from plant operating data covering  $10^6$  cycles of operation (Wagner et al. 2003). Bounding axial burnup profiles (Figure 4-1) are implemented through UNF-ST&DARDS and used in the criticality analysis.

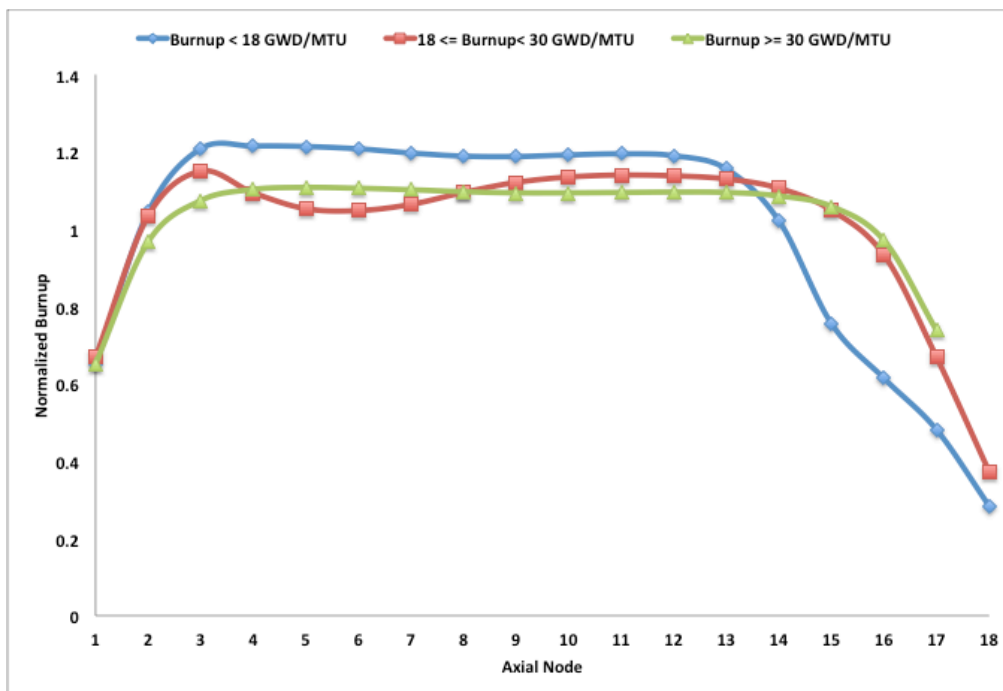


Figure 4-1. Axial burnup profiles for PWR assemblies, with normalized distribution and 18 nodes, with 1 being the bottom of the assembly

#### 4.2.2 Isotopes Included in the Criticality Model

The isotope set credited in criticality calculations is selected based on the burnup credit isotopes recommended by NUREG/CR-7108 and -7109 (Radulescu et al. 2012; Scaglione et al. 2012) for the UNF storage and transportation. The credited isotopes are listed in Table 4-1.

Table 4-1. Burnup analysis isotope set including actinides and 16 fission products

|                         |                   |                   |                   |                   |                   |
|-------------------------|-------------------|-------------------|-------------------|-------------------|-------------------|
| <b>Actinides</b>        |                   |                   |                   |                   |                   |
| <sup>234</sup> U        | <sup>235</sup> U  | <sup>236</sup> U  | <sup>238</sup> U  | <sup>238</sup> Pu | <sup>239</sup> Pu |
| <sup>240</sup> Pu       | <sup>241</sup> Pu | <sup>242</sup> Pu | <sup>241</sup> Am | <sup>243</sup> Am | <sup>237</sup> Np |
| <b>Fission products</b> |                   |                   |                   |                   |                   |
| <sup>95</sup> Mo        | <sup>99</sup> Tc  | <sup>101</sup> Ru | <sup>103</sup> Rh | <sup>109</sup> Ag | <sup>133</sup> Cs |
| <sup>143</sup> Nd       | <sup>145</sup> Nd | <sup>147</sup> Sm | <sup>149</sup> Sm | <sup>150</sup> Sm | <sup>151</sup> Sm |
| <sup>152</sup> Sm       | <sup>151</sup> Eu | <sup>153</sup> Eu | <sup>155</sup> Gd |                   |                   |

#### 4.2.3 Subcritical Limit

For simplicity, computational biases and uncertainties are not developed in this analysis, but are simply assumed to be  $\pm 2\%$  ( $\Delta k_{eff}$ ) resulting in a subcritical limit of  $k_{eff} < 0.98$ . The corresponding subcritical limit  $k_{eff} < 0.98$  is used in this study as a representative acceptance criteria for as-loaded calculations, recognizing that more complete validation and assessment of bias and uncertainties could be needed for disposal licensing.

Time-dependent reactivity calculation results are provided for the time range between the calendar years 2001 and 9999 (i.e., approximately 8000 years). Note that after the initial decrease, reactivity increases gradually from approximately 100 years to 10,000 years and beyond due to radioactive decay series, and reaches a second reactivity peak (Wagner and Parks 2003). However, the expected reactivity increase between 8,000 years and the second reactivity peak is not significant (less than  $0.005 \Delta k_{eff}$ ). As mentioned before, UNF-ST&DARDS is employed to carry out the as-loaded criticality analyses. Currently, a database restriction allows UNF-ST&DARDS to perform analyses only up to the calendar year 9999.

#### 4.2.4 Degradation Scenarios

An important assumption for criticality analysis is that water enters a breached waste package at some point during the repository performance period. While different geologic settings and material degradation mechanisms might yield a large number of potential configurations for analysis, two simplified and representative configurations are used in this analysis:

- **Loss-of-Absorber** – Total loss of neutron absorber components from unspecified degradation and material transport processes, with replacement by ground water. The degradation process for neutron absorber plates (e.g., aluminum based) in ground water is not well understood, and criticality may be sensitive to partial or local loss mechanisms. Thus, the reactivity effect of gradual, uniform loss of neutron absorber is studied here, culminating in complete loss.
- **Basket Degradation** – Loss of the internal basket structure (including the neutron absorber) with basket consolidation represented by negligible assembly-assembly spacings.

For both scenarios corrosion products are ignored. For aluminum-based absorber materials the quantities of corrosion products would be small relative to the interstitial volume of the fuel. For degradation of basket materials such as carbon steel there could be a slight moderator displacement effect which is conservatively ignored.

Figure 4-2 presents the reactivity reduction in terms of negative  $\Delta k_{eff}$  of a 32-assembly PWR canister as a function of  $^{10}\text{B}$  areal density in the neutron absorber panels, assuming the DPC is flooded with fresh water. For all the cases,  $\Delta k_{eff}$  for each step is calculated with respect to the  $k_{eff}$  corresponding to 0% of the minimum  $^{10}\text{B}$  areal density. This 32-assembly canister contains Westinghouse (W) 17x17WL (Lopar design) fuel assemblies. The  $^{10}\text{B}$  areal density study is performed for three uniform canister loadings: 10, 20 and 30 GW-d/MTU assemblies in all 32 locations, with 100 years of cooling time. The DPC licensing evaluations typically credit 75% of the minimum  $^{10}\text{B}$  areal density (NRC 2010a). Figure 4-2 indicates that loss of neutron absorber from the basket up to a certain threshold  $^{10}\text{B}$  areal density would not significantly increase reactivity. However, when the loss of neutron absorber from the basket passes the threshold  $^{10}\text{B}$  areal density, significant reactivity increase is expected. Note that the reactivity behavior with loss of neutron absorber from the basket is strongly related to the DPC geometry.

The extent of basket degradation in the disposal environment may be insignificant for criticality analysis, such that the basket degradation scenario would be unrealistically conservative. DPC fuel baskets generally have one of two designs: the “egg-crate” type fabricated from metal plates in reticular arrangement, and “tube-and-spacer-disk” structures fabricated from thin-wall tubes (holding each fuel assembly) held in place by a series of thicker, perpendicular metal spacer

disks. The egg-crate structures could retain structural integrity if the plates retain much of their mechanical thickness during long-term exposure to ground water. The tube-and-spacer-disk structures could continue to hold fuel assemblies apart even after degradation of the tubes, by the action of the spacer disks. Localized corrosion (pitting, crevice corrosion, stress corrosion, etc.) may not impact mechanical lifetime if the components retain their mechanical thickness. Of all the materials used in DPC basket construction, stainless steels (discussed in Section 8) are most likely to have the corrosion properties needed to retain mechanical thickness and obviate the basket degradation scenario.

**Effects from Basket Degradation on Reactivity** – On initial flooding, a DPC basket would be in original, undegraded condition so that criticality could not occur. Basket materials would begin to corrode on contact with ground water. The aluminum-based materials including neutron absorbers Boral® and Metamic® would likely be fastest to corrode. Thus, the loss-of-absorber degradation scenario would be realized first. Aluminum corrosion products would be produced but constitute a minor volume fraction.

Slower degradation of basket structural materials would produce corrosion products, particularly Fe-bearing oxides and oxyhydroxides. If basket materials are reactive, degradation could eventually proceed to partial, and then full basket collapse. The fully collapsed condition is represented by the basket degradation scenario, in which intact fuel assemblies are moved together in a nearly cylindrical configuration. No credit is taken for corrosion products, for moderator displacement and/or to maintain separation of fuel assemblies.

If degradation of the basket components can occur, some credit for the effects of moderator displacement in the available void volume could be realized. The effects would depend on the molar density of hydrogen atoms in the corrosion products compared to that of water, and on whether the interstitial volume of the fuel assemblies is completely filled. For example, if the molar density of corrosion products decreased by a factor of 4, and 50% of the internal DPC volume is interstitial space, then approximately 7,000 kg of steel would need to corrode, to fill the interstitial volume in a 32-PWR size DPC. This is comparable to the mass of the basket in a typical DPC. The resulting reactivity would be similar to that for a porous filler (Figure 9-3, and Figure 9-5 for aluminum powder) because the corrosion products are hydrous.

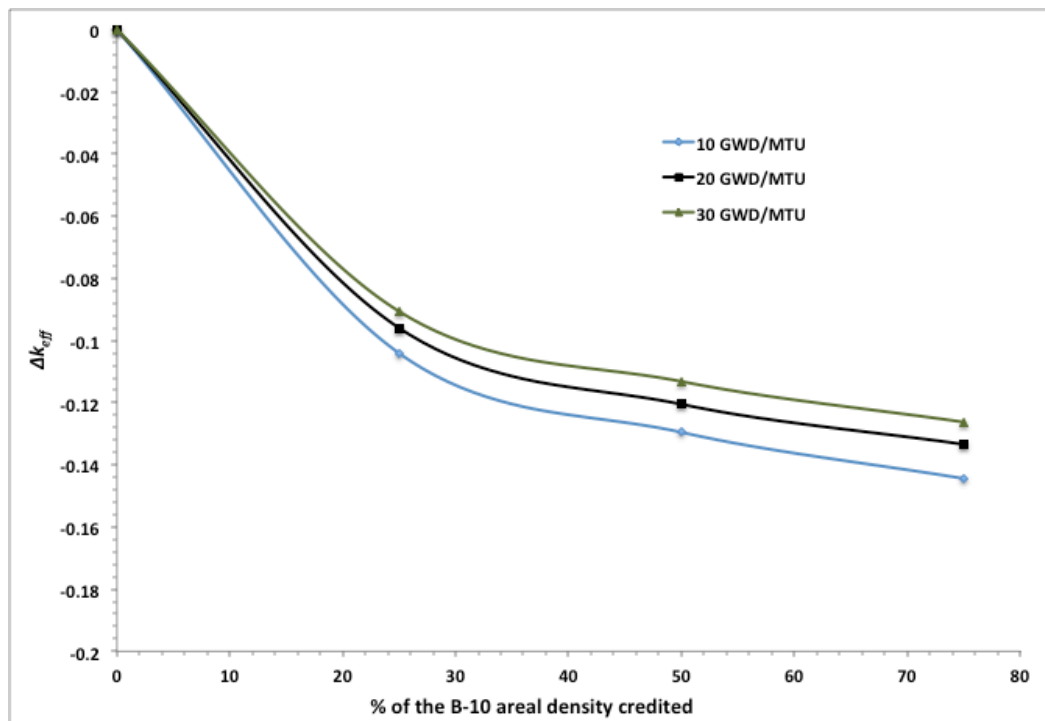


Figure 4-2. Reactivity impact of  $^{10}\text{B}$  areal density variation

### 4.3 Effects from Aqueous Species in Ground Water

As mentioned previously, neutron moderation by flooding with water is needed for a waste package to achieve criticality. However, the ground water (or pore water) that may potentially flood a breached waste package will contain various dissolved aqueous species that may be important. The dissolved aqueous species in the ground water can: 1) act as neutron absorbers (e.g.,  $^{35}\text{Cl}$  and  $^6\text{Li}$ ); and 2) displace moderating elements (e.g., H). Currently, a geologic repository site has not been identified, hence various geologic settings are being considered including crystalline rock, clay/shale, rock salt, and sedimentary rock among others (Hardin et al. 2012). Review of groundwater literature (Wang et al. 2012; Winterle et al. 2012; Jove-Colon et al. 2011; also see Section 5 of this report) shows that dissolved aqueous species vary widely. For example, pore water in Opalinus clay contains about 10,000 mg/L (ppm) of chlorine, while the chlorine content of a salt brine (in a salt repository) could be more than 150,000 mg/L.

As an alternative approach to using real groundwater composition data, the following elements are identified as good neutron absorbers in the natural environment, or they are abundant enough in ground water to warrant consideration: Ca, Li, Na, Mg, K, Fe, Al, Si, Ba, B, Mn, Sr, Cl, S, Br, N, and F. The reactivity impact of each of these elements is determined separately by varying the concentration over a wide range. Reactivity was examined using the two degraded canister scenarios introduced in Section 4.2.4: loss-of-absorber, and basket degradation.

These studies are performed for the representative MPC-32 canister from Holtec International, an egg-crate design with stainless steel plates. Uniform loading with specified burnup at all locations is assumed. Figures 4-3 and 4-4 illustrate the criticality models for the loss-of-absorber

and basket degradation scenarios, respectively. The basket degradation model reduces the assembly-assembly spacing uniformly and forms a closely packed cylindrical configuration. This configuration increases neutron interaction which in turn increases reactivity. The corrosion products from basket materials are represented as water, which is conservative with respect to increasing moderator effect.

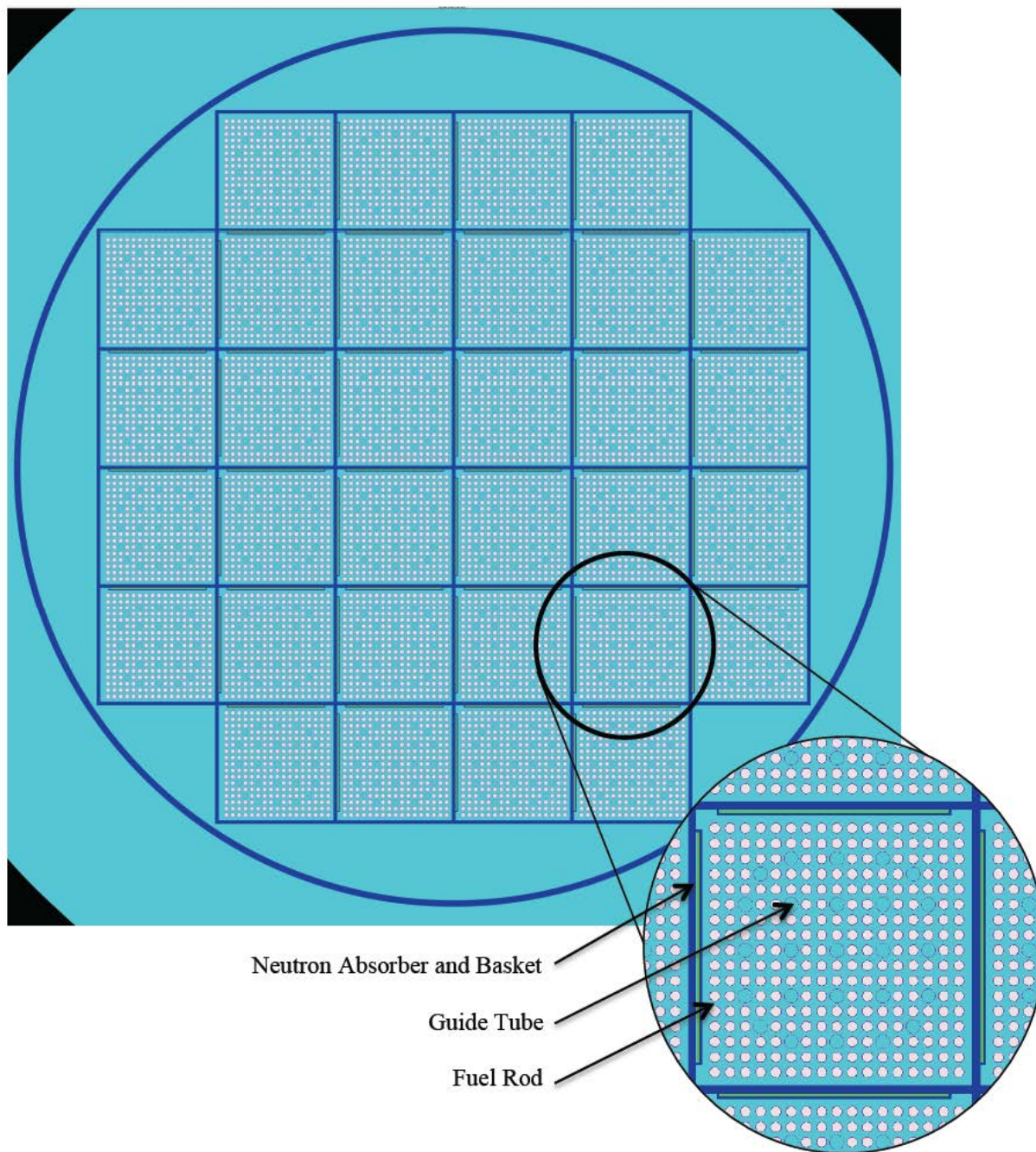


Figure 4-3. Graphical depiction of the center plane of the MPC-32 KENO-VI model used for ground water composition studies with varying  $^{10}\text{B}$  areal density in the neutron absorber panels

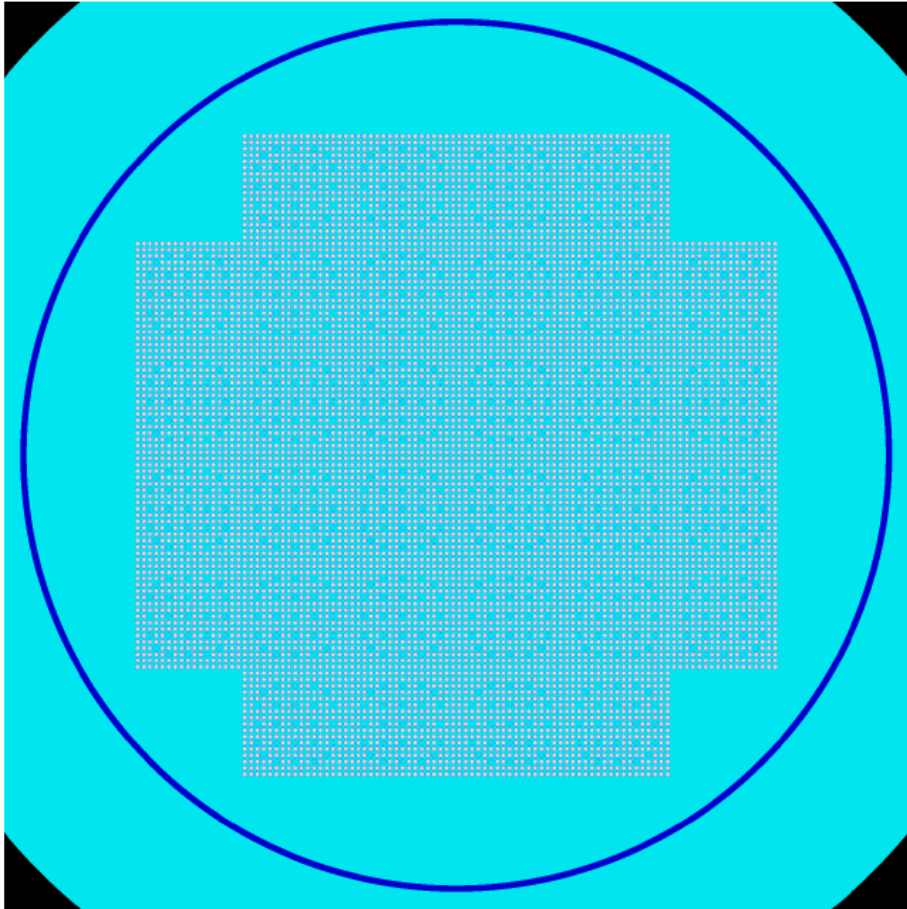
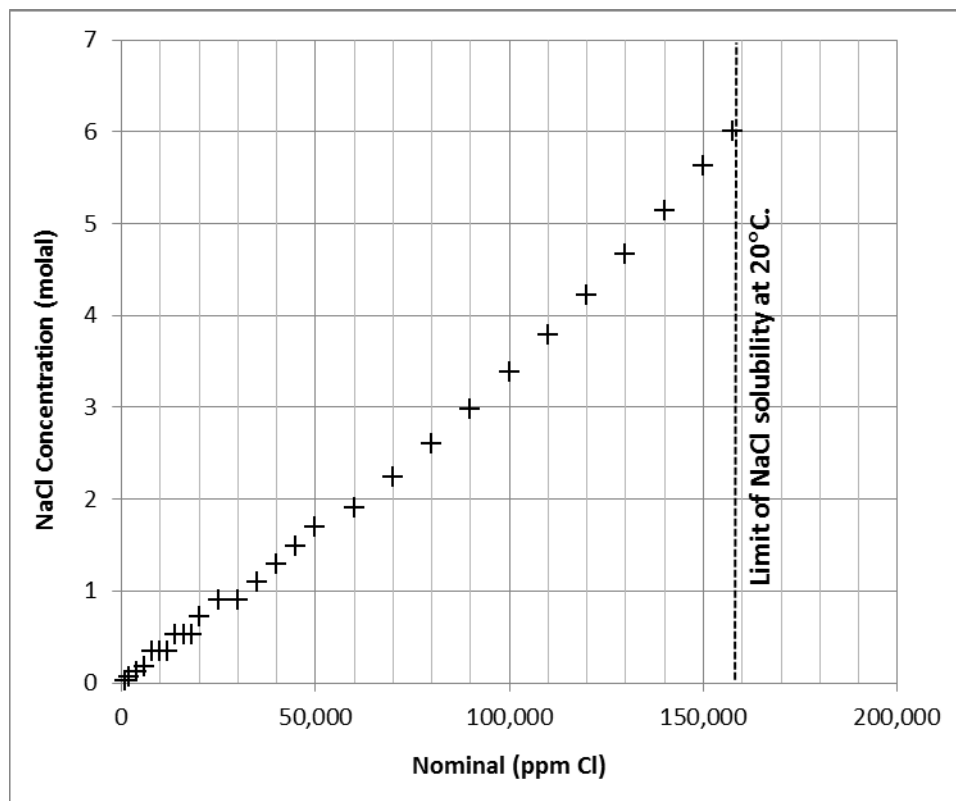


Figure 4-4. KENO-VI depiction of the MPC-32 basket degradation scenario

#### 4.3.1 Ground Water Study Results

The ppm units used in this discussion are based on number density distributions used in the neutronics calculations. For chlorine, they are correlated to NaCl concentrations as shown in Figure 4-5.

Among the dissolved aqueous species listed previously, Cl, Li, and B produce the greatest reduction in canister reactivity because of their large neutron absorption cross-sections. Figure 4-6(a) presents the impact of chlorine concentration in ground water on the reactivity of DPCs with different levels of neutron absorber in the basket, while Figure 4-6(b) illustrates the same for a degraded basket configuration. The negative  $\Delta k_{eff}$  indicates reactivity reduction with respect to the  $k_{eff}$  that corresponds to a configuration with fresh water. Similarly, Figures 4-7 and 4-8 present reactivity reduction for lithium and boron. Higher elemental concentrations (up to 150,000 ppm may be possible for chlorine, in a salt repository) are used for the basket degradation scenario because the configuration is more reactive.



Source of handbook solution specific gravity data (20°C): Weast and Astle (1981).

Figure 4-5. Correlation of ppm-chlorine units used in neutronics calculations (nominal) with NaCl concentration

These plots could be used to estimate reactivity impact ( $\Delta k_{eff}$ ) for a combination of different elements at different concentrations. For example, 100,000 ppm (mg/L) of chlorine with an average DPC assembly burnup of 10 GW-d/MTU provides approximately -0.20  $\Delta k_{eff}$  for the loss-of-absorber scenario, which could be enough to demonstrate subcriticality of many DPCs. Note that the concentration of chlorine (typically as chloride) in ground water varies widely among different geologic media. Also, lithium and boron are known to be scarce in ground water, so realistically they may not provide significant reactivity reduction. Bromine and manganese may offer slight reactivity reduction (Figure 4-9) while the other elements (N, Ba, Mg, F, S, Na, K, Sr, Ca, Fe, Al, and Si) would be insignificant (Figure 4-10).

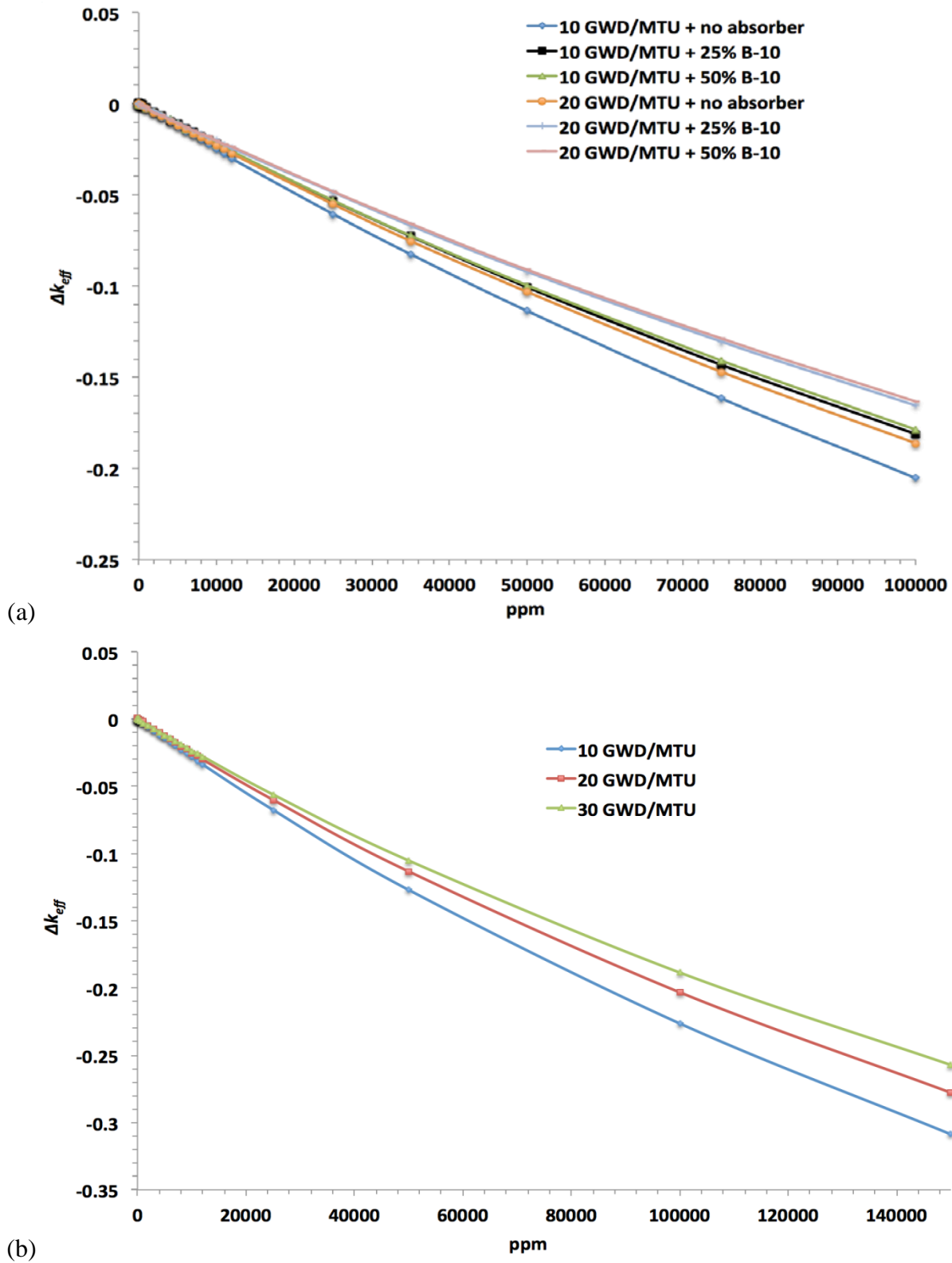


Figure 4-6. Impact on reactivity from chlorine concentration in ground water: (a) for different levels of neutron absorber; and (b) for degraded basket configuration

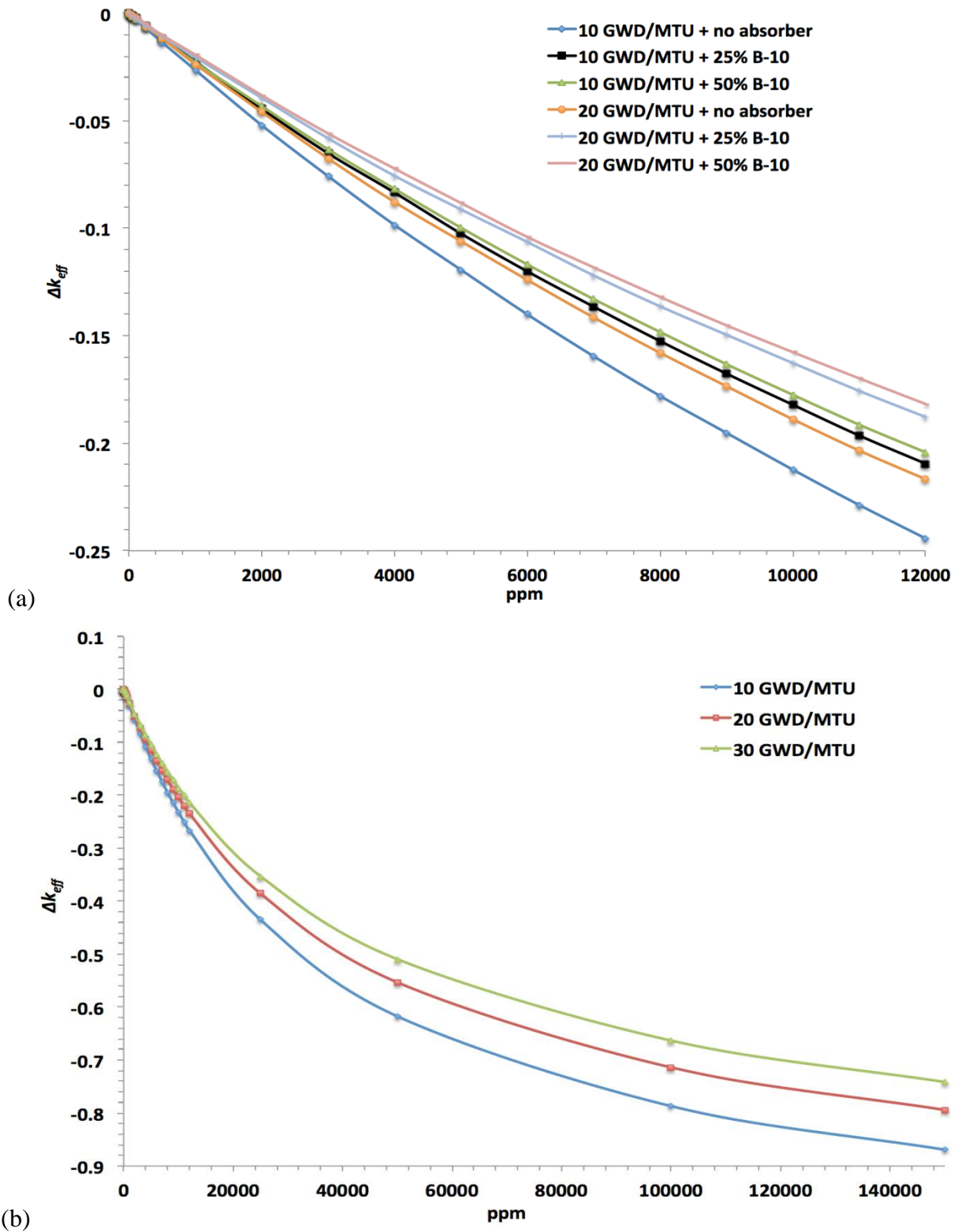
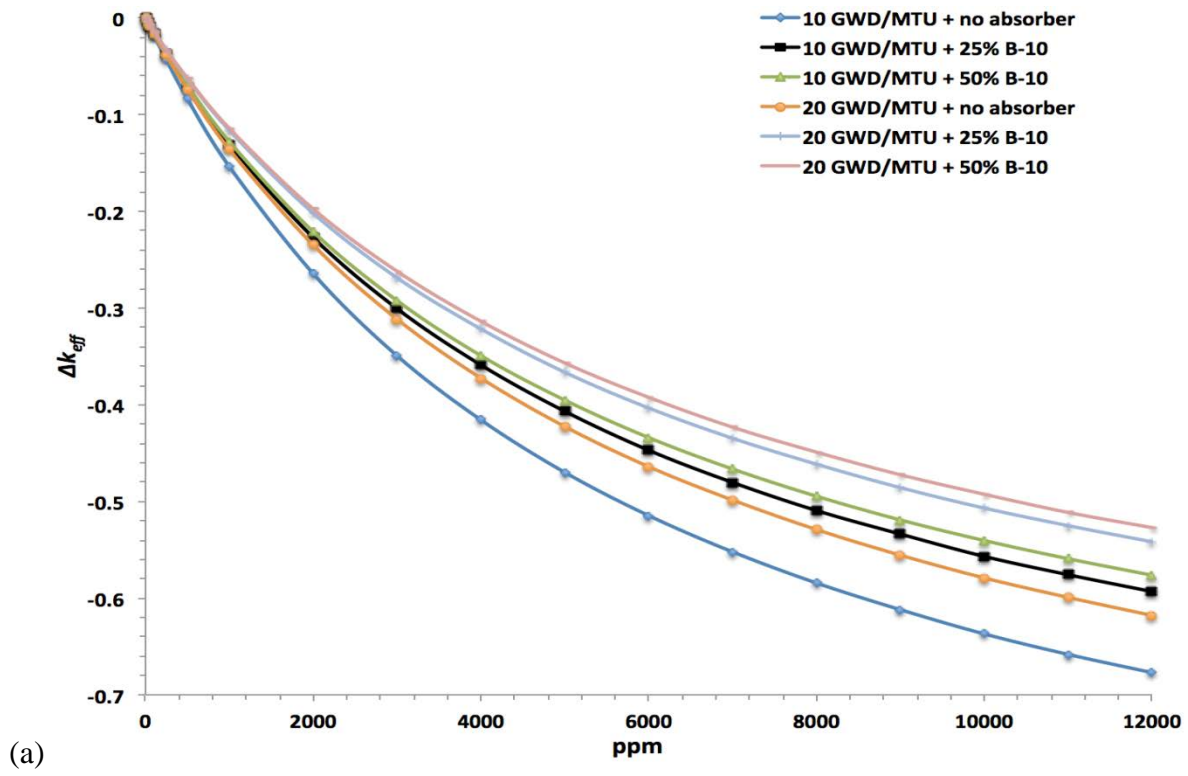
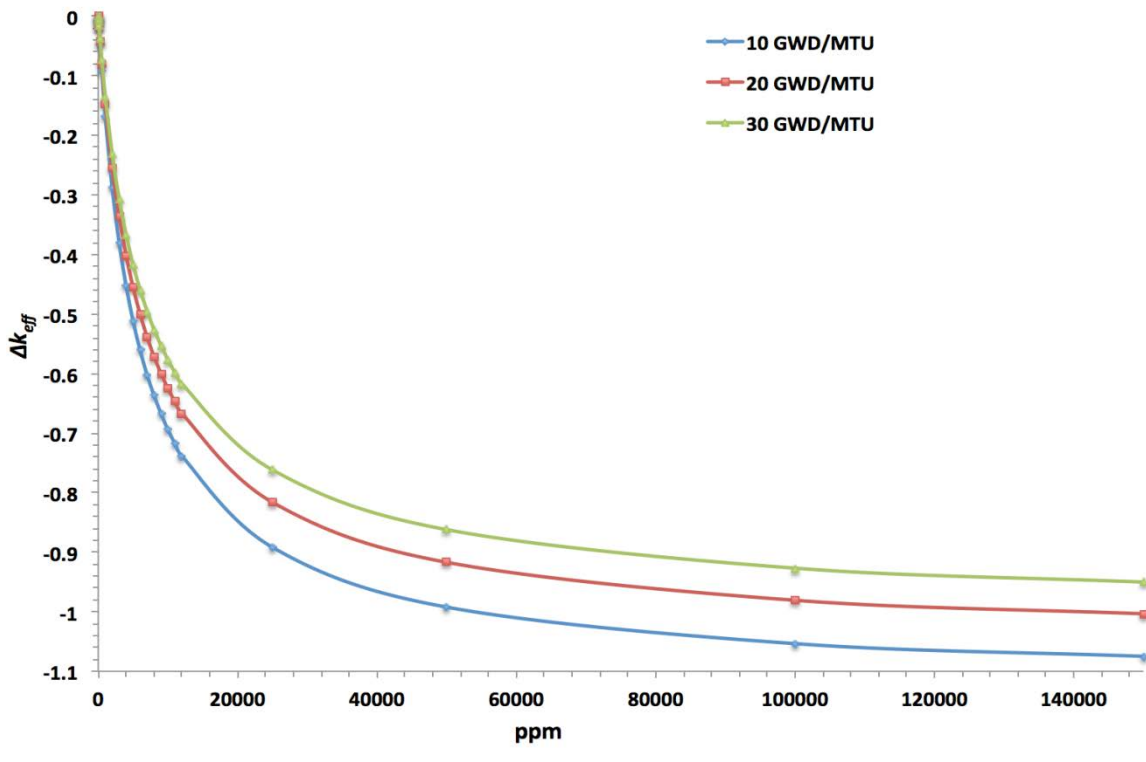


Figure 4-7. Impact on reactivity from lithium concentration in ground water: (a) for different levels of neutron absorber; and (b) for degraded basket configuration



(a)



(b)

Figure 4-8. Impact on reactivity from boron concentration in ground water: (a) for different levels of neutron absorber; and (b) for degraded basket configuration

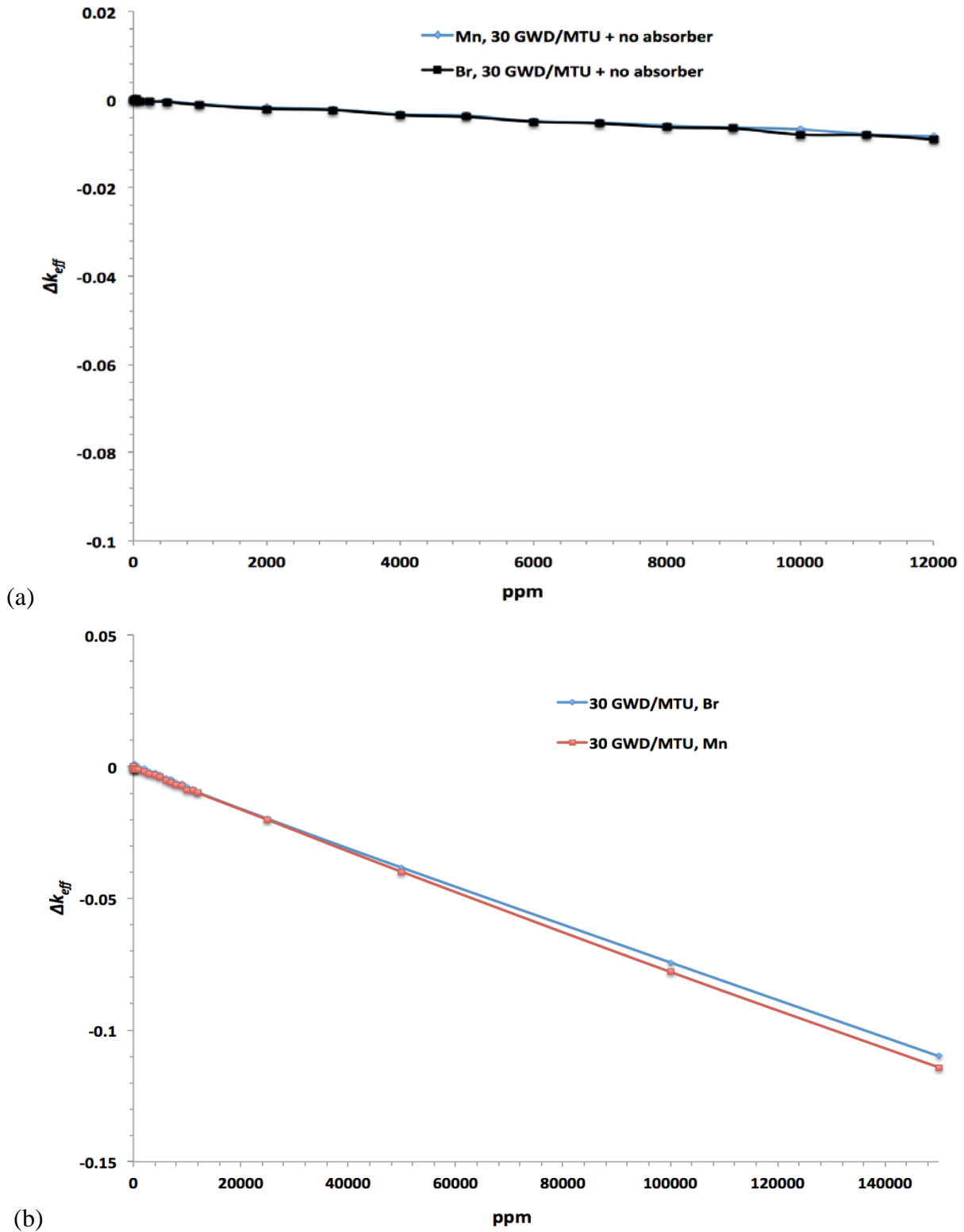


Figure 4-9. Impact on reactivity from Br and Mn concentration in ground water: (a) for complete loss of neutron absorber; and (b) for degraded basket configuration

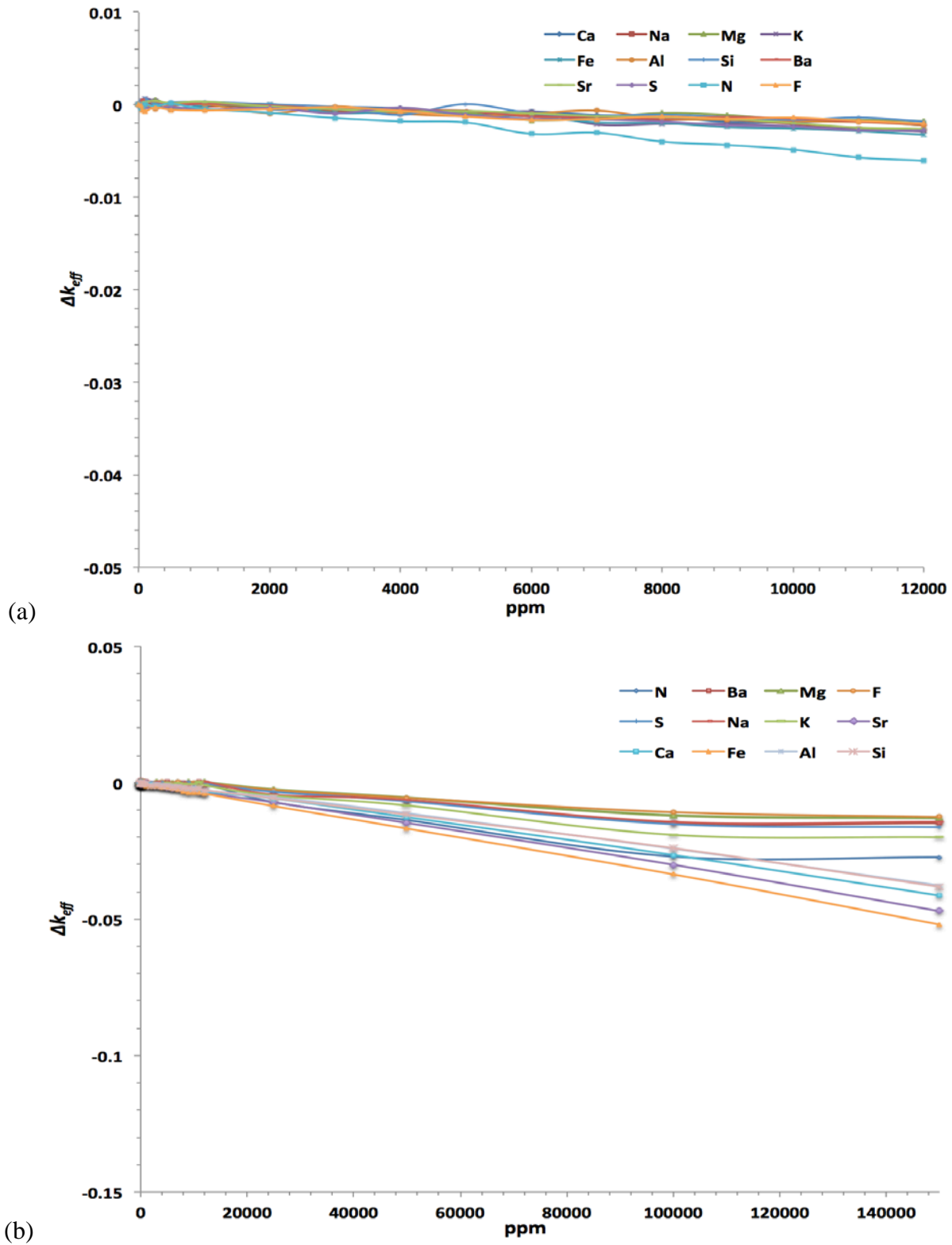


Figure 4-10. Impact on reactivity from other elements in ground water: (a) for complete loss of neutron absorber; and (b) for degraded basket configuration

#### 4.4 High-Reactivity Configuration

A hypothetical high-reactivity configuration is developed to conservatively estimate the minimum concentration of chlorine that would ensure subcriticality. This configuration is not intended to be credible. It consists of intact fuel rods from the fuel assemblies distributed on a triangular pitch within the canister boundary. The following assumptions are used:

- The MPC-32 canister loaded with fuel rods from W17x17WL assemblies. A total of 8,619 rods are used in the model arranged in a hexagonal lattice array (This is slightly more than the 8,448 rods present in 32 17x17 assemblies because of a modeling simplification which is appropriate for this specific representation).
- The fuel rods are modeled as fresh UO<sub>2</sub> fuel with 4 wt% and 5 wt% <sup>235</sup>U enrichment, and also with three uniform loadings with uniform burnup of 10, 20 and 30 GW-d/MTU.

Figure 4-11 shows the canister loaded with distributed fuel rods, while Figure 4-12 presents calculated reactivity as a function of chlorine concentration. A saturated NaCl brine has a concentration of approximately 6 molal (~158,000 ppm on Figure 4-5) which could ensure subcriticality of fresh fuel with 4% enrichment, or irradiated fuel with 5% enrichment and at least 10 GW-d/MTU burnup (Figure 4-12). Because concentrated chloride brine would be needed to ensure subcriticality of these cases, the bounding-type approach is suited mainly for DPC disposal in salt.

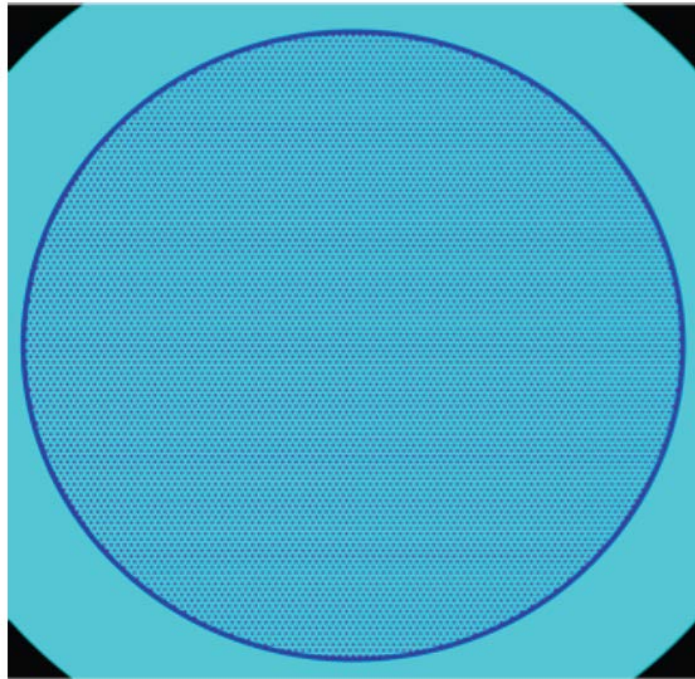
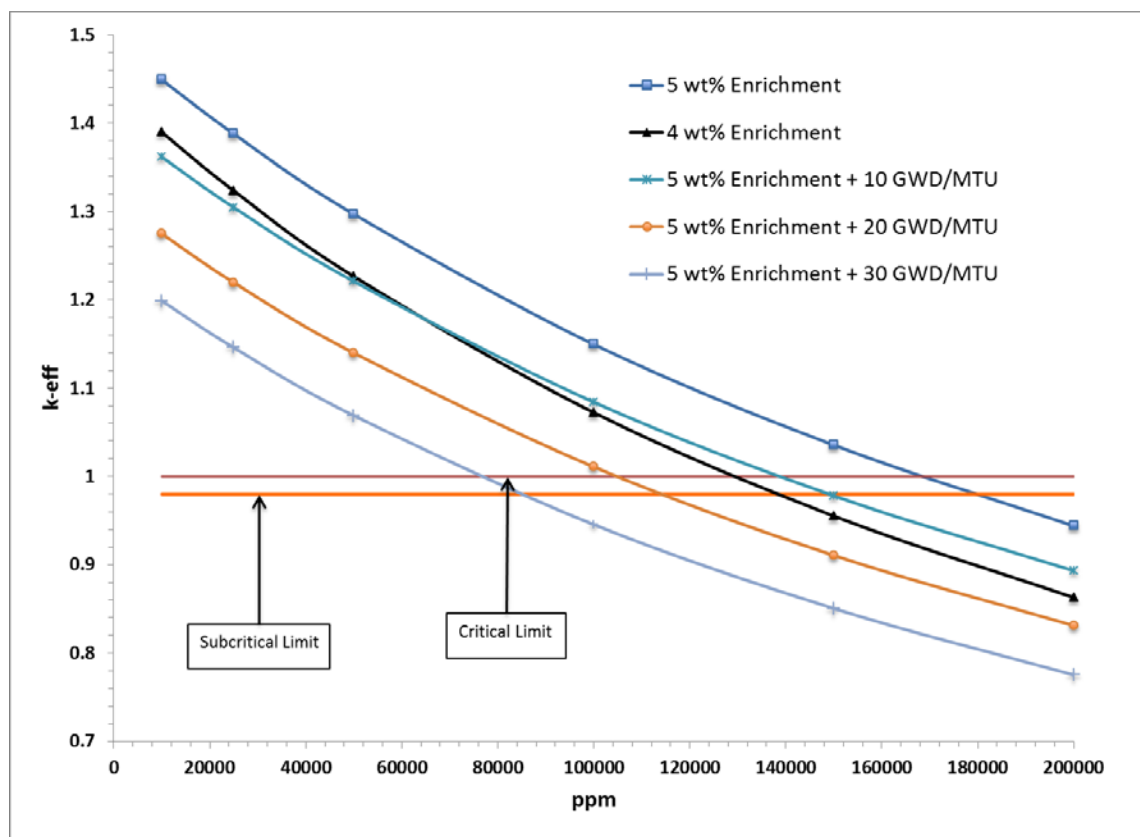


Figure 4-11. High-reactivity configuration as modeled in KENO-VI



Note: Solubility limit for NaCl at 20°C corresponds to 158,000 ppm (see Figure 4-5). Higher chlorine concentrations could possibly be obtained with naturally occurring divalent salts.

Figure 4-12. Reactivity effect from chlorine concentration in flooding ground water, for high-reactivity configuration

#### 4.5 Analysis with Canister-Specific Loading

The FSAR for a particular DPC-based cask system documents the bounding models and calculations used to demonstrate that the system meets the regulatory requirements (10 CFR 71.55 and 71.73). FSAR calculations and approved content specifications are intended to be bounding, and to certify cask systems for a variety of fuel characteristics without placing stringent requirements on where the assemblies are placed in the basket. Therefore, licensed cask systems in as-loaded condition generally have uncredited safety margins. This study simulates the reactivity of existing as-loaded canisters, and also simulates the conditions documented in the FSARs, to estimate the uncredited margins compared to the design basis. These calculations assume that the canister is flooded with fresh water, and that neutron absorber materials (panels) and coated carbon steel structural components are completely degraded and flushed from the system. However, stainless steel structural components are assumed to maintain mechanical integrity through the repository performance period (e.g., 10,000 years). Canisters loaded at five sites (A, B, C, D and E) are investigated.

UNF-ST&DARDS is employed for the as-loaded criticality analyses. UNF-ST&DARDS performs neutronics calculations for each unique assembly design, (e.g., Westinghouse 17×17

OFA or STD), accounting for initial enrichment, burnup, and age. It generates explicit criticality models for each fuel assembly and DPC with the appropriate canister loading pattern identified from canister-specific loading maps. Table 4-2 shows a representative loading map. The same criticality model is used for the design basis and as-loaded calculations. In the following subsections, the Site A evaluations are described first, followed by criticality analyses for Sites B, C, D and E.

Table 4-2. Representative loading map

| Assembly ID | Assembly Average Burnup (MW-d/MTU) | Initial Enrichment | Assembly Location |
|-------------|------------------------------------|--------------------|-------------------|
| NJ03GM      | 10,000                             | 3.062              | 1                 |
| NJ02GF      | 28,000                             | 3.143              | 2                 |
| 1B06        | 25,397                             | 2.673              | 3                 |
| 1B50        | 25,736                             | 2.676              | 4                 |
| NJ01GZ      | 32,000                             | 3.21               | 5                 |
| NJ02F8      | 21,000                             | 3.144              | 6                 |
| NJ030H      | 20,000                             | 3.19               | 7                 |
| 1C07        | 31,914                             | 2.99               | 8                 |
| 1B27        | 35,360                             | 2.67               | 9                 |
| NJ00DN      | 38,016                             | 3.2                | 10                |
| 1B14        | 25,706                             | 2.671              | 11                |
| 1A17        | 16,998                             | 2.007              | 12                |
| 1C24        | 29,320                             | 2.998              | 13                |
| 1B54        | 28,420                             | 2.664              | 14                |
| NJ00E0      | 36,545                             | 3.19               | 15                |
| 1C04        | 35,311                             | 2.993              | 16                |
| 1B20        | 27,611                             | 2.671              | 17                |
| NJ03GA      | 10,000                             | 3.06               | 18                |
| NJ03FA      | 10,000                             | 3.056              | 19                |
| NJ017Y      | 32,000                             | 3.041              | 20                |
| NJ016G      | 34,000                             | 3.041              | 21                |
| NJ00DH      | 28,054                             | 3.188              | 22                |
| NJ0179      | 24,804                             | 3.042              | 23                |
| NJ02FN      | 21,000                             | 3.141              | 24                |

#### 4.5.1 Site A

For this site 60 UMS canister systems from NAC International are analyzed. Each UMS canister (DPC) can contain up to 24 PWR fuel assemblies. The basket is of the tube-and-spacer-disk design. Neutron absorber sheets are attached on the four sides of the fuel tube, and the gaps between adjacent assemblies are flux traps. The Site A DPC basket components are stainless steel, so only the loss-of-absorber degradation scenario is considered. Figure 4-13 shows the 24-assembly DPC basket without neutron absorber, as modeled in SCALE.

The design basis for the UMS system is fresh, 4.2 wt% enriched Westinghouse 17x17 OFA (Optimized Fuel Assembly) assemblies (NAC 2004a). Table 4-3 summarizes the reactivity of the loss-of-absorber configuration with the design basis assembly.

Table 4-3. Calculated  $k_{eff}$  for the Site A DPCs with design basis fuel and loss of absorbers

| Enrichment<br>(w/w $^{235}\text{U}$ ) | Burnup<br>(GW-d/MTU) | $k_{eff}$        |
|---------------------------------------|----------------------|------------------|
| 4.2                                   | 0                    | 1.16584± 0.00040 |

Figure 4-14 presents the calculated  $k_{eff}$  for Site A canisters with the loss-of-absorber scenario, as a function of calendar year. A substantial number of these DPCs are below the subcritical limit ( $k_{eff} = 0.98$ ) defined in this report, for the duration of the simulations, which is attributed to canister-specific uncredited margin. Table 4-4 shows the number of Site A DPCs above the subcritical limit and the maximum  $k_{eff}$ . It also reports the approximate concentration of chlorine needed to maintain subcriticality in those canisters that are above the subcritical limit with fresh water (calculated by linearly interpolating the data in Figure 4-6).

Table 4-4. Final Site A DPC statistics in the year 9999

| Description  | Values            |
|--|-------------------|
| Number of canisters  | 60                |
| Number of canisters with $k_{eff} > 0.98$ (design basis loading)     | 60                |
| Number of canisters with $k_{eff} > 0.98$ (as-loaded)                | 4                 |
| Maximum $k_{eff}$  | 1.00696           |
| Approximate chlorine requirement (linear interpolation) <sup>a</sup> | 13,500 ppm (mg/L) |

Note: Chlorine reactivity worth based on a 32-assembly configuration is assumed to be applicable for this DPC.

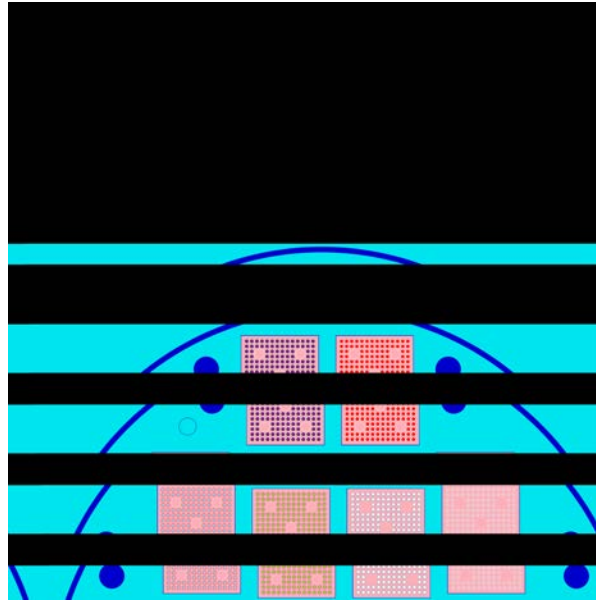


Figure 4-13. NAC UMS 24-assembly basket without neutron absorbers as modeled in SCALE

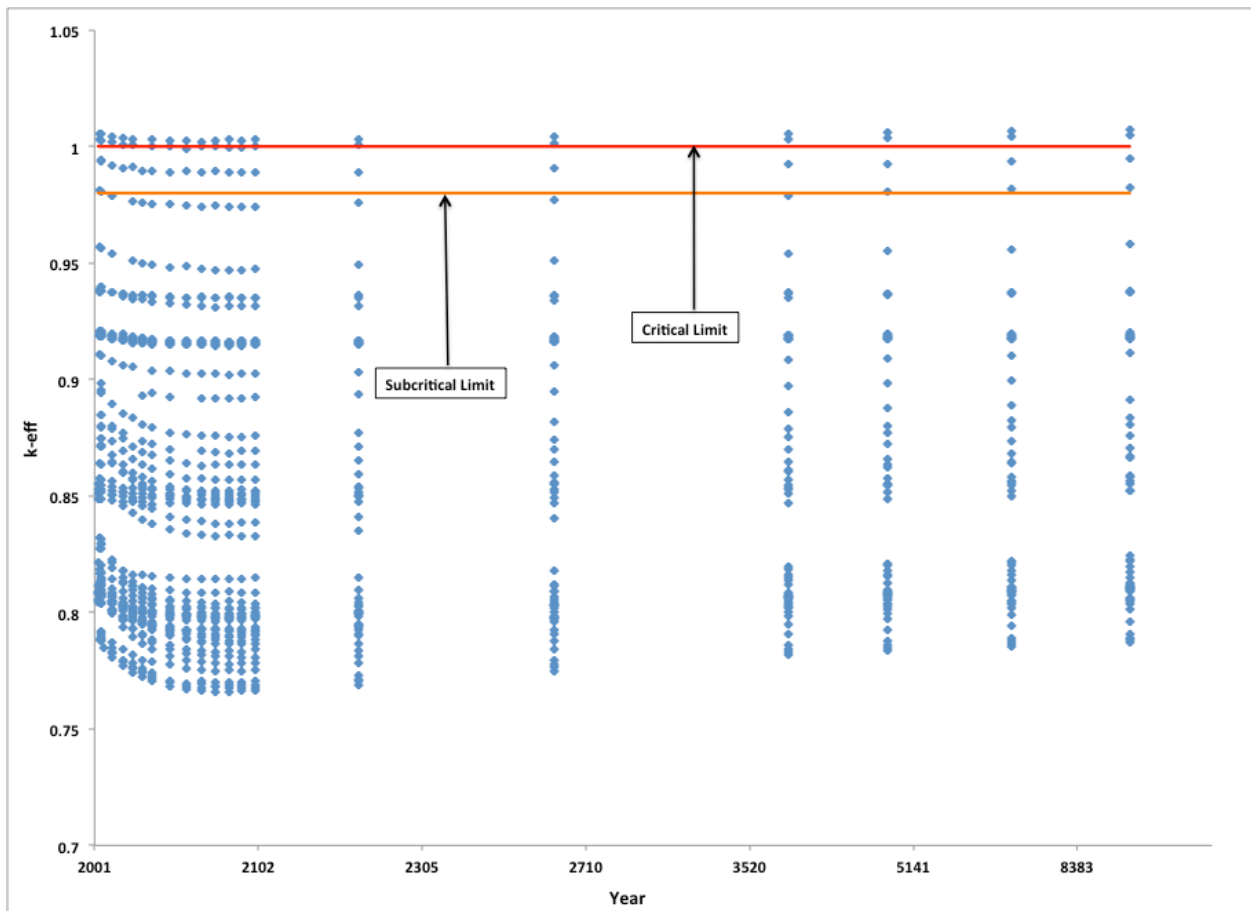


Figure 4-14. Calculated maximum neutron multiplication factor ( $k_{eff}$ ) vs. calendar year, for as-loaded Site A 24-assembly DPCs with loss-of-absorber configuration

### 4.5.2 Site B

For Site B, 39 DPCs from NAC International are analyzed. The DPC fuel basket at Site B is available for both a 26 and 24 assembly configuration. These two baskets are identical except that the top weldment of the 24-assembly configuration consists of 24 fuel tube penetrations (NAC 2004b). The 24-assembly basket is designed to accommodate higher enriched fuel assemblies than the 26-assembly basket. Site B baskets are made of stainless steel, so only the loss-of-absorber degradation scenario is considered. Table 4-5 lists the number of each type of DPC loaded at the Site B independent spent fuel storage installation (ISFSI). Figure 4-15 illustrates the 26-assembly basket without neutron absorber panels, while Figure 4-16 represents the 24-assembly basket without neutron absorber panels, as modeled in SCALE.

Table 4-5. Type and number of DPCs in the Site B ISFSI

| Site B DPC Configuration | Count |
|--------------------------|-------|
| 26-assembly              | 36    |
| 24-assembly              | 3     |

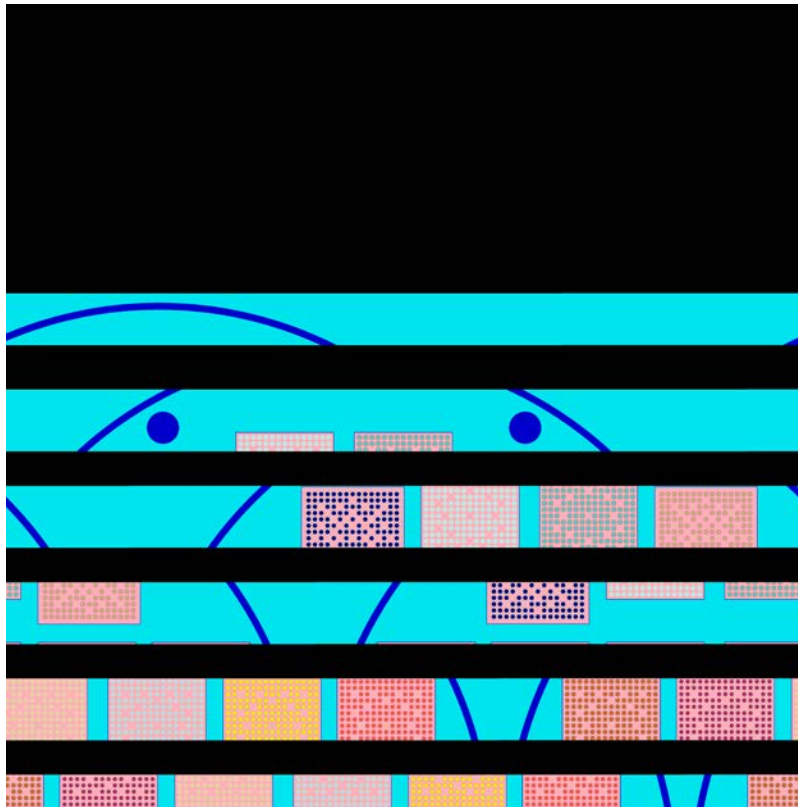


Figure 4-15. Radial layout of the Site B 26-assembly basket without neutron absorbers as modeled in SCALE

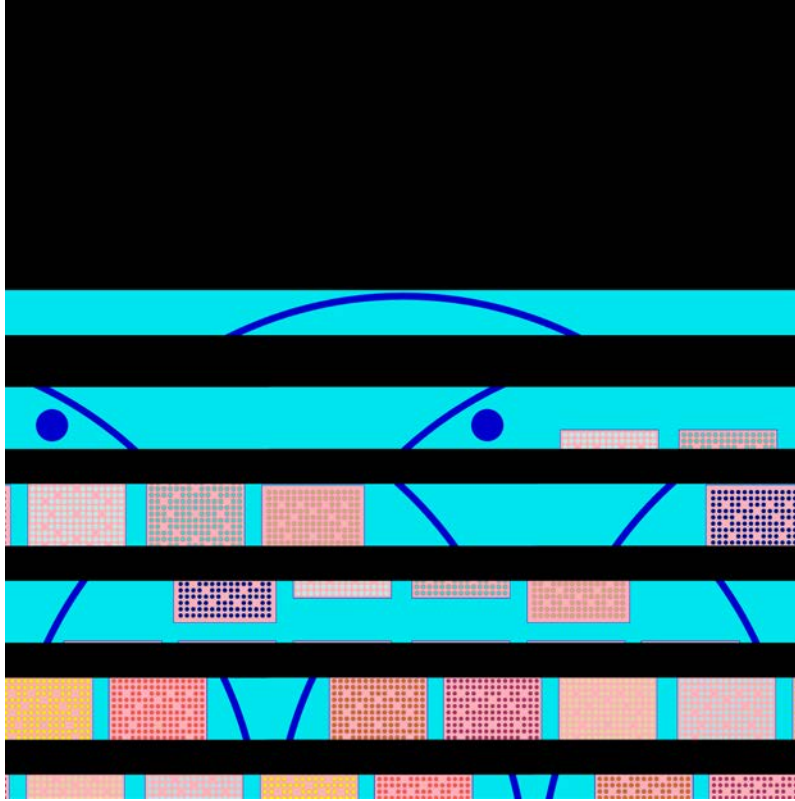


Figure 4-16. Radial layout of the Site B 24-assembly basket without neutron absorbers as modeled in SCALE

The Site B DPC licensing basis evaluations are performed using fresh fuel assemblies, with fuel characteristics defined as follows (NAC 2004b):

- 26-assembly basket:
  - 15 × 15 Zircaloy-clad fuel (Babcock and Wilcox or B&W) up to 3.93 wt% initial enrichment
  - 15 × 15 stainless steel-clad fuel up to 4.03 wt% initial enrichment. However, the stainless steel-clad assembly is bounded by the 3.93 wt% Zircaloy-clad fuel.
- 24-assembly basket:
  - 15 × 15 Zircaloy-clad fuel (Westinghouse Vantage 5H) up to 4.61 wt% initial enrichment
  - 24-assembly loading is allowed in the 26-assembly basket

Table 4-6 summarizes the reactivity of these DPCs for the loss-of-absorber scenario with the design basis loading.

Table 4-6. Calculated  $k_{eff}$  for the Site B DPCs with design basis fuel and loss of absorbers

| DPC Type    | Enrichment<br>(w/w $^{235}\text{U}$ ) | Burnup<br>(GW-d/MTU) | $k_{eff}$             |
|-------------|---------------------------------------|----------------------|-----------------------|
| 24-assembly | 4.61                                  | 0                    | $1.14546 \pm 0.00023$ |
| 26-assembly | 3.93                                  | 0                    | $1.14809 \pm 0.00024$ |

Figure 4-17 shows the calculated  $k_{eff}$  for Site B DPCs with the loss-of-absorber scenario, as a function of calendar year. A substantial number of these DPCs are below the subcritical limit ( $k_{eff} = 0.98$ ) defined in this report, for the duration of the simulations, which is attributed to canister-specific uncredited margin. Table 4-7 reports the number of Site B DPCs above the subcritical limit and the maximum  $k_{eff}$ . It also reports the approximate concentration of chlorine needed to maintain subcriticality in those canisters that are above the subcritical limit with fresh water (calculated by linearly interpolating the data in Figure 4-6).

Table 4-7. Final Site B DPC statistics in the year 9999

| Description  | Values            |
|--|-------------------|
| Number of canisters  | 39                |
| Number of canisters with $k_{eff} > 0.98$ (design basis loading)     | 39                |
| Number of canisters with $k_{eff} > 0.98$ (as-loaded)                | 3                 |
| Maximum $k_{eff}$  | 1.00118           |
| Approximate chlorine requirement (linear interpolation) <sup>a</sup> | 11,000 ppm (mg/L) |

Note: Chlorine reactivity worth based on a 32-assembly configuration is assumed to be applicable for this DPC.

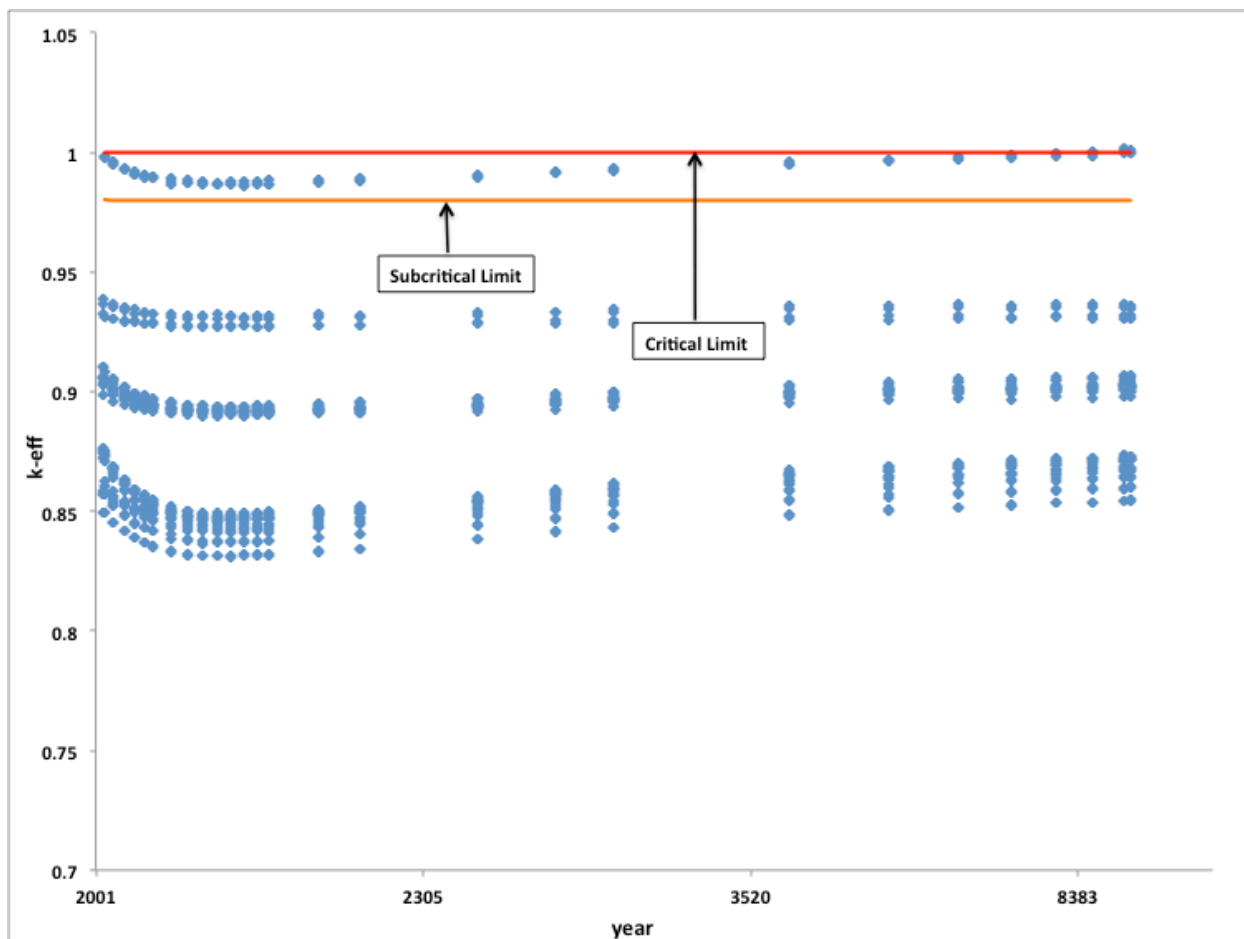


Figure 4-17. Calculated maximum neutron multiplication factor ( $k_{eff}$ ) vs. calendar year, for as-loaded Site B DPCs with loss of neutron absorber

### 4.5.3 Site C

For Site C, 20 NUHOMS as-loaded dry-shielded canisters (DSCs) (Transnuclear 2003) are evaluated. These DPCs can accommodate 24 intact PWR assemblies. Design basis criticality analyses are performed applying 3.43 wt% enriched B&W (Babcock and Wilcox)  $15 \times 15$  Mark B4 PWR intact fuel assemblies (Transnuclear 2003).

Fuel assemblies inside the DPCs are maintained in place by thin-wall guide sleeves. Each guide sleeve is made from stainless steel, with neutron absorber panels attached to each side of the sleeve that faces another assembly. The gaps between the neutron absorber panels facing each other form the flux-trap design. The guide sleeves are arranged inside the canister using radial spacer disks, made of coated carbon steel, to maintain the flux-trap configuration (Figure 4-18). Because of the carbon steel spacer disks, the following two degradation scenarios are considered:

- **Loss-of-Absorber** – The neutron absorber plates are replaced by fresh water. It is assumed that the degraded absorber materials are flushed from the canister while the guide sleeves are still in their original positions supported by spacer disks. This hypothetical configuration could result if the fuel assemblies, stainless steel guide

sleeves, and coated carbon steel spacer disks are more corrosion resistant than the neutron absorber. Figure 4-19(a) depicts the cross-section of the canister as modeled in SCALE, while Figure 4-19(b) presents calculated  $k_{eff}$  for as-loaded canisters as a function of calendar year. All of these DPCs are below the subcritical limit ( $k_{eff} = 0.98$ ) defined for this report, for the duration of the simulations. Note that the calculated  $k_{eff}$  for this scenario with design basis fuel is greater than 1 (Table 4-8).

- **Degraded Basket** – The loss-of-absorber configuration is extended to include complete degradation of the spacer disks, resulting in a close-packed configuration of collapsed guide sleeves. The degraded disk material is replaced by fresh water. Figure 4-20(a) illustrates the cross-section of the collapsed basket as modeled in KENO-VI. The results for as-loaded canisters are shown in Figure 4-20(b), which shows that  $k_{eff}$  values associated with some of the DPCs are above the subcritical limit defined in this report. An analysis of this configuration using the design basis fuel (Table 4-8) shows that  $k_{eff} > 1$  for all the DPCs.

Table 4-9 summarizes Site C DPC results for the two degradation scenarios, including the estimated chlorine concentration needed to ensure subcriticality.

Table 4-8. Calculated  $k_{eff}$  for the Site C DPCs with loss-of-absorber and basket degradation scenarios, and design basis fuel

| Degradation Scenario                      | Enrichment (w/w <sup>235</sup> U) | Burnup (GW-d/MTU) | $k_{eff}$         |
|---|-----------------------------------|-------------------|-------------------|
| Loss of neutron absorber                  | 3.43                              | 0                 | 1.09358 ± 0.00024 |
| Loss of neutron absorber and spacer disks | 3.43                              | 0                 | 1.27754 ± 0.00019 |

Table 4-9. Final Site C statistics in the year 9999

| Description  | Values for Loss-of-Absorber | Values for Degraded Basket |
|--|-----------------------------|----------------------------|
| Number of DSCs   | 20                          | 20                         |
| Number of DSCs with $k_{eff} > 0.98$ (design basis loading)          | 20                          | 20                         |
| Number of DSCs with $k_{eff} > 0.98$ (as-loaded)                     | 0                           | 18                         |
| Maximum $k_{eff}$  | 0.92691                     | 1.04468                    |
| Approximate chlorine requirement (linear interpolation) <sup>A</sup> | NA                          | 32,500 ppm (mg/L)          |

<sup>A</sup> Chlorine reactivity worth based on a 32-assembly configuration is assumed to be applicable for this DPC.

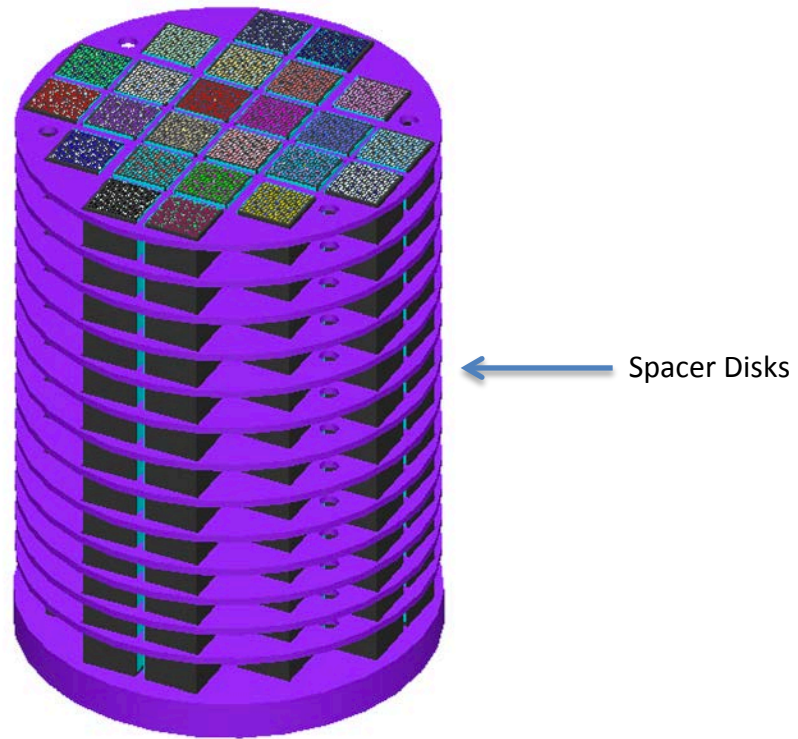


Figure 4-18. Isometric view of the Site C DPC as modeled in SCALE

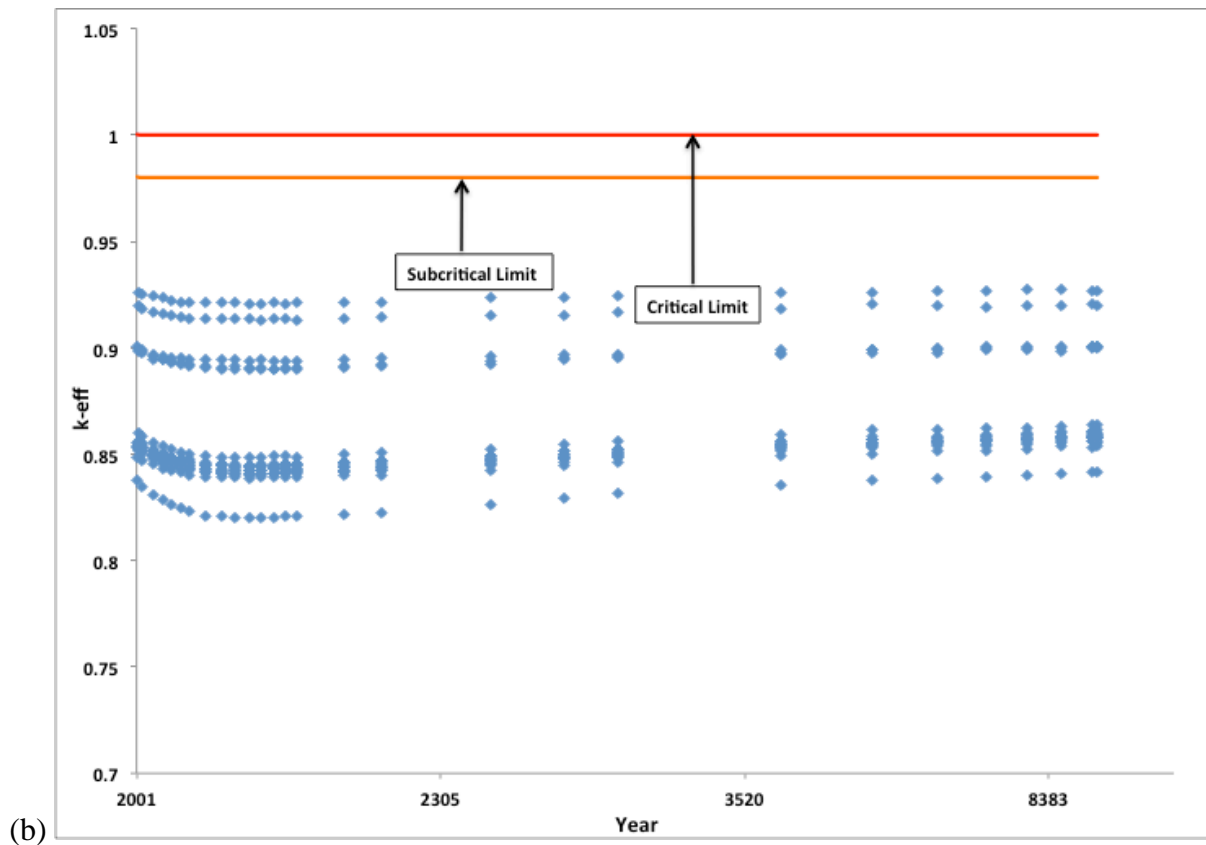
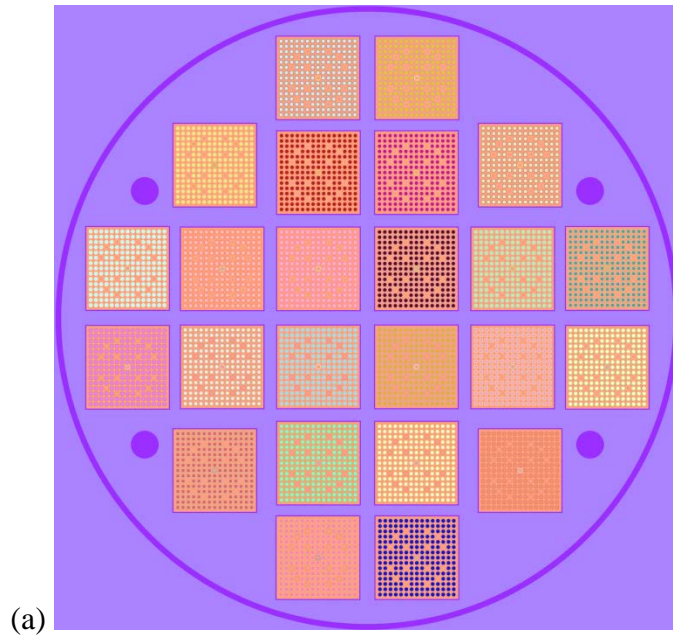


Figure 4-19. Calculated maximum neutron multiplication factor ( $k_{eff}$ ) for Site C DPCs: (a) loss of absorber configuration as modeled in KENO-VI; and (b)  $k_{eff}$  vs. calendar year, based on actual loading

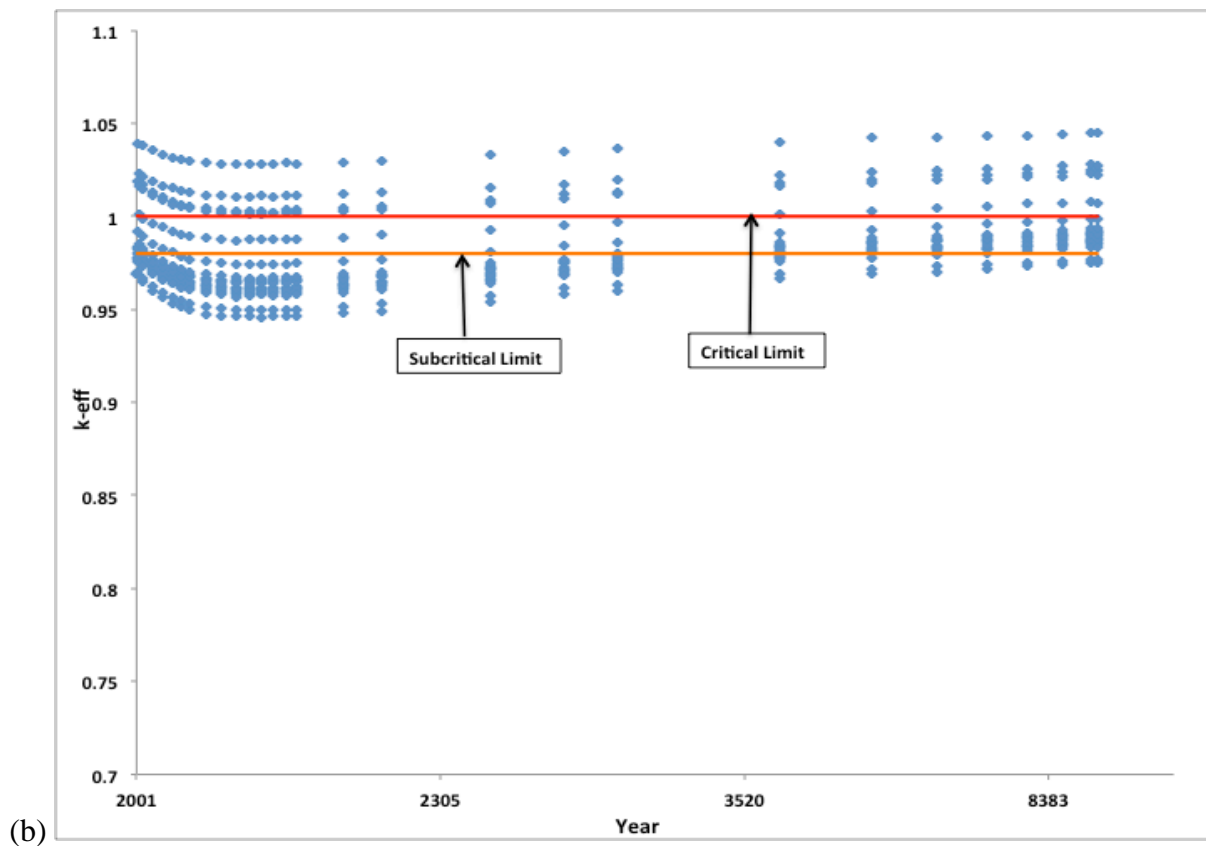
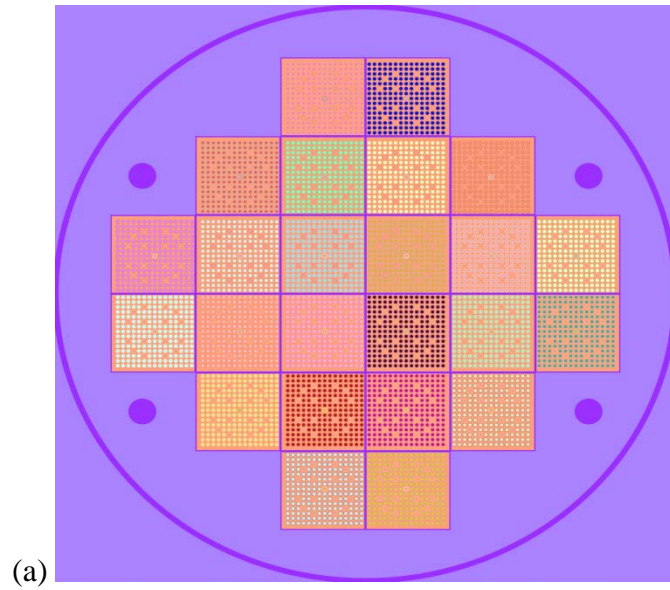


Figure 4-20. Calculated maximum neutron multiplication factor ( $k_{eff}$ ) for Site C DPCs: (a) degraded spacer disks configuration as modeled in KENO-VI; and (b)  $k_{eff}$  vs. calendar year, based on actual loading

#### 4.5.4 Site D

For Site D, 34 MPC-24E/EF canisters from Holtec International (Holtec 2010a) are analyzed. This DPC can accommodate up to 24 PWR fuel assemblies. The basket is of stainless steel construction, so only the loss-of-absorber scenario is considered here. Figure 4-21 illustrates the MPC-24E/EF basket without neutron absorber plates, as modeled in SCALE.

Design basis criticality analyses are performed applying 3.7 wt% enriched W17x17 STD (standard) assemblies (Holtec 2010a). Table 4-10 shows calculated reactivity for the loss-of-absorber scenario with the design basis assembly.

Table 4-10. Calculated  $k_{eff}$  for the Site D DPCs with design basis fuel and loss of absorbers

| Enrichment<br>(w/w $^{235}\text{U}$ ) | Burnup<br>(GW-d/MTU) | $k_{eff}$         |
|---------------------------------------|----------------------|-------------------|
| 3.7                                   | 0                    | 1.00569 ± 0.00020 |

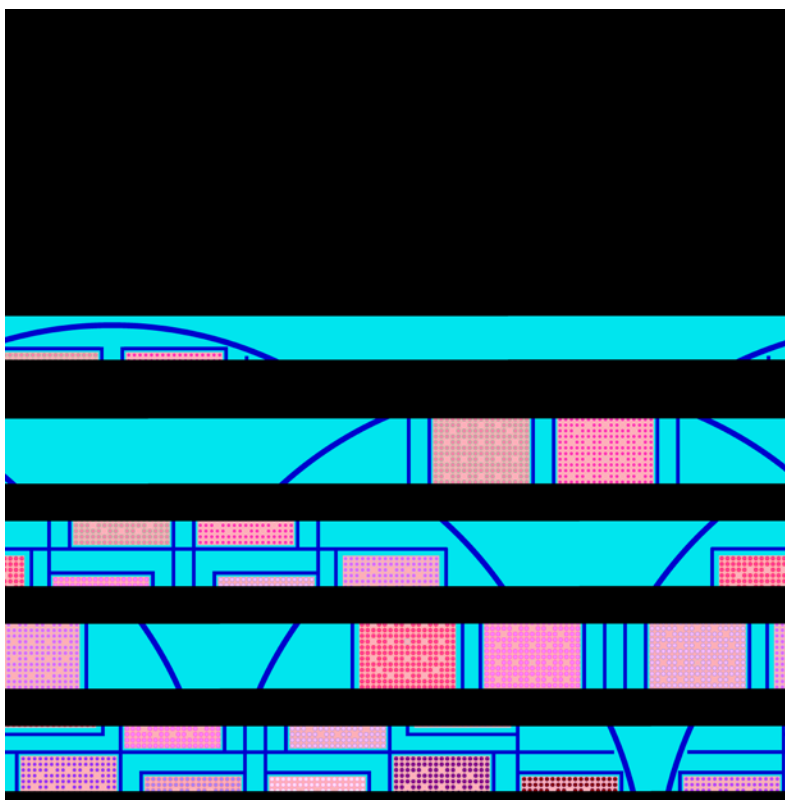


Figure 4-21. Radial layout of the MPC-24E/EF without neutron absorbers as modeled in SCALE

Figure 4-22 presents calculated  $k_{eff}$  for as-loaded canisters, with the loss-of-absorber scenario, as a function of calendar year. All of these DPCs are below the subcritical limit ( $k_{eff} = 0.98$ ) for the duration of the simulations, which is attributed to canister-specific uncredited margin. Note that

the calculated  $k_{eff}$  for this degradation scenario with design basis fuel is greater than 1 (Table 4-10). Table 4-11 summarizes the Site D results.

Table 4-11. Final Site D statistics in the year 9999

| Description  | Values  |
|--|---------|
| Number of canisters  | 34      |
| Number of canisters with $k_{eff} > 0.98$ (design basis loading) | 34      |
| Number of canisters with $k_{eff} > 0.98$ (as-loaded)            | 0       |
| Maximum $k_{eff}$  | 0.90476 |
| Approximate chlorine requirement (linear interpolation)          | NA      |

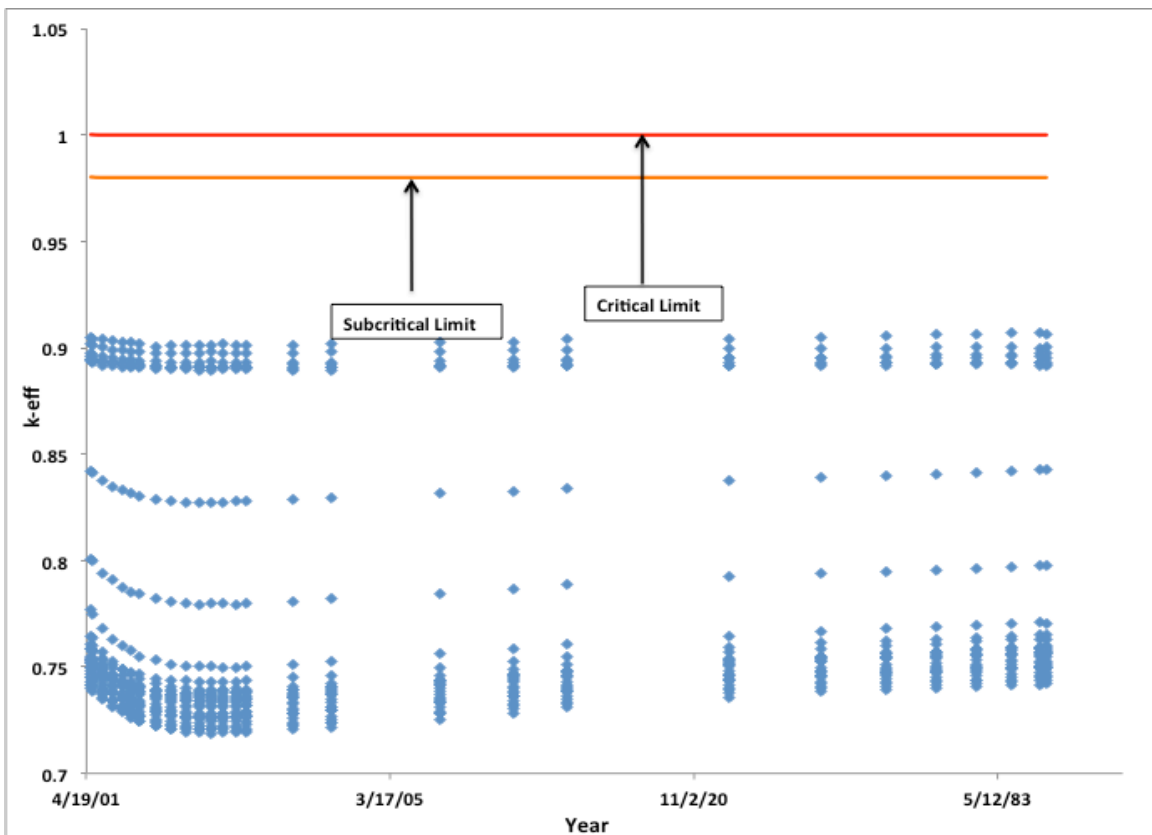


Figure 4-22. Calculated maximum neutron multiplication factor ( $k_{eff}$ ) vs. calendar year, for as-loaded Site D DPCs with loss of neutron absorber

#### 4.5.5 Site E

Site E is the only operating plant investigated in this analysis. It uses the HI-STORM 100 system from Holtec International (Holtec 2010b) with MPC-32 canisters. The MPC-32 is an all stainless steel canister that can accommodate 32 PWR assemblies and uses an egg-crate basket design with a single neutron absorber panel between adjacent assemblies. Accordingly, loss of neutron absorber is the only degradation scenario considered for the MPC-32. Figure 4-23 presents a cross-section view of the MPC-32 as modeled in SCALE. This analysis evaluated 26 loaded MPC-32 canisters at Site E.

Because of its high density, the MPC-32 is licensed for transportation by applying burnup credit for criticality analysis (NRC 2010b). Table 4-12 presents the design basis reactivity for the loss-of-absorber scenario.

Table 4-12. Calculated  $k_{eff}$  for the Site E DPCs with design basis fuel and loss of absorbers

| Fuel Type <sup>A</sup> | Configuration <sup>A</sup> | Enrichment<br>(w/w <sup>235</sup> U) | Burnup<br>(GW-d/MTU) | $k_{eff}$         |
|------------------------|----------------------------|--------------------------------------|----------------------|-------------------|
| 17x17A,B,C             | B                          | 4.0                                  | 49                   | 1.06812 ± 0.00040 |

<sup>A</sup> Source: NRC Certificate Number 9261, Rev. 8, *Certificate of Compliance for Radioactive Material Packages – HI-STAR 100*.

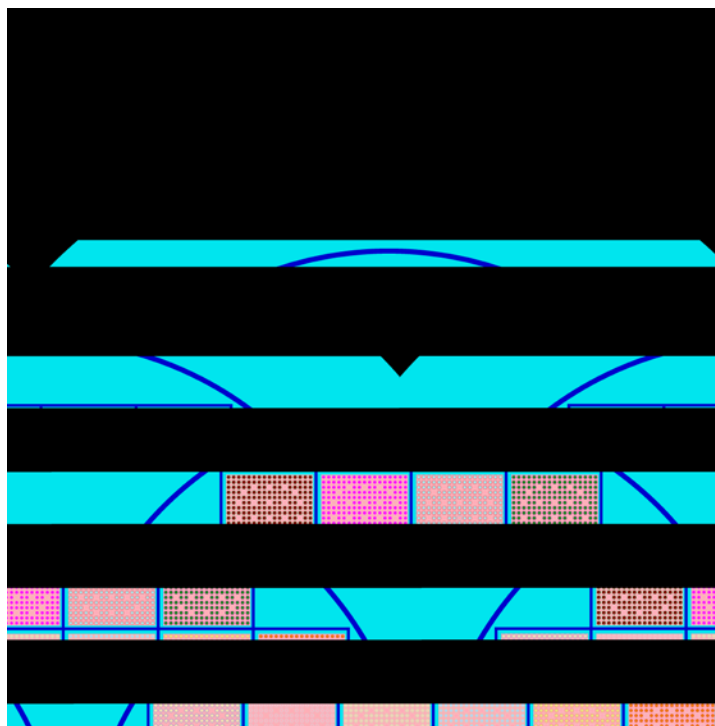


Figure 4-23. Radial layout of the MPC-32 without neutron absorbers as modeled in SCALE

Figure 4-24 presents the calculated  $k_{eff}$  for as-loaded DPCs, with the loss-of-absorber scenario, as a function of calendar year. Note that components in the guide tubes (Section 4.6), if present, are

credited in the calculations. Figure 4-24 shows that some of these DPCs remain below the subcritical limit defined in this report ( $k_{eff} = 0.98$ ) for the duration of the simulations. Note that the calculated  $k_{eff}$  for this scenario with design basis fuel is greater than 1 (Table 4-12). Table 4-13 shows the number of Site E DPCs above the subcritical limit for the loss-of-absorber scenario, and the maximum  $k_{eff}$ . It also indicates the approximate concentration of chlorine required to maintain subcritical condition in the 16 identified DPCs that are above the subcritical limit when flooded with fresh water.

Table 4-13. Final Site E statistics in the year 9999

| Description  | Values            |
|--|-------------------|
| Number of canisters  | 26                |
| Number of canisters with $k_{eff} > 0.98$ (design basis loading)     | 26                |
| Number of canisters with $k_{eff} > 0.98$ (as-loaded)                | 16                |
| Maximum $k_{eff}$  | 1.00623           |
| Approximate chlorine requirement (linear interpolation) <sup>A</sup> | 13,500 ppm (mg/L) |

<sup>A</sup> Chlorine reactivity worth based on a 32-assembly configuration is assumed to be applicable for this DPC.

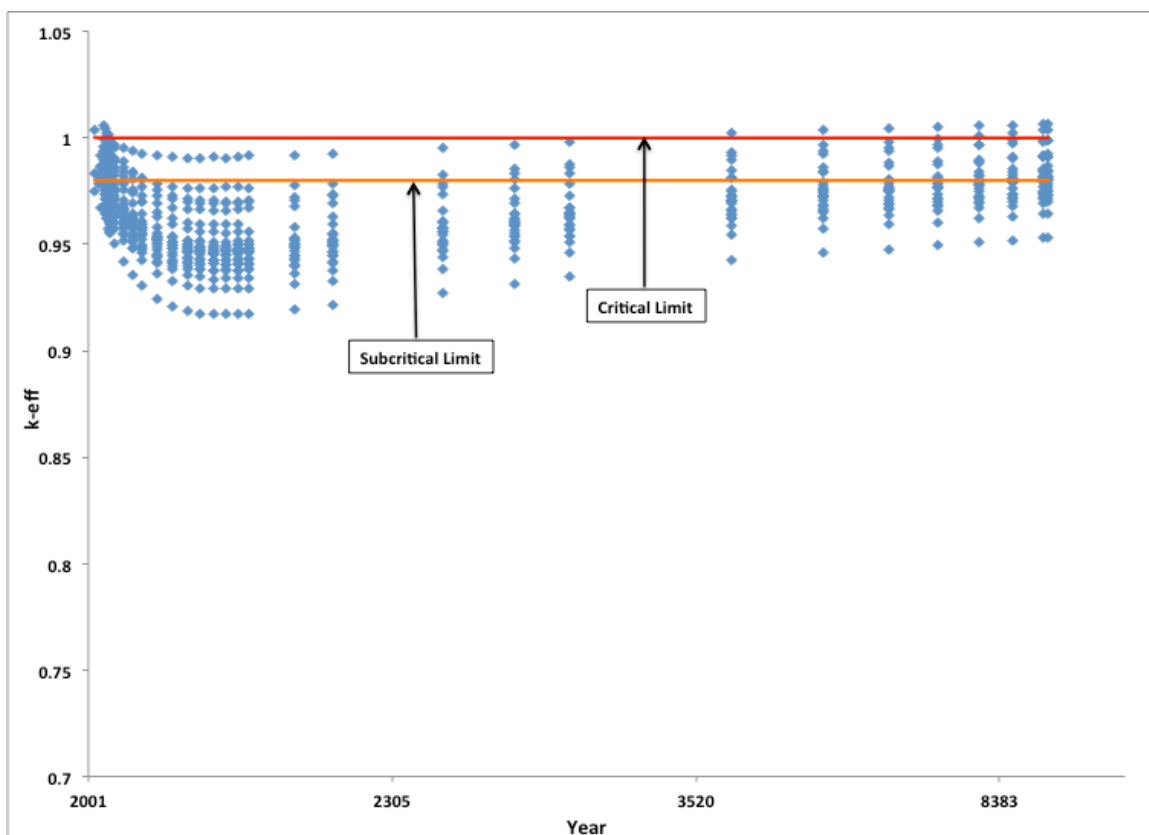


Figure 4-24. Calculated maximum neutron multiplication factor ( $k_{eff}$ ) vs. calendar year, for as-loaded Site E DPCs with loss of neutron absorber

#### 4.6 Component Credit Analysis

Many plant operators are currently placing non-fuel components such as burnable poison rods and control rods into DPCs for storage. Regulatory guidance (NRC 2002) allows that materials that are positioned or operated within the envelope of a fuel assembly during reactor operation may be approved for storage in a DPC. The guidance also states: "...credit for water displacement may be taken provided adequate structural integrity and placement under accident conditions is demonstrated."

The typical non-fuel components that are currently stored in the guide tubes of used fuel assemblies include burnable poison rod assemblies (BPRAs), wet annular burnable absorbers (WABAs), and control rod assemblies (CRAs). BPRAs rods are either solid or annular (with dry annular gap), while WABAs contain wet annular gaps. CRAs typically contain solid control rods. The number of rods (or rodlets) in each type of component can also vary (e.g., for W17x17 PWR assemblies the number of component rods can vary from 4 to 24).

Some of the DPCs at Site E contain BPRAs and WABA assemblies with 4 to 24 rods inserted, including asymmetrical configurations (e.g., with 9 rods). The remainder of this section describes how these components are represented in criticality calculations presented above for Site E. The approach is simple because the available information does not completely describe the component geometry and composition. These components are credited only for water displacement. The following assumptions are used:

- WABA design is considered for all the components as it provides the least amount of water displacement because of the wet annular gap. WABA radial dimensions are obtained from CRWMS M&O (1998). Figure 4-25 illustrates a cross section view of the WABA model used for the Site E DPCs.
- As a simplification, WABAs are modeled to cover the entire axial length of the active fuel. Although a WABA is longer than the active fuel length when placed in the guide tube, the bottom end of a WABA is about 11 cm higher than that of the active fuel. The upper part of the WABA above the active fuel height is not credited for water displacement.
- 16 WABA rods are considered for all components irrespective of the actual number of rods.
- The absorber material (e.g.,  $\text{Al}_2\text{O}_3\text{-B}_4\text{C}$ ) is modeled as void.

This approach can be refined in the future to include the actual number and geometry of the components when more data are available. Table 4-14 presents the typical reactivity reduction obtained from the water displacement by the components in the guide tubes. A reactivity reduction of approximately  $0.06 \Delta k_{eff}$  is obtained with the simplified approach described here.

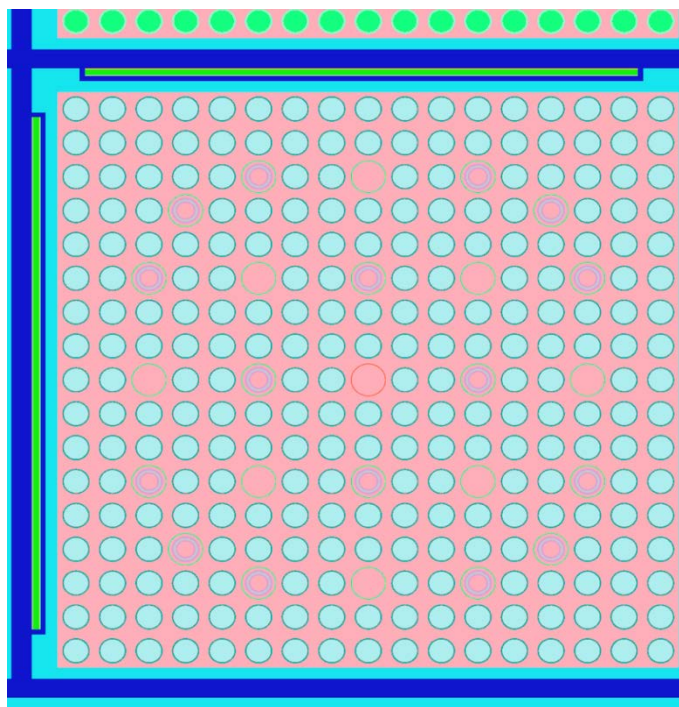


Figure 4-25. Radial view of WABAs in guide tubes as modeled in SCALE for Site E DPCs

Table 4-14. Reactivity reduction from non-fuel assembly components for Site E DPCs with loss of neutron absorber

| Site E DPC | $k_{eff}$ without Component @ Calendar 9999 | $k_{eff}$ with Component @ Calendar 9999 | $\Delta k$ |
|------------|---|--|------------|
| MPC-005    | 1.0048                                      | 0.99868                                  | 0.00612    |
| MPC-006    | 0.9808                                      | 0.97466                                  | 0.00614    |
| MPC-0109   | 0.9705                                      | 0.96418                                  | 0.00632    |
| MPC-0110   | 0.95872                                     | 0.95314                                  | 0.00558    |
| MPC-0177   | 0.99812                                     | 0.99254                                  | 0.00558    |
| MPC-068    | 0.98747                                     | 0.9818                                   | 0.00567    |
| MPC-070    | 0.97858                                     | 0.97276                                  | 0.00582    |

#### 4.7 Summary and Conclusions

Direct disposal of SNF currently stored in DPCs, would involve a disposal overpack designed to provide support and containment in the specific disposal environment. There is a small probability that one or more of these overpacks could fail within the regulatory performance period for disposal, e.g., within 10,000 years.(SNL 2007, Sections 6.4 and 6.5) This could then expose the DPC and its contents to ground water for thousands of years, with the possibility of flooding. Neutron absorber materials used in current DPC designs are typically aluminum based, and would readily degrade under long-term exposure to ground water. Further, some DPCs have

internal structural components made from materials such as aluminum or low-alloy steel, which would also degrade. Note that if ground water can be excluded from waste packages, there is virtually no potential for criticality.

Criticality analyses are performed assuming flooding with fresh water, for two canister degradation scenarios: loss-of-absorber and basket degradation. Five types of DPCs, presently located at five respective dry storage sites, are analyzed. The licensing basis for DPCs involves criticality analysis for the event of flooding. Fuel characteristics assumed for that analysis are generally conservative compared to fuel that is actually loaded. The difference is uncredited reactivity margin, mainly associated with enrichment, burnup, and loading positions for assemblies in as-loaded DPCs.

In the analysis, neutron absorber and structural materials degraded by corrosion are replaced by water moderator, and corrosion products are assumed to be flushed away. For the basket degradation scenario fuel assemblies are relocated so they are in close contact, forming a cylindrical array. For some DPCs (Site E) credit for water displacement by control rods and similar components of the fuel assemblies is included.

Another set of analyses is used to generate reactivity reduction curves for a representative DPC flooded with ground water, as functions of the concentrations of various aqueous species. Available groundwater data indicates that chlorine (as chloride) is the only naturally abundant, neutron-absorbing element in ground water that can provide significant reduction of reactivity. The chloride concentration in seawater (approximately 19,400 ppm chloride by weight; Stumm and Morgan 1981) may be enough to ensure subcriticality of some DPCs (Table 4-15). More concentrated salt brines could ensure subcriticality for all DPCs, a result which could be useful for DPC disposal in salt.

Table 4-15 summarizes the analyses reported in this section. Of the 179 DPCs analyzed all would exceed the subcritical limit ( $k_{eff} > 0.98$ ) with loss of neutron absorbers, if loaded with the design-basis fuel used for licensing. Using as-loaded fuel characteristics and burnup credit (28 nuclides) only 23 of the 179 would exceed the subcritical limit for the loss-of-absorber scenario, unless the chlorine concentration of flooding ground water is at least 13,500 ppm (less than seawater at 19,400 ppm chloride). For the Site C DPCs, 18 of the 20 DPCs would exceed the subcritical limit with the basket degradation scenario, unless the chlorine concentration is at least 32,500 ppm. The prevalence of chloride concentrations in ground waters from crystalline and sedimentary settings is discussed in Section 5. Many geologic settings are potentially viable for waste disposal in salt deposits, and in old, deep crystalline rock formations associated with brines. However, if marine sediments containing seawater are included (i.e., lower chlorine concentration required) the number of potentially viable settings could be much greater. More than 1,900 DPCs have already been loaded in the U.S., so more analysis is needed to extend these results to a greater sample.

The analyses performed in this report indicate that subcriticality can be demonstrated for typical DPCs by detailed canister-specific analysis and by crediting the available ground water composition. However, better understanding of the corrosion and physical degradation of basket materials, as well as the probability of flooding, could significantly influence the analysis of criticality.

**Criticality Consequence Analysis** – The possibility of one or more criticality events does not by itself lead to a conclusion that DPC direct disposal is not technically feasible. Including

criticality consequence analysis in the performance assessment for a geologic repository, is allowed in the current licensing framework (DOE 2003) and is part of a general strategy for screening criticality events (Scaglione et al. 2014).

The primary attributes of a criticality event in a DPC loaded with commercial SNF, are concerned with how the boundary conditions could affect reactivity (Scaglione et al. 2014):

- **Under- or Optimal Moderation** – Because the only means to a criticality event in a DPC is through flooding with water, onset of criticality must occur at under-moderated or optimally moderated conditions. Once a critical configuration is formed, it will reduce moderation by increasing water temperature and decreasing the density. Although over-moderated configurations might occur hypothetically for a brief period of time (e.g., basket collapse), consistently under-moderated or optimally moderated conditions leading to criticality would be more likely.
- **Quasi-Steady State** – DPCs must be breached to allow flooding, so there is little potential for over-pressurization. Additionally, the SNF in DPCs does not have significant excess reactivity due to the configuration and the presence of neutron absorbers and poisons in the depleted fuel, so a quasi-steady state criticality is most likely. A rapid transient criticality event with a rapid increase in the power generation rate in a non-pressurized, under- or optimally moderated DPC is implausible. Additionally, any rapid transient would be short-lived due to changes in geometry, reduced water density due to heating, and Doppler broadening.

Reactivity analyses based on actual DPC designs, fuel loading, and corrosion behavior of canister and basket materials would be needed to evaluate the potential for a significant rapid transient criticality event in a breached DPC. Similar calculations were performed for a repository in volcanic tuff (e.g., CRWMS 1999). A quasi-steady state criticality event in a DPC would oscillate between critical and subcritical configurations as a function of water flow rate and density, fuel temperature, generation of neutron poisons, depletion and decay of fissile material, and decay of neutron absorbers into fissile material. The last two decay items are relevant only if the criticality analyses are not based on peak reactivity during the repository performance period.

The primary parameters of repository performance that could be impacted by a criticality event are the radionuclide inventory, water flow rates and distribution (influenced by thermal power), and near-field chemistry (related to temperature and radiolysis). Radionuclide inventory changes have been thoroughly investigated (e.g., Rechar et al. 2003) and found to be insignificant for a small number of criticality events. The consequences of a criticality event are a function of several factors, but are strongly tied to water flow rates in and out of the DPC. Thermal output and the episodic nature of a criticality event would be coupled with DPC degradation and repository hydrogeology. Degradation of the DPC internals and the repository near field, possibly influenced by criticality, could determine when criticality ceases.

Table 4-15. Summary of DPC criticality analyses

| Description  | Values                   |   |
|--|--------------------------|---|
| Total DPCs analyzed  | 179                      |   |
| Failed subcriticality with loss-of-absorber (design basis loading) | 179                      |   |
| Fail subcriticality (as-loaded)                                    | Loss of neutron absorber | Loss of neutron absorber + basket degradation |
|  | 23<br>(of 179 DPCs)      | 18<br>(of 20 DPCs at Site C)                  |
| Approximate chlorine requirement                                   | 13,500 ppm (mg/L)        | 32,500 ppm (mg/L)                             |

#### References for Section 4

BSC (Bechtel-SAIC Co.) 2003. *The Potential of Using Commercial Dual Purpose Canisters for Direct Disposal*. TDR-CRW-SE-000030 Rev 00. U.S. Department of Energy, Office of Civilian Radioactive Waste Management. November, 2003.

Clarity, J.B. and J.M Scaglione 2013. *Feasibility of Direct Disposal of Dual-Purpose Canisters-Criticality Evaluations*. ORNL/LTR-2013/213. Oak Ridge National Laboratory, Oak Ridge, TN. June, 2013.

CRWMS M&O (Civilian Radioactive Waste Management System Management & Operating Contractor) 1998. *Summary Report of Commercial Reactor Criticality Data for Unit 2*. B00000000-01717-57054064 Rev. 01. Las Vegas, NV. April 14, 1998.

CRWMS M&O (Office of Civilian Radioactive Waste Management Management & Operating Contractor) 1999. *Sensitivity Study of Reactivity Consequences to Waste Package Egress Area*. CAL-EBS-NU-000001 Rev. 00. U.S. Department of Energy, Las Vegas, NV.

DOE (U.S. Department of Energy) 2003. *Disposal Criticality Analysis Methodology Topical Report*. YMP/TR-004Q Rev. 2. Office of Civilian Radioactive Waste Management. November, 2003.

EPRI (Electric Power Research Institute) 2008. *Feasibility of Direct Disposal of Dual-Purpose Canisters: Options for Assuring Criticality Control*. Palo Alto, CA. 1016629.

EPRI (Electric Power Research Institute) 2009. *Handbook of Neutron Absorber Materials for Spent Nuclear Fuel Transportation and Storage Applications*. Palo Alto, CA. 1019110.

Hardin, E., T. Hadgu, D. Clayton, R. Howard, H. Greenberg, J. Blink, M. Sharma, M. Sutton, J. Carter, M. Dupont and P. Rodwell 2012. *Repository Reference Disposal Concepts and Thermal Management Analysis*. FCRD-USED-2012-000219 Rev. 2. U.S. Department of Energy, Office of Used Nuclear Fuel Disposition. November, 2012.

Holtec (Holtec International) 2010a. *HI-STAR SAR Report HI-951251 Rev. 15*. U.S. Nuclear Regulatory Commission Docket No. 72-1014. October 11, 2010.

Holtec (Holtec International) 2010b. *Holtec Final Safety Analysis Report for the HI-STORM 100 Cask System, Rev. 9*. February 13, 2010. ADAMS Accession Number ML101400161.

Jove-Colon, C.F., et al. 2011. *Disposal Systems Evaluations and Tool Development—Engineered Barrier System (EBS) Evaluation*. SAND2010-8200. Sandia National Laboratories, Albuquerque, NM.

ORNL (Oak Ridge National Laboratory) 2011. *SCALE: A Comprehensive Modeling and Simulation Suite for Nuclear Safety Analysis and Design*. ORNL/TM-2005/39, V.6.1. Radiation Safety Information Computational Center, Oak Ridge National Laboratory, Oak Ridge, TN.

NAC (NAC International) 2004a. *NAC-UMS Final Safety Analyses Report, Rev. 3*. U.S. Nuclear Regulatory Commission Docket No. 72-1015. January, 2004.

NAC (NAC International) 2004b. *NAC-STC Safety Analysis Report, Rev. 15*. U.S. Nuclear Regulatory Commission Docket No. 71-9235. March, 2004.

NRC (U.S. Nuclear Regulatory Commission) 2002. *Interim Staff Guidance – 9, Revision 1, Storage of Components Associated with Fuel Assemblies*. Spent Fuel Project Office.

NRC (U.S. Nuclear Regulatory Commission) 2010a. *Standard Review Plan for Spent Fuel Dry Storage Systems at a General License Facility*. NUREG-1536 Rev. 1. Office of Nuclear Material Safety and Safeguards. July, 2010.

NRC (U.S. Nuclear Regulatory Commission) 2010b. *Certificate Number 9261, Revision 8, Certificate of Compliance HI-STAR 100 for Radioactive Material Packages – HI-STAR 100*. October, 2010.

Radulescu, G., I.C. Gauld, G. Ilas and J.C. Wagner 2012. *An Approach for Validating Actinide and Fission Product Burnup Credit Criticality Safety Analyses – Isotopic Composition Predictions*. NUREG/CR-7108 (ORNL/TM-2011/514). Prepared for the U.S. Nuclear Regulatory Commission by Oak Ridge National Laboratory. Oak Ridge, TN. April, 2012.

Rechard, R.P., L.C. Sanchez and H.R. Trelue 2003. “Consideration of Nuclear Criticality When Directly Disposing Highly Enriched Spent Nuclear Fuel in Unsaturated Tuff - I: Nuclear Criticality Constraints.” *Nuclear Technology*. V.144, N.2.

Scaglione, J.M., D.E. Mueller, J.C. Wagner and W.J. Marshall 2012. *An Approach for Validating Actinide and Fission Product Burnup Credit Criticality Safety Analyses – Criticality ( $k_{eff}$ ) Predictions*. NUREG/CR-7109 (ORNL/TM-2011/514). Prepared for the U.S. Nuclear Regulatory Commission by Oak Ridge National Laboratory. Oak Ridge, TN. April, 2012.

Scaglione, J.M., et al. 2013. “Integrated Data and Analysis System for Commercial Used Nuclear Fuel Safety Assessments.” *Proceedings of the 17<sup>th</sup> International Symposium on the Packaging and Transportation of Radioactive Materials (PATRAM)*. August 18-23, 2013. San Francisco, CA.

Scaglione, J.M., R.L. Howard, A.A. Alsaed, C.L. Bryan and E.L. Hardin 2014. *Criticality Analysis Process for Direct Disposal of Dual Purpose Canisters*. ORNL/LTR-2014/80. Oak Ridge National Laboratory, Oak Ridge, TN. Prepared for the U.S. Department of Energy, Office of Used Nuclear Fuel Disposition.

Smith, H., et al. 2012. *Fuel Assembly Modeling for the Modeling and Simulation Toolset*. ORNL/LTR-2012-555. Oak Ridge National Laboratory, Oak Ridge, TN. November, 2012.

SNL (Sandia National Laboratories) 2007. *Analysis of Mechanisms for Early Waste Package/Drip Shield Failure*. ANL-EBS-MD-000076 Rev. 0. Prepared for the U.S. Department of Energy, Las Vegas, Nevada.

Stumm, W. and J.J. Morgan 1996. *Aquatic Chemistry: Chemical Equilibria and Rates in Natural Waters*, 3rd Edition. Wiley-Interscience.

Transnuclear (Transnuclear, Inc.) 2003. *Multi-Purpose Cask, Rev. 17, Safety Analysis Report-NUHOMS-MP187*. Fremont, CA. July, 2003. (vendor provided)

Wagner, J.C., M.D. DeHart and C.V. Parks 2003. *Recommendations for Addressing Axial Burnup in PWR Burnup Credit Analyses*. NUREG/CR-6801 (ORNL/TM-2001/273). Prepared for the U.S. Nuclear Regulatory Commission by Oak Ridge National Laboratory, Oak Ridge, TN. March, 2003.

Wagner, J.C. and C.V. Parks 2003. *Recommendations on the Credit for Cooling Time in PWR Burnup Credit Analyses*. NUREG/CR-6781 (ORNL/TM-2001/272). Prepared for the U.S. Nuclear Regulatory Commission by Oak Ridge National Laboratory, Oak Ridge, TN. January, 2003.

Wang, Y., T. Hadgu, S. Painter, D.R. Harp, S. Chu, T. Wolery and J. Houseworth 2012. *Integrated Tool Development for Used Fuel Disposition Natural System Evaluation—Phase I Report*. FCRD-UFD-2012-000229. U.S. Department of Energy, Office of Used Nuclear Fuel Disposition. September, 2012.

Weast. R.C. and M.J. Astle 1981. *CRC Handbook of Chemistry and Physics*. CRC Press, Boca Raton, FL.

Winterle, J., G. Ofoegbu, R. Pabalan, C. Manepally, T. Mintz, E. Percy, K. Smart, J. McMurry, R. Pauline and R. Fedors 2012. *Geological Disposal of High-Level Radioactive Waste in Salt Formations*. Center for Nuclear Waste Regulatory Analyses. San Antonio, TX. Prepared for the U.S. Nuclear Regulatory Commission (Contract NRC-02-07-006).

THIS PAGE INTENTIONALLY LEFT BLANK

## 5. Survey of Ground Water Compositions in Representative Geologic Settings

One aspect of the technical feasibility for direct disposal of spent nuclear fuel (SNF) in dual-purpose canisters (DPCs) is analysis of nuclear criticality in the event of canister breach, flooding with ground water, and possible changes in canister composition and geometry (Hardin et al. 2013). Flooding with water provides a neutron moderator and increases the reactivity of SNF assemblies. Dissolved species at high enough concentrations could lower reactivity by absorbing neutrons and decreasing the fractional density of water molecules. Chlorine-35 is a moderately effective neutron absorber because of its neutron capture cross-section and natural abundance. This survey identifies example ground water compositions, and the hydrogeologic settings where they occur, with emphasis on waters with high chloride concentration (at least several times that of seawater). As shown in Section 4 of this report, these are waters that could significantly lower the reactivity of breached waste packages in a repository.

### 5.1 Overview of Chloride and Total Dissolved Solids

Chloride is a common dissolved anion in many ground waters. Typical counter ions in saline ground water include  $\text{Na}^+$ ,  $\text{K}^+$ ,  $\text{Ca}^{2+}$  and  $\text{Mg}^{2+}$ . Calcium-chloride waters are more common with increasing depth particularly in granite due to alteration of plagioclase to albite (Gascoyne 2004). The salinity of groundwater is nearly equivalent to the term total dissolved solids (TDS), which can also include other soluble compounds such as carbonates and organics, although these generally do not reach high concentrations. Groundwater salinity is classified in terms of TDS, from fresh water with low TDS to saline waters with high TDS.

Using the classification for salinity summarized in Kharaka and Hanor (2003), fresh water has TDS of less than 1,000 mg/L, brackish waters have 1,000 to 10,000 mg/L, and saline waters have 10,000 to 35,000 mg/L (the upper end being equivalent to average seawater). Waters that have TDS greater than 35,000 mg/L (more saline than seawater) are termed brines. The natural limit of TDS in groundwaters is about 350,000 mg/L due to solubility limits (DeMaio and Bates 2013). Based on data for TDS and chloride in sedimentary basins presented by Kharaka and Hanor (2003), chloride concentration is linearly correlated with TDS and represents about 60% ( $\pm$  approximately 10%) of total TDS.

In both sedimentary and crystalline rock terranes, groundwater (i.e., formation water) typically becomes more saline with depth (Figure 1), although salinity reversals in sedimentary basins are known to occur (Kharaka and Hanor 2003). The salinity of groundwater is due to several possible processes including mineral-rock interactions, advection or diffusion of salt from adjacent formations, or the trapping and later modification of connate seawater in the pore spaces of marine sediments (Hanor 1994; Kharaka and Hanor 2003; Frape et al. 2003; Gascoyne 2004; Rebeix et al. 2014). Once present in a deep and stable geologic environment (several hundred meters or more), saline waters will tend to remain saline and stagnant because their higher density makes them resistant to mixing with more dilute waters from meteoric sources (Phillips and Castro 2003), and, in the case of deep water in crystalline rocks, because of the low permeability of the rock and closed fractures at depth that limit connectivity and mixing with shallower meteoric waters (Frape et al. 2003). Pore waters in deep sedimentary basins are potentially more mobile because of the presence of permeable sandstones and carbonates, but pore waters in impermeable shale intervals are essentially immobile except for slow diffusion of ionic species across concentration gradients (Clark et al. 2013; Rebeix et al. 2013).

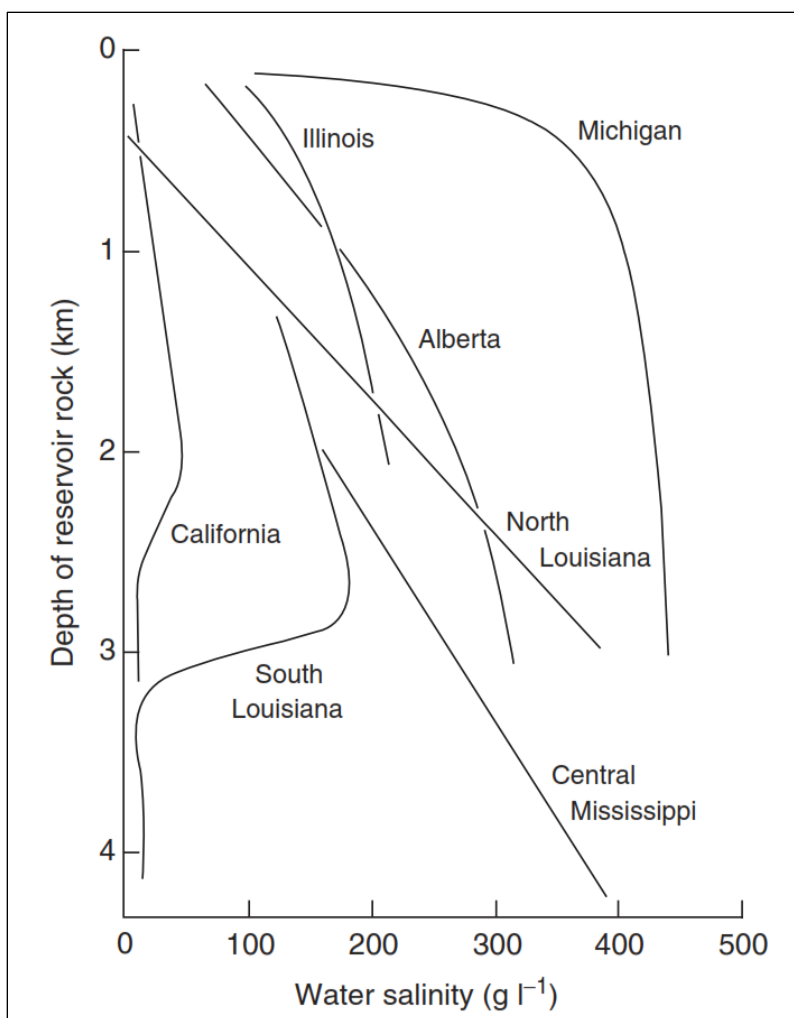


Figure 5-1. Salinity vs. depth for sedimentary basins in North America (from Kharaka and Hanor 2003)

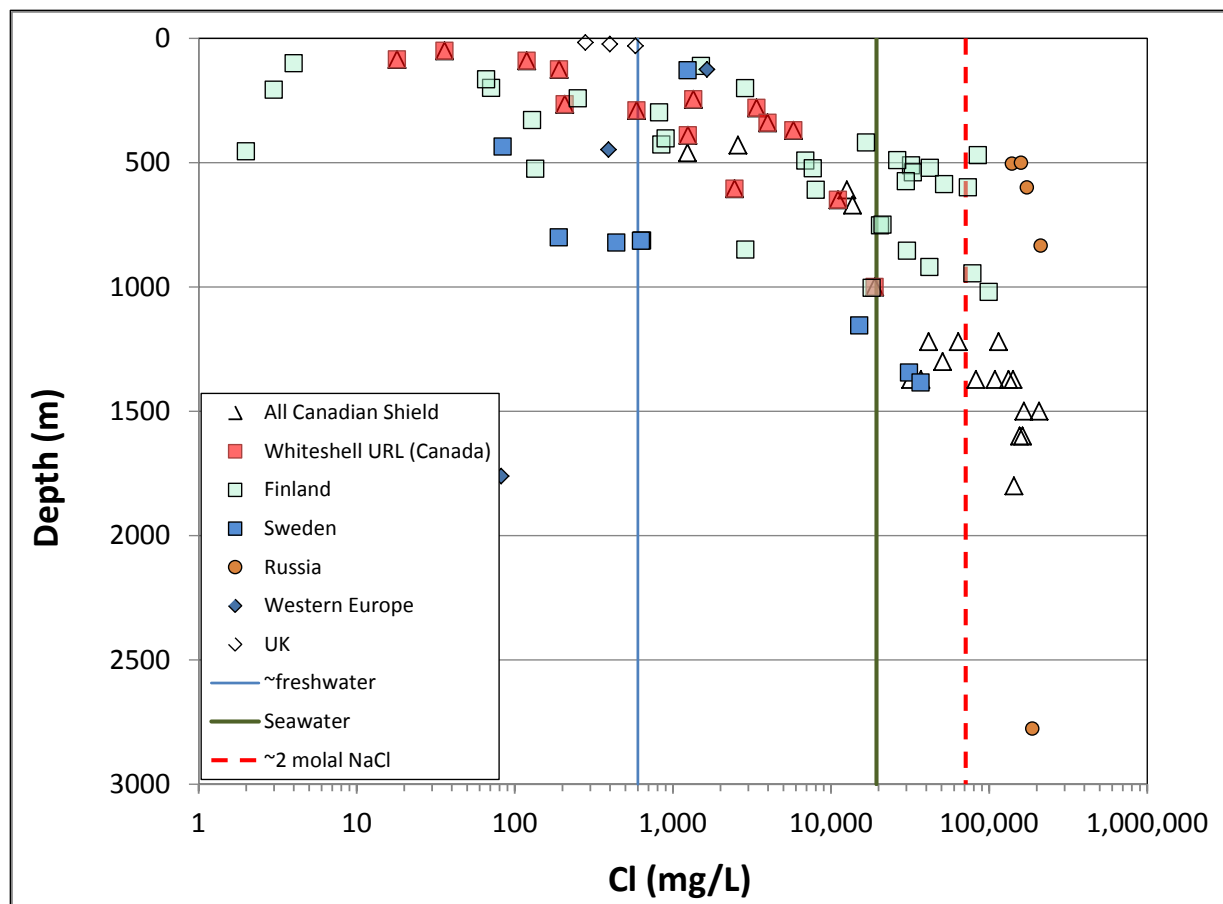
## 5.2 Chloride Data for Crystalline and Shale Formation Waters

In this section, data for chloride concentrations in granite and shale pore waters are described and compared. These data were obtained primarily for the purposes of characterizing the geologic environments for HLW disposal in Canadian or European repository development programs. Chloride data are also available from the oil and gas industry and carbon sequestration programs, but these data are obtained mostly from permeable rocks such as sandstones and carbonates.

Ground water can be sampled by well pumping or with a bailer sampler. In low-permeability media (e.g., clay/shale or intact granite) water is often sampled by isolating and sampling depth intervals in vertical boreholes, by extracting pore water from drill core in the laboratory, or by horizontal drilling from subsurface openings such as mines or tunnels. Sampling methods are reviewed in detail by Frapre et al. (2003) and Kharaka and Hanor (2003).

Chloride concentrations reported for both shale and crystalline rock span a range of values, from approximately 100 mg/L or less (fresh water) to approximately 210,000 mg/L which is near saturation for dissolved NaCl at temperatures less than 100°C (Figures 5-2 and 5-3). Some reported data for chloride concentration vs. depth in granitic pore waters from different

crystalline terranes are summarized in Figure 5-2. Also shown are reference lines for fresh water, seawater, and a 2 molal solution of NaCl (approximately 3.6 times the chloride content of seawater). The 2 molal reference was chosen because flooded DPCs would have significantly less likelihood of criticality compared to flooding with fresh water (Hardin et al. 2013).



Source: Frappe et al. (2003). Reference lines are the chloride concentration limits for fresh water and average seawater, and the chloride concentration for 2 molal NaCl. Reference lines are the upper limits of chloride concentration for fresh water and average seawater, and the chloride concentration of 2 molal NaCl brine.

Figure 5-2. Chloride concentration vs. depth for various crystalline terranes

The main trend in crystalline rocks is increasing chloride concentration with depth (Figure 5-2). Nearly all fresh water samples (TDS < 1,000 mg/L; Cl < 600 mg/L) are restricted to depths of less than 500 m, reflecting the domination of meteoric waters. At depths greater than about 500 m pore water compositions become increasingly more saline, with chloride concentrations reaching maximum values of greater than 200,000 mg/L. A number of samples, primarily at depths greater than 1,000 to 1,500 m exceed chloride values equivalent to a 2 molal NaCl (Figure 5-2). Samples from the Russian Siberian Platform are notably saline at relatively shallow depth (500-1000) m (Figure 2), which has been attributed to the influence of extensive overlying evaporate deposits (Frappé et al. 2003). Highly saline waters (greater than seawater or > 2 molal NaCl) are apparently common in Archean basement at depths greater than about 500 m based on

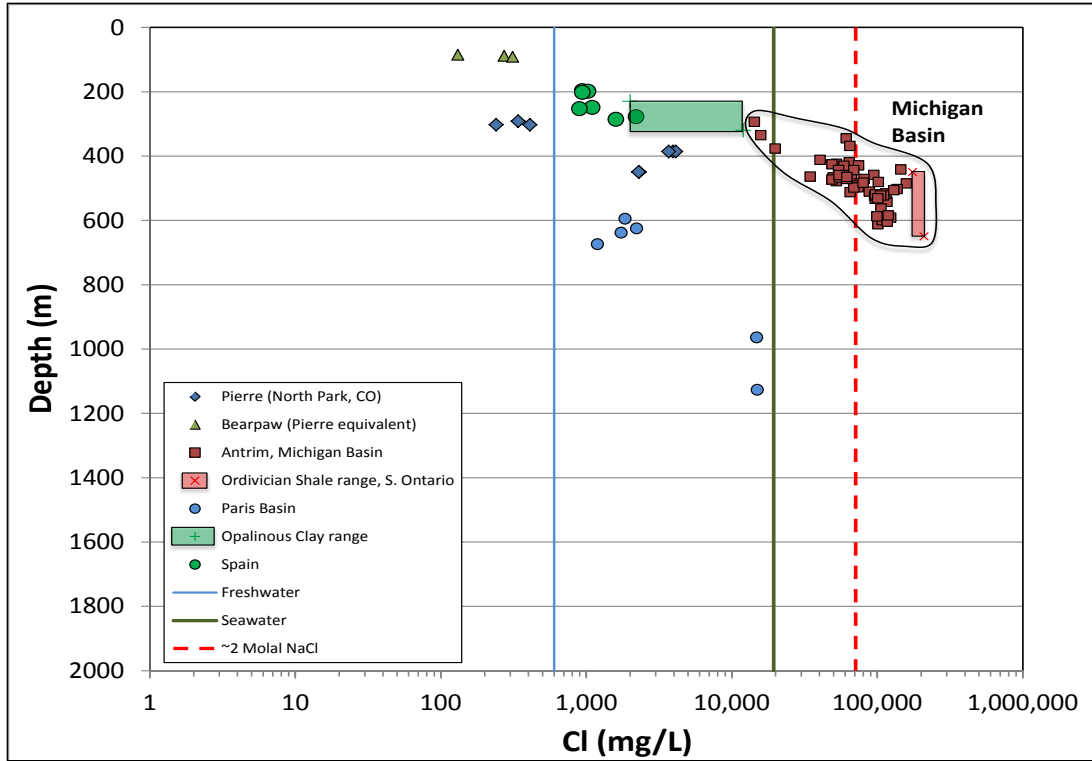
data from Canada, Finland and Russia (Figure 2). The high salinity is likely the result of a long geologic history of water-rock interactions and the emplacement of marine brines from external sources (Frape et al. 2003).

Compared to crystalline rocks, data for pore water or formation water in shales are relatively sparse (Figure 5-3) reflecting the difficulty in extracting pore water from shale and less interest in determining the pore water compositions of aquitards compared to more permeable reservoir rocks. This situation is changing with hydrocarbon extraction from shales, but the literature data are dominated by data from produced waters under less than ideally controlled conditions. Some data sources present only graphs and those are shown in Figure 5-3 as fields representing the approximate range of data. Better controlled data for shale pore waters have come from international repository R&D programs. As is the case with granites, pore waters reflect input from relatively fresh meteoric water at shallow depths (<500 m) and are increasingly saline with depth. Most reported shale pore waters have chloride concentrations corresponding to salinity less than that of seawater. The notable exceptions are two shale intervals that lie within the Michigan Basin. These shales (the Antrim Shale and Ordovician shales below the southern Ontario portion of the Michigan Basin) have chloride values exceeding the equivalent of 2 molal NaCl. Although the Michigan Basin has major intervals of bedded salt (both above and below these shales as shown in Figure 5-4) the high chloride contents are not simply attributed to dissolution and transport of waters from nearby evaporates, but to more complex processes as discussed below.

### **5.3 Geologic Environments and the Origins of Saline Pore Waters**

Geochemical and isotopic evidence indicates that saline pore waters can originate through several processes or combinations, that are either internal to the rock mass or that involve transport of saline waters from outside the rock mass (Kharaka and Hanor 2003; Frape et al. 2003). In granitic rocks, internal processes mainly involve water-rock reactions and alteration of minerals such as feldspars. External processes include movement of saline waters into the rock mass from basinal brines or dissolution of evaporate deposits. In shales, internal processes include incorporation of the original marine connate seawater trapped in pore spaces during sedimentation and lithification as well as subsequent modification of pore waters through water-rock interactions. External processes controlling salinity in shales include transport of basin brines, dissolution and transport of evaporate deposits and diffusion across concentration gradients (Kharaka and Hanor 2003).

Origins of saline waters in shales of the Michigan Basin have been described in detail for the Devonian Antrim Shale and an interval of Ordovician shale in Ontario (Figure 5-4). For the Antrim Shale McIntosh et al. (2004) have attributed the origin of highly saline waters in the central part of the basin to exchange with brine originating in underlying Devonian carbonates, which have Cl/Br ratios reflecting evaporated seawater. In contrast, shale pore waters near the basin margins have lower chloride concentration reflecting recharge by meteoric water (McIntosh et al. 2004, Figure 3B). High chloride concentrations in the Ordovician shale interval are attributed by Clark et al. (2013) to diffusive mixing with overlying evaporative brines of the Silurian Salina Formation, which includes major intervals of bedded salt (Figure 5-4).

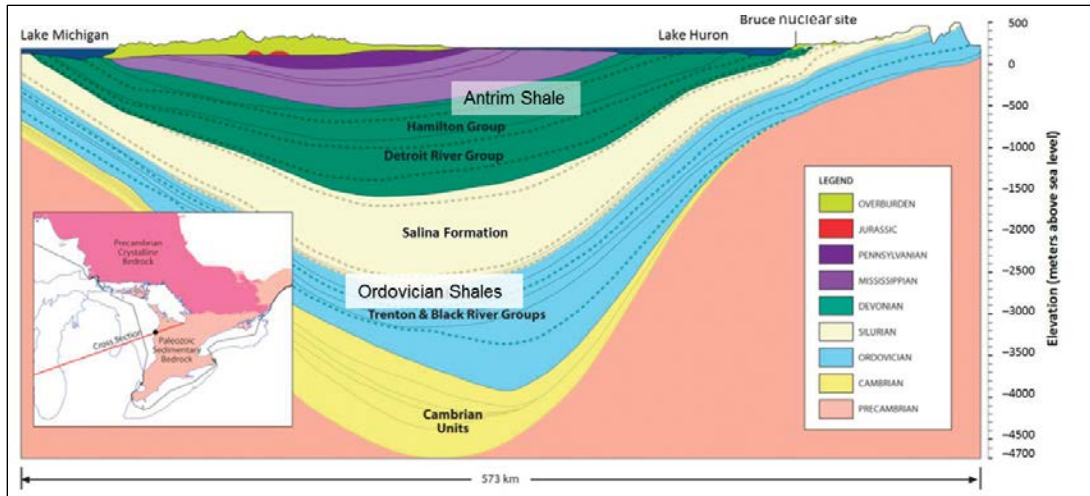


Sources:

1. Pierre Shale in North Park Basin, Colorado (Blondes et al. 2014)
2. Bearpaw Shale in southern Saskatchewan (Hendry et al. 2000)
3. Antrim Shale in Michigan Basin (Blondes et al. 2014)
4. Ordovician shales in southern Ontario (Clark et al. 2013)
5. Paris Basin, France (Bensenouci et al. 2013)
6. and 7. Opalinus Clay, Mont Terri, Switzerland and Jurassic mudrock, Spain (Turrero et al. 2006)

Reference lines are the upper limits of chloride concentration for fresh water and average seawater, and the chloride concentration of 2 molal NaCl brine.

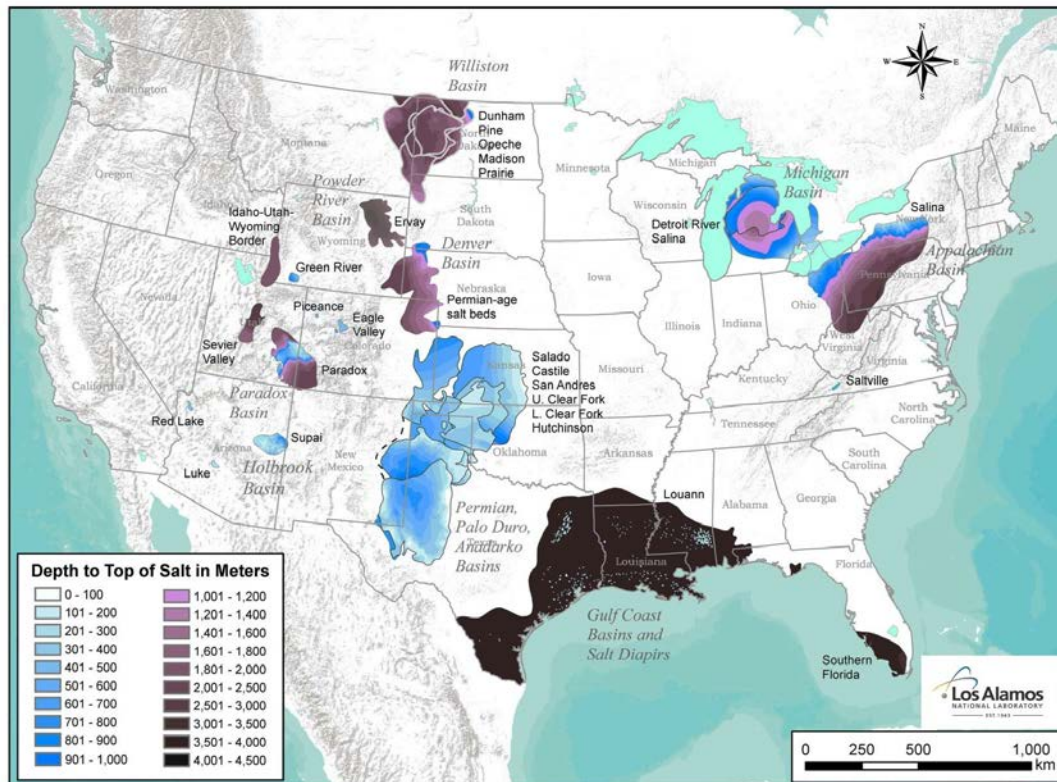
Figure 5-3. Depth vs. chloride concentrations vs. depth for selected shale formations in North America and Europe



Notes:

1. Ordovician shales with high chloride concentrations are present in the upper part of the formations shown in blue. The stratigraphic position of the Devonian-age Antrim shale is also indicated.
2. Major bedded salt units occur within the Salina Formation and the Detroit River Group.

Figure 5-4. Stratigraphic cross-section of the Michigan Basin beneath Michigan and southern Ontario (from Clark et al. 2013)



Note: Basins with a long history of marine deposition, including deposition of bedded salts and marine shales, are more likely to contain shale with highly saline pore waters

Figure 5-5. Distribution and depth of salt formations in the US (from Perry et al. 2014)

Shales with highly saline pore waters are clearly the product of highly saline geologic environments (Kharaka and Hanor 2003). The major Paleozoic sedimentary basins of the U.S., which include the Michigan, Appalachian, Williston and Permian Basins (Figure 5-5), are characterized by bedded salt deposits and evaporative basinal brines that resulted from multiple marine transgressions. These environments provide the high salinity that produce high-chloride shale pore waters as connate features or products of diffusive mixing with brines in adjacent brine-bearing formations.

High salinity in produced waters has been documented from the Marcellus formation in the Appalachian Basin where salinity approaches 2 molal NaCl (Barbot et al. 2013). The chemistry of these waters suggests that the salinity originated primarily from seawater that evaporated and concentrated to form brines. The middle unit of the Bakken Formation in the Williston Basin is a fine-grained siltstone while the upper and lower units are black shales. The middle unit is highly saline, possibly due to ion filtration by the surrounding tight shales (Peterman et al. 2014). The salinity values for the upper and lower Bakken shale have not been reported.

An example of the mixed origin of saline pore waters in crystalline rock is provided by a study of the Lac du Bonnet granite batholith, part of the Archean Canadian Shield (Gascoyne 2004). The batholith hosts the Whiteshell underground research laboratory (URL) in Manitoba. Pore water salinity is less than in other areas of the Canadian Shield but lies along the Canadian Shield trend (Figure 5-2). Chloride concentrations increase with depth and reach that of seawater at a depth of approximately 1,000 m (Figure 5-2). Gascoyne (2004) discussed several alternative origins for the salinity of water at depth in both fractures and pore fluids. The pore fluids have the highest salinity and are dominated by Ca-Cl type water, indicating prolonged ( $>>1$  Ma) water-rock interactions involving albitization of plagioclase and a reduction of Na/Cl in the reacting fluid. These saline waters probably contributed to the salinity of the deeper fracture-filling groundwater. Although the Ca-Cl composition of the saline pore waters indicates prolonged rock-water interactions, the degree of salinity suggests that the salinity could not have originated solely within the granite mass. Low Br/Cl ratios of the deeper waters lie between those of seawater and basinal brines of the Manitoba Basin to the west, suggesting that the primary source of salinity was marine brines that infiltrated the granite during marine sedimentation in the Paleozoic. The timing also indicates that the resulting deep saline waters are old and stagnant over periods exceeding millions of years (Gascoyne 2004).

#### **5.4 Conclusions**

High-salinity pore waters occur at depth in both crystalline rock and shale under certain geologic conditions. Pore waters with greater than the chloride equivalent of 2 molal NaCl, sufficient to significantly reduce the likelihood of criticality in flooded DPCs, are common in geologically ancient crystalline basement terranes at depths of greater than 500 m. These saline waters primarily originated through a long history of water-rock interactions following infiltration of crystalline rocks masses by marine brines derived from overlying sedimentary rocks. The origin of highly saline waters in shale generally involves more complex processes, but shales with concentrations greater than the chloride equivalent of 2 molal NaCl are likely to be found in sedimentary basins with bedded salt deposits or histories of marine shale deposition that concentrated chloride in connate pore waters through evaporative processes and post-depositional water-rock interactions. In both crystalline and sedimentary environments, highly saline waters tend to be old and stagnant as a result of density differences and low rock permeabilities that would inhibit mixing with more dilute waters.

The correlation with age suggests that high-chloride waters may not be common in geologically young granites that occur more frequently in the U.S. (i.e., post-Archean) or for granites in tectonically active regions (potentially allowing more connectivity between shallow and deep waters). More data may be available for pore water compositions in major sedimentary basins in the U.S. that contain marine sediments. High-chloride shales have been documented in the Michigan Basin and likely occur in both the Appalachian and Williston Basins, although the extent of these occurrences is not well documented. Based on similarity of geologic environments, high-chloride shales would be expected to occur in the Permian Basin, but no data have been identified to support this conjecture.

### References for Section 5

Barbot, E., N. Vidic, K. Gregory and R. Vidic 2013. "Spatial and Temporal Correlation of Water Quality Parameters of Produced Waters from Devonian-Age Shale following Hydraulic Fracturing." *Environmental Science and Technology*. pp. 2562-2569.

Bensenouci, F., J. Michelot, S. Savoye, J. Tremosa and S. Gaboreau 2011. "Profiles of chloride and stable isotopes in pore-water obtained from a 2000 m-deep borehole through the Mesozoic sedimentary series in the eastern Paris Basin." *Physics and Chemistry of the Earth*. V.65, pp.1-10.

Blondes, M.S., K.D. Gans, J.J. Thordsen, M.E. Reidy, B. Thomas, M.A. Engle, Y.K. Kharaka and E.L. Rowan 2014. National Produced Waters Geochemical Database V2.0 (PROVISIONAL). U.S. Geological Survey. April, 2014.

(<http://energy.usgs.gov/EnvironmentalAspects/EnvironmentalAspectsOfEnergyProductionandUse/ProducedWaters.aspx#3822349-data>)

Clark, I., T. Al, M. Jensen, M. Mazurek, R. Mohapatra and K. Raven 2013. "Paleozoic-aged brine and authigenic preserved in an Ordovician shale aquiclude." *Geology*. V.41, pp. 951-954.

DeMaio, W. and E. Bates 2013. *Salinity and Density in Deep Boreholes*. Massachusetts Institute of Technology. UROP REPORT: October 29, 2013. 14 p.

Frape, S., A. Blyth, R. Blomqvist, R. McNutt and M. Gascoyne 2003. "5.17 Deep Fluids in the Continents: II. Crystalline Rocks." In: *Treatise on Geochemistry* (Eds. H. Holland, and K. Turekian). pp. 541-580.

Gascoyne, M. 2004. "Hydrochemistry, groundwater ages and sources of salts in granitic batholith on the Canadian Shield, southeastern Manitoba." *Applied Geochemistry*. V.19, pp. 519-560.

Hardin, E., D. Clayton, R. Howard, J. Scaglione, E. Pierce, K. Banerjee, M.D. Voegelé, H. Greenberg, J. Wen, T. Buscheck, J. Carter and T. Severynse 2013. *Preliminary Report on Dual-Purpose Canister Disposal Alternatives*. FCRD-UFD-2013-000171 Rev. 0. U.S. Department of Energy, Office of Used Nuclear Fuel Disposition. August, 2013.

Hendry, M., L. Wassenaar and T. Kotzer 2000. "Chloride and chlorine isotopes ( $^{36}\text{Cl}$  and  $\delta^{37}\text{Cl}$ ) as tracers of solute migration in a thick, clay-rich aquitard system." *Water Resources Research*. V.36, pp. 285-296.

Kharaka, Y. and J. Hanor 2003. "5.16 Deep Fluids in the Continents: I. Sedimentary Basins." In: *Treatise on Geochemistry* (Eds. H. Holland, and K. Turekian). pp. 1-48.

McIntosh, J., L. Walter and A. Martini 2004. "Extensive microbial modification of formation water geochemistry: Case study from a Midcontinent sedimentary basin, United States." *Geological Society of America Bulletin*. V.116, pp. 743-759.

Perry, F., R. Kelly, S. Birdsell, P. Dobson and J. Houseworth 2014. *Regional Geology: A GIS Database for Alternative Host Rocks and Potential Siting Guidelines*. FCRD-UFD-2014-000068. U.S. Department of Energy, Office of Used Nuclear Fuel Disposition. Los Alamos Unlimited Release LA-UR-14-20368. 168 p.

Peterman, Z. E., J. Thamke, L. Neymark, T. Oliver and K. Futa 2014. *Bakken Formation Water Salinity and the Role of Ion Filtration, Williston Basin*. Retrieved from The Geological Society of America: <https://gsa.confex.com/gsa/2014RM/webprogram/Paper238366.html>

Phillips, F. and M. Castro 2003. "5.15 Groundwater Dating and Residence-time Measurements." In: *Treatise on Geochemistry* (H. Holland, and K. Turekian, editors). pp. 452-497.

Rebeix, R., C. Le Gal La Salle, P. Jean-Baptiste, V. Lavastre, E. Fourré, F. Bensenouci and J. Lancelot 2013. "Chlorine transport process through a 2000 m aquifer/aquitard system." *Marine and Petroleum Geology*. V.53, pp. 102-116.

Turrero, M., A. Fernandez, J. Peña, M. Sánchez, P. Wersin, P. Bossart and P. Hernán 2006. "Pore water chemistry of a Paleogene continental mudrock in Spain and a Jurassic marine mudrock in Switzerland: Sampling methods and geochemical interpretation." *Journal of Iberian Geology*. pp. 233-258.

THIS PAGE INTENTIONALLY LEFT BLANK

## 6. Thermally-Driven Coupled Processes in Clay/Shale Media

This study analyzes thermally driven processes that could occur in clay-rich host geologic media with direct disposal of DPC in waste packages that are large and hot, relative to reference disposal concepts (Hardin et al. 2012a) and concepts proposed in other countries. DPC-based waste packages could contain 6 to 9 times as much SNF as the small waste packages proposed for clay/shale repositories in Europe (NAGRA 2002; ANDRA 2005) and they would have roughly twice the diameter.

Clay/shale media are of particular interest for waste disposal because of low permeability and small radionuclide diffusion coefficients, which produce high retention capacity for radionuclides (Zheng et al. 2012). Clay minerals have self-sealing properties due to swelling when in contact with water (Hicks et al. 2009), that promote radionuclide retardation and inhibit microbial development. These properties make argillaceous media desirable as host rock and also backfill, however, argillaceous media generally have low thermal conductivity and low tolerance for elevated temperature compared to other media such as salt and granite. Recently, concepts for direct disposal of DPCs in various media were proposed (Hardin et al. 2013) including disposal in argillaceous sedimentary rock. In-drift emplacement (e.g., on the floor) was selected for large, heavy DPC-based waste packages. The emplaced waste would be ventilated for up to 50 years, then the emplacement drifts would be backfilled with clay-based engineered material. This

Temperature limits for clay/shale host media and clay-based backfill are typically 100°C or less, as selected by international repository R&D programs (ANDRA 2005, Section 1.2.3.4; SKB 2011, Section 5.5.1). To meet 100°C peak temperature limits with DPC-based waste packages, could require a large repository layout and more than 150 years of decay storage before permanent disposal. With packages spaced 20 to 30 m apart, it could be helpful from a thermal management perspective to heat small regions of the host rock and backfill around each waste package to temperatures greater than 100°C. This could irreversibly change certain properties of these clay-rich materials, but it could also allow a smaller repository and earlier disposal of the DPCs. The motivation for this study is to evaluate how large such a region could be, and the nature and extent of changes in material properties that could be expected.

Significant progress has been made in the U.S. and international repository R&D programs to understand the coupled thermal-hydrologic-mechanical-chemical (THMC) processes that could alter argillaceous host media and backfill materials. For direct disposal of DPCs, some differences with respect to disposal concepts proposed in other countries could include: 1) an initial ventilation period after waste package emplacement in the repository; 2) larger drift openings to accommodate large waste packages and handling equipment; 3) asymmetrical layout of the waste package, backfill and drift opening when viewed in cross-section; and 4) a liner constructed of concrete or shotcrete, possibly with steel supports. Each of these differences is represented explicitly in the models described below.

After a brief introduction of the calculation tools, this section presents results from modeling desaturation of the host rock and thermal-hydrologic-mechanical (THM) processes considering realistic layout geometry and backfill.

**Coupled Process Simulator** – The modeling work presented here is conducted with TOUGH2, a finite-volume, multiphase fluid flow code for nonisothermal multicomponent fluid and heat

flow (Pruess et al. 1999). A broad range of subsurface thermo-physical-chemical processes can be investigated, and the program can be applied to one-, two- or three-dimensional problems in porous and fractured media. The THM simulation was conducted with TOUGH-FLAC3D (Rutqvist et al. 2011) which sequentially couples the finite-difference geomechanical code FLAC3D (Itasca, 2009).

### 6.1 TOUGH2 Model for Desaturation of the Host Rock

TOUGH2 models simulate a 2D cross section (Figure 6-1) of an emplacement drift with surrounding argillite. The model represents an emplacement drift located at 500 m depth (z-axis), in a large panel with spacing of 45 m (center-center) between drifts, and with waste packages spaced 20 m apart (center-center) along each drift. The symmetry model domain is one-half the horizontal spacing from the package center to the mid-point of a pillar between drifts (22.5 m, x-axis). Boundary conditions are chosen so that the model represents an array of parallel emplacement drifts. The engineered barrier system (EBS) consists of the canister, surrounded by unsaturated air during the ventilation period with a perforated steel liner, followed by backfilling of the tunnels. The perforated steel liner is open to moisture exchange, so the model provides an upper-bound-type estimate of the effects of dewatering during ventilation. The tunnel radius is 2.26 m (denoted with an asterisk in Figure 6-1). The waste package is placed concentrically in the drift opening, for comparison of TOUGH2 calculations with analytical solutions (more realistic in-drift emplacement geometry is discussed in Section 6.3).

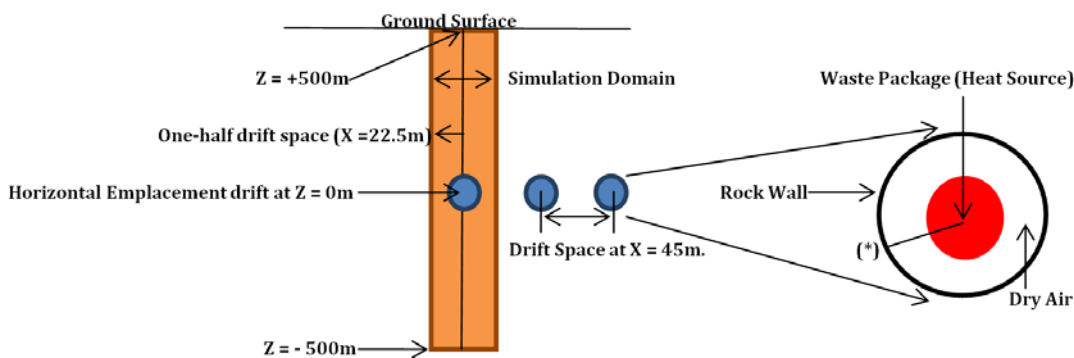


Figure 6-1. Repository layout for modeling drift at 500 m below ground surface

Pressure and temperature are fixed at the top and bottom of the model domain. During the ventilation period, a time-dependent temperature boundary condition is prescribed at the drift wall, while the relative humidity of the air in the drift tunnel is maintained at 53%. The time-dependent temperature condition is based on an analytical model (Greenberg et al. 2012). After ventilation ends, clay-based backfill with an initial gas saturation of 35% is installed, and a heat source is applied at the waste package.

Table 6-1 lists the thermal and hydrodynamic parameters used in the model. Parameters for the backfill are largely taken from Birkholzer et al. (2008), based on properties of the Opalinus Clay (Thury 2002; Bossart 2011), except for thermal conductivity (Hardin et al. 2012b) and permeability. Regarding permeability, Soler (2001) reported that the Opalinus permeability ranges from  $10^{-21}$  to  $10^{-18}$   $m^2$ , with lower values from laboratory measurements ( $10^{-21}$  to  $8 \cdot 10^{-21}$

m<sup>2</sup>; Harrington and Horseman 1999; De Windt and Palut 1999), and higher values from field tests ( $10^{-18}$  m<sup>2</sup>; NAGRA 1989). A medial permeability value of  $5.0 \cdot 10^{-19}$  m<sup>2</sup> is used here.

Table 6-1. Thermal and hydrodynamic parameters for host rock and bentonite buffer

| Parameter                                | Host rock                | Bentonite backfill      |
|--|--------------------------|-------------------------|
| Grain density (kg/m <sup>3</sup> )       | 2,700                    | 2,700                   |
| Porosity, $\phi$                         | 0.15                     | 0.39                    |
| Saturated permeability (m <sup>2</sup> ) | $5.0 \cdot 10^{-19}$     | $5.0 \cdot 10^{-20}$    |
| Relative permeability, $k_{rl}$          | $m = 0.6, S_{rl} = 0.01$ | $K_{rl} = S^3$          |
| Van Genuchten, $\alpha$ (1/Pa)           | $6.8 \cdot 10^{-7}$      | $3.3 \cdot 10^{-8}$     |
| Van Genuchten, $m$                       | 0.6                      | 0.3                     |
| Compressibility, $\beta$ (1/Pa)          | $3.2 \cdot 10^{-9}$      | $5.0 \cdot 10^{-8}$     |
| Thermal expansion coeff. (1/K)           | 0.0                      | $1.0 \cdot 10^{-4}$     |
| Dry specific heat (J/kg°C)               | 800                      | 1,247                   |
| Thermal conductivity (W/m·K)             | 1.48 (dry)/1.75 (wet)    | 0.6 (dry)/1.2 (wet)     |
| Tortuosity for vapor phase               | $\phi^{1/3} S_g^{10/3}$  | $\phi^{1/3} S_g^{10/3}$ |
| Bulk modulus (GPa)                       | 4.17                     | 0.02                    |
| Shear modulus (GPa)                      | 1.92                     | 0.0067                  |

## 6.2 TOUGH2 Initial Scoping Results

This section presents thermal-hydrologic simulations starting with constant thermal conductivity (for comparison to analytical solutions) and proceeding to saturation-dependent conductivity and analyses of permeability and disturbed rock zone (DRZ) effects. Mechanical effects and asymmetrical placement of the waste package in the drift opening are discussed in Section 6.3.

Calculations are performed with SNF that has 40 GW-d/MTU burnup, emplaced at age of 50 years from reactor discharge, and ventilated in the repository for 40 years or 350 years. The latter duration is not proposed as a disposal option (see assumptions in Hardin and Howard 2013) but represents a bounding case of maximal cooling for comparison to ventilation for 40 years which is relatively brief. Ventilation efficiency is assumed to be 75% of heat removed (Hardin et al. 2012a).

In TOUGH2 the thermal conductivity  $K_{th}$  is calculated as:

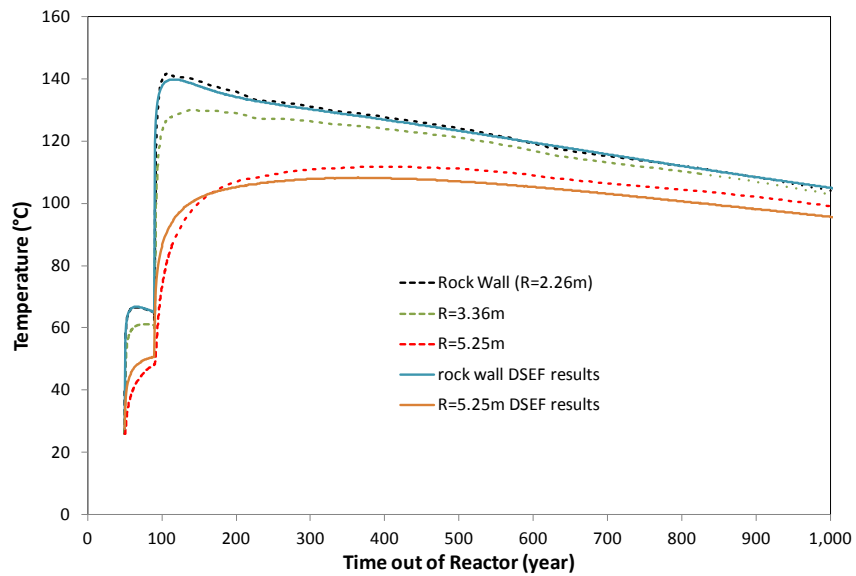
$$K_{th} = K_{wet} + S_l (K_{wet} - K_{dry}) \quad (6-1)$$

where  $K_{wet}$  is the thermal conductivity under fully liquid-saturated conditions,  $K_{dry}$  is the thermal conductivity under desaturated conditions, and  $S_l$  is the liquid saturation. For initial scoping calculations  $K_{wet} = K_{dry} = 1.75$  W/m·K, which means that thermal conductivity is unaffected by saturation changes. This effective value for isotropic thermal conductivity of clay/shale media is consistent with the Opalinus Clay and other geologic units (Hardin et al. 2012b; Hansen et al. 2010).

**40-Year Ventilation Case** – Figure 6-2 depicts the temperature profile simulated with TOUGH2 at the rock wall. The simulations start at 50 years because waste packages are emplaced after 50 years of surface decay storage. After emplacement, temperature rises rapidly to a maximum of

approximately 65°C at rock wall during ventilation, then decreases slowly as the heat output of the waste decays. When ventilation stops 40 years later, there is a steep increase of the rock wall temperature to about 140°C.

Gas saturation increases as the host medium dewateres during ventilation (Figure 6-3). Ventilation causes desaturation but the effect does not persist very far into the rock. Near the drift wall the gas saturation increases to a maximum of ~0.48, but just 0.3 meters further into the rock the gas saturation is only ~0.25. No desaturation effect is seen at a radial distance of 5.25 meters and beyond. As ventilation ceases, there is no strong driving force for drying out the near-field host rock, and the system resaturates within about 10 years.



Note: DSEF refers to an Excel-based calculation using analytical solutions (Greenberg et al. 2012).

Figure 6-2. Temperature evolution at several locations for backfill and non-backfill operation modes for the 40-year ventilation case

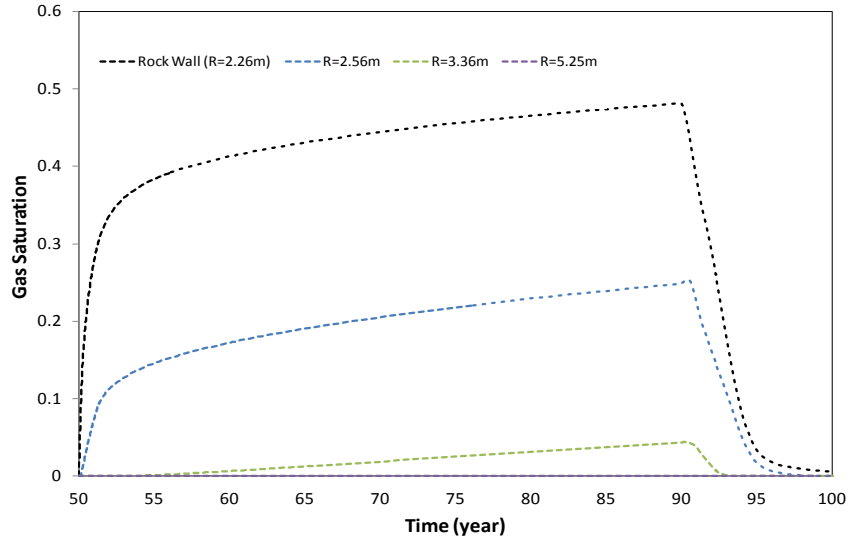
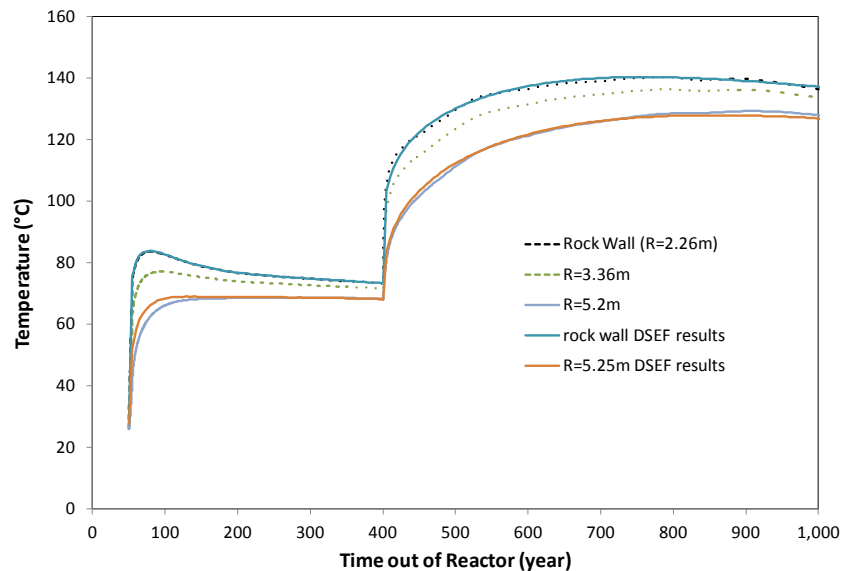


Figure 6-3. Gas saturation evolution at several locations for the 40-year ventilation case

**350-Year Ventilation Case** – Thermal transients at multiple locations are shown in Figure 6-4 for the 350-year ventilation scenario. Like the 40-year scenario, ventilation keeps the temperature low, after which the host rock temperature increases. The longer ventilation period impacts the saturation profiles (Figure 6-5). Desaturation of the near-field rock is stronger (higher gas saturations) and it extends further into the host rock.



Note: DSEF refers to an Excel-based calculation using analytical solutions (Greenberg et al. 2012).

Figure 6-4. Temperature evolution at several locations for the 350-year ventilation case

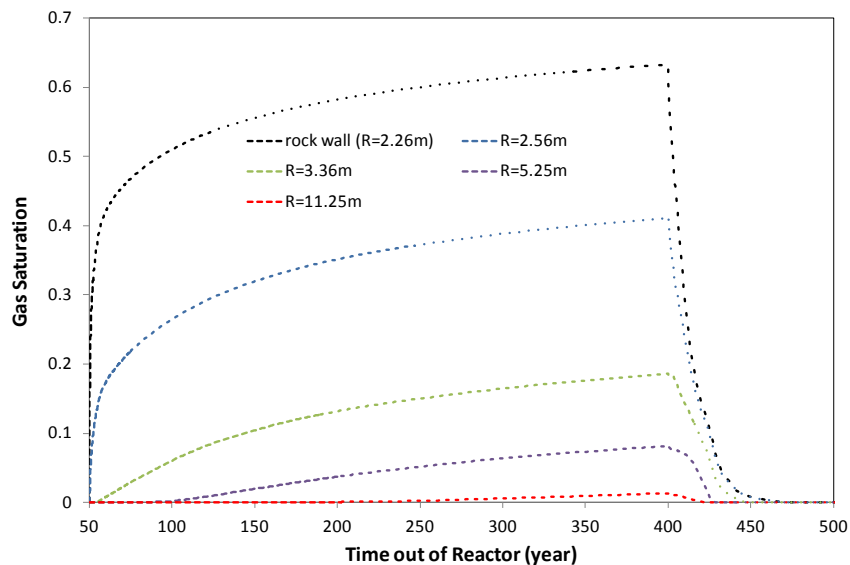


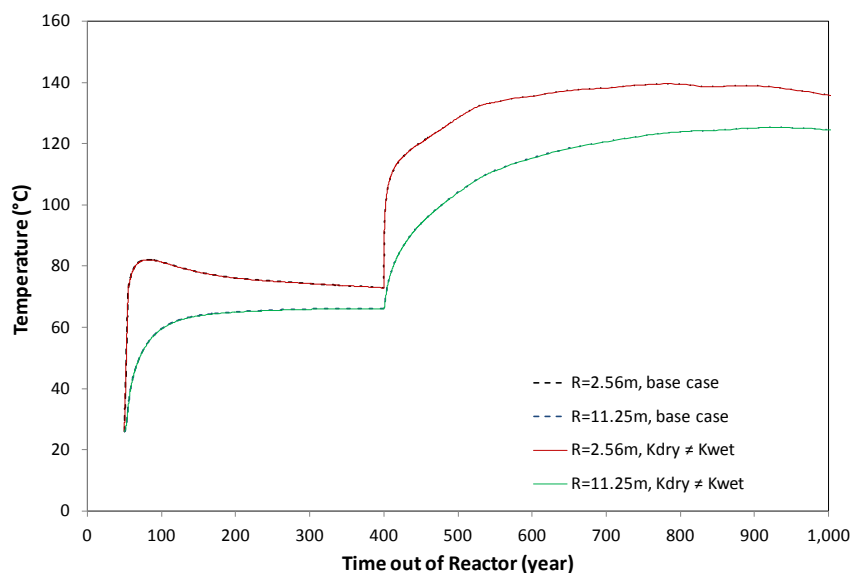
Figure 6-5. Gas saturation evolution at several locations for the 350-year ventilation case

The drift wall desaturates during 350 years of ventilation, reaching a gas saturation value of ~0.63, which may be regarded as a bound for this model. Just 0.3 meters into the host rock the gas saturation value has a maximum of ~0.41. After ventilation stops, the resaturation time is approximately 50 to 75 years, whereas resaturation takes about 10 years for the 40-year ventilation case.

**Saturation Dependent Thermal Conductivity** – Host rock thermal conductivity and hydraulic permeability are two important properties that determine thermal-hydrologic (TH) evolution in clay/shale media. This calculation evaluates TH changes in the host rock if  $K_{th}$  varies between saturation-dependent values. The assumption that thermal conductivity is constant during heating and desaturation of the host rock is a necessary simplification for comparing to analytical solutions. However, it is known that thermal conductivity decreases when a porous medium desaturates. In models of this type the effective thermal conductivity  $K_{th}$  is typically a function of  $S_b$ ,  $K_{wet}$  and  $K_{dry}$ . Here we use

$$K_{th} = \alpha \left( \frac{V_{air}}{V} \right) + K_{wet} \quad (6-2)$$

where  $\alpha = -K_{wet}$  and  $(V_{air}/V) = 0.15$  (porosity, Table 6-1).  $V_{air}$  is the product of volume  $V$ , porosity  $\phi$ , and the complement of liquid saturation  $(1-S_l)$ . This function was selected from several alternatives (e.g., Tang et al. 2008) and implemented in TOUGH2. In this case  $K_{wet}$  is 1.75 W/m·K (as before) and  $K_{dry}$  is 1.48 W/m·K. Small temperature differences are observed, as exemplified for the 350-year ventilation scenario (Figure 6-6). This is because  $K_{th}$  exhibits only small variation within the limited desaturated zone, so the smallest value of  $K_{dry}$  is 1.68 W/m·K in the 40-year case and 1.64 W/m·K in the 350-year case. These results show that assuming constant thermal conductivity for clay/shale media produces only small differences in calculated temperature. It is possible that some clay/shale media could have greater porosity, in which case  $K_{dry}$  and  $K_{wet}$  could be more different, and differences between wet and dry temperatures could be greater.



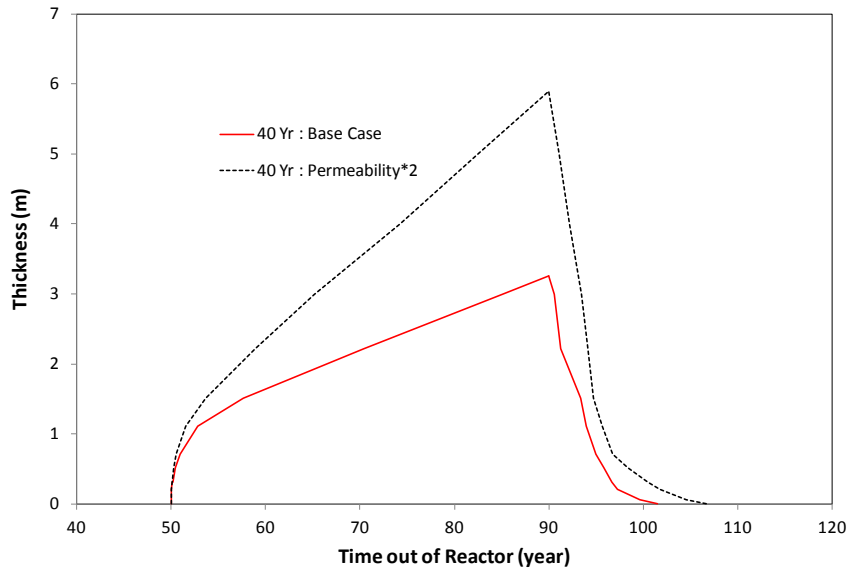
Note: The base case is the TOUGH2 initial scoping calculation with constant thermal conductivity.

Figure 6-6. Temperature evolution for the 350-year ventilation scenario ( $K_{wet} = 1.75 \text{ W/m}\cdot\text{K}$  and  $K_{dry} = 1.48 \text{ W/m}\cdot\text{K}$ )

Additional calculations (Zheng et al. 2014) show that a lower  $K_{th}$  values leads to higher temperatures in the host rock, which produces a slightly larger desaturated zone. For instance, in the 40-year ventilation case, the desaturated zone extends 3.63 meters into the host rock when  $K_{th}$  is  $1.0 \text{ W/m}\cdot\text{K}$  compared to 3.26 meters when  $K_{th} = 1.75 \text{ W/m}\cdot\text{K}$  in the base case. Similarly, increasing  $K_{th}$  decreases the extent of desaturated zone by a small amount.

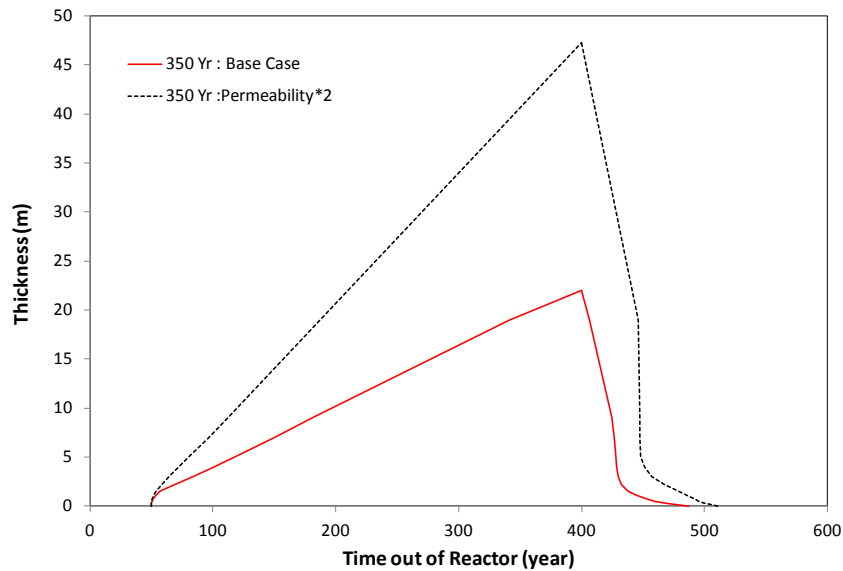
**Sensitivity to Permeability** – Permeability affects the migration of fluids and gases in porous media, and is directly related to porosity, which in turn depends on grain shape, size, and sorting. For this calculation the host rock permeability is increased by a factor of 2 to examine the effect on TH behavior in the host rock. Greater permeability leads to a larger desaturated zone (Figures 6-7 and 6-8) due to faster moisture migration during ventilation. In these calculations the host rock thermal conductivity is not a function of liquid saturation, but permeability would have little effect on temperature because as demonstrated previously, liquid saturation has a small effect on temperature.

**Effect of a Disturbed Rock Zone** – In this discussion the term DRZ is used to describe a zone of altered properties caused by excavation and ensuing activities, including a near region where changes may be permanent (the EDZ), and a distal region where changes may be reversible over time. The model described here tests the sensitivity of TH processes to altered properties assumed for a specified region around the opening, and does not describe the processes that could reverse the alteration or determine the extent of an EDZ.



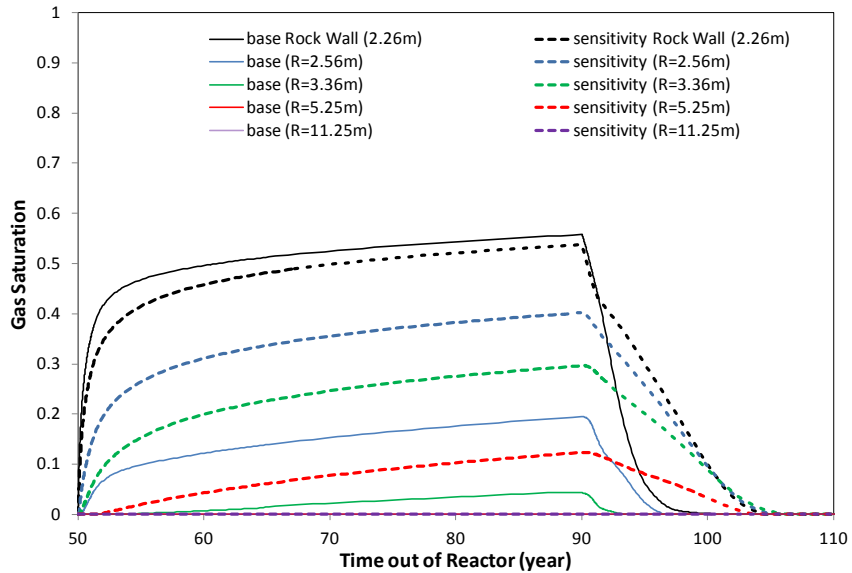
Note: The base case is the TOUGH2 initial scoping calculation with constant thermal conductivity.

Figure 6-7. Thickness of the desaturated zone for the 40-year ventilation case, with doubled permeability



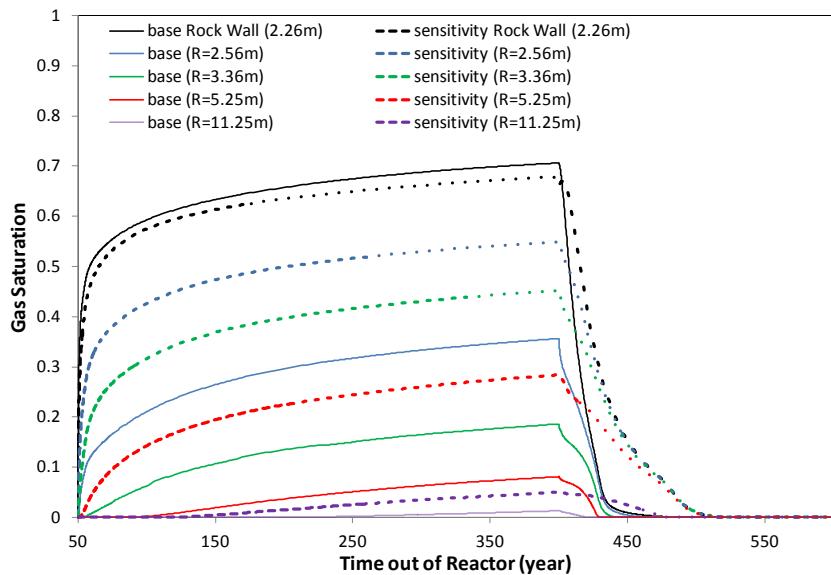
Note: The base case is the TOUGH2 initial scoping calculation with constant thermal conductivity.

Figure 6-8. Thickness of the desaturated zone for the 350-year ventilation case, with doubled permeability



Note: The base case is the TOUGH2 initial scoping calculation with constant thermal conductivity.

Figure 6-9. Gas saturation evolution at several points for the 40-year ventilation scenario: with DRZ (sensitivity) and without DRZ (base)



Note: The base case is the TOUGH2 initial scoping calculation with constant thermal conductivity.

Figure 6-10. Gas saturation evolution at several points for the 350-year ventilation scenario: with DRZ (sensitivity) and without DRZ (base)

The thickness and permeability of a DRZ can vary, for example, the DRZ in Opalinus Clay at the Mont Terri site (Thury 2002) ranges from 0.5 to 3 m thick, with permeability that is one to several orders of magnitude greater than the undisturbed rock. For this calculation host rock permeability is increased by one order of magnitude in a 1-m DRZ at the drift wall. Figures 6-9 and 6-10 show the gas saturation at several points for the 40-year and 350-year ventilation cases, respectively. The existence of a DRZ leads to lower gas saturation at the drift wall but greater gas saturation inside the host rock, producing a flatter gas saturation gradient from the drift wall outward. Because of the higher permeability moisture is more readily transported to the drift during ventilation, so the desaturated zone penetrates deeper into the host rock.

### **6.3 Thermal-Hydrologic-Mechanical Model**

The THM model geometry is more realistic than the scoping model represented in Figure 6-1. The drift has a concrete liner and a concrete invert forming a floor (Figure 6-11). The waste package is emplaced directly on the floor, and is ventilated and later backfilled. Heat transport differs from the waste package to the top vs. the bottom of the opening, so temperature evolution differs. The model grid used for this calculation is shown in Figure 6-12. The model domain size, boundary conditions, and symmetry conditions are the same as those described in Section 6.2.

Only the 40-year ventilation case is simulated; the 350-year case is helpful for understanding the effects from prolonged ventilation, but is not realistic. To represent the ventilation period the temperature at the waste package surface, calculated using an analytical solution that includes thermal radiation, is used as the boundary condition. The relative humidity of the air in the drift is set to 53% during ventilation. After ventilation ends and backfill is installed, a heat source is used to represent the canister, with heating rate shown in Figure 6-13. This heating function is calculated by dividing the waste package heat generation (32 PWR assemblies; 40 GW-d/MTU fuel burnup) by the waste package spacing (20 m).

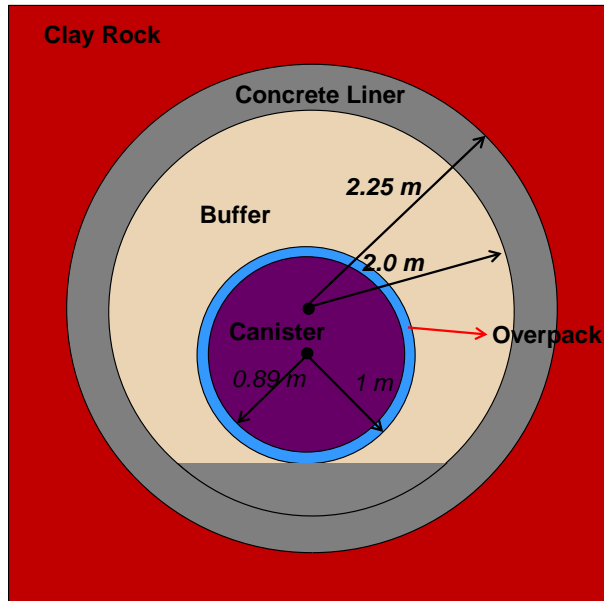


Figure 6-11. Geometry of a cross section of a drift for DPC disposal

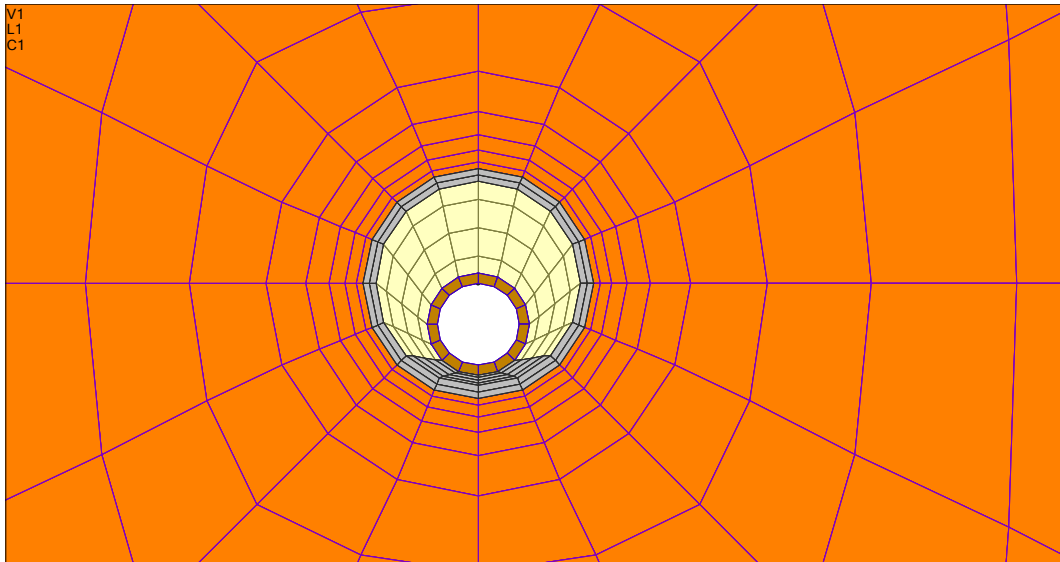


Figure 6-12. Mesh used in THM model for the configuration shown in Figure 6-11

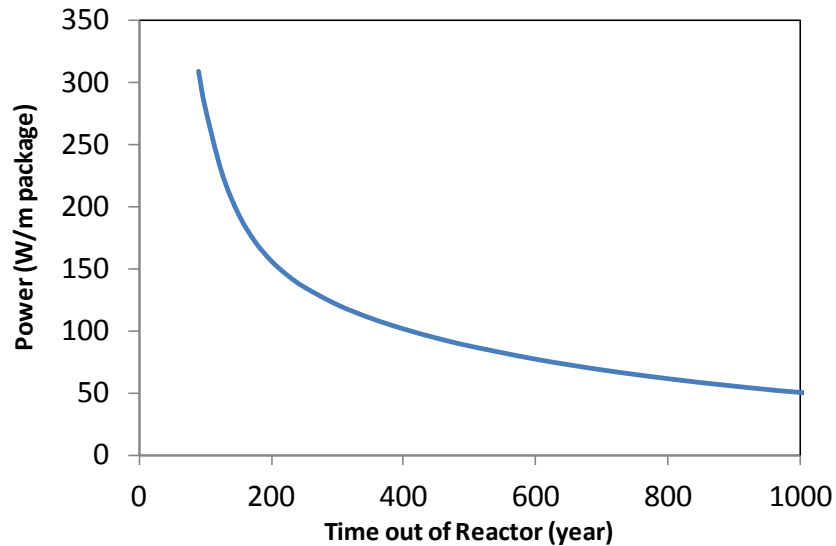


Figure 6-13. Heat load for the 2D THM model

**Mechanical Constitutive Models and Properties** – The rock properties for argillite are listed in Table 6-1. They correspond to the Opalinus Clay, with values taken from Gens et al. (2007) as well as Corkum and Martin (2007). The FLAC3D ubiquitous joint model is used, as previously used by Corkum and Martin (2007) when simulating *in situ* experiments in Opalinus Clay at the Mont Terri Underground Research Laboratory. The theory and implementation of this model are described in the FLAC3D manual (Itasca, 2009).

A linear-elastic swelling model (Rutqvist et al. 2011) is used for the bentonite backfill. Under mechanically constrained conditions, a swelling stress,  $\sigma_s$ , is linearly proportional to the saturation:

$$d\sigma_s = 3K\beta_{sw}dS_l \quad (6-3)$$

where  $K$  is the bulk modulus and  $\beta_{sw}$  is a dimensionless moisture-swelling coefficient ( $\beta_{sw} = 0.0108$ ). Other properties used in the model are shown in Tables 6-1 and 6-2. An elastic model is used for the concrete liner; liner properties are from Kim et al. (2013) except for thermal conductivity. Gibbon and Ballim (1998) cite concrete thermal conductivity values in the range 0.6–2.6 W/m·K, so for this calculation a medial value of 1.6 W/m·K is used for wet conditions, and 1.35 W/m·K for dry concrete applying Eq. 6-2.

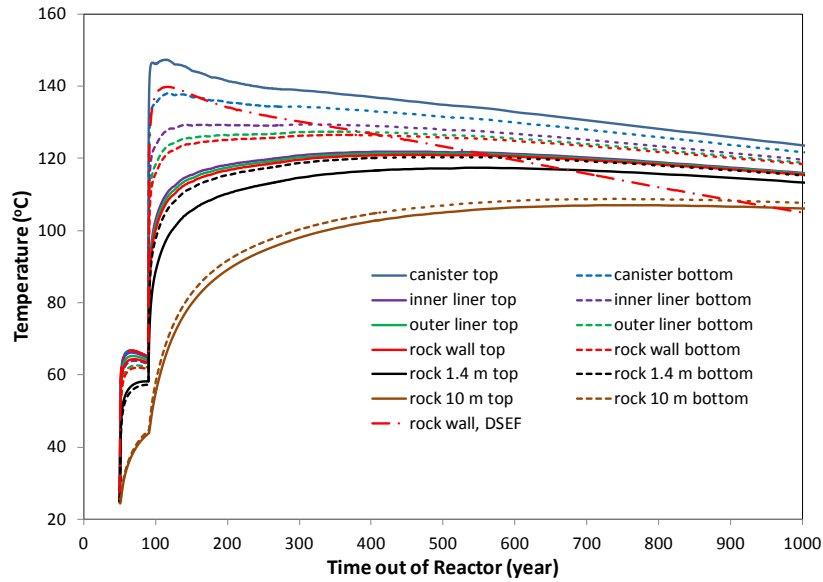
Table 6-2. Thermal, mechanical and hydrodynamic parameters for concrete liner

| Parameter                                | Concrete liner          |
|--|-------------------------|
| Grain density (kg/m <sup>3</sup> )       | 2700                    |
| Porosity $\phi$                          | 0.15                    |
| Saturated permeability (m <sup>2</sup> ) | $5.0 \cdot 10^{-20}$    |
| Relative permeability, $k_{rl}$          | $K_{rl} = S^3$          |
| Van Genuchten $\alpha$ (1/Pa)            | $3.3 \cdot 10^{-8}$     |
| Van Genuchten $m$                        | 0.3                     |
| Compressibility, $\beta$ (1/Pa)          | $5.0 \cdot 10^{-8}$     |
| Thermal expansion coeff. (1/K)           | $1.0 \cdot 10^{-4}$     |
| Dry specific heat (J/kg <sup>o</sup> C)  | 1000                    |
| Thermal conductivity (W/m·K)             | 1.35(dry)/1.6(wet)      |
| Tortuosity for vapor phase               | $\phi^{1/3} S_g^{10/3}$ |
| Young's modulus (GPa)                    | 23                      |
| Poisson's ratio                          | 0.2                     |

**Simulation Results** – Temperature evolution is asymmetrical around the waste package (Figure 6-14). Because of geometry, heat dissipates faster at the bottom, and temperatures are lower than at the top of the waste package. In the concrete liner, peak temperature at the bottom is typically 7 to 10 C° greater than that at the top, and peaks earlier. At the rock wall the maximum temperature is about 126°C at the bottom vs. 120°C at the top. In a 3D model (these TOUGH2-FLAC3D cases are 2D) the regions between waste packages would be much cooler. Figure 6-15 shows the temperature in the backfill starting from 90 years when it is installed. The temperature in the backfill next to the waste package peaks at 140°C and remains near 120°C for 1,000 years (the limit of the simulation time).

Figure 6-16 shows the gas saturation at different locations. During the ventilation period, at the top of the drift, the liner and host rock undergo stronger desaturation than at the bottom of the drift. After the installation of backfill the concrete liner and host rock are rapidly hydrated by moisture transported from the far field, and gas saturation decreases sharply. However, the concrete liner and host rock remain unsaturated until approximately 280 years, although the gas saturation is low.

Initially, the backfill has a gas saturation of 0.35, but after being emplaced in the hot drift, evaporation causes desaturation (Figure 6-17). After some cooling, the backfill is hydrated from the surrounding host rock, and gas saturation decreases. But as with the concrete liner, the backfill does not reach full saturation until approximately 280 years.



Note: DSEF refers to an Excel-based calculation using analytical solutions (Greenberg et al. 2012).

Figure 6-14. Temperature evolution at several locations, solid lines represent the temperature at locations above of the waste package and dashed lines are the temperature at locations below the waste package.

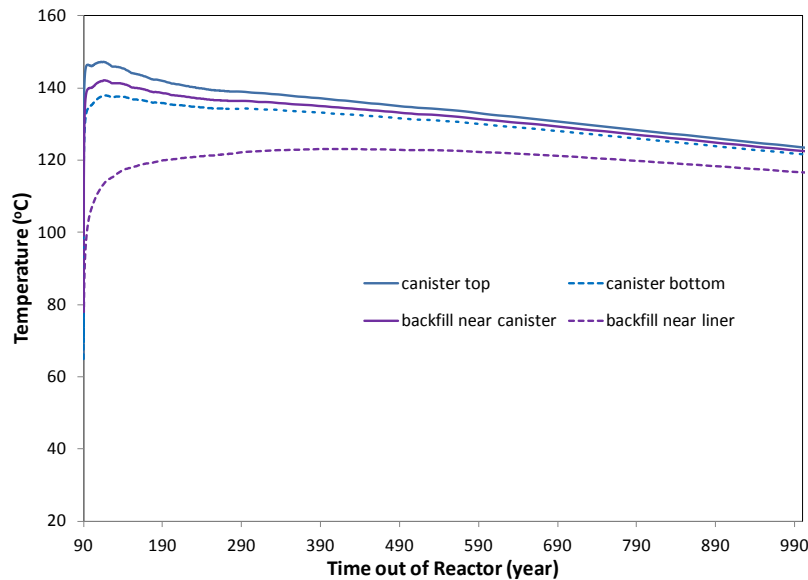


Figure 6-15. Temperature evolution at canister surface and in the backfill

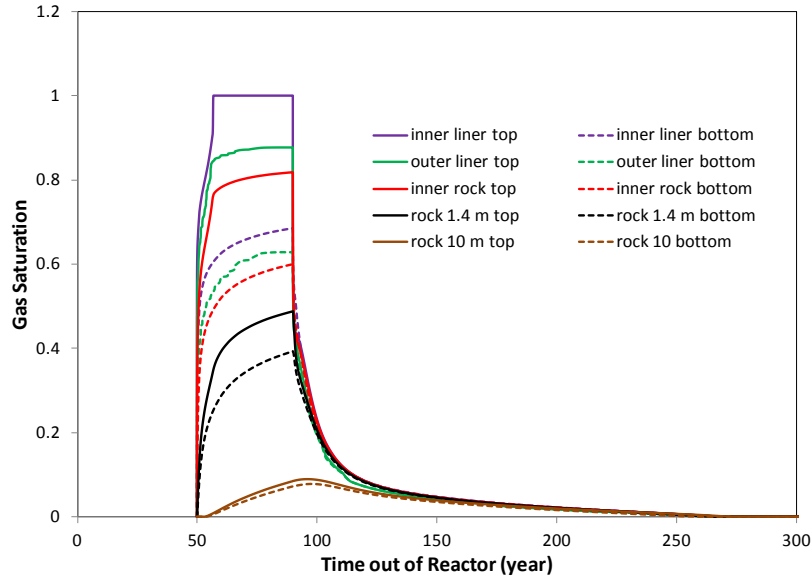


Figure 6-16. Gas saturation evolution at several locations. Solid lines represent locations above the waste package, and dashed lines indicate locations below the waste package

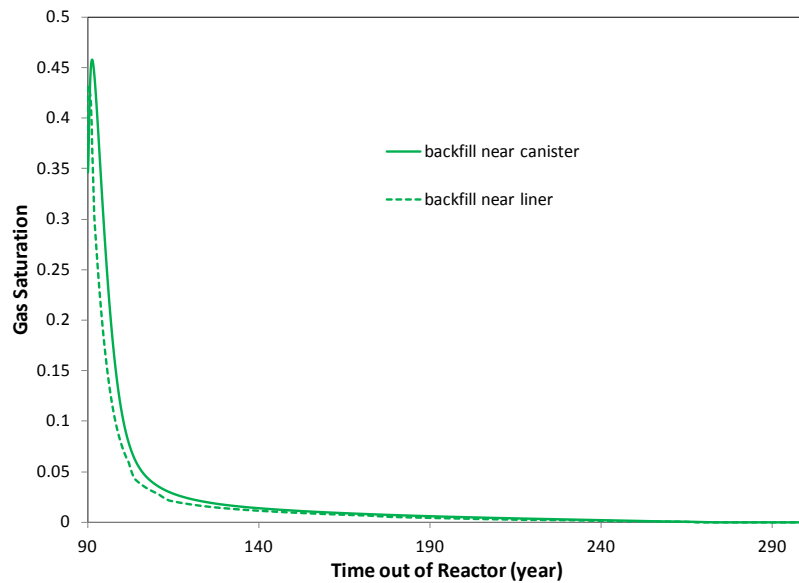


Figure 6-17. Gas saturation evolution at two points in the backfill

The whole system undergoes large changes in pore pressure during heating and cooling. Starting from hydrostatic conditions, the ventilation quickly drives the pore pressure in the concrete and host rock to atmospheric pressure as in the open drift (Figure 6-18). Even after the cessation of ventilation and installation of backfill, the pore pressure remains low as the media remains unsaturated. After it becomes fully saturated everywhere, the pore pressure goes up, and thermal pressurization makes the pressure even higher than hydrostatic fluid pressure, which is  $4.5 \times 10^6$  Pa under ambient temperature conditions.

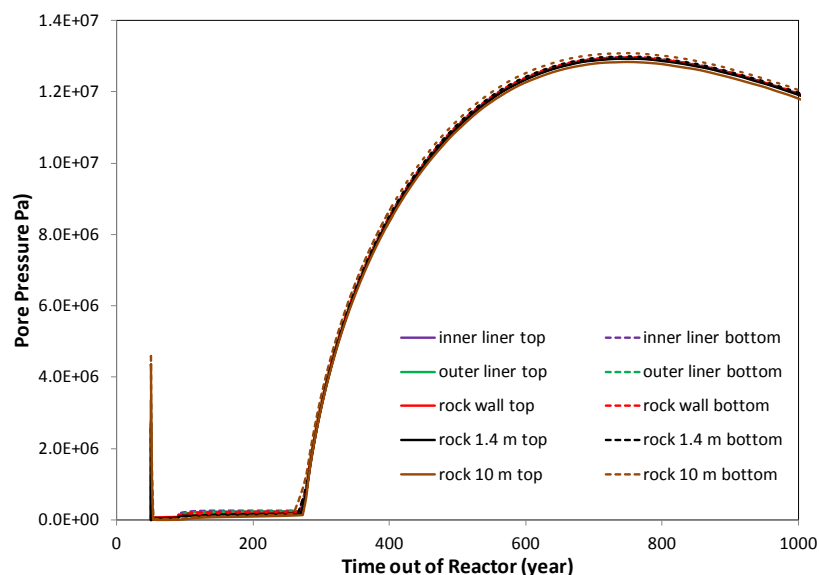


Figure 6-18. Pore pressure evolution at several locations. Solid lines represent the pressure at locations above the waste package, and dashed lines indicate the pressure at locations below the waste package

Figure 6-19 presents the evolution of total stress in the backfill near the canister. The total stress combines far-field loading and body forces, with poroelastic effects, saturation-dependent swelling, and thermal expansion of the solid framework and the pore fluid. In this calculation, the total stress evolves mainly from poroelastic changes in fluid pressure, whereas the effects of swelling (saturation change) and temperature are relatively small. In comparison with the stress evolution in backfill for smaller canisters (4 PWR canister) as assumed in the model of Rutqvist et al. (2014), the stress is higher, mainly because of higher pore pressure resulting from thermal pressurization. The stress changes within the backfill are fairly uniform.

Figure 6-20 shows the maximum and minimum principal stresses in the liner at the bottom of the drift. Increases in pore pressure at early time lead to greater (less negative) minimum compressive principal stress in the liner, and then a gradual decrease (more negative) as the pore pressure decreases. The maximum principal stress in the liner, which is horizontal at the bottom, appears to peak at roughly 700 years.

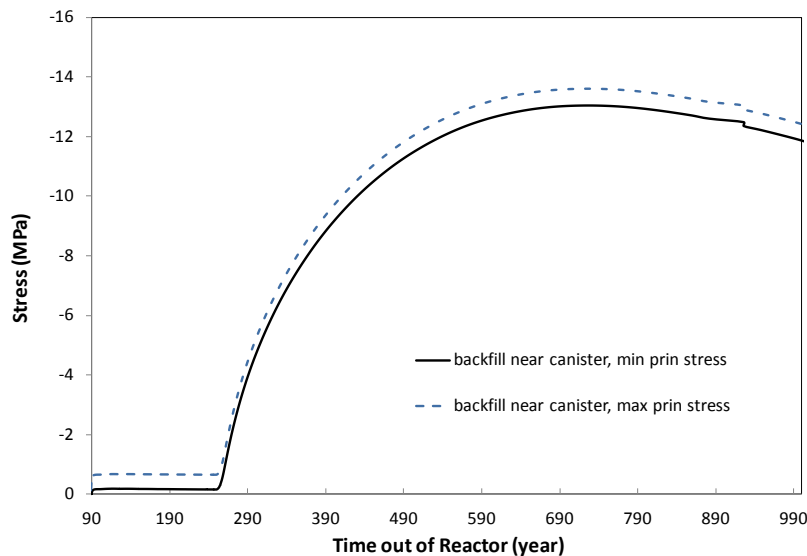


Figure 6-19. Minimum and maximum compressive principal stress within the backfill near the canister

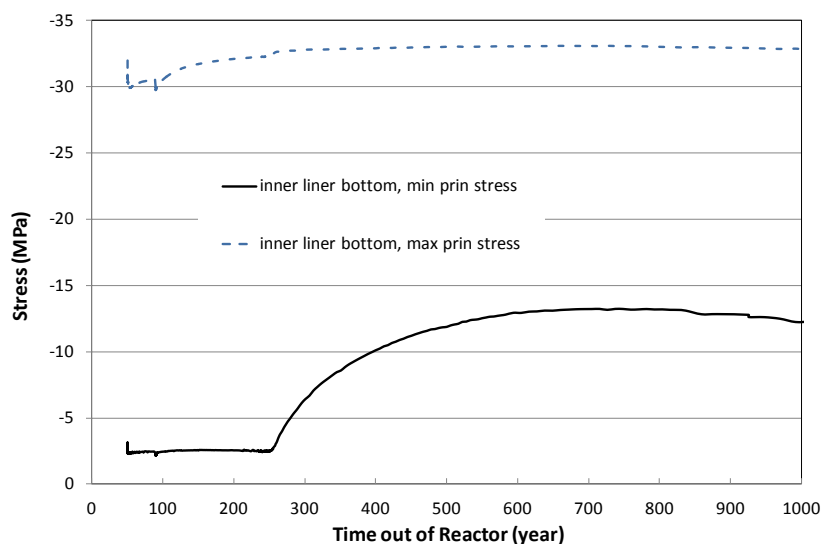


Figure 6-20. Minimum and maximum compressive principal stress within the concrete liner at the bottom

Figure 6-21 shows the maximum and minimum compressive principal stress at the rock wall. Results show a significant increase in the maximum principal stress, which is affected by both temperature and fluid pressure changes. The minimum principal stress, which is the stress normal to the drift wall at this location, is equivalent to the maximum stress in the backfill.

Figure 6-22 shows the maximum and minimum principal stresses in the host rock 10 m away from the rock wall, above the drift crown. While the minimum principal stress does change much

after the initial perturbation by desaturation and resaturation, there is a significant increase in the maximum principal stress, which is affected by the displacement-constrained lateral boundary conditions (and thus the repository layout, which gives rise to the boundary conditions).

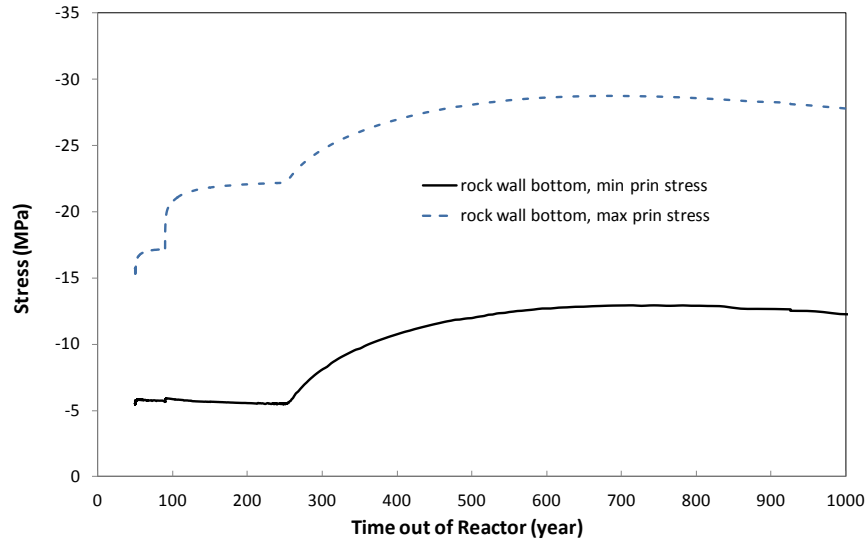


Figure 6-21. Minimum and maximum compressive principal stress at the drift wall

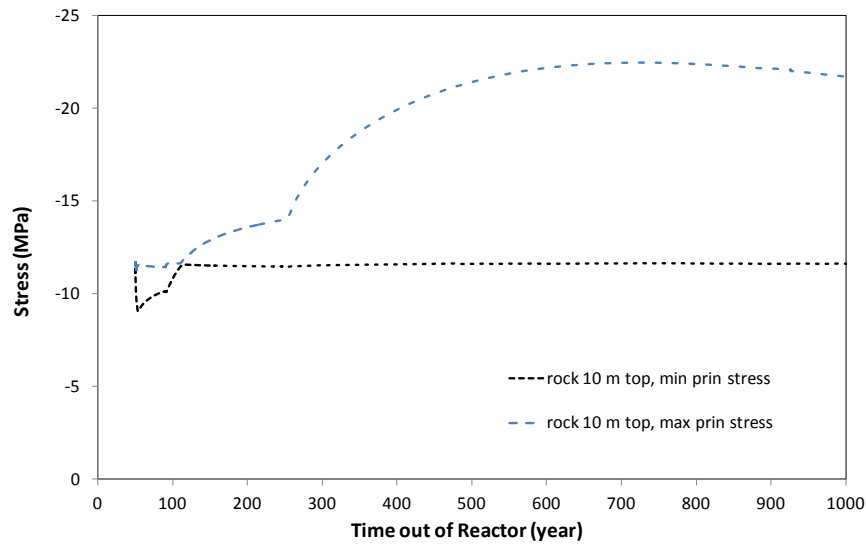


Figure 6-22. Minimum and maximum compressive principal stress in the host rock 10 m away from the drift wall

## 6.4 Summary and Conclusions

Disposal of DPC-based waste packages in argillaceous sedimentary rock has been proposed, but with technical challenges related to thermal management because of the relatively low thermal conductivity and limited temperature tolerance of clay/shale media. Peak temperature limits of 100°C or lower for argillaceous materials have been selected by international programs (SKB 2011, Section 5.5.1; ANDRA 2005, Section 1.2.3.4), and could be applied for SNF disposal in the U.S. However, a limit above 100°C could help to limit the duration of surface decay storage or repository ventilation needed for DPC-based waste packages. The effects of locally higher temperatures on repository performance need to be evaluated (in addition to the effects at lower temperature) and this section demonstrates some of the models that would be used.

The disposal of DPC-based waste packages has technical aspects that differ from concepts for smaller canisters, such as an initial ventilation period, larger emplacement openings, asymmetrical layout of waste packages in the EBS, and possibly a thicker concrete or steel liner to maintain stability. Therefore, investigation of DPC disposal would be supported by a unique set of 2D and 3D models. This section describes progress toward building those models, using a modeling approach that couples the TOUGH2 and FLAC3D codes to represent thermally driven THM processes.

Coupled constitutive models used to evaluate SNF disposal in clay/shale media would be site specific. Clay/shale media tend to vary widely according to composition and properties (thermal, hydrologic, mechanical, chemical). The models presented here are based on properties of the Opalinus Clay, but are essentially generic. More complicated constitutive models are available and could be appropriate, but they tend to involve more parameters for which site-specific laboratory and field investigations would be needed. For example, creep is not modeled here, consistent with observations of little or no creep in the Opalinus Clay over timescales of years to tens of years. However, creep may be important in other clay/shale media such as the Mol Clay (ONDRAF/NIRAS 2001) or the Pierre Shale (Section 2).

A 2D TH model using TOUGH2 (Pruess et al. 1999) is used to evaluate the desaturation of argillaceous host rock as a result of heating, particularly during the preclosure ventilation period. The TOUGH2 model was formulated with a highly permeable drift liner, for a bounding-type calculation of moisture loss. A comparison of temperatures calculated using TOUGH2 and analytical solutions shows similar results, indicating that changes in thermal conductivity with water saturation in the host rock and backfill have minimal effect.

This 2D TH model does not include a steel or concrete liner, and therefore tends to overestimate moisture loss from the host rock during repository ventilation. As noted in Section 2 one of the functions of the liner would be to isolate the host rock to control shrinkage or other potentially destabilizing effects from desiccation. The calculated extent of desaturation from this simulation is a few meters, with smaller influence calculated to more than 10 m. Saturation in the affected zone is predicted to recover within tens to a few hundred years after ventilation ceases and backfill is installed (Figures 6-9 and 6-10). Again, these are overestimates because the model does not include a liner.

A more realistic 2D THM model is used to examine the THM behavior in backfill and host rock. The model represents in-drift emplacement on the floor, with a thick concrete liner and invert. Like the TH model, a bentonite backfill is installed at repository closure. Several observations are made from the model results:

- Temperature in the backfill and liner is a few Celsius degrees higher in the lower part of the drift, and maximum temperatures are immediately below the waste package. This vertical asymmetry in temperature diminishes with distance into the rock.
- During ventilation, the concrete liner and host rock at the top of drift undergo more desaturation than that at the bottom. Longer ventilation duration, greater host rock permeability, and the existence of a DRZ tend to increase the extent of the desaturated zone. After ventilation ceases and backfill is installed, resaturation (moisture migrating from the far field) takes place over a period of tens to a few hundred years.
- Significant, transient increases in stress are calculated in the host rock and backfill, due to thermally and mechanically induced increases in pore pressure, and thermal expansion of the solid framework.
- With installation of a thick concrete liner and swelling-clay backfill, stability is predicted for emplacement drift openings at a depth of 500 m, in a host medium with characteristics similar to the Opalinus Clay.

The models used in this work are 2D and therefore have underestimated peak temperatures, desaturation, and stresses in the immediate vicinity of waste packages. The estimates improve at greater than a few meters distance, so the models can be used to approximate the extent of disturbance in to the host rock. The effect from 2D models is noticeable from comparison to 3D analytical solutions (DSEF, Figure 6-14). The regions between waste packages are known to be cooler, and these results indicate that peak temperature in the backfill at the midpoint between waste packages spaced 20 m or more apart could be less than 100°C (Greenberg et al. 2012; Hardin et al. 2013).

### References for Section 6

ANDRA (National Radioactive Waste Management Agency) 2005. *Dossier 2005 argile – architecture and management of a geological disposal system*. December, 2005.

<http://www.andra.fr/international/pages/en/menu21/waste-management/research-and-development/dossier-2005-1636.html>.

Bossart, P. 2011. *Characteristics of the Opalinus Clay at Mont Terri*.

([http://www.montterri.ch/internet/mont-terri/en/home/geology/key\\_characteristics.html](http://www.montterri.ch/internet/mont-terri/en/home/geology/key_characteristics.html))

Corkum, A.G. and C.D. Martin 2007. “The mechanical behaviour of weak mudstone (Opalinus Clay) at low stresses.” *Int. J. Rock Mech. Min. Sci.* V.44, pp. 196-209.

De Windt, L. and J.M. Palut 1999. “Tracer feasibility experiment FM-C, DI.” In: *Mont Terri Rock Laboratory: Results of the Hydrogeological, Geochemical and Geotechnical Experiments Performed in 1996 and 1997* (Editors: M.Ž. Thury and P. Bossart). Geol. Ber., V.23. Swiss National Hydrological and Geological Survey, Bern.

Gens, A., B. Garitte and Y. Wileveau 2007. “In situ behaviour of a stiff layered clay subject to thermal loading: Observations and interpretation.” *Geotechnique*. V.57, pp. 207-228.

Gibbon, G.J. and Y. Ballim 1998. “Determination of the thermal conductivity of concrete during the early stages of hydration.” *Magazine of Concrete Research*. V.50, pp. 229-235

Greenberg, H.R., M. Sharma, M. Sutton and A.V. Barnwell 2012. *Repository Near-Field Thermal Modeling Update Including Analysis of Open Mode Design Concepts*. Lawrence Livermore National Laboratory. LLNL-TR-572252.

Hardin, E., T. Hadgu, D. Clayton, R. Howard, H. Greenberg, J. Blink, M. Sharma, M. Sutton, J. Carter, M. Dupont and P. Rodwell 2012a. *Repository Reference Disposal Concepts and Thermal Management Analysis*. FCRD-USED-2012-000219 Rev. 2. U.S. Department of Energy, Office of Used Nuclear Fuel Disposition. November, 2012.

Hardin, E., T. Hadgu, H. Greenberg and M. Dupont 2012b. *Parameter Uncertainty for Repository Thermal Analysis*. FCRD-UFD-2012-000097. U.S. Department of Energy, Office of Used Nuclear Fuel Disposition. April, 2012.

Hardin, E. and R. Howard 2013. *Assumptions for Evaluating Feasibility of Direct Geologic Disposal of Existing Dual Purpose Canisters*. FCRD-UFD-2012-000352 Rev. 1. U.S. Department of Energy, Office of Used Nuclear Fuel Disposition. November, 2013.

Hardin, E., D. Clayton, R. Howard, J.M. Scaglione, E. Pierce, K. Banerjee, M.D. Voegelé, H. Greenberg, J. Wen, T.A. Buscheck, J.T. Carter, T. Severynse and W.M. Nutt 2013. *Preliminary Report on Dual-Purpose Canister Disposal Alternatives (FY13)*. FCRD-UFD-2013-000171 Rev. 0. U.S. Department of Energy, Office of Used Nuclear Fuel Disposition. August, 2013.

Harrington, J.F. and S.T. Horseman 1999. "Laboratory experiments on hydraulic and osmotic flow." In: *Mont Terri Rock Laboratory: Results of the Hydrogeological, Geochemical and Geotechnical Experiments Performed in 1996 and 1997* (Editors: M.Ž. Thury and P. Bossart). Geol. Ber., V.23. Swiss National Hydrological and Geological Survey, Bern.

Hicks, T.W., M.J. White and P.J. Hooker 2009. *Role of Bentonite in Determination of thermal Limits on Geological Disposal Facility Design*. Galson Sciences Limited.

Itasca (Itasca Consulting Group) 2009. *FLAC3D V4.0, Fast Lagrangian Analysis of Continua in 3 Dimensions, User's Guide*. Minneapolis, MN.

Kim, H.-M., J. Rutqvist, J.-H. Jeong, B.-H. Choi, D.-W. Ryu and W.K. Song 2013. "Characterizing Excavation Damaged Zone and Stability of Pressurized Lined Rock Caverns for Underground Compressed Air Energy Storage." *Rock Mechanics and Rock Engineering*. V.46, N.5, pp. 1113-1124.

NAGRA (National Cooperative for the Disposal of Radioactive Waste) 1989. *Sedimentstudie-Zwischenbericht, 1988. Möglichkeiten zur Endlagerung Langlebiger Radioaktiver Abfälle in den Sedimenten der Schweiz*. NAGRA Technischer Bericht 88-25. NAGRA, Baden, Switzerland. Executive summary in English.

ONDRAF/NIRAS (Belgian Agency for Radioactive Waste and Enriched Fissile Materials) 2001. *SAFIR 2: Safety Assessment and Feasibility Interim Report 2*. NIROND 2001-06 E, December, 2001.

Pruess, K., C. Oldenburg and G. Moridis 1999. *TOUGH2 User's Guide, Version 2.0*. Lawrence Berkeley National Laboratory, Berkeley, CA.

Rutqvist, J., Y. Ijiri and H. Yamamoto 2011. "Implementation of the Barcelona Basic Model into TOUGH-FLAC for simulations of the geomechanical behavior of unsaturated soils." *Computers & Geosciences*. V.37, pp. 751-762.

Rutqvist, J., L. Zheng, F. Chen, H.-H. Liu and J.T. Birkholzer 2014. “Modeling of Coupled Thermo-Hydro-Mechanical Processes with Links to Geochemistry Associated with Bentonite-Backfilled Repository Tunnels in Clay Formations.” *Rock Mechanics and Rock Engineering*. V.47, N.1, pp. 167-186.

SKB (Swedish Nuclear Fuel and Waste Management Co.) 2011. *Long-term safety for the final repository for spent nuclear fuel at Forsmark: Main report of the SR-Site project, Volume I*. Technical Report TR-11-01.

Birkholzer, J., J. Rutqvist, E. Sonnenthal and Barr, D. 2008. *DECOVALEX-THMC Project Task D Final Report*. Chapter 5: Long-Term Permeability/Porosity Changes in the EDZ and Near Field due to THM and THC Processes in Volcanic and Crystalline-Bentonite Systems.

Soler, J.M. 2001. “The effect of coupled transport phenomena in the Opalinus Clay and implications for radionuclide transport.” *Journal of Contaminant Hydrology*. V.53, N.1–2, pp. 63-84.

Tang, A.M., Y. Cui and T.T. Le 2008. “A Study on the Thermal Conductivity of Compacted Bentonites.” *Applied Clay Science*. V.41, pp. 181-189.

Thury, M. 2002. “The characteristics of the Opalinus Clay investigated in the Mont Terri underground rock laboratory in Switzerland.” *Comptes Rendus Physique*. V.3, N.7-8, pp. 923-933.

Zheng, L., L. Li, J. Rutqvist, H.-H. Liu and J.T. Birkholzer 2012. *Modeling Radionuclide Transport in Clays*. Lawrence Berkeley National Laboratory. FCRD-UFD-2012-000128. U.S. Department of Energy, Office of Used Nuclear Fuel Disposition.

Zheng, L., J. Rutqvist, H. Greenberg and J. Birkholzer 2014. *Model Evaluation of the Thermo-Hydrological-Mechanical Response in Argillaceous Sedimentary Rock Repository for Direct Disposal of Dual-Purpose Canisters*. FCRD-UFD-2014-000515. U.S. Department of Energy, Office of Used Nuclear Fuel Disposition. June, 2014.

## 7. Potential for Vertical Movement of Waste Packages in a Salt Repository

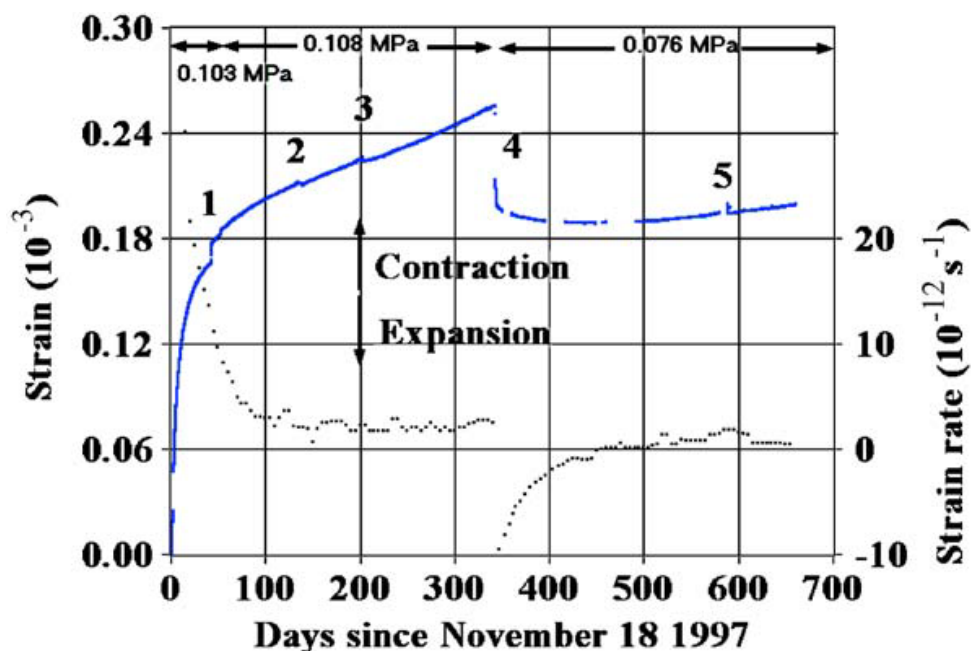
A salt repository has been identified with superior heat dissipation and neutron absorption properties, both of which are conducive to DPC direct disposal. Vertical movement (sinking) of heavy DPC-based waste packages in salt has also been identified as a potentially important process in salt repository performance (Winterle et al. 2012; OECD/NEA 2000). Extensive sinking (e.g., more than 1 m per  $10^4$  years) could move waste packages out of the host unit especially in bedded salt, where they could be exposed to different strata and possible ground water flux. Creep constitutive laws for salt that have been used for decades do not predict significant waste package sinking (Clayton et al. 2013). However, recent creep tests on salt cores at low deviatoric stress similar to what could be produced by a heavy waste package, show the potential for creep that is not predicted by those creep laws.

The possibility of waste package vertical movement over 10,000 years or longer has been recognized for decades (e.g., Dawson and Tillerson 1978) but has received little attention compared to other processes such as crushed salt backfill reconsolidation and brine migration. Simulations using widely known constitutive models suggest that waste package vertical movement due to negative buoyancy would be very small (Clayton et al. 2013). However, interpretation of recent salt creep tests (Bérest et al. 2005, 2012) suggests that LS-LSR deformation could produce significant movement. This section explores the implications of LS-LSR creep for vertical package movement, and presents a working hypothesis that can be tested to determine the importance of LS-LSR creep.

Salt rheology has been extensively studied using *in situ* observations and laboratory tests. Constitutive models have been developed and conditioned on laboratory data and multi-year observations of room and borehole closure. However, the strain rates associated with these observations are orders of magnitude greater than that which could be associated with slow sinking of waste packages for thousands of years (on the order of 1 meter per  $10^4$  years or greater).

A possible mechanism for salt creep that prevails at low temperature, low stress, and low strain-rate conditions was recognized decades ago (Munson and Dawson 1984) but only in the past few years have attempts been made to measure it (Bérest et al. 2005, 2012). In these tests, creep strains on the order of  $10^{-4}$  are produced at rates on the order of  $10^{-12}$ /sec. An example from Bérest et al. (2005) of long-term (22 months) creep test results is shown in Figure 7-1. Creep strain was defined as change in length divided by initial length. These tests were dead-loaded, and performed underground in a remote part of a salt mine with stable temperature and humidity conditions. The mechanism is thought to involve pressure solution because it is similar to deformation at greater strain rates, that is known to depend on moisture content.

**Pressure Solution Mechanism** – Regarding pressure solution, Weinberg (1993) wrote: “...several laboratory studies have indicated that dry salt deforms by dislocation creep and behaves as a power-law fluid at high strain rates” and that “traces of brine in confined salt deforming at slow strain rates cause a change in the deformation mechanism from dislocation creep to solution-transfer creep in relatively fine grained salt (Urai et al. 1986). The salt then becomes weaker and behaves like a Newtonian fluid with a viscosity that is directly proportional to the cube of grain size.”



Source: Bérest et al. (2005, Figure 7). Core size 7 cm dia. × 16 cm long.

Figure 7-1. Strain vs. time and strain-rate vs. time, for a core of Etrez salt, unconfined and axially dead-loaded at the levels shown

Spiers et al. (1986) concluded that rheology of surrounding bedded salts may be important to control long-term stability, that stresses around a repository may equilibrate faster than previously thought, and that brine migration toward hot canisters may cause softening and increased rates of sinking (bounded at 1 m per  $10^4$  yr). Thus, brine intrusion into an excavation could accelerate and possibly localize low strain-rate deformation. Spiers et al. (1990) introduced a power law for pressure solution

$$\dot{\epsilon} = 6.95 \cdot V_m \cdot 10^{-15} \frac{\exp(-Q/RT) \sigma}{T d^3} \quad (7-1)$$

where

- $V_m$  = molar volume ( $2.693 \cdot 10^{-5}$  m<sup>3</sup>/mole)
- $Q$  = Activation energy (24,530 J/mole)
- $R$  = Gas constant (8.314 J/mole-K)
- $T$  = absolute temperature (K)
- $\sigma$  = differential stress (Pa)
- $d$  = grain size (m)

This power law incorporates Newtonian behavior (stress exponent  $n=1$ ) with strong grain size dependence ( $d^{-3}$ ). Spiers et al. (1990) concluded in part that the relative importance of pressure solution (as judged from natural microstructural observations) diminishes during natural diapirism due to: 1) water loss during progressive shearing; 2) increased deformation rates as diapir structures evolve; and 3) some other mechanism (possible dislocation related). For the LS-LSR test conditions of Bérest et al. (2005, 2012) and grain size of 1 cm, expression (7-1) yields

strain rates on the order of  $10^{-15}$ /sec at 25°C. For grain size of 1 cm, the expression yields viscosity on the order of  $10^{19}$  Pa-sec at 300 K. These results are too slow and viscous to represent the Bérest et al. data.

The Newtonian form of expression (7-1) contrasts with power laws conditioned on laboratory data and multi-year observations of room and borehole closure, where strain rates are much greater. For example, the compilation by Weinberg (1993) includes a power law for Permian Salado formation salt:

$$\dot{\epsilon} = 2.42 \cdot 10^{-44} \sigma^{4.9} \quad (7-2)$$

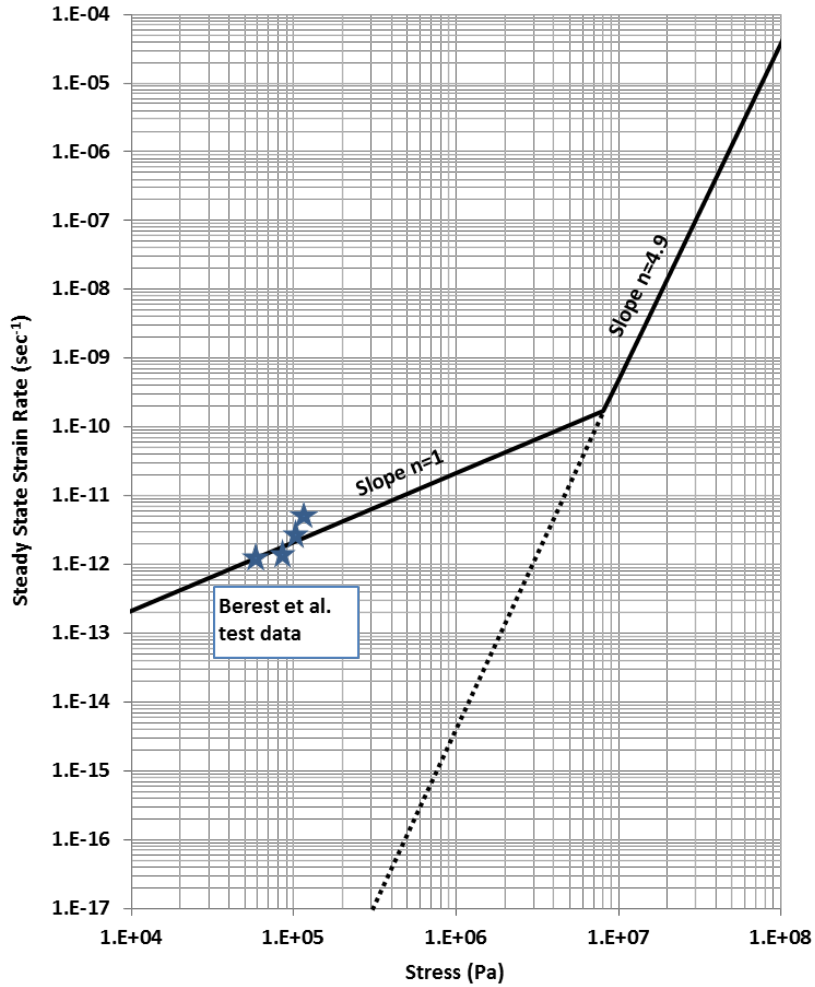
with stress units of Pa, and temperature of 300 K.

**Spliced Constitutive Model** – To explore the modeling implications of these different laws, expressions (7-1) and (7-2) are spliced. The intercept of the segments with different slopes on a log-log plot, as shown in Figure 7-2(a), is constrained by the Bérest et al. (2005, 2012) data so that the transition stress is  $\sigma = 8$  MPa. This value is model dependent, and does not signify a sharp transition in salt response. The approach is similar to that of Bérest et al. (2012) who analyzed the LS-LSR deformation of a solution-mined storage cavity using a transition stress of 4 MPa.

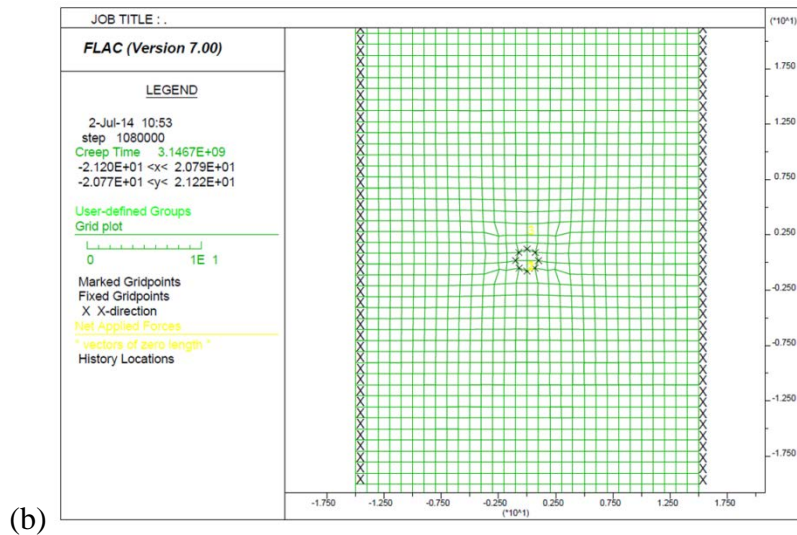
**Repository Simulation Comparative Analysis** – The spliced constitutive model is used in the FLAC code (Itasca 2011) with a grid representing a cross-section through a repository drift, shown in Figure 7-2(b). The drift opening is filled with crushed salt installed at initial porosity of 36% with creep-consolidation behavior represented by the *cwipp* constitutive model in FLAC. A 2-m diameter waste package rests on the floor. The waste package is assigned the density of steel ( $8 \cdot 10^3$  kg/m<sup>3</sup>, greater than the average density expected for DPC-based waste packages  $\sim 5 \cdot 10^3$  kg/m<sup>3</sup>).

The simulation was run for 100 years, and vertical displacements plotted for the drift crown, and the floor below the waste package (Figure 7-3). The plots show initial displacements when the opening is excavated (down at the crown, up at the floor), followed by creep response as the opening closes and the backfill consolidates. The figure compares results with the original Norton law for Salado salt (Weinberg 1993) with the spliced model. The Norton law produces gradual creep response, then stability as the backfill approaches intact density and the stress state returns to lithostatic. Importantly, the spliced model exhibits rapid creep response, followed by steady-state downward movement of the waste package and the surrounding salt. The velocity of this movement is approximately 1 meter per  $10^4$  years.

The rapid creep response with the spliced model is unrealistic. This modeling exercise shows that if LS-LSR creep can occur throughout the rockmass, then salt in the far field creeps rapidly, shifting load to the near field around openings where salt creep accelerates because of greater stress. This modeling situation leads to questions about the role of the mean stress, i.e., confining stress, in constitutive models that include LS-LSR behavior.

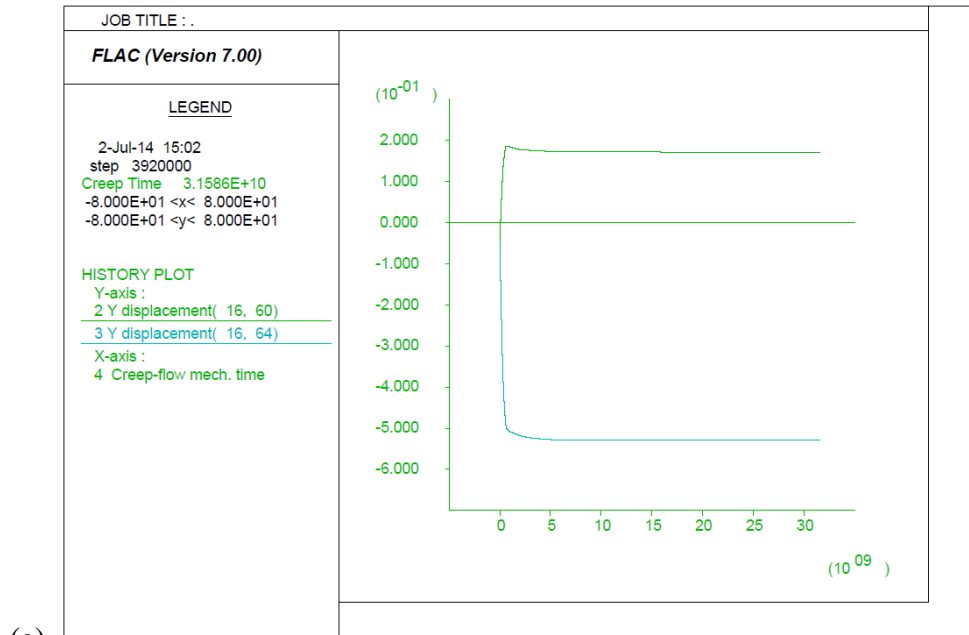


(a)

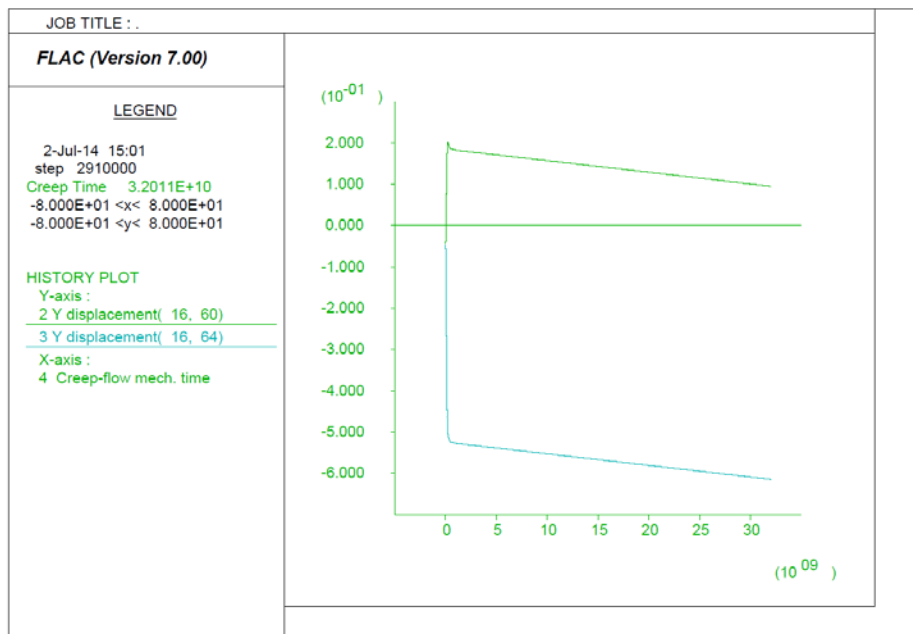


(b)

Figure 7-2. Modeling details: (a) spliced Norton and Newtonian constitutive laws, and (b) FLAC model grid used in comparative analysis.



(a)



(b)

Note: In each plot the drift crown is the lower trace, and the floor is the upper trace. Thus, the crown moves downward and the floor upward in response to initial excavation of the drift opening.

Figure 7-3. Time dependent crown and invert displacements for a rectangular waste emplacement opening in salt, for 100 years, using: (a) a Norton-type constitutive power law, and (b) a Norton-type power law spliced to a Newtonian LS-LSR at stresses less than 8.1 MPa.

If the LS-LSR creep strain rate is attenuated by confining stress, then existing creep models hold and sinking of DPC-based packages would be insignificant. If LS-LSR creep occurs at confined as well as unconfined conditions, then waste packages could sink at velocities of 1 m per  $10^4$  years or greater. This assessment does not take into account the effects of heating, which lasts only about 1,000 years but could increase strain rates by 2 to 3 orders of magnitude (activation energy of  $50.2 \cdot 10^3$  J/mol-K; Weinberg 1993). An R&D approach that tests the effect of confinement on LS-LSR creep, could use a predictive model based on the following research hypothesis.

**Research Hypothesis** – Pressure solution occurs at grain boundaries where they are bridged by contacts. A film of moisture covers each contact, and remains even after salt cores are drilled and thus unloaded (dilation that occurs with unloading can produce unsaturated conditions in grain-boundary porosity). Dissolution and solute diffusion can occur in the brine film as deduced by Hickman and Evans (1995). When cores are subjected to loading, framework stress is concentrated through the grain boundary contacts. The more highly stressed salt at the contacts dissolves into the brine film and diffuses outward to the edge of the contact where stress is smaller.

Following the model of Rutter (1976) the convergence rate at each circular contact is proportional to the contact force, and inversely proportional to the 4<sup>th</sup> power of the contact radius. Thus, as the mean stress increases, contact force increases, the contact radius grows, and pressure solution slows down. The physical interpretation is that diffusive transport through the brine film slows down as the path length increases. To help quantify the effect, volume strain observed in the laboratory at low confining pressure could be interrogated to estimate contact abundance and radius. Using this conceptual model, the slope of an experimentally determined volume strain vs. confining pressure curve, at pressures in the range of interest (e.g., 0.1 to 5 MPa), would be inversely proportional to contact radius assuming a grain size and the number of contacts between grains. By substituting, an inverse relationship between the rate of pressure-solution creep and confining pressure could be developed. In this way the LS-LSR data of Bérest et al. (2005, 2012) could be accommodated, while higher stress, higher strain-rate simulations show behavior more typical of that observed in large-scale *in situ* tests underground.

This semi-mechanistic constitutive modeling approach could be useful because direct measurements at LS-LSR conditions are difficult, and have not yet been done at lithostatic conditions. Additional testing is needed to better understand LS-LSR behavior over a wider range of stress conditions in different salt media, and to confirm the role of moisture. Observation of LS-LSR deformation in carefully dried samples could confirm the role of brine, and help to verify the deductions of Hickman and Evans (1995). An observation that LS-LSR creep slows significantly at confined conditions would greatly improve understanding of grain boundary effects. Another challenge is to characterize the long-term accumulation of larger strain due to LS-LSR creep which could be prohibitive to measure directly.

### References for Section 7

Bérest, P., P.A. Blum, J.P. Charpentier, H. Gharbi and F. Valès 2005. “Very slow creep tests on rock samples.” *Int. J. Rock Mech. & Mining Sci.* V.42. pp. 569–576.

Bérest, P., J.F. Béraud, M. Bourcier, A. Dimanov, H. Gharbi, B. Brouard, K. DeVries and D. Tribout 2012. “Very slow creep tests on rock samples.” in: *Proc. Mechanical Behavior of Salt VII* (P. Bérest et al. editors). April 16-19, 2012. Paris, France. CRC Press.

Clayton, D.R., M.J. Martinez and E.L. Hardin 2013. *Potential Vertical Movement of Large Heat-Generating Waste Packages in Salt*. Sandia National Laboratories, Albuquerque, NM. SAND2013-3596.

Dawson, P.R. and J.R. Tillerson 1978. *Nuclear Waste Canister Thermally Induced Motion*. Sandia National Laboratories, Albuquerque, NM. SAND-78-0566.

Hickman, S.H. and B. Evans 1995. "Kinetics of pressure solution at halite-silica interfaces and intergranular clay films." *J. Geophys. Res.* V. 100, N. B7, pp. 13,113-13,132.

Itasca (Itasca Consulting Group) 2011. *FLAC Version 7.00 User's Guide*. Minneapolis, MN.

Munson, D.E. and P.R. Dawson 1984. "Salt constitutive modeling using mechanism maps." In: *Proc. Mechanical Behavior of Salt II* (Hardy, H.R. Jr. and M.N. Langer, editors). Trans. Tech. Publications. Hanover, Germany. pp. 717-737.

OECD/NEA (Organisation for Economic Co-operation and Development/Nuclear Energy Agency 2000. *Features, Events, and Processes (FEPs) for Geologic Disposal of Radioactive Waste—An International Database*. Proceedings of OECD/NEA Conference, January 23–25, 2007. Paris, France.

Spiers, C.J., J.L. Urai, G.S. Lister, J.N. Boland and H.J. Zwart 1986. *The influence of fluid-rock interaction on the rheology of salt rock*. Commission of the European Communities, Nuclear Science and Technology. Report EUR-10399.

Spiers, C.J., P.M.T.M. Schutjens, R.H. Brzesowsky, C.J. Peach, J.L. Liezenberg and H.J. Zwart 1990. "Experimental determination of constitutive parameters governing creep of rocksalt by pressure solution." In: *Deformation Mechanisms, Rheology and Tectonics* (R.J. Knipe and E.H. Rutter, editors). Geol. Soc. London, Spec. Publ. 54. pp. 215-227.

Urai, J.L., D.J. Spiers, H.J. Zwart and G.S. Lister 1986. "Weakening of rock salt by water during long-term creep." *Nature*. V. 324, N. 11, pp. 554-557.

Weinberg, R.F. 1993. "The upward transport of inclusions in Newtonian and power-law salt diapirs." *Tectonophysics*. V.22, pp. 141-150.

Winterle, J., G. Ofoegbu, R. Pabalan, C. Manepally, T. Mintz, E. Percy, K. Smart, J. McMurry, R. Pauline and R. Fedors 2012. *Geologic Disposal of High-Level Radioactive Waste in Salt Formations*. Contract NRC-02-07-006. U.S. Nuclear Regulatory Commission. March, 2012. 45 pp.

THIS PAGE INTENTIONALLY LEFT BLANK

## 8. DPC Materials and Corrosion Environments

This section summarizes information on DPC materials (Greene et al. 2013; Hardin et al. 2013) and their mechanisms of corrosion in expected disposal environments, emphasizing basket materials particularly stainless steel. The materials used in existing DPCs are summarized in Table 8-1.

### 8.1 Materials Used in DPCs

Canister shells are nearly all constructed from stainless steel alloys, with the exception of some versions of the NAC-MPC canister that use carbon steel (Table 8-1). Typical canister shells are made from stainless steel SS-304L or 316 (Hardin et al. 2013). Holtec International lists “alloy X” as the preferred canister material, where the four stainless steel alloys that meet the requirements for “alloy X” are 316, 316LN, 304, and 304L (BSC 2003).

Baskets maintain spacings between fuel assemblies, transfer heat, and support neutron absorber elements. A number of common DPC designs use stainless steel for major basket components (e.g., Holtec HI-STAR 100 MPC®, NAC Universal MPC® system, and most of the NUHOMS® systems) (BSC 2003; Greene et al. 2013). In general, baskets are fabricated with square stainless steel tubes, or egg-crate arrangements of stainless steel plates, to which sheets of neutron absorbing material are affixed between assemblies. Besides stainless steels 304/304L and 316/316L, other basket materials can include: precipitation-hardened Type 17-4 (for PWR support disks), SA-533 (for BWR support disks), and aluminum (for heat transfer disks) (NAC UMS and Yankee systems; BSC 2003). In some NUHOMS® systems, aluminum-coated carbon steel is used to support flux traps in the basket, and in the BNFL Fuel Solutions DPC some of the basket components can be fabricated with nickel-coated carbon steel (BSC 2003).

Metal matrix composite (MMC) materials are commonly used for neutron absorbers. MMC sheets are fabricated with finely divided boron carbide ( $B_4C$ ) evenly dispersed in an aluminum matrix (Lindquist 2009). Commonly used MMC materials (e.g., Boral® or Metamic®) perform in fuel pools and are used in DPCs licensed for transportation, but can readily corrode over time frames relevant to disposal: on the order of  $1.91 \text{ mg cm}^{-2} \text{ yr}^{-1}$  giving estimated corrosion lifetime of as few as 40 years (Lindquist 2009). Accordingly, these materials cannot be relied on as neutron absorbers during long-term exposure to ground water in geologic disposal environments.

More durable neutron absorber materials include borated stainless steel and nickel-gadolinium alloys (Wells 2008). Laboratory testing using electrochemical methods show estimated general corrosion rates for these materials ranging from  $0.03$  to  $0.65 \text{ } \mu\text{m yr}^{-1}$  for borated stainless steel 304B4, and from  $0.96$  to  $94 \text{ } \mu\text{m yr}^{-1}$  for a Ni-Cr-Mo-Gd alloy (Lister et al. 2007). A few DPC systems offered by vendors would use longer-lasting neutron absorber materials, but implementation has been very limited and is not significant with respect to the overall inventory of existing DPCs (BSC 2003; Greene et al. 2013).

Whereas aluminum-based materials such as Boral® or Metamic® are expected to readily corrode in any disposal environment where exposed to ground water, stainless steel basket structures could maintain configuration stability depending on corrosion modes and rates, and basket component thicknesses. Structural integrity is unlikely to be significantly affected by localized corrosion (crevice corrosion, pitting, and stress corrosion cracking) especially for basket components that are loaded in compression. The basket fits closely into the canister

shell, which provides confinement, and the shell fits into the disposal overpack, which provides additional confinement.

Details of basket degradation are beyond the scope of the current study, and are called out as information needs (Sections 10.4 and 10.5). This review focuses on the performance of basket materials that could be exposed to ground water over thousands of years, and prospective disposal overpack materials that could possibly be used to protect DPCs in disposal environments.

Table 8-1. DPC materials summary (data from Greene et al. 2013)

| Storage/Transport System | Canister Materials                                       | Internals/Basket Materials   | Shield Plug Materials  |
|--------------------------|--|--|--|
| FuelSolutions™           | SS   | Steel/Boral®   | DU/SS or SS/CS   |
| HI-STORM 100®            | SS   | SS/Metamic®/Al   | SS   |
| HI-STAR 100®             | SS   | SS/Boral®/Al<br>SS/Metamic®/Al   | SS<br>SS   |
| HI-STAR 190®             | N/A  | N/A  |  |
| NAC-MPC®                 | SS<br>Concrete/CS<br>CS/Pb                               | SS/Boral®/Al<br>NS-4-FR<br>NS-4-FR   | SS<br>SS<br>SS   |
| NAC-UMS®                 | SS<br>SS<br>Concrete/Steel                               | SS/Al/Boral®<br>SS/CS/Boral®/Al<br>NS-4-FR   | SS<br>SS<br>NS-4-FR  |
| NAC-MAGNASTOR®           | SS   | Ni-plated CS/SS  | SS   |
| NUHOMS®                  | SS<br>SS<br>SS<br>SS<br>SS<br>SS<br>SS<br>SS<br>SS<br>SS | Steel<br>Steel/B-Al/Al<br>SS/Boral®<br>SS/B-Al/Boral®/MMC<br>SS/Al/MMC<br>SS/Al-B sheets<br>SS/Boron plates<br>SS/Boral®<br>CS/B-SS<br>CS/B-Al/MMC/Boral®/Al | CS or SS/Pb<br>Steel/Pb<br>Steel or<br>Steel/Pb<br>Steel<br>Steel<br>CS or Steel/Pb<br>CS<br>SS/Pb<br>CS<br>CS |

Note: CS = carbon steel; SS = stainless steel; DU = depleted U; other symbols are trademarks as noted, or chemical elements.

## 8.2 Factors Controlling Material Corrosion Rates in Disposal Environments

Based on the driving forces and mechanisms, the following corrosion types have been identified: galvanic or bimetallic, uniform or general attack, localized corrosion (crevice,

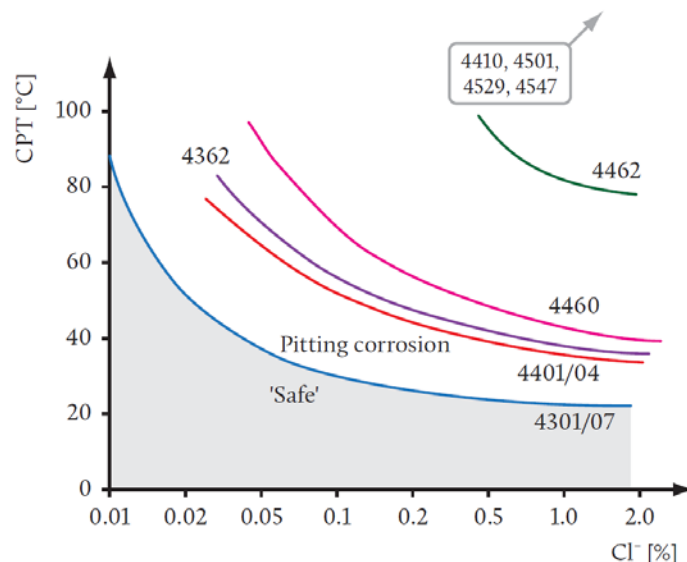
pitting, intergranular, and stress corrosion cracking; APV 2008), and microbial. The local geochemical environment plays a significant role in corrosion processes, and prominent physico-chemical drivers include availability of moisture, ion concentrations, pH, and temperature.

Galvanic corrosion occurs when two conducting materials are in electrical contact with each other in an electrolyte solution. As a result, galvanic current is generated between these two metals. This galvanic current generally causes a reduction in the total corrosion rate of the cathodic member of the couple, while amplifying the corrosion of the anode (which is sometimes called the sacrificial anode) (Zhang 2011). This process is well understood for various metallic material couples, and is not expected to impact stainless steel. The aluminum-based neutron absorbers will serve as protective anodes for stainless steel basket materials (one reason why these neutron absorbers would be relatively short-lived). For stainless steel to be anodically corroded would require a cathode that is significantly more noble (higher on the galvanic series). Corrosion resistant materials such as copper, titanium, Zircaloy and nickel-chromium alloys that might be used in the disposal overpack, do not produce sufficient potential differences with stainless steel to support galvanic corrosion. Hence, galvanic corrosion would not be important to long-term behavior of stainless steel in DPCs, in disposal environments.

Uniform or general corrosion is characterized by both anode and cathode reactions across the entire surface of the material. As a result, a overall uniform loss of material (due to the oxidation and dissolution of the oxide layer) is observed. In corrosion allowance materials such as carbon steel, uniform corrosion is the most common corrosion type yet it is considered negligible in many industrial applications. Uniform corrosion is slow in corrosion-resistant materials (generally passivating metals, including stainless steels) and is generally detectable only in aggressive chemical media such as concentrated acids or bases (Jessen 2011).

Localized corrosion can take place within days, and therefore can significantly limit containment lifetime of materials such as stainless steel (although it may be of minor importance to basket structural lifetime as discussed above). For example, pitting penetration of a 0.5 mm thick stainless sheet in the presence of chloride and hydrogen peroxide was observed after 4 days (Jessen 2011). Pitting and crevice corrosion are the most common localized corrosion types for stainless steels.

The formation of pits on stainless steel surfaces proceeds due to the local breakdown of the passive oxide layer. The pit behaves as an anode, while the oxide film over the rest of the surface behaves as a cathode, with the resulting internal galvanic coupling driving pit growth (Jessen 2011). Temperature, chloride concentration, availability of oxidants, and pH are the most important chemical drivers for local corrosion including pitting (Kursten et al. 2004; Smart et al. 2004). The corrosion rate increases with increasing temperature, chloride content, availability of oxidants (e.g., hydrogen peroxide, perchlorate, dissolved oxygen), and decreasing pH. Laboratory measurements of stainless steel pitting in well-aerated, semi-neutral solutions show that concentration of chloride controls the critical pitting temperature. Critical pitting temperature curves as a function of chloride content for several stainless steel alloys are shown in Figure 8-1. However, it should be noted that these data are for the base metals; sensitization and residual stresses in weld heat-affected zones (HAZ) lower the critical pitting temperature for a given chloride concentration.



## Notes:

1. ISO grades shown.
2. ISO4401 is comparable to Grade SS 316, and ISO4301 is comparable to SS 304.
3. Other grades shown are high-performance austenitic and/or martensitic compositions.

Figure 8-1. Critical pitting temperature for stainless steel alloys as a function of chloride concentration (from Jassen 2011)

Crevice corrosion is controlled by the same chemical drivers as pitting. However, these two corrosion processes differ in how fluids are replaced: crevice corrosion evolves in confined spaces where the fluid is replaced by diffusion, while fluids are free to move convectively during pitting corrosion (Jassen 2011). Diffusion-limited fluid transport causes the evolution of localized conditions favoring enhanced corrosion (e.g., lower local pH and ion concentrations; APV 2008). Linear dimensions of the confined space determine whether crevice corrosion is likely to initiate; it usually occurs in gaps of a few hundred microns or less, and is rarely observed in crevices deeper than 2 mm (APV 2008). The initiation of crevice corrosion can happen within a few hours to several months, and can proceed rapidly after initiation (APV 2008).

Stress corrosion cracking (SCC) is observed in corrosion resistant materials including stainless steel. It is localized around areas of residual stress produced from welding, thermal cycling, or mechanical stress to yield (cold-work). SCC can cause rapid penetration and loss of structural integrity in some applications. Similar to the other localized corrosion processes, SCC is controlled by the presence of water vapor or an aqueous phase, corrosive species (particularly chloride), oxidizers, pH, and temperature.

In addition to the five main corrosion drivers (moisture, pH, temperature, oxidizers, and chloride) a variety of geochemical constituents can significantly enhance or inhibit the rate and extent of general and localized corrosion. Metal corrosion in soils (which can be analogous to repository environments) is a multi-scale, multivariate process controlled by the local chemical environment at the corroding surface. The geometry and liquid phase chemistry of surface

films/droplets and the thickness and composition of the oxide layer affect the diffusion of oxidizing species to the corroding surface (Cole and Marney 2012).

Chemical species that are not redox active, and do not attack the passive layer, can potentially decrease corrosion (Jack and Wilmott 2011). For example, the presence of dissolved organic compounds can significantly reduce corrosion rates by blocking the surface from the aggressive species (Jassen 2011). Similarly, dissolved sulfate ( $\text{SO}_4^{2-}$ ) and phosphate ( $\text{PO}_4^{3-}$ ) can also adsorb and protect the surface (Jassen 2011). Under normal conditions sulfate acts as a corrosion inhibitor; however, both sulfate and phosphate can serve as nutrients for microbial communities, and thereby contribute to microbially influenced corrosion (Jack and Wilmott 2011).

Microbially influenced corrosion has been described for stainless steels, and has been observed in piping in the waste water plants. Some types of bacteria can significantly lower the corrosion resistance of stainless steel. Microbial biofilms can act as crevices and change the local environment at the corroding surface (Jassen 2011). Microbial populations are ubiquitous in the subsurface, including prospective hard rock and argillaceous repository types, and possibly salt host media as well. Microbial processes therefore need to be considered when evaluating material performance and expected corrosion rates.

The following sections summarizes major physico-chemical corrosion drivers in the three repository types: hard rock (crystalline), salt, and argillaceous rock. The general geochemical features of these repository types are summarized in Figure 8-2. The range of groundwater compositions encountered in these repository settings is described in Table 8-2.

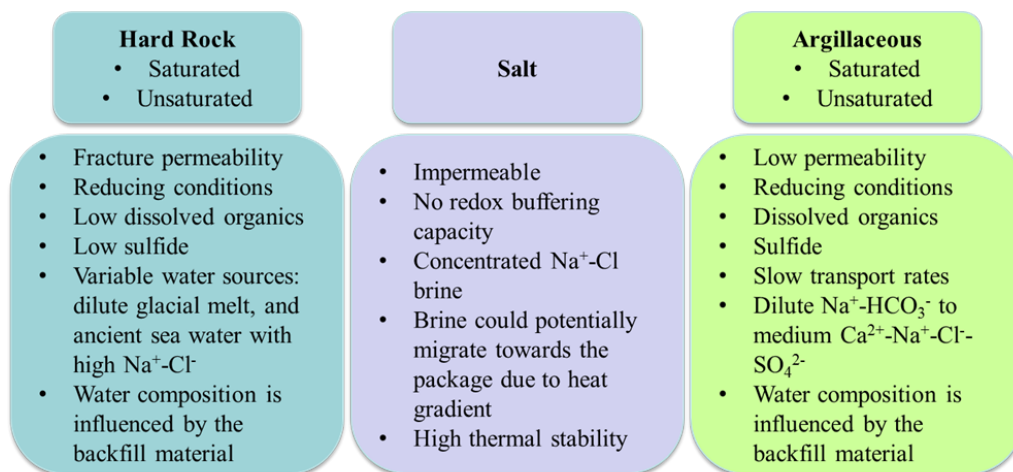


Figure 8-2. General disposal environments and geochemical conditions

### 8.2.1 Hard Rock (Crystalline) Disposal Environments

Hard rock host media are also referred to as crystalline, or granite, and are being pursued by Swedish (Marsal et al. 2007) and Finnish (Andersson et al. 2007) repository programs. Hard rock repositories can be either saturated or unsaturated depending on the depth of the water table. They may have low or high fracture permeability, and oxidizing or reducing conditions. Concentrations of dissolved organics and sulfide are typically low. The composition of

infiltrating waters is variable, but can be bounded by two chemical end members selected here: glacial melt or ancient trapped sea water.

Table 8-2. Range of geochemical conditions in three main geologic repository types (concentration values in mg/L, temperature in degrees Celsius)

| Hard rock (granite)       |        |        |                 |                |                  |                  |                 |                               |                              |                               |                 |                |                               |
|---------------------------|--------|--------|-----------------|----------------|------------------|------------------|-----------------|-------------------------------|------------------------------|-------------------------------|-----------------|----------------|-------------------------------|
|                           | pH     | Temp.  | Na <sup>+</sup> | K <sup>+</sup> | Ca <sup>2+</sup> | Mg <sup>2+</sup> | Cl <sup>-</sup> | HCO <sub>3</sub> <sup>-</sup> | NO <sub>3</sub> <sup>-</sup> | SO <sub>4</sub> <sup>2-</sup> | HS <sup>-</sup> | F <sup>-</sup> | PO <sub>4</sub> <sup>3-</sup> |
| High                      | -      | -      | 63900           | 17678          | 108747           | 15306            | 212280          | 525                           | -                            | 3206                          | -               | -              | -                             |
| Low                       | -      | -      | 10              | 0              | 9                | 0                | 2               | 2                             | -                            | 1                             | -               | -              | -                             |
| Mean                      | -      | -      | 7490            | 542            | 15283            | 1106             | 40926           | 85                            | -                            | 317                           | -               | -              | -                             |
| Median                    | -      | -      | 2935            | 19             | 3415             | 25               | 10186           | 54                            | -                            | 114                           | -               | -              | -                             |
| Salt                      |        |        |                 |                |                  |                  |                 |                               |                              |                               |                 |                |                               |
|                           | pH     | Temp.  | Na <sup>+</sup> | K <sup>+</sup> | Ca <sup>2+</sup> | Mg <sup>2+</sup> | Cl <sup>-</sup> | HCO <sub>3</sub> <sup>-</sup> | NO <sub>3</sub> <sup>-</sup> | SO <sub>4</sub> <sup>2-</sup> | HS <sup>-</sup> | F <sup>-</sup> | PO <sub>4</sub> <sup>3-</sup> |
| High                      | 8.1    | -      | 123000          | 30000          | 18700            | 45000            | 204000          | 30                            | -                            | 17500                         | -               | 7              | -                             |
| Low                       | 6      | -      | 10651           | 15             | 100              | 10               | 18980           | 3.8                           | -                            | 250                           | -               | 4              | -                             |
| Mean                      | -      | -      | -               | -              | -                | -                | -               | -                             | -                            | -                             | -               | -              | -                             |
| Median                    | -      | -      | -               | -              | -                | -                | -               | -                             | -                            | -                             | -               | -              | -                             |
| Argillaceous (Clay/Shale) |        |        |                 |                |                  |                  |                 |                               |                              |                               |                 |                |                               |
|                           | pH     | Temp.  | Na <sup>+</sup> | K <sup>+</sup> | Ca <sup>2+</sup> | Mg <sup>2+</sup> | Cl <sup>-</sup> | HCO <sub>3</sub> <sup>-</sup> | NO <sub>3</sub> <sup>-</sup> | SO <sub>4</sub> <sup>2-</sup> | HS <sup>-</sup> | F <sup>-</sup> | PO <sub>4</sub> <sup>3-</sup> |
| High                      | 12     | 242    | 126957          | 1575           | 37300            | 22632            | 204000          | 8150                          | -                            | 15000                         | -               | 0.51           | -                             |
| Low                       | 1.0404 | 97     | 3               | 3              | 1                | 1                | 6               | 4.56                          | -                            | 1                             | -               | 0.51           | -                             |
| Mean                      | 7.39   | 142.32 | 19099           | 135            | 3088             | 708              | 35830           | 964                           | -                            | 1270                          | -               | 0.51           | -                             |
|                           | 7.3    | 135    | 12143           | 48             | 1140             | 290              | 21588           | 448                           | -                            | 682                           | -               | 0.51           | -                             |

#### Number of Data Points for the Argillaceous (clay/shale) Section

| Parameter        | # of Data Points | Parameter                     | # of Data Points |
|------------------|------------------|-------------------------------|------------------|
| pH               | 710              | HCO <sub>3</sub> <sup>-</sup> | 762              |
| Temp.            | 26               | NO <sub>3</sub> <sup>-</sup>  | 0                |
| Na <sup>+</sup>  | 772              | SO <sub>4</sub> <sup>2-</sup> | 721              |
| K <sup>+</sup>   | 167              | HS <sup>-</sup>               | 0                |
| Ca <sup>2+</sup> | 787              | F <sup>-</sup>                | 1                |
| Mg <sup>2+</sup> | 776              | PO <sub>4</sub> <sup>3-</sup> | 0                |
| Cl <sup>-</sup>  | 794              |                               |                  |

#### Notes:

1. The granite data are from Frappe et al. (2003). These data are for sites in Canada, Sweden, Finland, Russia, Western Europe, and the UK.
2. Salt data are from Tables 21 and 23 of Bryan et al. (2011), Stein and Krumhansl (1987), and Deal et al. (1995).
3. Shale data are from the U.S. Geological Survey National Produced Waters Geochemical Database V2.0 (Blondes et al. 2014). The data are for U.S. geological formations only, and are based on produced waters. They span a range of dates, with the most recent being in 1980.

### 8.2.2 Salt Repository Disposal Environments

The main characteristics of salt repositories are summarized from the literature review compiled by Bryan et al. (2011). Creep closure is expected to seal the drifts or boreholes used to emplace radioactive waste, and the creep closure rate depends on the lithostatic pressure and the temperature. A typical salt repository is considered impermeable due to viscoplastic behavior.

Water content depends on the salt formation. Bedded salt has brine content that ranges from a few tenths to a few weight percent. Domal salt has less brine, from a few thousandths to tenths

of a weight percent (Bryan et al. 2011). The brine exists in the intragranular spaces, within fluid inclusions, and as structural water in hydrous minerals (clay minerals, gypsum, and polyhalite).

Typical brines contain sodium and chloride ions, and sometimes significant amounts of dissolved magnesium (Table 8-2). Overall, salt formations provide little or no pH or redox buffer capacity, and the redox conditions adjacent to the waste package are expected to be controlled by reactions involving package materials (including radiolysis products), controlled by the availability of brine, and limited oxygen fugacity. Waste heating of the salt may cause brine migration which could change brine availability.

### **8.2.3 Argillaceous Disposal Environments**

Argillaceous (clay/shale) host media can be either saturated or unsaturated. Argillaceous rocks are characterized by low permeability, reducing conditions, presence of sulfide and organic matter, with variable compositions of pore water. These waters range from dilute sodium bicarbonate to medium-strength calcium-sodium-chloride-sulfate type (Table 8-2).

## **8.3 Survey of Corrosion Rates and Mechanisms, and Corrosion Products for Stainless Steels AISI 304L and 316L**

Alloys 304L and 316L are the most common materials in DPC shells and basket structural components. A schematic representation of the corrosion drivers and corrosion products for Fe-based alloys (carbon and stainless steels) is shown in Figure 8-3.

### **8.3.1 Redox Effects**

The redox potential of the system, particularly the availability of dissolved oxygen, controls the corrosion pathway and formation of corrosion products. Both oxic and anoxic conditions are expected during the postclosure performance period of a repository. General and localized corrosion proceed faster in oxic conditions, but oxic conditions are expected to exist early during the evolution of repositories in low-permeability host media or backfill/buffer materials.

Under oxic conditions cathodic reactions on metallic surfaces are dominated by the reduction of dissolved oxygen (Figure 8-3) (Rebak 2011). Major solid corrosion products of the Fe-based alloys (carbon and stainless steels) under oxic conditions are iron oxy(hydr)oxides goethite ( $\text{FeOOH}$ ), lepidocrosite ( $\text{Fe}_2\text{O}_3$ ), hematite ( $\text{Fe}_2\text{O}_3$ ), maghemite ( $\text{Fe}_2\text{O}_3$ ), and magnetite ( $\text{Fe}_3\text{O}_4$ ) (Jack and Wilmott 2011).

Most DPC direct disposal concepts (and other disposal concepts as well) are expected to return to anoxic or anaerobic conditions shortly after backfilling and closure (Bryan et al. 2011). This is especially true for low-permeability, water saturated host media that contain reducing minerals (e.g., pyrite) or natural organic matter. Under reducing conditions, water acts as an electron acceptor for metallic iron, and the cathodic reaction is controlled by hydrogen evolution (Figure 8-3) (Rebak 2011). The ubiquity of water as a possible electron acceptor is one reason that steels continue to corrode, albeit slowly, at anoxic aqueous conditions. Under anoxic conditions, siderite ( $\text{FeCO}_3$ ), iron hydroxide  $\text{Fe}(\text{OH})_2$  and magnetite ( $\text{Fe}_3\text{O}_4$ ) are the predominant corrosion products of the Fe-based alloys (Jack and Wilmott 2011). During anaerobic microbial assisted corrosion a different assemblage may form including siderite, amorphous iron-sulfide ( $\text{FeS}$ ), mackinawite ( $\text{FeS}$ ), greigite ( $\text{FeS}$ ), and pyrite ( $\text{FeS}_2$ ) (Jack and Wilmott 2011).

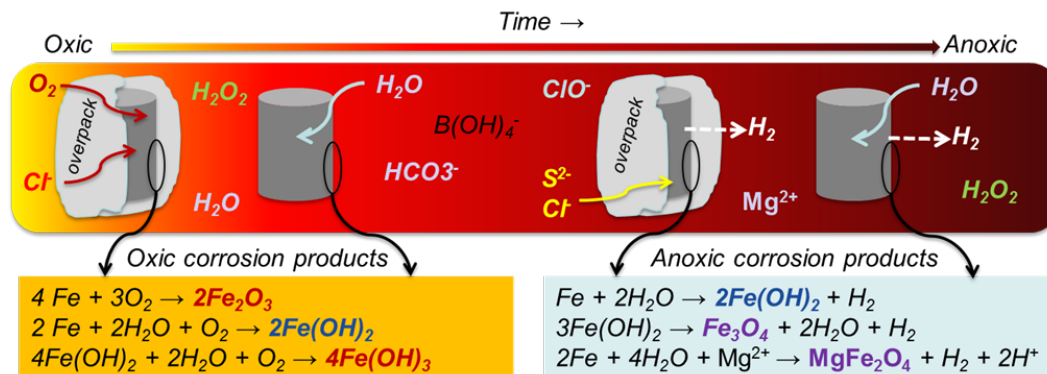


Figure 8-3. Time-dependent chemical corrosion drivers for Fe-based materials (carbon steel and stainless steel)

While steel corrosion is generally anticipated to be slower under anoxic conditions, environmental factors such as sulfide concentration or microbial activity may result in rapid corrosion even under anoxic conditions. For instance, a qualitative soil corrosivity classification has been developed based on the soil oxidation-reduction potential (ORP) by (Jack and Wilmott 2011). They observed an increase in corrosion with increasingly reducing (lower ORP) conditions; no corrosion at ORP > 400 mV, slight corrosion at 200 to 400 mV, moderate corrosion at 100 to 200 mV, and severe corrosion at ORP < 100 mV. This was attributed to the effects of anaerobic microbial activity in the anoxic soils. The relative importance of microbial activity in repository settings may vary with the host rock. It is generally believed to be suppressed in highly compacted swelling clay backfill materials such as those used in granite repository concepts (Kwong 2011). However, tests in the Opalinus Clay at Mont Terri (e.g., Wersin et al. 2011; Vinsot et al., 2014) have shown high rates of microbial activity when electron donors (H<sub>2</sub> or incidental organic matter) were introduced via boreholes; sulfate was the electron acceptor. Hence, the potential for microbially mediated corrosion cannot be ignored.

### 8.3.2 Effects from pH and Chemical Composition on Corrosion Mechanisms and Rates

As discussed above, pH and composition of the aqueous phase are major controls on corrosion rates and mechanisms. Typically, soil pH falls within the range 3.5 to 10. Corrosion of Fe-based alloys increases significantly as pH falls below 4 (Jack and Wilmott 2011). Figure 8-4 illustrates the dependence of steel corrosion rates on pH and resistivity of ground water, for steel pipes buried in near-surface soils where redox conditions are typically oxidizing. Groundwater resistivity is a surrogate for greater salt content. The effects of pH and salt content are similar under anoxic conditions, but uniform corrosion rates are expected to be lower (compared to Figure 8-4).

Under anoxic conditions, localized corrosion modes include hydrogen blistering, hydrogen-induced cracking, stress-oriented hydrogen-induced cracking, and sulfide stress cracking (Elboujdaini 2011). Hydrogen gas is one of the corrosion products of Fe-based alloys in anoxic conditions (Figure 8-3). Hydrogen embrittlement, induced blistering, and cracking occur due to the evolution of atomic hydrogen at the surface, followed by its diffusion into the steel. Once entrained within the steel, the hydrogen accumulates in hydrogen traps (e.g., around inclusions), leading to localized pressure increase within the material (Elboujdaini 2011). Sulfide stress

cracking is a variety of hydrogen-induced cracking, and is usually localized in weld zones (Elboujdaini 2011). It can occur in mildly corrosive media at temperatures below 90°C. Sulfide reaction with ferrous iron:



produces atomic hydrogen, and dissolved sulfide hinders hydrogen recombination reaction at the corroding surface (combining two atomic  $\text{H}^0$  into gas  $\text{H}_2$ ). Abundant atomic hydrogen easily diffuses into steel (Elboujdaini 2011).

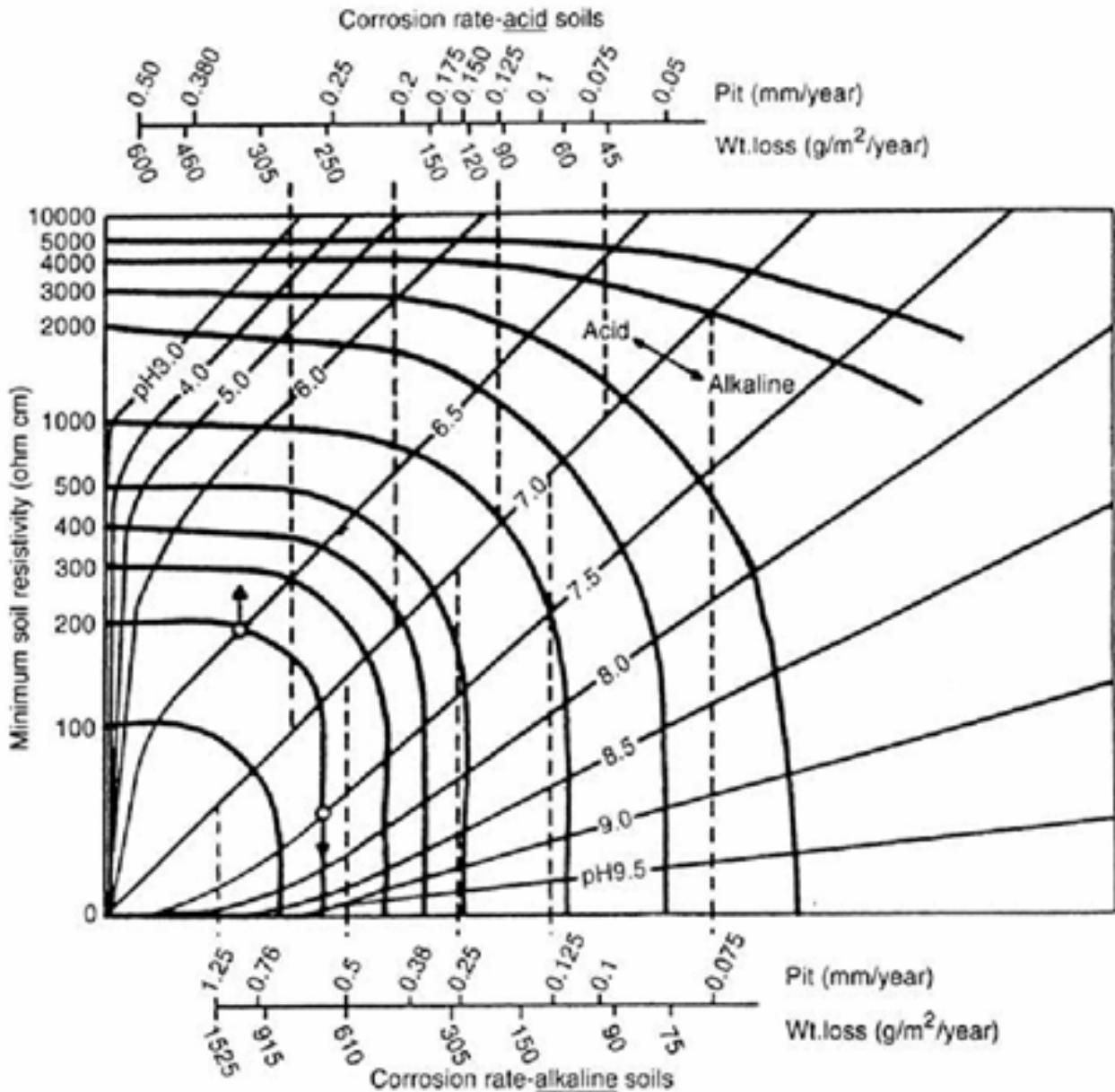


Figure 8-4. Nomogram relating soil resistivity, pH, and corrosion rate for steel pipe in soil (from Jack and Wilmott 2011; original source King 1977)

### 8.3.3 Radiation Flux Effects

Radiation exposure has a strong effect on the corrosion environment. Container corrosion rates, particularly in anoxic repository settings, could be significantly increased by radicals produced by radiolysis. The following short discussion on radiolysis is a summary from the recent report by Buck et al. (2012).

The redox conditions in a waste repository environment are expected to evolve due to the time-dependent generation of radiolytic redox active species (both oxidants and reductants), and the corrosion of Fe-bearing canister materials. In the presence of water vapor or a thin-film of water, the  $\gamma$ -radiation from SNF triggers complex radiolysis reactions (about 100 have been identified). Some of the products of these reactions include hydroxide ( $\text{OH}\bullet$ ) and hydrogen ( $\text{H}\bullet$ ) radicals, oxygen ions ( $\text{O}_2^-$ ), aqueous electrons ( $\text{e}_{\text{aq}}^-$ ), hydrogen peroxide ( $\text{H}_2\text{O}_2$ ), hydrogen gas ( $\text{H}_2$ ), and the secondary radiolysis product, oxygen ( $\text{O}_2$ ). These species are highly reactive, and are expected to increase both the degradation rate of the SNF, and the corrosion rate of the container. Hydrogen peroxide ( $\text{H}_2\text{O}_2$ ) can significantly increase pitting rates of stainless steel (see below) and is expected to be the predominant oxidant for SNF under anoxic conditions (Buck et al. 2012).

### 8.3.4 Survey of Corrosion Rate Data for Stainless Steel

Stainless steel types 304/304L and 316/316L are the most common alloys used in the construction of DPCs and their internal components. Type 304 is a chromium-nickel alloy, and type 316 is a chromium-nickel alloy containing 2 to 3% molybdenum.

**Uniform Corrosion of Stainless Steel** – Under oxic, alkaline conditions, and the water chemistry typical of a clay repository (no added chloride) uniform corrosion rates for 316L vary from  $<0.1 \mu\text{m yr}^{-1}$  at  $30^\circ\text{C}$  to  $0.2\text{-}0.8 \mu\text{m yr}^{-1}$  at  $80^\circ\text{C}$  (Kursten et al. 2004). Estimated corrosion rates under anoxic conditions are from  $0.001 \mu\text{m yr}^{-1}$  to  $0.1 \mu\text{m yr}^{-1}$  over the same temperature range (Kursten et al. 2004). A proposed long-term general corrosion rate for stainless steels under anaerobic conditions is  $<0.01 \mu\text{m yr}^{-1}$  (Kursten et al. 2004).

**Localized Corrosion of Stainless Steel** – Experimental testing of indicated no pitting of 316L in alkaline solutions containing up to  $100 \text{ g L}^{-1}$  chloride at room temperature (Kursten et al. 2004). When the concentration of chloride was decreased to  $50 \text{ g L}^{-1}$  the critical pitting temperature is increased to  $45^\circ\text{C}$  (Kursten et al. 2004). Similar chloride concentration threshold behavior was observed for pitting of 304L: pitting was observed at  $60^\circ\text{C}$  with  $>50 \text{ g L}^{-1}$  chloride (Kursten et al. 2004). Crevice corrosion of 304L is observed at  $80^\circ\text{C}$  and background chloride concentrations of  $20 \text{ g L}^{-1}$  or greater; and no crevice corrosion is observed at  $40^\circ\text{C}$  and chloride concentrations up to  $20 \text{ g L}^{-1}$  (Kursten et al. 2004). Pit initiation testing for 304/304L and 316/316L indicates that pitting is variable (Table 8-3). The oxidative history of the sample was associated with a large difference in the number of pits for the 316/316L alloys, but not for 304/304L.

Stress corrosion cracking was observed in an unstressed sample of 304L stainless steel that had been aged in cementitious material containing  $100 \text{ g L}^{-1}$  chloride for 2 years. Additional testing in alkaline solutions indicated that increased chloride ( $17.7 \text{ g/L}$ ) and thiosulfate ( $\text{S}_2\text{O}_3^{2-}$  at  $3.4 \text{ g/L}$ ) increased both pitting and stress corrosion cracking of the 316L and 304L alloys (Kursten et al. 2004).

In aggressive environments (e.g., 45% MgCl or 26% NaCl), stress corrosion cracking is observed to take place within hours to days. Cracking is observed in less than 3 hours in magnesium chloride solution at 155°C, and after 48 to 72 hours in sodium chloride tests at 102 and 200°C (Streicher and Grubb 2011).

Table 8-3. Pit initiation in stainless steels 304/304L and 316/316L exposed to 0.1N NaCl at 25°C (from Streicher and Grubb 2011)

| Alloy | Element % |       |      |       |       |      | Pits per cm <sup>2</sup> (Note 1) |                         |
|-------|-----------|-------|------|-------|-------|------|-----------------------------------|-------------------------|
|       | Cr        | Ni    | Mo   | C     | N     | Si   | Clean <sup>2</sup>                | Passivated <sup>3</sup> |
| 304   | 18.45     | 8.90  |      | 0.063 |       | 0.58 | 3.4                               | 2.2                     |
| 304L  | 18.30     | 11.02 |      | 0.020 | 0.033 | 0.37 | 1.6                               | 2.8                     |
| 316   | 17.93     | 13.50 | 2.47 | 0.031 |       | 0.31 | 0.46                              | 15.8                    |
| 316L  | 17.71     | 11.17 | 2.44 | 0.02  | 0.032 |      | 0.17                              | 29.0                    |

Notes:

1. Pits produced by anodic polarization.
2. Surface cleaned in nitric-hydrofluoric-hydrochloric HNO<sub>3</sub>-HF-HCl mixture prior to the experiment.
3. Surface passivated in nitric acid HNO<sub>3</sub> with potassium dichromate K<sub>2</sub>Cr<sub>2</sub>O<sub>7</sub>.

#### 8.4 Research Needs for Predicting Stability of DPC Materials in Disposal Environments

The neutron absorber materials in current DPCs are largely aluminum-based and are not anticipated to survive long in a breached, flooded waste package. The aluminum-based neutron absorber will actually act as a sacrificial anode with respect to the steel. Borated stainless steel, used in a few DPC packages, is anticipated to have a longer lifetime. Corrosion of borated stainless steel under reducing conditions has not been explored, and further testing is needed to assess this material if it will be used in future canisters.

Criticality analysis (Section 4) has shown that the basket degradation case is the most reactive configuration, but might be avoided if stainless steel basket structures maintain the SNF configuration during the postclosure repository performance period (e.g., up to 10,000 years). A rough estimate of the expected loss of thickness of a stainless steel plate or sheet, after 10,000 years exposure to ground water, is 0.01 to 1 mm (1-sided surface retreat). This estimate is based on the following assumptions:

- Anoxic conditions, non-corrosive water composition, and pH >4
- Estimated stainless steel corrosion rates for anoxic conditions are 0.001 to 0.1 μm yr<sup>-1</sup> over the temperature range 30 to 80°C (Kursten et al. 2004)
- Localized corrosion (e.g., pitting) may occur but does not cause loss of structural integrity
- Crevice corrosion and stress corrosion cracking do not occur, or if they do occur damage to the basket does not impact structural integrity
- Microbially influenced corrosion does not occur
- Hydrogen that evolves at corroding surfaces diffuses away and does not accumulate in the uncorroded steel, so the extent of any hydrogen-embrittlement or hydrogen-induced cracking is not significant
- Radiolysis products (e.g., H<sub>2</sub>O<sub>2</sub>) predominantly react with UO<sub>2</sub> in the SNF, or recombine, and do not react with basket materials to any significant extent because the cladding is mostly intact

Using this estimate, a stainless steel basket structure could maintain the SNF configuration for 10,000 years (e.g., in the event of early breach of the disposal overpack).

Some of these assumptions should be tested experimentally. Investigation should focus on container-specific corrosion rates, and testing or analysis to evaluate the assumptions used for this estimate of basket lifetime. Corrosion processes are complex, and there are no existing mechanistic process models that could more reliably predict corrosion rates. Whereas some basket designs have relatively thin-wall stainless steel tubing or sheets, under reducing conditions general corrosion rates are generally slow. However, within a waste package radiolysis may create oxidizing conditions that could locally increase corrosion rates. While stainless steels will pit in reducing, saline ground waters it is not clear that this will structurally weaken the basket. Crevice corrosion and SCC of basket materials may be more important in limiting basket lifetime. Crevice corrosion may occur at any contact, while SCC may occur in weld zones or areas of high loading. Another potential factor may be hydrogen embrittlement associated with anoxic metal corrosion reactions or by radiolytic breakdown of water.

Key areas of uncertainty that should be addressed by future investigations include the evolution of disposal environments through time:

- Changes in redox conditions, temperature, hydrogen buildup/diffusion, interactions between products of corrosion (e.g.,  $\text{Fe}^{2+}$ ) and the clay buffer
- Diffusion of corrosion-active species (e.g., chloride or sulfide) through buffer material, and potential effects on long-term corrosion rate
- Feedbacks between  $\text{H}_2$  production and transport
- Likelihood of localized corrosion in basket materials
- Radiation effects on the corrosion environment, particularly in anoxic repository settings, from radicals produced by radiolysis (e.g.,  $\text{H}_2\text{O}_2$ )
- Competition for oxidizing radicals between  $\text{UO}_2$  and container materials

and aspects of container design and fabrication that can affect corrosion:

- Effects of thermal treatments and welding of the basket
- Metallurgical modifications due to long-term radiation flux or thermal aging

## 8.5 Prospective Overpack Materials

For DPCs, barrier functions will be assigned to the overpack because the 1.27 to 1.59 cm (1/2 to 5/8 inch) shell is not expected to provide structural strength for handling and emplacement, or corrosion resistance to isolate the waste for the required repository performance period. To be an effective barrier, the overpack/waste package system must resist damage during handling and emplacement. Additionally, for clay and salt repositories after backfilling, pressures will rise to those of the host rock with magnitude between hydrostatic and lithostatic. Any overpack must resist crushing under such loading conditions.

There are two general strategies for overpack material selection: corrosion allowance material and corrosion-resistant material. Corrosion allowance has been used in European clay/shale and salt repository designs, with selection of thick-wall carbon steel waste packages. A thick wall can resist crushing until the overpack is degraded by corrosion. Although carbon steel corrodes

relatively rapidly via general corrosion, it is not susceptible to pitting or crevice corrosion. Hence, canister degradation rates can be reliably calculated. Containment penetration times for thick carbon steel overpacks or waste packages are typically estimated to be on the order of 10,000 years, which can be consistent with repository performance objectives if other engineered and natural barriers continue to perform isolation functions. Accordingly, the use of corrosion allowance materials may be limited to salt and other repository concepts where the natural system is an effective long-term isolation barrier.

Corrosion-resistant materials such titanium or copper, and including stainless steels, can produce longer estimates containment lifetime. Materials such as titanium and stainless steel passivate under the environmental conditions being considered, forming a resistant surface oxide layer leading to very low general corrosion rates. Passive materials are by their nature susceptible to localized corrosion, or disruption of the passive layer with rapid local penetration (e.g., pitting, crevice corrosion, or stress corrosion cracking). Copper is a special case because it does not passivate. Rather, the metal is thermodynamically stable in the presence of water, and will not corrode under anoxic conditions in pure water. However, it will corrode in natural anoxic groundwater systems due to the presence of sulfide, with which it reacts to form Cu-sulfides. Among corrosion-resistant materials, only copper is currently being considered for a waste package (although other corrosion-resistant materials have been considered in the past). Because corrosion-resistant materials are more expensive than carbon steel, they would likely be used in a relatively thin layer as part of a DPC disposal overpack. Structural requirements of the overpack could then be met by another, potentially thicker layer (e.g., stainless steel).

In European repository concepts using corrosion allowance materials, criticality concerns are addressed using two strategies. In French, Swiss, and Belgian clay repository designs, the SNF capacity is restricted (e.g., 4 PWR size, or typically 9 BWR assemblies) which can be small enough to prevent criticality. For the German POLLUX fuel rod consolidation is proposed, which significantly decreases the amount of moderating water that can combine with the fuel. DPCs have much greater capacity, and contain intact fuel assemblies, so these strategies are not applicable. Hence, an overpack lifetime of 10,000 years could be needed for DPC disposal overpacks, to exclude ground water. Note that the 10,000 year time requirement is a regulatory one (Hardin and Howard 2013). Carbon steel corrosion rates under anoxic conditions are well known and can be used to calculate the needed thickness.

For overpacks constructed of a corrosion-resistant material, work by the European research groups has focused mainly on copper. Stainless steel and Ni-based alloys are susceptible to localized corrosion and potentially, rapid penetration. Moreover, under anoxic conditions, corrosion will occur via reduction of water, producing hydrogen. Both stainless steel and low-iron nickel alloys are susceptible to hydrogen uptake and embrittlement when this reaction occurs. Corrosion reactions with hydrogen sulfide present in reducing groundwaters can also lead to hydrogen embrittlement of steel and Ni-based alloys. Titanium is not affected by hydrogen sulfide, unless it is galvanically coupled to a less noble metal (e.g., a steel alloy). Copper is also not affected by hydrogen embrittlement. If nickel alloys or stainless steels are proposed for an overpack material, then corrosion rates, and pitting penetration rates for these materials would be determined for each relevant environment.

Other materials currently under consideration for engineered barriers, which may include disposal overpacks, include: gray cast iron, 1018 carbon steel, 4130 alloy steel, 2.25Cr-1Mo type 304 and 316 stainless steels, Monel 400, Incoloy 825, Inconel 625, Hastelloys C-4 and C-

22, and Ti (Grades 2, 7, 12, 16 and 29) (Rebak 2011). Some corrosion studies for two types of prospective overpack materials (carbon steel and Hastelloys C-4 and C-22) are summarized below.

### 8.5.1 Corrosion of Carbon Steels

Corrosion of a waste container is expected to depend mainly on the immediate geochemical environment of the container. For example, if a backfill material is used (e.g., bentonite clay backfill in a granite repository) then geochemical conditions within the backfill will drive the corrosion of waste package materials. Relevant corrosion data for two types of carbon steel (BS4360 grade 43A and TStE 355) are discussed here. For the former, data are presented for exposure to bentonite systems, while for the latter, data are reported for exposure to brine.

Experiments were completed to measure the rates of carbon steel (BS4360 grade 43A) corrosion in a bentonite clay slurry, compact bentonite, and pore water simulants. The measured uniform corrosion rates for carbon steel ranged depending on temperature and whether it was exposed to the compact media, slurry, or homogeneous (pore water) phases. The observed corrosion rates varied with time. Fresh carbon steel surfaces corroded rapidly, with the rate increasing with increasing temperature. The initial rate was around 25 to 30  $\mu\text{m yr}^{-1}$  for bentonite slurries at 30 and 50°C. This high rate was sustained for a short time, and dropped to 1.5 to 4  $\mu\text{m yr}^{-1}$  after ~3,000 hours of reaction for all studied systems (Smart et al. 2006). In the homogeneous systems the long-term (>2,500 days) carbon steel general corrosion rates in anoxic alkaline conditions at 30, 50 and 80°C were <0.1  $\mu\text{m yr}^{-1}$  (Smart et al. 2004). The decrease in corrosion rate is due to the development of oxide layers, namely ferrous hydroxide at 30°C and magnetite at 50 and 80°C (Smart et al. 2004).

Carbon steel TStE 355 corrosion rates vary widely depending on the chemical conditions of the experiment. From *in situ* studies where the amount of brine was limited, an estimated general corrosion rate was <0.1  $\mu\text{m yr}^{-1}$  (90 and 170°C) (Kursten et al. 2004). In the laboratory experiment with excess brine, the resulting corrosion rates were 70  $\mu\text{m yr}^{-1}$  (90°C) and 199  $\mu\text{m yr}^{-1}$  (170°C) in magnesium-rich brines, and 5  $\mu\text{m yr}^{-1}$  (90°C) and 46  $\mu\text{m yr}^{-1}$  (170°C) in sodium chloride brines (Kursten et al. 2004). The predominant corrosion mode for carbon steel is uniform corrosion, but sometimes stress corrosion cracking can occur when the environmental conditions allow for development of a passivating layer, for example in the presence of anodic inhibitors: nitrates, hydroxides, carbonates, or phosphates (Parkins 2011).

### 8.5.2 Survey of Corrosion Rate Data for Hastelloys C-4 and C-22

The corrosion behaviors of stainless steels, nickel-based alloys (Hastelloys C-4 and C-22), Ti99.8-Pd and copper-based materials in rock salt, granite and clay environments were assessed in the laboratory by Smailos et al. (2004). The corrosion results for Hastelloys C-4 and C-22 are summarized below. Overall, the study concluded that the most promising materials for disposal in granitic formations are Hastelloy C-22, Cu and Cu-Ni-alloys. For clay/shale formations, the most important candidate materials for thin-walled containers are stainless steels, nickel-based alloys (Hastelloys C-4 and C-22), and Ti99.8-Pd (Smailos et al. 2004).

Corrosion studies on the nickel-based alloys Hastelloy C-4 and C-22 in rock salt, granite, and clay environments indicate that these materials exhibit excellent general and local corrosion resistance. For anoxic conditions in granitic environments ( $\text{Cl}^-$  up to 50,000 mg/L, temperature up to 90°C) Hastelloy C-22 exhibits the highest corrosion resistance among all tested materials.

It is resistant to pitting corrosion, crevice corrosion, stress corrosion cracking and microbially influenced corrosion. For clay/shale repository conditions (100 to 50,000 mg/L  $\text{Cl}^-$ , at 16°C and up to 140°C) Hastelloys C-4 and C-22 show slight crevice corrosion under severe test conditions (oxidizing, 140°C,  $\text{Cl}^- > 20,000$  mg/L) (Smailos et al. 2004).

Under aerobic (oxic) conditions at 140°C, Hastelloys C-4 and C-22 are resistant to general and pitting corrosion. However, signs of pitting were observed in some tests with high  $\text{Cl}^-$  ( $> 20,000$  mg/L) (Smailos et al. 2004). The addition of hydrogen peroxide ( $\text{H}_2\text{O}_2$ ) to the solutions (to mimic the effect of potential radiolysis products) did not affect the corrosion behavior of Hastelloys C-4 and C-22 in both oxic and anoxic conditions at 90°C (Smailos et al. 2004).

## **8.6 Summary and Application to DPC Inventory**

The foregoing discussion shows that stainless steel corrosion rates may be low enough to sustain DPC basket structural integrity for performance periods of as long as 10,000 years, especially in reducing conditions. Uncertainties include basket component design, disposal environment conditions, and the in-package chemical environment including any localized effects from radiolysis.

Published data briefly reviewed above support an observation that prospective disposal overpack materials exist for most disposal environments, including both corrosion allowance and corrosion resistant materials. Whereas the behavior of corrosion allowance materials is understood for a wide range of corrosion environments, demonstrating corrosion resistance could be more technically challenging and require environment-specific testing.

Not all DPCs have stainless steel basket structures, as noted for the Site C canisters analyzed in Section 4. The following sections describe a preliminary screening of the existing inventory of DPCs and other types of canisters, according to the type of closure, whether they can be readily transported, and what types of materials are used in basket construction.

### **8.6.1 Cask Closure**

Storage and transportation casks can be broadly subdivided into two categories, those in which UNF fuel is stored in thin-wall, welded metal canisters and those in which fuel is stored in metallic canisters with bolted closures. DPCs are welded metal canisters that can be transferred between overpacks for storage, transportation and possibly disposal.

Bolted-closure systems are typically referred to as “casks” because they are massive and self-shielding, and cannot be inserted into overpacks for other purposes such as disposal (and in some cases, transportation). Bolted-closure systems may also be referred to as “bare fuel casks” because they are designed for fuel retrieval (as bare assemblies) and cask reuse. Regulatory requirements for bolted closures include periodically monitoring the inerting gas pressure over the life of the cask, whereas welded canisters are known to be leak-tight. Metal gaskets are typically used to aid in the sealing of bolted lids, and must be replaced if a leak occurs. Gamma and neutron shielding are typically integral to the bolted container.

A bolted system could be suitable for disposal if a disposal overpack with appropriate dimensions and postclosure performance is available. Bolted closures must be monitored and maintained and thus would not be suitable for direct disposal without an additional, permanent containment envelope. Since there are relatively few existing dry storage systems in the U.S.

with bolted closures, and they can be readily opened to retrieve the fuel for disposal, they are not considered in the canister screening exercise described below (Section 8.6.5).

### **8.6.2 Transportability**

For purposes of this screening the existing DPC inventory is divided into canisters designed for storage and transportation and those that are considered to be storage only. Canisters are considered to be transportable if they have a 10CFR71 certificate of compliance, or if they are new designs that have not completed the 10CFR71 licensing process. It may be possible in the future to license some older storage-only canisters for transportation, but that is beyond the scope of this analysis.

### **8.6.3 Repository Degradation Susceptibility**

As shown in Section 4, structural integrity of the fuel basket (e.g., for up to 10,000 years) greatly increases the fraction of analyzed DPCs that could remain subcritical after flooding. Basket integrity will be determined by the susceptibility of the basket materials to corrosion. As discussed above, stainless steel is the most degradation resistant material used in canister construction, and may retain sufficient structural integrity in the repository environment after exposure to ground water. By obviating the basket degradation reactivity scenario, stainless baskets could prevent criticality. For this analysis, stainless steel is assumed to be the only material in existing DPC that could perform in this manner. A working definition of degradation susceptibility for basket materials is provided below.

### **8.6.4 Basket Designs and Structural Components**

There are two major types of baskets used in DPCs: the “tube-and-spacer-disk” design (Figure 8-5) and the “egg-crate” design (Figure 8-6). The tube-and-disk design consists of a series of fuel tubes (also called guide sleeves) which maintain the position of each fuel assembly. The fuel tubes are held in place by mechanical coupling to a set of disks, which are secured to the canister body by tie rods. The disks maintain the tube spacing and provide heat transfer to the canister shell. Some of the disks may be fabricated from aluminum or other materials to aid heat transfer. The egg-crate designs typically comprise fuel support tubes or cells made from tubing or plates welded together. The entire basket is connected to the canister by supports attached at the basket periphery. Egg crate designs may also incorporate interstitial material between the fuel tubes in order to improve heat conduction out of the basket.

For screening of tube-and-disk canisters the materials of construction of the spacer disks, support rods, and fuel tubes were examined. For screening the egg-crate canisters only the fuel tube materials were considered, eliminating some of the support design details because it seems likely that the supports could fail without causing a structural failure of the basket.

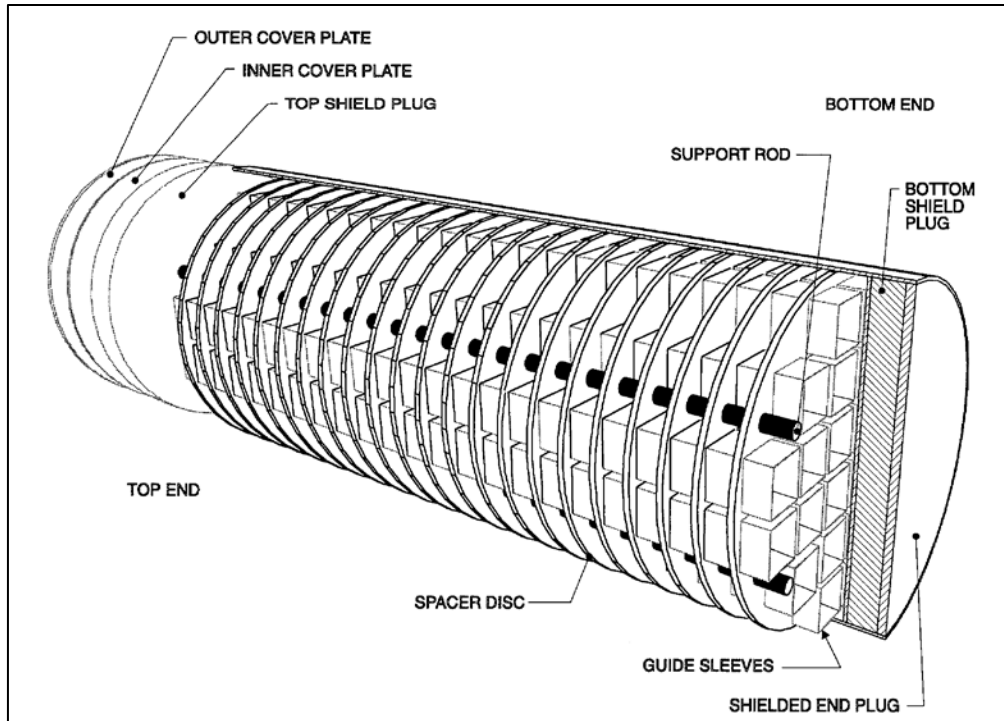


Figure 8-5. Schematic cutaway of the FO/FC-DSC manufactured by Transnuclear, an example of tube-and-disk basket design

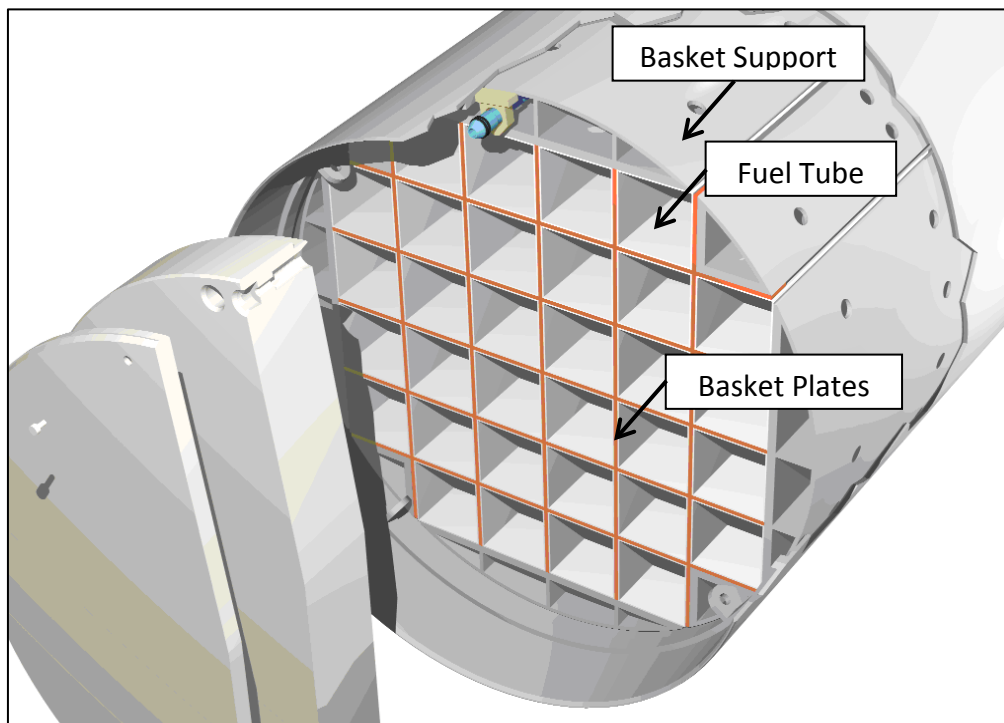


Figure 8-6. Schematic cutaway of the DSC-32PTH manufactured by Transnuclear, an example of egg-crate basket design

### 8.6.5 Canister Inventory and Screening

Screening to determine the fraction of canisters or fuel assemblies that may be stored in disposable containers (as defined) begins with canister inventory, PWR and BWR assembly counts, and other data from a table compiled by an industry newsletter publication (Ux Consulting 2014). The materials of construction of each canister were extracted from licensing documents (Transnuclear 2002, 2012; McLean 1990; NAC 2003, 2004, 2010; NRC 2014; Holtec 2010; Energy Solutions 2002, 2003). The compilation for existing DPCs is presented in Table 8-4.

Based on the criteria discussed above the canisters were grouped into the following categories:

- Transportable canisters without degradation-susceptible components
- Transportable canisters with degradation susceptible-components
- Non-Transportable canisters without degradation-susceptible components
- Non-Transportable canisters with degradation-susceptible components
- Bolted casks

Degradation susceptibility is defined here to mean non-stainless steel structural components. Thus, DPCs that have carbon steel spacer disks (including plated steel), or aluminum-based (e.g., Metamic®) basket structures, would be degradation-susceptible. DPCs that contain non-stainless materials that are not used in structural applications (e.g., thermal shunts) would not be susceptible as long as the structure is stainless steel. This categorization does not imply that stainless steel degradation could not occur. It is intended to show which canisters could have sufficient structural lifetime in relatively fresh ground waters, that the criticality analysis could consider the loss-of-absorber scenario but not necessarily the basket degradation scenario.

The results of the screening process are shown in Figures 8-7 through 8-9, and Table 8-5. Approximately 2/3 of the overall inventory of storage casks and canisters are considered transportable with basket structural components made from stainless steel, while 6% are transportable but with non-stainless components. The remaining 25% consists of storage-only canisters and bolted casks. The fraction of BWR assemblies in transportable canisters with stainless steel basket components (83% of all BWR fuel), is greater than the fraction of PWR assemblies (65% of all PWR fuel).

It should be reiterated that these screening results are based on assumptions that stainless steel is the best existing basket material for disposability, that component thickness (e.g., guide sleeves, Figure 8-5) is sufficient to sustain structural integrity, and that basket supports and interstitial materials (Figures 8-5 and 8-6) are not critical to basket structural integrity.

Table 8-4. Domestic inventory of UNF in dry storage, by canister type, transportability, and susceptibility to degradation in disposal environments

| Canister/Cask Name | Closure Mechanism | Reactor Type | Number of Canisters Loaded | Number of Assemblies in Storage | Transportable | Susceptible to Repository Degradation | Reference (see notes) |
|--------------------|-------------------|--------------|----------------------------|---------------------------------|---------------|---------------------------------------|-----------------------|
| TN-32              | Bolted            | PWR          | 63                         | 2016                            | Not Included  | Not Included                          | Not Included          |
| TN-40              |                   | PWR          | 35                         | 1400                            |               |                                       |                       |
| TN-68              |                   | BWR          | 68                         | 4624                            |               |                                       |                       |
| V/21&X33           |                   | PWR          | 26                         | 558                             |               |                                       |                       |
| MC-10              |                   | PWR          | 1                          | 24                              |               |                                       |                       |
| NAC-I28            |                   | PWR          | 2                          | 56                              |               |                                       |                       |
| DSC-24PTH          | Welded            | PWR          | 27                         | 648                             | Yes           | No                                    | 1                     |
| DSC-32P            |                   | PWR          | 24                         | 768                             | No            | No                                    | 2                     |
| DSC-32PT           |                   | PWR          | 76                         | 2432                            | Yes           | No                                    | 1                     |
| DSC-32PTH          |                   | PWR          | 98                         | 3136                            | Yes           | No                                    | 1                     |
| DSC-61BT           |                   | BWR          | 129                        | 7869                            | Yes           | No                                    | 1                     |
| DSC-61BTH          |                   | BWR          | 51                         | 3111                            | Yes           | No                                    | 1                     |
| MPC-24             |                   | PWR          | 20                         | 480                             | Yes           | No                                    | 3                     |
| MPC-24EEF          |                   | PWR          | 34                         | 790                             | Yes           | No                                    | 3                     |
| MPC-32             |                   | PWR          | 272                        | 10324                           | Yes           | No                                    | 3                     |
| MPC-68             |                   | BWR          | 300                        | 20400                           | Yes           | No                                    | 3                     |
| MPC-HB             |                   | BWR          | 6                          | 390                             | Yes           | No                                    | 3                     |
| TSC-37             |                   | PWR          | 23                         | 851                             | Yes           | Yes                                   | 4                     |
| DSC-24P            |                   | PWR          | 135                        | 3240                            | No            | Yes                                   | 2                     |
| DSC-24PHB          |                   | PWR          | 48                         | 1152                            | No            | Yes                                   | 2                     |
| DSC-24PT1          |                   | PWR          | 18                         | 395                             | Yes           | Yes                                   | 5                     |
| DSC-24PT4          |                   | PWR          | 33                         | 792                             | Yes           | Yes                                   | 1                     |
| DSC-52B            |                   | BWR          | 27                         | 1404                            | No            | Yes                                   | 2                     |
| DSC-7P             |                   | PWR          | 8                          | 56                              | Yes           | No                                    | 6                     |
| DSC-FO/FC          |                   | PWR          | 22                         | 493                             | Yes           | Yes                                   | 5                     |
| CY-MPC             |                   | PWR          | 43                         | 1019                            | Yes           | No                                    | 7                     |
| MPC-LACBWR         |                   | BWR          | 5                          | 333                             | Yes           | No                                    | 7                     |
| MSB                |                   | PWR          | 58                         | 1392                            | No            | Yes                                   | 8                     |
| TSC-24             |                   | PWR          | 236                        | 5562                            | Yes           | No                                    | 9                     |
| W74                |                   | BWR          | 8                          | 441                             | Yes           | Yes                                   | 10                    |
| Yankee-DPC         | PWR               | 16           | 533                        | Yes                             | No            | 7                                     |                       |

Notes:

|                        |                            |                             |
|------------------------|----------------------------|-----------------------------|
| 1. Transnuclear (2012) | 5. NRC (2014)              | 9. NAC (2004)               |
| 2. Transnuclear (2002) | 6. McClean (1990)          | 10. Energy Solutions (2003) |
| 3. Holtec (2010)       | 7. NAC (2003)              |                             |
| 4. NAC (2010)          | 8. Energy Solutions (2002) |                             |

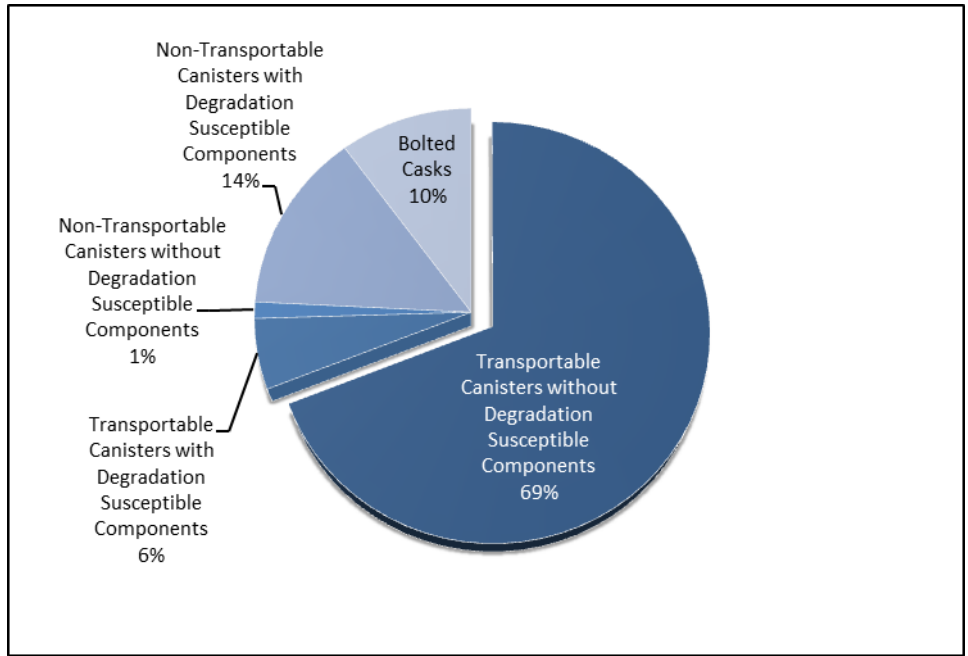


Figure 8-7. Fractional representation of the total number of DPCs and bare fuel casks by canister type and material susceptibility

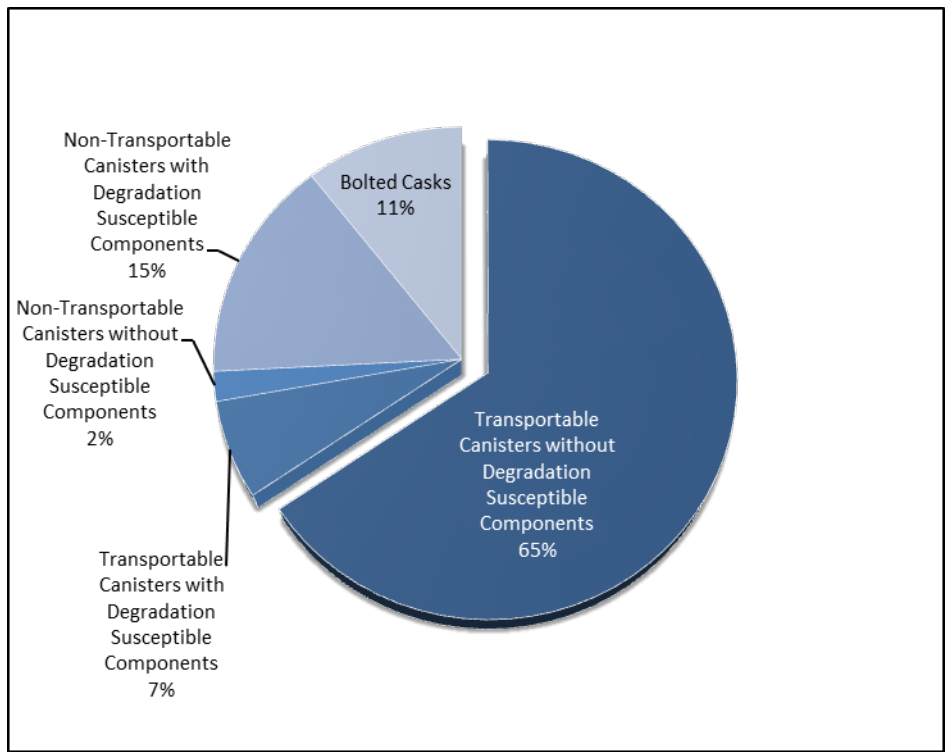


Figure 8-8. Fractional representation of PWR fuel assemblies by canister type and material susceptibility

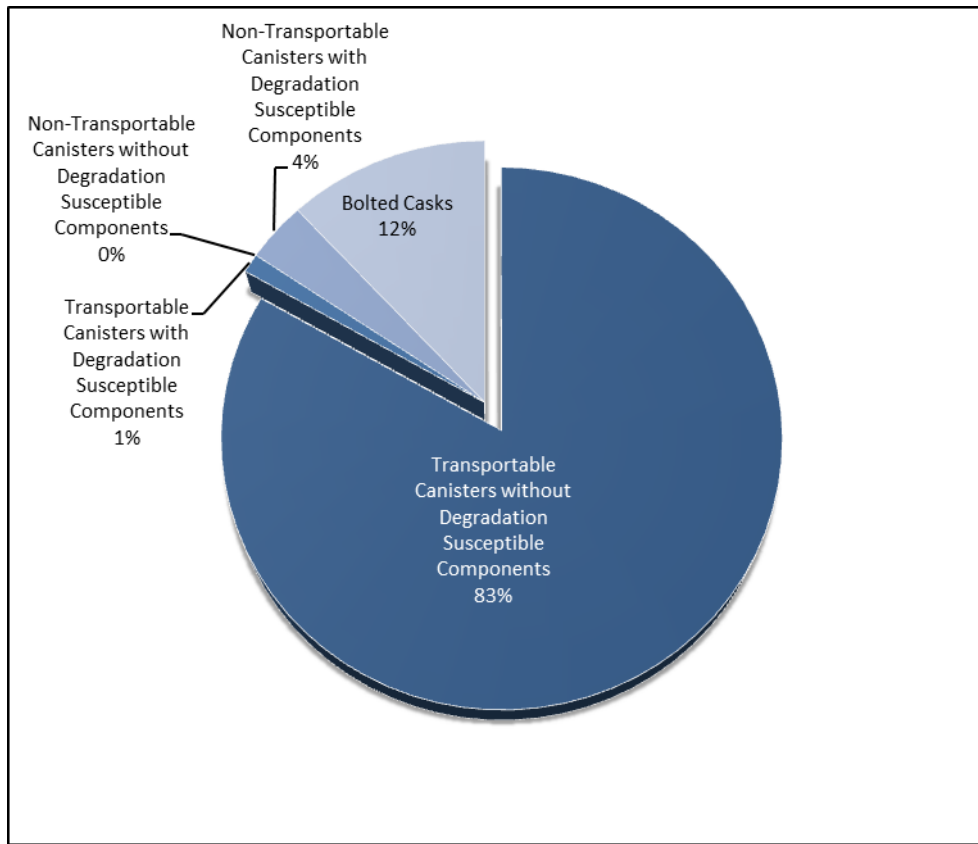


Figure 8-9. Fractional representation of BWR fuel assemblies by canister type and material susceptibility

Table 8-5. Summary of the distribution of canisters and fuel types, by canister type and material susceptibility

| Canister Classification  | # of Canisters in Storage (July, 2014) | # of PWR Fuel Assemblies in Storage (July, 2014) | # of BWR Fuel Assemblies in Storage (July, 2014) |
|--|--|--|--|
| Transportable Canisters without Degradation-Susceptible Components     | 1,321 (69.1%)                          | 24,980 (65.5%)                                   | 32,103 (83.2%)                                   |
| Transportable Canisters with Degradation-Susceptible Components        | 104 (5.4%)                             | 2,531 (6.6%)                                     | 441 (1.1%)                                       |
| Non-Transportable Canisters without Degradation-Susceptible Components | 24 (1.3%)                              | 768 (2.0%)                                       | 0 (0%)   |
| Non-Transportable Canisters with Degradation-Susceptible Components    | 268 (14.0%)                            | 5,784 (15.2%)                                    | 1,404 (3.6%)                                     |
| Bolted Casks   | 195 (10.2%)                            | 4,054 (10.6%)                                    | 4,624 (12.0%)                                    |
| <b>Total</b>   | <b>1,912</b>                           | <b>38,117</b>                                    | <b>38,572</b>                                    |

## References for Section 8

- Andersson, J., H. Ahokas, J.A. Hudson, L. Koskinen, A. Luukkonen, J. Löfman, V. Keto, P. Pitkänen, J. Mattila, A.T.K. Ikonen and M. Ylä-Mella 2007. *Olkiluoto site description 2006*. POSIVA 2007-03, Olkiluoto: Posiva Oy.
- APV (SPX Corporation) 2008. *Corrosion Handbook*. Issued August, 2008.
- Blondes, M.S., K.D. Gans, J.J. Thordsen, M.E. Reidy, B. Thomas, M.A. Engle, Y.K. Kharaka and E.L. Rowan 2014. U.S. Geological Survey National Produced Waters Geochemical Database v2.0 (Provisional), April, 2014.
- Bryan C.R., D.G. Enos, L. Brush, A. Miller, K. Norman and N.R. Brown 2011. *Engineered Materials Performance: Gap Analysis and Status of Existing Work*. FCRD-USED-2011-000407. U.S. Department of Energy, Office of Used Nuclear Fuel Disposition. October, 2011.
- BSC (Bechtel-SAIC Co.) 2003. *The Potential of Using Commercial Dual-Purpose Canisters for Direct Disposal*. TDR-CRW-SE-000030 REV 00. U.S. Department of Energy. Las Vegas, NV.
- Buck E. C., Wittman R. S., Skomurski F. N., Cantrell K. J., McNamara B. K., and Soderquist C. Z. *Radiolysis Process Modeling Results for Scenarios*. FCRD-UFD-2012-000199. U.S. Department of Energy, Office of Used Nuclear Fuel Disposition. Pacific Northwest National Laboratory, PNNL-21554.
- Cole I.S. and D. Marney 2012. "The science of pipe corrosion: a review of literature on the corrosion of ferrous metals in soils." *Corrosion Science* 56, 5-16
- Deal, D.E., R.J. Abitz, D.S. Belski, J.B. Case, M.E. Crawley, C.A. Givens, P.P.J. Lipponer, D.J. Milligan, J. Myers, D.W. Powers and M.A. Valdivia 1995. *Brine Sampling and Evaluation Program 1992-1993 Report and Summary of BSEP Data Since 1982*. DOE-WIPP 94-011. U.S. Department of Energy, WIPP Project Office. Carlsbad, NM.
- Elboujdaini, M. 2011. "Hydrogen-induced cracking and sulfide stress cracking." In: *Uhlig's Corrosion Handbook, 3<sup>rd</sup> edition* (Editor: R.W. Revie). John Wiley & Sons, Inc.
- Energy Solutions 2002. *VSC-24 Ventilated Storage Cask System Final Safety Analysis Report, Revision 5*. September, 2002.
- Energy Solutions 2003. *FuelSolutions Storage System Final Analysis Report*. April, 2003.
- Frape, S., A. Blyth, R. Blomqvist, R. McNutt and M. Gascoyne 2003. "5.17 Deep Fluids in the Continents: II. Crystalline Rocks." In: *Treatise on Geochemistry* (Eds. H. Holland, and K. Turekian). pp. 541-580.
- Hardin, E. and R. Howard 2013. *Assumptions for Evaluating Feasibility of Direct Geologic Disposal of Existing Dual Purpose Canisters*. FCRD-UFD-2012-000352 Rev. 1. U.S. Department of Energy, Office of Used Nuclear Fuel Disposition. November, 2013.
- Hardin E.L, D.J. Clayton, R.L. Howard, J.M. Scaglione, E. Pierce, K. Banerjee, M.D. Voegelé, H.R. Greenberg, J. Wen, T.A. Buscheck, J.T. Carter, T. Severynse and W.M. Nutt 2013. *Preliminary Report on Dual-Purpose Canister Disposal Alternatives*. FCRD-UFD-2013-000171 Rev. 1. U.S. Department of Energy, Office of Used Nuclear Fuel Disposition. December, 2013.

- Hardin, E.L. 2013. *Spent Fuel Canister Disposability Baseline Report*. FCRD-UFD-2014-000330 Rev. 0. U.S. Department of Energy, Office of Used Nuclear Fuel Disposition. December, 2013.
- Holtec (Holtec International) 2010. *Storage, Transportation, and Repository Cask System Safety Analysis Report, Revision 10*. May, 2010.
- Jack, T.R. and M.J. Wilmott 2011. "Corrosion by soils." In: *Uhlig's Corrosion Handbook, 3<sup>rd</sup> edition* (Editor: R.W. Revie). John Wiley & Sons, Inc.
- Jessen, C.Q. 2011. *Stainless Steel and Corrosion*. Damstahl Stainless Steel Solutions, Denmark.
- King, R.A. 1977. *A review of soil corrosiveness with particular reference to reinforced earths*. TRRL Supplemental Report 316. Transport and Road Research Laboratory, Crowthorne, UK.
- Kursten, B., E. Smailos, I. Azkarate, L. Werme, N.R. Smart and G. Santarini 2004. *COBECOMA: State-of-the-art document on the CORrosion BEhaviour of COntainer MAterials*. European Commission 5th Euratom Framework Programme, 1998-2002. Contract # FIKW-CT-20014-20138 Final Report: European Commission.
- Kwong, G. M. 2011. *Status of corrosion studies for copper fuel containers under low salinity conditions*. NWMO TR-2011-14. Toronto: Nuclear Waste Management Organization.
- Lister T., R. Mizia, A. Erickson and T. Trowbridge 2007. *Electrochemical Corrosion Testing of Neutron Absorber Materials*. INL/EXT-06-11772 Rev. 1. Idaho National Engineering Laboratory, Idaho Falls, ID.
- Lindquist, K. 2009. *Handbook of Neutron Absorber Materials for Spent Nuclear Fuel Transportation and Storage Applications: 2009 Edition*. Electric Power Research Institute. Palo Alto, CA. 1019110.
- Marsal F., L. De Windt and D. Pellegrini 2007. *Modelling of long term geochemical evolution of the bentonite buffer of a KBS-3 repository*. Project SSI P 1596.07 "IRSN support of the SR-Can review." Institute for Radiological Protection and Nuclear Safety. September, 2007.
- McLean, J.C. 1990. *NUHOMS Modular Spent-Fuel Storage System: Design, Licensing, and Construction, Carolina Power and Light*. Raleigh, North Carolina. August, 1990.
- NAC (NAC International) 2003. *NAC-MPC Final Safety Analysis Report, Revision 3*. October, 2003.
- NAC (NAC International) 2004. *NAC-UMS Final Safety Analysis Report, Revision 4*. November, 2004.
- NAC (NAC International) 2010. *MAGNASTOR Final Safety Analysis Report, Revision 10*. August, 2010.
- NRC (U.S. Nuclear Regulatory Commission) 2014. *Certificate of Compliance 71-9255 for the MP-187 Multi-Purpose Cask, Revision 12*. Issued March, 2014.
- Parkins, R.N. 2011. "Stress corrosion cracking." In: *Uhlig's Corrosion Handbook, 3<sup>rd</sup> edition* (Editor: R.W. Revie). John Wiley & Sons, Inc.
- Rebak, R.B. 2011. "Environmental Degradation of Engineered Barrier Materials in Nuclear Waste Repositories". In: *Uhlig's Corrosion Handbook, 3<sup>rd</sup> edition* (Editor: R.W. Revie). John Wiley & Sons, Inc.

Smailos, E., M.A. Cunado, B. Kursten, I. Azkarate and G. Marx 2004. *Long-term performance of candidate materials for HLW/spent fuel disposal containers*. European Commission 5th Euratom Framework Programme, 1998-2002. Contract # FIKW-CT-2000-00004 Final Report: European Commission.

Smart, N.R., D.J. Blackwood, G.P. Marsh, C.C. Naish, T.M. O'Brien, A.P. Rance and M.I. Thomas 2004. *The anaerobic corrosion of carbon and stainless steels in simulated cementitious repository environments: A summary review of NIREX research*. AEAT/ERRA-0313, Harwell, England: AEA Technology.

Smart N.R., A.P. Rance, L. Carlson and L.O. Werme 2006. "Further Studies of the Anaerobic Corrosion of Steel in Bentonite." *Mat. Res. Soc. Symp. Proc.* V. 932.

Stein, C.L. and J.L. Krumhansl 1987. "A model for the evolution of brines in salt from the lower Salado Formation, southwestern New Mexico." *Geochimica et Cosmochimica Acta*. V.52, pp. 1037-1046.

Streicher, M.A. and J.F. Grubb 2011. "Austenitic and ferritic stainless steels." In: *Uhlig's Corrosion Handbook, 3<sup>rd</sup> edition* (Editor: R.W. Revie). John Wiley & Sons, Inc.

Transnuclear (Transnuclear, Inc.) 2002. *Final Safety Analysis Report for the Standardized NUHOMS Horizontal Modular Storage System for Irradiated Nuclear Fuel, Revision 6*. September, 2002.

Transnuclear (Transnuclear, Inc.) 2012. *MP-197 Transportation Safety Analysis Report, Revision 12 2/2012*.

Ux Consulting 2014. *Store Fuel*. V.15, N.190. June, 2014.

Vinsot, A., C. A. J. Appelo, et al. 2014. "In situ diffusion test of hydrogen gas in the Opalinus Clay." Special Publication 400. Geological Society, London.

Wells, A. 2008. *Feasibility of Direct Disposal of Dual-Purpose Canisters: Options for Assuring Criticality Control*. Electric Power Research Institute. Palo Alto, CA. 1016629.

Wersin, P., O. X. Leupin, et al. 2011. "Biogeochemical processes in a clay formation in situ experiment: Part A – Overview, experimental design and water data of an experiment in the Opalinus Clay at the Mont Terri Underground Research Laboratory, Switzerland." *Applied Geochemistry*. V.26, N.6. pp. 931-953.

Zhang X.G. 2011. "Galvanic corrosion." In: *Uhlig's Corrosion Handbook, 3<sup>rd</sup> edition* (Editor: R.W. Revie). John Wiley & Sons, Inc.

THIS PAGE INTENTIONALLY LEFT BLANK

## 9. Potential DPC Filler Materials

One alternative to direct disposal of existing DPCs, is to treat the DPCs in preparation for disposal by opening them, adding filler materials, and re-sealing them. The main reason for doing so would be for control of postclosure criticality, by adding material for moderator displacement (in the event of flooding) and/or neutron absorption. Note that in this discussion the terminology “criticality control” implies maintaining subcritical conditions, and is equivalent to “criticality avoidance.”

Fillers could render DPCs more suitable for direct disposal, and obviate the need to cut them open and re-package the SNF. Fillers could also potentially enhance waste isolation performance, heat dissipation, and structural stability of the fuel. This section identifies canister filler materials that could be used in existing and future DPCs to mitigate the potential for postclosure criticality, based on the report of Jubin et al. (2014). This topic was previously identified as a key R&D need for DPC disposal evaluation (Hardin et al. 2013).

The approach is generic, such that fillers might be used with DPCs to be disposed of in crystalline, sedimentary (e.g., clay/shale), or salt media. Fillers may have more benefit for some media than others. This evaluation assumes that fillers would be installed at or near the repository, so that the effects on SNF transportation would be secondary.

Addition of fillers to canistered fuel has been considered since the early concepts for dry storage and transportation of SNF were conceived. An earlier study performed by Maheras et al. (2012) evaluated the use of filler materials to meet 10 CFR Parts 71 and 72 requirements to allow extended storage and subsequent transport of the UNF. During extended storage of the fuel, components relied on for safety may degrade due to thermal, chemical, mechanical, or radiological effects. Use of filler materials could eliminate the challenge of verifying that fuel is “intact” prior to shipment and disposal. Fillers could possibly prevent the necessity of re-packaging “failed fuel” to ensure transportation safety for both normal and accident conditions. Based on the estimated R&D and licensing efforts that would be needed, and the expected benefits, these authors concluded that the use of filler materials for stabilizing UNF during storage and transport was not recommended.

The International Atomic Energy Agency (IAEA 2000) discussed the addition of filler material for moderator exclusion. Such an approach could also involve adding neutron-absorbing materials that were selected to last longer than those typically considered for transportation and storage. The report (IAEA 2000) states the following:

“The moderator exclusion substance shall have an expected useful life that exceeds that of the fuel while it remains reactive. This approach will complicate the design of a system where canisters are welded and are intended for use in the geological repository. This consideration will require the designer of a canister to be able to demonstrate the ability to open and reseal the container after the addition of additive materials, unless the additive materials have been already introduced at the time of the first loading of the canister.”

For disposal, the geologic timescale following repository emplacement makes postclosure criticality a concern (BSC 2003). DPC designs are based on the assumption that water could flood the canister during a transport accident, and design features (e.g., flux traps, neutron absorbers) are provided to prevent nuclear criticality. Due to degradation and mobility of these

materials in certain environments, they cannot currently be credited for maintaining subcritical configurations during long-term exposure to ground water (i.e., thousands of years).

This section develops a list of candidate filler materials to meet the postclosure criticality control objective. Further studies to evaluate the suitability of selected fillers in specific disposal media, and cost/benefit analyses to determine if the DPCs can be filled without re-packaging of the fuel, would be performed as part of a future R&D program (Figure 9-1).

In addition to criticality control, advantages of filler materials in emplaced DPCs could also include the following (Cogar 1996):

- Chemical buffering to reduce radionuclide migration following breach of containment barriers and water intrusion into the waste package
- Cathodic protection, by use of filler material with the highest electrochemical activity, in the event of water intrusion to minimize the effects of corrosion
- Mechanical supports to maintain geometry, inhibit movement, and retain structural integrity of the fuel and waste package
- Improved heat transfer to protect fuel cladding and engineered barriers in the disposal system



Source: Forsberg (1997).

Figure 9-1. Surrogate waste package with bead filler

## 9.1 Filler Material Requirements

Requirements for filler materials to be provided at the repository would be similar, but not identical, to requirements for fillers to be used for storage and transportation. Table 9-1 compares potential evaluation metrics for filler materials when applied to storage and transportation, vs. those for control of postclosure criticality. This table is an adaptation of metrics proposed by Maheras et al. (2012). Evaluation criteria for filler material performance fall into two general groups (Puig et al. 2008a): those required for criticality control (Table 9-2), and other general attributes of the materials (Table 9-3).

Filler material requirements that would be applicable to storage and transportation but are of relatively minor importance for repository performance include the following:

- **Radiation Shielding** – Package emplacement in the repository is assumed to be performed using shielded transporters and handling equipment
- **Filler Weight** – The incremental weight of the filler may contribute significantly to the weight of the transportation package, requiring re-packaging into smaller DPCs to meet weight limits. The incremental weight of the filler is not expected to contribute significantly to the weight (approximately 80 to 100 MT) of the emplaced waste package
- **Filler Performance During Shipment** – The filler material will not be subject to hypothetical accident conditions or normal conditions of transport, since movement will be restricted to transfer from the fill station to the repository
- **Fuel Retrieval** – Individual fuel assemblies will not be retrievable from the DPC once filled

## 9.2 Canister Filling Requirements

Filling operations are assumed to require access to sealed canisters received at the repository. For existing canisters access can be obtained through the vent and drain lines, removal of the canister lid to expose the fuel, or a new penetration into the top or sidewall of the canister. The access selected may depend on the physical and chemical form of the selected filler material and the DPC design variant. Placement of the filler material must ensure (Wallin 1996):

- **No Damage** – Fillers should not cause degradation of canister structural integrity, or damage to the fuel
- **Minimum Fill** – At least 60% of the canister void space should be filled
- **No Re-Packaging** – Filling can be completed without requiring re-packaging
- **Quality Control** – Filler materials and filling methods should allow for measurement of completeness of void fill
- **Re-Sealing of DPCs** – Filler materials and filling methods should allow for re-sealing the DPC
- **DPC Atmosphere** – The inert atmosphere (e.g., He charge) can be re-established after filling to provide corrosion protection and heat transportation while the canister is intact

Table 9-1. Comparison of DPC filler metrics relevant to transportation and postclosure criticality control

| Evaluation Criteria for Candidate Canister Fill Material | Elements   | Relevant to Storage and Transportation <sup>A</sup> | Relevant to Control of Postclosure Criticality <sup>A</sup> |
|--|--|---|---|
| <b>Criticality Control</b>                               | • Provide moderator exclusion  | X   | X   |
|  | • Neutron absorption capability  | <b>X</b>  | <b>Secondary</b>  |
|  | • Minimize neutron moderation  | <b>X</b>  | <b>Secondary</b>  |
|  | • Provide dilution of fissile radionuclides  | <b>X</b>  | <b>Secondary</b>  |
|  | • Capacity to fill over 60% of the inner free volume of the canister   | X   | X   |
|  | • Fill material does not compact by more than 10% of its original volume under its own weight or as the result of shipping or handling   | X   | X   |
| <b>Heat Transfer or Thermodynamic Properties</b>         | • Promote heat transfer from the fuel  | <b>X</b>  | <b>Secondary</b>  |
|  | • Thermal stability  | <b>X</b>  | <b>Secondary</b>  |
|  | • Chemical stability   | <b>X</b>  | <b>Secondary</b>  |
|  | • Radiation stability  | <b>X</b>  | <b>Secondary</b>  |
|  | • Chemically compatible with fuel cladding, fuel, neutron poisons, fuel baskets, and other structural materials within canister  | <b>X</b>  | <b>Secondary</b>  |
| <b>Homogeneity and Rheological Properties</b>            | • Homogeneous batches  | X   | X   |
|  | • Good rheological properties to ensure proper filling   | X   | X   |
|  | • Ability to be placed in the canister without damaging fuel assemblies  | X   | X   |
| <b>Retrievability</b>                                    | • Allows for safe retrieval of UNF from a canister without need to resort to time-consuming or costly measures and without further compromise of the integrity of UNF assemblies | <b>X</b>  | <b>NA</b>   |
| <b>Material Availability and Cost</b>                    | • Low cost   | X   | X   |
|  | • Material available in required purity  | X   | X   |
| <b>Weight and Radiation Shielding</b>                    | • Fill material does not add significantly to the weight of the container/cask system  | <b>X</b>  | <b>NA</b>   |
|  | • Good radiation shielding properties  | <b>X</b>  | <b>NA</b>   |
| <b>Operational Considerations</b>                        | • Easy to emplace  | X   | X   |
|  | • Fill material does not adversely react to normal conditions of transport or hypothetical accident conditions   | <b>X</b>  | <b>NA</b>   |

<sup>A</sup> The “X” indicates the associated element in the criteria list is highly important. Differences between the last two columns are highlighted in bold text.

Table 9-2. Criticality control criteria

| Attribute                      | Basis   |
|--------------------------------|---|
| <b>Low water solubility</b>    | Prevents dissolution and migration of filler following package degradation and water inflow |
| <b>Low compaction ratio</b>    | Ensures that the void volume remains constant after filling                                 |
| <b>Low neutron moderation</b>  | Low content of hydrogen or other light elements allows neutrons to escape the package       |
| <b>High neutron absorbance</b> | Presence of neutron absorbers (B, Cd) can reduce the $\Delta k_{\text{eff}}$ of the system  |
| <b>Water exclusion</b>         | Filler material may physically block the introduction of water to a degraded package        |
| <b>Isotope dilution</b>        | Depleted uranium can reduce the bulk $^{235}\text{U}$ concentration from failed fuel        |

Table 9-3. General performance criteria

| Attribute   | Basis   |
|---|---|
| <b>Thermal, chemical, mechanical, radiological stability</b>                      | Ensures that the filler properties are consistent and compatible with application                 |
| <b>Good rheological properties</b>  | Provides for continuous, replicable filling of the canister                                       |
| <b>Good heat transfer</b>   | Reduces thermal loading on fuel cladding  |
| <b>Chemical compatibility with, fuel, waste package, and disposal environment</b> | Reduces corrosion and delays/eliminates the migration of radionuclides to the environment         |
| <b>Material availability</b>  | Provides domestic supplies of sufficient quantity and purity, with minimal environmental impacts  |
| <b>Material cost</b>  | Ensures incremental cost of material is insignificant with cost of filling and disposal of the WP |

Oversby and Werme (1995) suggest the following three-tier approach to design requirements. The first tier comprises those requirements necessary to ensure void spaces are filled and that the fill material remains in place. Three items were identified as sufficient to ensure meeting this requirement:

- I. The fill material must be able to be placed in the canister in a manner that does not damage the fuel and results in a residual void volume of less than 40% of the original void volume. This also assumes that virtually the entire DPC is filled and that the voids are inter-particulate voids. See the discussion on criticality (Section 6).
- II. The fill material has a solubility of less than 100 mg/L at 50°C in pure water and in the water of the anticipated repository environment.

- III. The fill material shall not compact by more than 10% of its original volume under its own weight or as the result of handling or emplacement. To demonstrate moderator displacement characteristics for criticality control, the limit of 10% compaction is based on analysis showing that a minimum volume displacement ratio must be maintained to ensure subcriticality.

The second tier of requirements suggested by Oversby and Werme (1995) is considered “desirable properties.” These include the following:

- A. The material is in dynamic equilibrium with the disposal system, thus ensuring chemical compatibility.
- B. The material has homogeneous properties within a batch and between batches, thus making quality control and performance modeling more certain.
- C. Material has well-documented, long-term durability, thus allowing more certain predictions concerning the condition of material through time.
- D. Material has good rheological properties for emplacement in the canister.
- E. Material contains a burn poison to absorb neutrons, thus enhancing criticality control.
- F. The material has the potential to absorb radionuclides from an aqueous solution, thus limiting potential releases from a breached waste package.
- G. Material has the potential to suppress the generation of hydrogen.
- H. Material has low cost.
- I. Material has low density, thus reducing the total weight of the fill canister.

Oversby and Werme (1995) also listed the following five traits as “undesirable properties” of filler materials:

- a) Limited availability.
- b) Potential to enhance the corrosion of the canister, fuel cladding, or the fuel itself.
- c) Material generates gas when it is altered or reacted.
- d) Material contains water.
- e) Material has an affinity for absorbing air.

### **9.3 Candidate Filler Materials**

Extensive investigation has been conducted into the identification and evaluation of canister filler materials to support storage, transportation, and disposition of SNF (Maheras et al. 2012; Oversby and Werme 1995; Puig et al. 2008a, 2008b, 2009). Potential materials that can satisfy the criteria described above are assumed to be solids introduced directly, or liquids or molten materials that solidify after emplacement. Although liquids and gases have been evaluated previously, they are not considered viable candidates because of the potential for escape after waste package breach.

Examples of filler materials introduced as liquids which then solidify are provided in Table 9-4. Materials introduced as solids are shown in Table 9-5. The suitability of a particular material is not only dependent on its physical and chemical properties but also on the properties of the fuel,

DPC geometry, and the disposal environment. The choice of filler material may vary if the principal performance requirement changes from criticality control to water displacement or radionuclide sequestration.

Limited testing has been performed using filler materials on surrogate fuel and canister assemblies. An more extensive test program would likely be needed to ensure that all performance requirements for materials, fuel, and waste packages are satisfied. In addition, the performance of the filled canister must be evaluated for each disposal environment under consideration to determine the postclosure impacts to the repository.

Table 9-4. Filler materials emplaced as liquids

|                                      | Advantages  | Disadvantages  | Examples                |
|--------------------------------------|---|--|-------------------------|
| <b>Molten (solidify on cooling)</b>  |   |  |                         |
| <b>Metals</b>                        | <ul style="list-style-type: none"> <li>• Good heat transfer</li> <li>• Good void fill</li> <li>• Water exclusion</li> </ul> | <ul style="list-style-type: none"> <li>• Need low melting point</li> <li>• Must be non-reactive with fuel and canister</li> </ul>  | Tin, lead, zinc, alloys |
| <b>Non-metals</b>                    | <ul style="list-style-type: none"> <li>• Good void fill</li> </ul>  | <ul style="list-style-type: none"> <li>• Neutron moderation</li> <li>• H<sub>2</sub> generation</li> <li>• Unstable to radiation</li> <li>• Low thermal conductivity</li> <li>• Low melting point</li> </ul> | Plastics                |
| <b>Liquid (solidify on reaction)</b> |   |  |                         |
|                                      | <ul style="list-style-type: none"> <li>• Good void fill</li> </ul>  | <ul style="list-style-type: none"> <li>• High organic and/or water content</li> <li>• Neutron moderation</li> <li>• Unstable to radiation</li> <li>• High viscosity</li> </ul>                               | Resins, foam, grout     |

Table 9-5. Filler materials emplaced as solids

|                     | Advantages   | Disadvantages  | Examples  |
|---------------------|--|--|---|
| <b>Particulates</b> | <ul style="list-style-type: none"> <li>• Good heat transfer</li> <li>• Maintain water exclusion</li> <li>• Isotopic dilution (depleted UO<sub>2</sub>)</li> <li>• Radionuclide absorption</li> </ul> | <ul style="list-style-type: none"> <li>• Compaction after filling</li> <li>• Dust generation during filling</li> </ul>   | Minerals (rutile, hematite, olivine, magnetite), crushed rock (granite), sand, depleted UO <sub>2</sub> |
| <b>Beads</b>        | <ul style="list-style-type: none"> <li>• Good heat transfer</li> <li>• Water exclusion</li> <li>• Neutron absorber addition</li> </ul>   | <ul style="list-style-type: none"> <li>• Compaction after filling</li> </ul>   | Metal (copper, lead, steel), glass (borosilicate, DUO <sub>2</sub> silicate)                            |
| <b>Clays</b>        | <ul style="list-style-type: none"> <li>• Radionuclide absorption</li> </ul>  | <ul style="list-style-type: none"> <li>• Requires alignment of flat surfaces for void fill</li> <li>• Possible compaction after filling</li> <li>• High water content</li> </ul> | Bentonite   |

### 9.3.1 Liquid Fill Materials That Solidify

A draft report from the Civilian Radioactive Waste Management System Management & Operating Contractor (CRWMS M&O 1999) discusses several low-melting point solids. These include tin, lead, zinc, and a zinc-aluminum alloy commercially used for die casting. The melting points for tin and lead are below 350°C. In this evaluation, tin was eliminated from further consideration due to limited availability and lead was eliminated due to its toxicity, mass, and the potential to embrittle other materials in the waste package. Zinc may interact with the Zircaloy cladding. Based on this concern both zinc and the zinc-aluminum alloys were rejected.

However, for this application there may be merit in re-examining the liquid fill options if some of the potential cladding interactions are less important. Lead and tin remain the most common low-melting-point metals. By combining lead and tin in the proper ratio, a lower-melting-point eutectic can be formed. The Sn63–Pb37 alloy, a solder used in electronics, has a melting point of 183°C. A number of lead-free solders are also available. These include Sn95.6–Ag3.5–Cu0.9 with a melting point of 217°C and Sn91–Zn9 with a melting point of 199°C. The melting point of zinc is 419.5°C, and the Zn–Al eutectic alloy is 382°C. Table 9-6 provides a summary of possible liquid fill materials and their melting points.

Maheras et al. (2012) summarized a study by the Canadian Nuclear Waste Management Organization which also considered a system where cast metal surrounded the fuel bundles and formed a layer between the outer bundles and the shell of the container. Lead, zinc, and aluminum metals and lead-antimony, aluminum-silicon, and aluminum-copper alloys were studied as candidate casting materials. Lead and zinc were recommended as the preferred casting materials.

Several other liquid or molten materials were also reviewed by Maheras et al. (2012), including paraffin, resins, foams and grout. They found no previous studies on the use of paraffin wax as a fill material for UNF canisters. Paraffin wax is a mixture of pure alkanes and has a melting point between about 46 and 68°C. It has a density of about 0.9 g/cm<sup>3</sup>. The thermal conductivity is 0.25 W/m·K. Handling would be relatively easy due to the low melting point, but there are also a number of potential issues associated with the use of paraffin as a fill material. Paraffin is a hydrocarbon and would be an effective moderator. This could be mitigated by adding a neutron absorber to the melt. A second aspect is the potential for radiolytic decomposition and the associated hydrogenation. Paraffin is also flammable and would require the addition of a flame retardant to the melt.

Maheras et al. (2012) also found no previous studies on the use of resins as a fillers for UNF canisters. Resins have potential as a fill material because they can be poured into a canister as a liquid and then solidify. Resin densities range from about 1.0 to 2.0 g/cm<sup>3</sup>. The thermal conductivity is in the range of 0.1 to 1.0 W/m·K. However, like paraffin, resins are hydrocarbons and would be effective moderators. This could be mitigated by adding a neutron absorber to the resin. The resin would also be subject to radiation damage, but some resins show resistance to doses greater than 10<sup>6</sup> Gy. Ignition temperatures for some resins can be >400°C, depending on the type; for example, the ignition temperature of unsaturated polyester is 500°C. If needed, an ignition retardant could be added.

Foams were also discussed by Maheras et al. (2012) but no studies were found on their use as fillers for UNF canisters. Foams have potential but injection methods must be demonstrated to ensure that significant voids can be avoided. Foam densities range from about 0.01 to 1.0 g/cm<sup>3</sup>.

Thermal conductivity is in the range of 0.03 to 5.8 W/m·K, depending on density and composition (the highest conductivity is associated with metallic foams). Issues associated with the use of foams would be similar to those with resins and paraffin. Most foams are organic and would be effective moderators. Foam would also be subject to radiation damage, but some foams show resistance to doses greater than  $10^6$  Gy. Organic foams can burn possibly necessitating addition of an ignition retardant. Metal or ceramic foams could avoid some of these issues.

Grout has already been used in a number of waste management applications (Maheras et al. 2012). There are, however, a number of issues associated with its application as a filler material. The first concern is the ability of the grout to flow between the fuel pins and the structural materials in the canister. The second is the fact that grout contains waters of hydration within its structure. A neutron absorber might be required in the grout to limit the moderating effect. The third issue is its compatibility with the fuel cladding and other material in the DPC. The use of grout may also require venting during the curing phase to allow the release of excess water.

### 9.3.2 Solid Fill Materials

**Sweden** – The Swedish repository R&D program has evaluated a number of candidate materials (Oversby and Werme 1995). These materials include glass beads, lead shot, copper spheres, sand, olivine, hematite, magnetite, crushed rock, bentonite clay, other clays, and concrete. Of these, glass beads were reported as the leading candidate because they can be made to contain one or more burnable poisons and have a number of other positive features, including the ability to manufacture the beads with homogeneous properties, well-documented studies of the performance of glass waste, and relatively low density. Copper spheres were also considered a leading candidate because copper is already present in the Swedish disposal concept. Magnetite was a third candidate since it is likely to be present in the host rock of the Swedish repository.

Table 9-6. Melting points of potential liquid fill materials

| Candidate Liquid Fill Material       | Eutectic? | Melting Point (°C) |
|--------------------------------------|-----------|--------------------|
| <b>Pb</b>                            | No        | 327.6              |
| <b>Sn</b>                            | No        | 231.9              |
| <b>Zn</b>                            | No        | 419.5              |
| <b>Pb–Sn (60/40) (common solder)</b> | No        | 188                |
| <b>Pb–Sn (37/63)</b>                 | Yes       | 183                |
| <b>Sn–Ag–Cu (95.6/3.5/0.9)</b>       | Yes       | 217                |
| <b>Sn–Zn (91/9)</b>                  | Yes       | 199                |
| <b>Zn–Al (95/5)</b>                  | Yes       | 382                |
| <b>Paraffin</b>                      | No        | 46–68              |

**Canada** – Forsberg (1997) described Canadian work on fillers. During a 15-year development program of its repository concept for CANadian Deuterium Uranium (CANDU) reactor SNF, the use of a glass-bead or silica-sand fill was explored. The would be loaded into empty waste

packages, and the void spaces filled with small particles. The waste packages would then be sealed and emplaced in the repository. Canadian waste package filler requirements were that it fill all empty spaces within the waste package and that it be chemically inert, structurally strong, and inexpensive. The fill was also required to support the waste package wall against 10 MPa of external hydrostatic pressure.

A comparison between CANDU and PWR characteristics is shown in Table 9-7. A key difference is that the internal clearances between pins in the CANDU fuel assembly are, on average, smaller than those of PWR assemblies (Figure 9-2). In the CANDU fuel assembly the minimum clearance between rods is 1.3 mm, while in a standard PWR fuel assembly the clearance is 3.4 mm. It is expected that filling these void spaces inside CANDU fuel assemblies would be more difficult than filling void spaces within PWR fuel assemblies (Forsberg 1997).

The Canadian test program demonstrated backfilling of the loaded waste packages with small particulates. Twelve fill materials were studied, including (Forsberg 1997):

- Wedron sand (0.2 to 0.85 mm)
- Fine glass beads (0.002–0.3 mm)
- Coarse glass beads (0.8–1.2 mm)
- Steel shot (0.6–1.0 mm)
- Aluminum oxide powder
- Crushed bauxite grains (up to 1 mm)
- Sintered bauxite powder
- Interprop hydraulic fracturing proppant
- Ceramic zirconia powder
- Rutile-Zircon-Garnet mixture
- Zircon powder
- Rutile powder

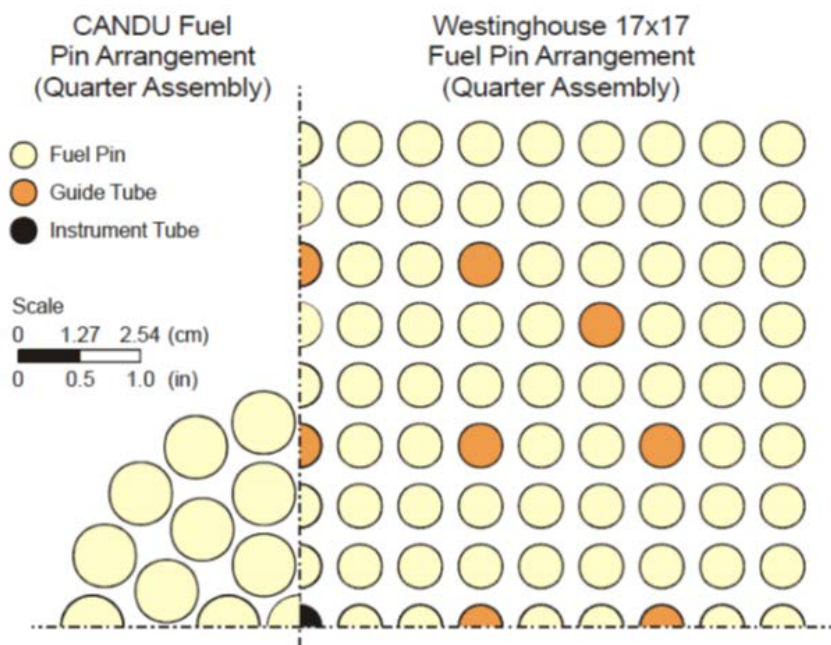
Extensive fill tests were conducted to define the particle size, vibration frequencies, and accelerations that provided the most rapid and reliable filling. These tests indicated that the maximum practical packing density was about 70%. Vibratory filling was identified as the preferred option for this type of waste package as it provided higher fill densities and shorter fill times (Forsberg 1997).

The review by Maheras et al. (2012) indicated that the Canadian program considered three fill materials as viable: glass beads, interprop, and sintered bauxite. Coarse glass beads generated the least amount of dust during compaction and produced the highest bulk modulus of elasticity in the compacted state. The glass beads were selected as the candidate fill material; however, they were later abandoned because glass beads could not provide the necessary assurance that the waste package would not collapse. If the structural requirement is removed, then glass beads may still be viable for the purpose of moderator exclusion.

Table 9-7. Characteristics of CANDU and PWR SNF (Forsberg 1997)

| Property                                 | Fuel-Assembly Type |                  |
|--|--------------------|------------------|
|  | CANDU              | PWR <sup>A</sup> |
| Weight, kg                               | 21.2               | 611.5            |
| Uranium, kg/assembly                     | 19                 | 401              |
| Initial enrichment, <sup>235</sup> U wt% | 0.71–0.9           | 3–5              |
| Burnup, MWd/t                            | 6,850 (design)     | 30,000–50,000    |
| <b>Assembly</b>                          |                    |                  |
| Geometry                                 | Circular           | Square           |
| Length, m                                | 0.495              | 4.063            |
| Width (diameter), cm                     | 10.2               | 21.4             |
| Fuel pins, number                        | 37                 | 264              |
| Nonfuel pins/tubes, number               | 0                  | 25               |
| Ratio of pin area to total area          | 0.613              | 0.414            |
| Minimum pin gap, mm                      | 1.3                | 3.4              |
| <b>Pins</b>                              |                    |                  |
| Fuel type                                | UO <sub>2</sub>    | UO <sub>2</sub>  |
| Clad type                                | Zircaloy           | Zircaloy         |
| Length, m                                | 0.493              | 3.868            |
| Diameter, cm                             | 1.3                | 0.914            |
| Clad thickness, mm                       | 0.4                | 0.57             |
| <b>Spacers (grids)</b>                   | 3                  | 6                |

<sup>A</sup> The 17 × 17 PWR fuel assembly has a total of 289 rod positions. Twenty-five positions may contain guide tubes for control rods, instrument tubes, and/or burnable absorber rods.



Source: Forsberg (2002).

Figure 9-2. Comparison of void space and pin arrangement for CANDU and PWR fuel assemblies

**United States** – Forsberg et al. (1996) and Pope et al. (1996) discussed the benefits of using a depleted uranium silicate (DUS) glass as a filler for spent fuel packages. In this concept, waste packages are filled with SNF and then backfilled with DUS (0.2 wt%  $^{235}\text{U}/\text{U}$ ) glass beads. The DUS beads are relatively small (<1 mm), so they easily flow into the SNF coolant channels. The DUS would contain >20 wt% depleted uranium (DU) such that the total fissile concentration in the waste package is below 1 wt%. One of the proposed benefits is that if ground water penetrates the waste package, the DUS glass would chemically saturate the water in the waste package with uranium and slow the SNF dissolution process (Forsberg et al. 1996). Forsberg (2000b) stated that field studies have shown that parts of natural uranium ore bodies have remained intact for geological time periods with oxidizing ground water nearby. In addition, it is reported that the silicate in the glass would lower the solubility of uranium in ground water. This would mean that additional ground water would be needed to dissolve the same amount of uranium. It was also proposed that a precipitated uranium silicate phase would tend to form a coating on exposed  $\text{UO}_2$  which would act as an additional barrier to dissolution (Forsberg et al. 1996).

Pope et al. (1996) provide the following as the proposed glass properties:

- Composition: 29.5 wt%  $\text{U}_3\text{O}_8$ , 11.2 wt%  $\text{CaO}$ , 7.4 wt%  $\text{Na}_2\text{O}$ , and 51.9 wt%  $\text{SiO}_2$
- Uranium isotopics: DU (i.e., 0.0014 wt%  $^{234}\text{U}$ , 0.2 wt%  $^{235}\text{U}$ , 0.0009 wt%  $^{236}\text{U}$ , and 99.7977 wt%  $^{238}\text{U}$ )
- DUS glass density: 4.1  $\text{g}/\text{cm}^3$  with an effective density of 2.7  $\text{g}/\text{cm}^3$ , assuming 65% of space is DUS glass beads
- Thermal conductivity: 0.33  $\text{W}/\text{m}\cdot\text{K}$  (same as dry sand)

Forsberg (2000a,b) discusses the use of  $\text{DUO}_2$  as a fill material, which has several of the same benefits as those discussed for DUS glass. Oxidation of  $\text{UO}_2$  to  $\text{U}_3\text{O}_8$  could result in a reduction of ground water flow due to a 36% increase in molar volume, and the swelling would fill inter-particle voids, creating a low-permeability zone. It could be expected that the water would then flow around the waste package rather than through it. Other materials such as iron would also expand upon oxidation.

Forsberg (2000a) discusses the use of  $\text{DUO}_2$  to control the radionuclide release rate from the waste package. It is proposed that the  $\text{DUO}_2$  fill would create a chemically reducing environment in the local area that would slow the release of radionuclides from the SNF by slowing the degradation of the SNF and by reducing the ground water flow through the waste package. The DU would also minimize the potential for criticality by isotopic dilution. The thermal conductivity of a  $\text{DUO}_2$ -helium particulate bed is expected to be  $\sim 1 \text{ W}/\text{m}\cdot\text{K}$  (Forsberg et al. 2001).

A number of processes have been developed to produce microspheres for nuclear fuel fabrication. These same techniques can be used to fabricate  $\text{DUO}_2$  microspheres (Forsberg et al. 1995, 2001). The proposed particle size is from 0.5 to 1 mm. Fill densities  $\sim 65\%$  can be achieved using a narrow size range of particles. Forsberg et al. (2001) indicated that this can be increased to  $>80\%$  with an appropriate binary-size mixture. Forsberg also indicates that the filling operation with a single particulate size can be accomplished with little or no vibration.

A study conducted by CRWMS M&O (1999) included low-melting point materials that could be placed in a molten state and allowed to solidify, particulate solids (e.g., DUS, iron shot, or iron oxide), and hygroscopic materials which would be reacted and solidified by water entering a breached waste package. Of these, iron shot, iron oxide (hematite,  $\text{Fe}_2\text{O}_3$ ), DUS, and an integral filler concept were selected for further study. The integral fill concept would incorporate the added material into the canister structure and is not applicable to the current study. It was noted that aluminum shot and aluminum oxides ( $\text{Al}_2\text{O}_3$ ) were available commercially in large quantities; however, aluminum oxides do not have the beneficial radionuclide sorption properties of iron oxides. Two structural concerns were identified from inclusion of filler material. The first stems from the increased waste package mass, which could cause larger deformations of the structural components, making the structure more susceptible to breach during a design basis event. Second, the reduction in void space within the waste package coupled with internal pressure increase that could result from failure of the fuel rods is expected to be greater than that for a waste package with no filler material.

Several field tests are discussed in the CRWMS M&O (1999) report. Filling with either 0.7 mm or 1.0 mm shot could be accomplished by gravity flow without the need for vibration.

**Spain** – Puig et al. (2008a, 2008b, 2009) evaluated eight alternative fill materials that could be relied on to control criticality once the fuel canister was flooded with ground water in a geological repository. The materials evaluated included the following.

- Cast iron or steel
- Borosilicate glass
- Spinel
- DU
- Dehydrated zeolites
- Hematite
- Phosphates
- Olivine

Of these, cast iron or steel, borosilicate glass, spinel, and DU were determined to be adequate but some uncertainties were associated with all of the candidate materials. In the case of cast iron or steel, nodular cast iron was used as the basis of assessment but it was noted that moderator displacement by steel shot would be better. In the case of borosilicate glass it was noted that devitrification was possible at high temperatures. The dissolution rate of borosilicate glass was anticipated to be slow, and even in the event of boron selective leaching and removal, volume occupation was assessed to be great enough to avoid criticality. Fillers containing  $\text{DUO}_2$  could be stable under reducing conditions and would behave similarly to SNF.

#### **9.4 Criticality Analysis of Filled DPCs**

The potential for criticality in a filled waste package that has breached and flooded with ground water, is measured by the effective neutron multiplication factor ( $k_{eff}$ , also referred to as reactivity here). System reactivity for commercial LWR fuel typically increases in the presence of a moderator (i.e., water) that slows neutrons to lower energies at which they can be more

readily absorbed by fissile nuclides, causing additional fission reactions. When  $k_{eff} = 1.0$  the system is considered critical. Note that DPC postclosure criticality is only possible if flooding with water occurs. This section investigates: 1) moderator displacement; and 2) neutron absorption aspects of the filler performance.

The methodology for criticality analysis is described in Section 4 and supporting references. Criticality analysis with fillers was performed using the same codes, input data, burnup credit approach, fuel assembly burnup profiles, and so on. The analysis also considers corrosion of DPC materials over hundreds to thousands of years, using the degradation scenarios introduced in Section 4.

**Degradation Scenarios** – An important assumption for criticality analysis is that water enters a waste package at some point during the repository performance period, and the waste package subsequently remains flooded. While the different geologic settings and material degradation mechanisms might yield a large number of potential configurations, two simplified and conservative configurations are used here to assess moderator displacement and neutron absorption by fillers:

- **Loss-of-Absorber** – Total loss of neutron absorber from unspecified degradation and material transport processes (Figure 9-3).
- **Basket Degradation** – Loss of the internal basket structure (including neutron absorbers) resulting in elimination of assembly-to-assembly spacing (Figure 9-4). Conceptually, this scenario consists of the assembly-to-assembly spacing reduced uniformly to zero, and the assemblies arranged in a closely packed cylindrical geometry. Corrosion products from basket degradation are assumed to be flushed from the system.

These degraded configurations are analyzed for a representative DPC emplaced in a horizontal orientation, flooded with fresh water, and filled with different fractional volumes of filler materials. For both scenarios corrosion products are ignored. For aluminum-based absorber materials the quantities of corrosion products would be small relative to the interstitial volume of the fuel. For degradation of basket materials such as carbon steel there could be a slight moderator displacement effect which is conservatively ignored.

Holtec International's MPC-32 is selected as the representative DPC, with modifications for the two degradation scenarios. Three representative filler materials are considered: aluminum in the form of metal powder, gibbsite, and  $B_4C$ . While the aluminum provides water displacement,  $B_4C$  provides both water displacement and neutron absorption. Gibbsite ( $Al(OH)_3$ ) is a common corrosion product of aluminum in the presence of water (OCRWM 2007) and is included to evaluate the effectiveness of a corrosion product that contains hydrogen in its formula. Packing densities of 58% and 68% are considered, and modeled as volumetric mixtures (e.g., 58% by volume aluminum powder, gibbsite, or  $B_4C$ , and 42% water). The criticality analysis is performed for three uniform fuel loadings: 10, 20, and 30 GW-d/MTU burnup, with 100 years of cooling time in all 32 assembly locations. Filler material is shown in Figures 9-3 and 9-4; for the basket degradation scenario the entire canister is filled or partially filled with filler, while for the loss-of-neutron absorber scenario filler material is dispersed more uniformly, filling or partially filling each cell containing a fuel assembly.

### 9.4.1 Criticality Analysis Results

The volume fractions used to present the criticality results depend on the degradation scenario. The volume fraction is calculated by dividing the volume of the filler material in a basket cell by the free volume of that basket cell for the loss-of-absorber case. The free volume of a cell is calculated by subtracting the volume of the assembly from the total volume of the cell. Note that assembly volume only includes the active fuel region (fuel rods, guide tubes, and instrument tubes) without the spacer grids. Guide tubes and instrument tubes are modeled as filled with water. The filler material volume in a cell is calculated by subtracting the part of the assembly volume covered by the filler material from the filler material volume. On the other hand, the volume fraction is calculated by dividing the filler material volume by the free canister volume for the basket degradation scenario. Figure 9-5 presents the reactivity reduction in terms of negative  $\Delta k_{eff}$ , as a function of fractional volume of powdered aluminum, for the loss-of-absorber and basket degradation scenarios. Figure 9-5(a) indicates monotonic reduction of reactivity with increasing filler volume for the loss of neutron absorber scenario, whereas Figure 9-5(b) shows that the reactivity reduction up to a certain threshold volume fraction is insignificant, with greater reduction beyond the threshold, for the basket degradation scenario. However, for both scenarios significant volume fraction (~90%) may be required with powdered aluminum, to maintain subcriticality over the repository performance period.

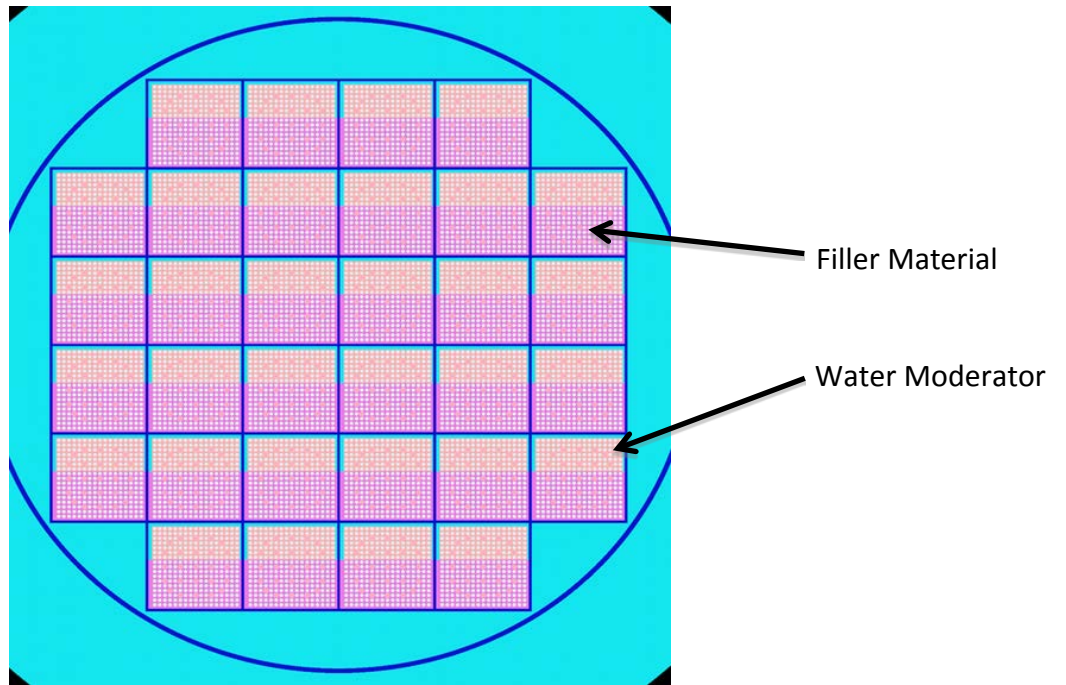


Figure 9-3. Graphical depiction of the center plane of the MPC-32 KENO-VI model with complete loss of neutron absorber used for filler materials study

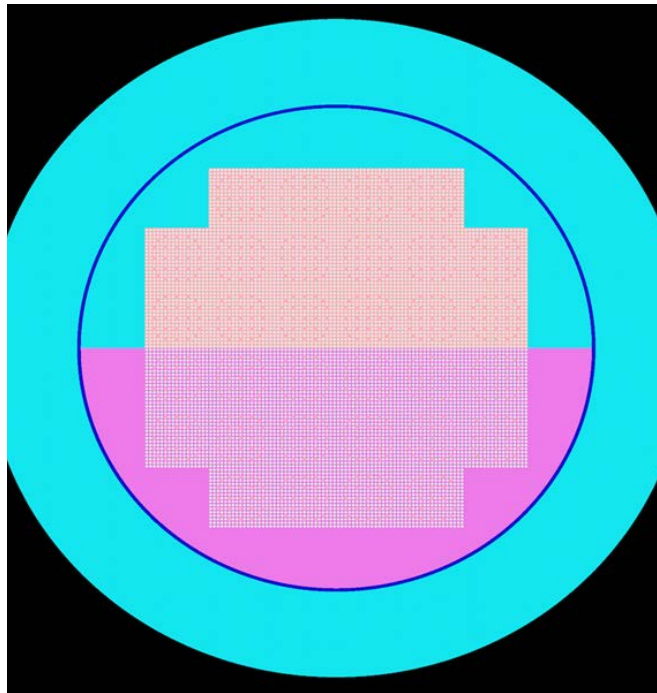


Figure 9-4. KENO-VI depiction of the MPC-32 basket degradation scenario with filler material

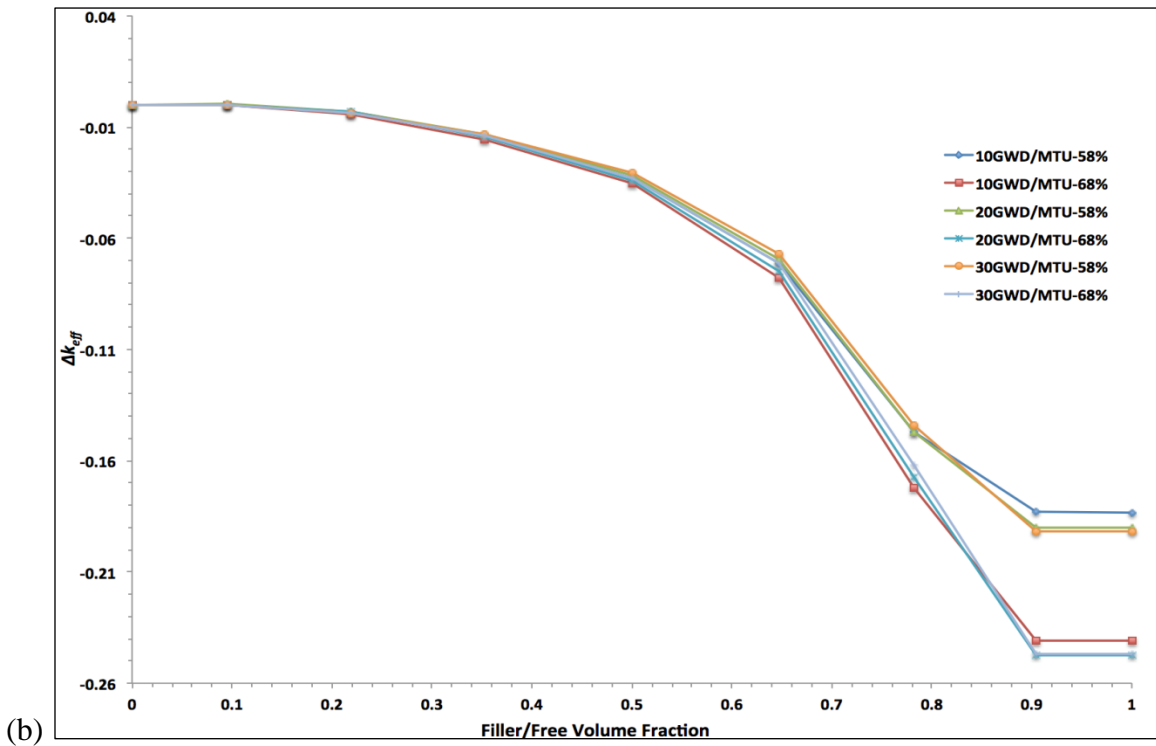
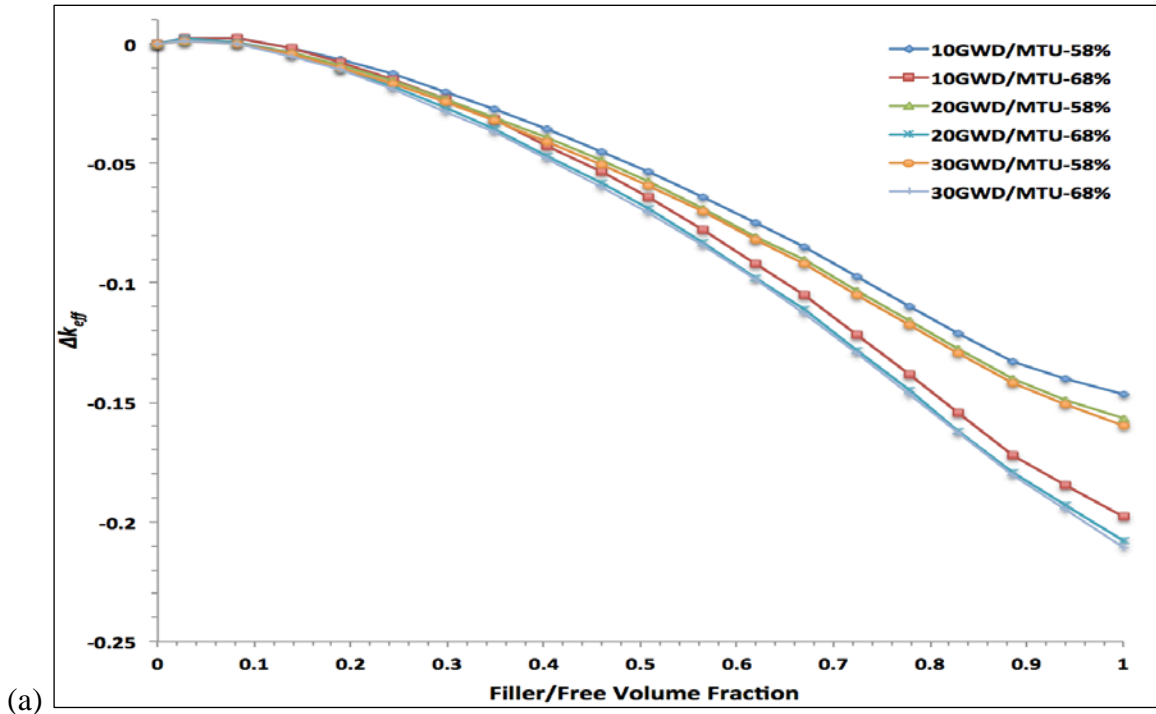


Figure 9-5. Reactivity reduction ( $\Delta k_{eff}$ ) as a function of aluminum powder volume fraction for: (a) complete loss of neutron absorber; and (b) basket degradation scenario

Figure 9-6(a) shows reactivity reduction as a function of  $B_4C$  filler volume fraction for the loss-of-absorber scenario. It shows that significant reactivity reduction can be realized with as little as 10% of the free volume filled by  $B_4C$  in the presence of fresh water. An important assumption here is that  $B_4C$  occupies the same volume inside each basket cell and is uniformly distributed throughout the axial length, as shown in Figure 9-1. This uniform  $B_4C$  filler material distribution throughout the axial length could be difficult to achieve in practice. Figure 9-6(b) shows that for the basket degradation scenario significant reactivity reduction can be obtained beyond a certain threshold volume fraction. In other words, only a few assemblies, completely flooded by water, may form a potential critical configuration if there are no basket materials in between the assemblies and the assemblies are virtually in contact with each other.

It is observed that if aluminum turns into gibbsite (or other similar materials that react with water to form a hydrogenous compound) in the presence of water over the repository time frame, the aluminum has a potential to lose its moderator displacement functionality. Figure 9-7 presents reduction in reactivity as a function of gibbsite volume fraction for the loss-of-absorber scenario and shows insignificant reactivity reduction. Similar to the aluminum study, gibbsite is modeled with 58% and 68% packing density. Therefore, any volume change that may occur because of an aluminum-to-gibbsite conversion is not accounted for in this study.

An important observation of the filler materials criticality study is that a filler material, irrespective of whether it is a neutron absorber, should occupy most or all of the free DPC volume to provide criticality control over the repository time frame. The study suggests that more than 90% of the free volume should be filled to provide conservative criticality control. Additionally, the eventual corrosion product of a filler material and its neutron moderating and absorbing properties must be considered.

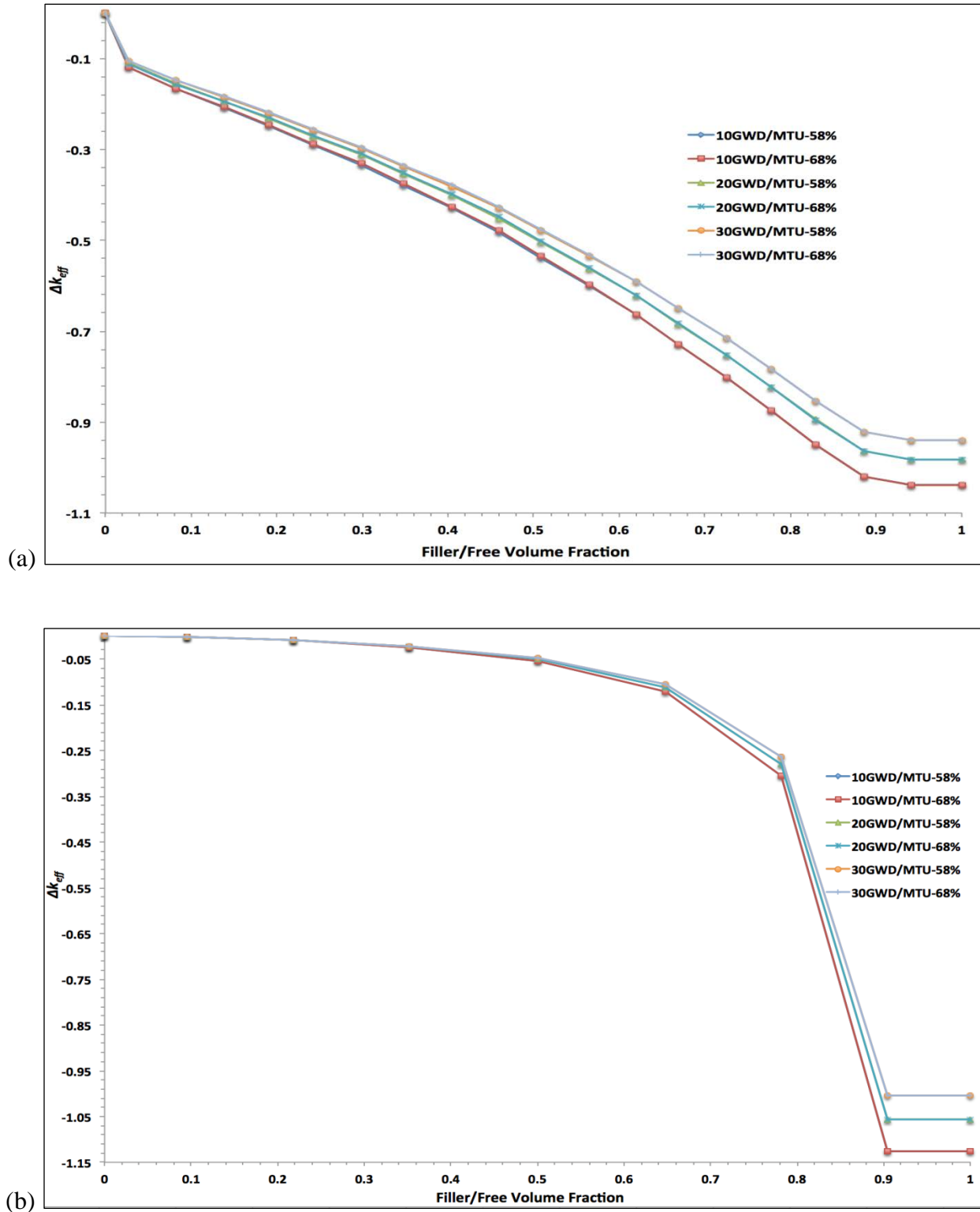


Figure 9-6. Reactivity reduction ( $\Delta k_{eff}$ ) as a function of  $B_4C$  volume fraction for: (a) complete loss of neutron absorber, and (b) basket degradation scenario

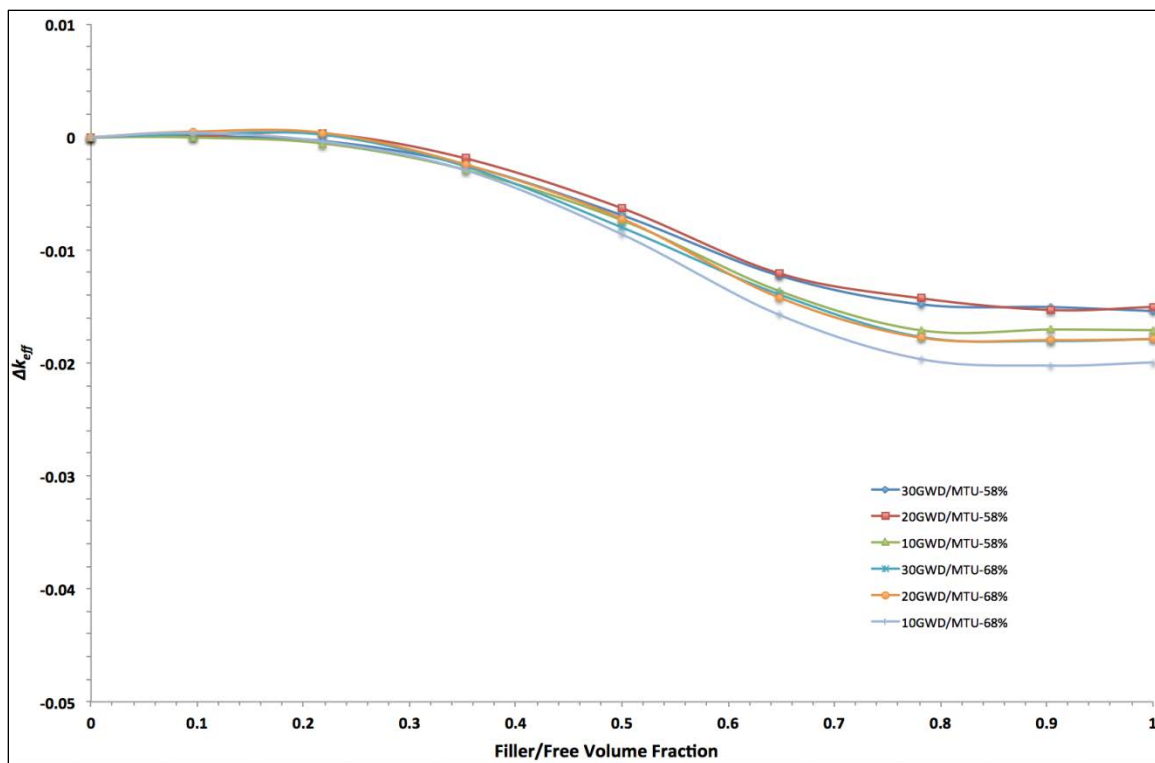
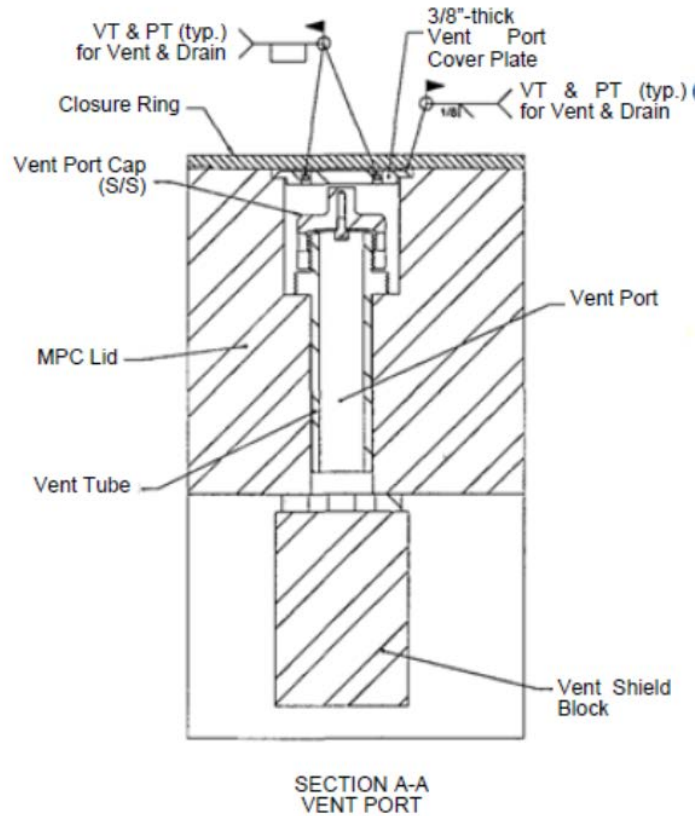


Figure 9-7. Reactivity reduction ( $\Delta k_{eff}$ ) as a function of gibbsite volume fraction for complete loss of neutron absorber

## 9.5 Filling Methods

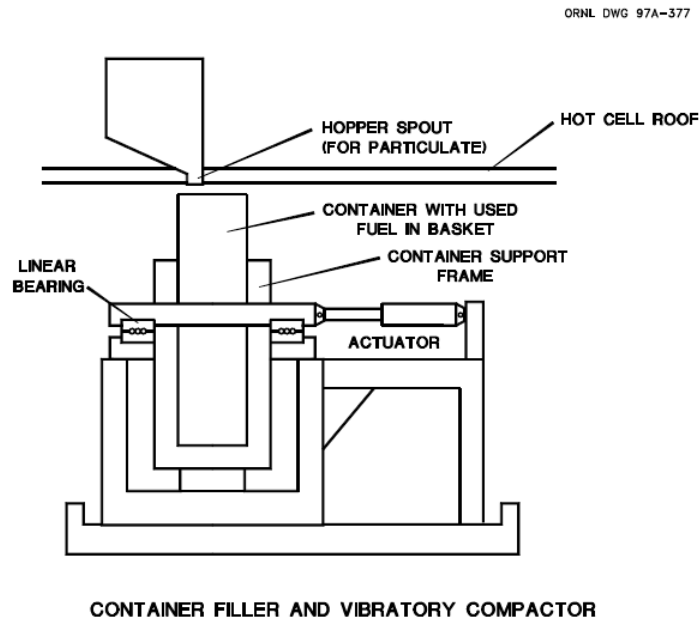
There are two different approaches to filling a DPC. The first approach would use a combination of the vent and drain ports as the means for introducing the filler material and venting the displaced gas. Such an approach would limit direct exposure to the fuel as the shielding would remain in place. However, some form of containment would still probably be required as there could be a potential for release of airborne particulates upon opening the DPC. Figure 9-8 shows details of the vent port (Chopra et al. 2013).

The second approach would involve cutting open the DPC. This operation would need to be conducted in a shielded facility such as a hot cell. Forsberg et al. (1995) proposed that glass beads could be loaded into a fuel canister while it is open or added through a small hole in the lid once the canister is closed. Figure 9-9 presents a conceptual drawing of the Canadian waste package fill station and compactor. In this concept, the waste package containing SNF is placed on a vibratory table located in a hot cell facility and the particulate fill is added while the entire waste package is vibrated. The particulate loading station hopper, metering device, and other components are located outside the hot cell. A filler hose that passes through the hot cell roof connects the hopper to the waste package (Forsberg 1997). A similar arrangement would be used for liquid fillers, except that for molten fillers the entire waste package would be pre-heated in an oven.



Source: Chopra et al. (2013).

Figure 9-8. Vent port details



Source: Forsberg (1997).

Figure 9-9. Canadian waste package filler and vibrator compactor concept

Under 10CFR72 all cask designs have some design features that would allow them to be opened to recover the fuel if necessary. Several options are available for a welded cask. These are described in a reports prepared by AREVA (2013) and CBI (2013) for the U.S. Department of Energy. The methods included:

- Plasma torch cutting
- Laser cutting
- Grinding
- Water jet cutting
- Lathing (skiving) and end mill cutting

It was assessed that all could effectively open a fuel canister, but several of the methods did not meet all of the following criteria (CBI 2013):

- Not causing damage to the SNF
- Not creating a foreign material concern
- Not damaging the transfer cask
- Cutting open the canister within a reasonable time
- Performing the operation remotely or semi-remotely
- Allowing initial access to the vent and drain ports for water filling
- Maintaining the capability to unload the canister and recover it for re-use
- Accommodating canister geometry changes (e.g., warping)

The preferred method from both assessments was lathing. This operation has been demonstrated by AREVA on the NUHOMS®-type canister (AREVA 2013). Plasma torch cutting resulted in a significant risk of molten metal being blown into the cask and onto the fuel assemblies. Laser cutting reduced the amount of slag, but controlling the depth of cut was difficult. Grinding was rejected due to the time required to cut the welds and the dust created. Water jet cutting was rejected primarily due to coating of the fuel with Garnet grit and metal, and the accumulation of water in the cask (CBI 2013). Since this operation results in the removal of the canister top, these operations would need to be carried out in a shielded hot cell (AREVA 2013).

## **9.6 Conclusions and Recommendations**

Based on this analysis, the most promising fill materials for use in DPCs to control postclosure criticality are: 1) low-melting-point metals such as Pb/Sn, Sn/Ag/Cu or Sn/Zn; and 2) small solid particles such as glass beads, including glass beads that contain DU or UO<sub>2</sub>. In the case of low-melting-point metals, provisions would be needed to pre-heat the entire DPC and its contents to temperatures of 225 to 250°C to ensure that the liquid flows to all parts of the container without solidifying.

Two potential filling methods are possible: 1) using the drain and vent ports accessed by removing the welded covers; and 2) removal of the lid from each DPC. The first approach would use both ports to optimize filler delivery and allow exit of the displaced phase. For solid particulate fillers, some provision for vibrating the entire DPC may be needed to ensure adequate

settling and complete filling. The second approach would involve cutting open the canisters using a method such as lathing (skiving). Depending on the approach chosen, a separate hot cell facility may be needed for receipt, opening, filling, closure and final testing of the filling result. In any case, containment will be required to control potential radiological releases when DPCs are opened and during filling and subsequent closure operations.

An important result from the criticality part of this study is that a filler material, irrespective of whether it is a neutron absorber, should occupy most part of the free DPC volume to provide criticality control over the duration of the repository performance period. Also, the eventual corrosion product of a filler material and its effect on reactivity should be considered in filler selection.

There has been relatively little experimental work conducted on the filling of dry storage canisters with molten and particulate materials. The results of this study suggest two follow-on activities:

- Assess the availability of candidate materials, and compatibility with the materials of DPC construction and with fuel assemblies
- Perform a demonstration of the proposed filling operation at a fractional scale

For the use of solid particles, tests similar to those conducted by Atomic Energy of Canada Limited (AECL) could demonstrate the capability to fill voids within fuel assemblies and between compartments in the DPC. Such tests should look at both glass beads and glass beads containing DU. Desired data would include packing density as a function of particle size, post-test identification of voids and particle size classification, and the need for vibration. For both liquid/molten and solid fillers, demonstrations are needed using access to both the drain and vent ports, and access only to the vent port.

If the use of fillers becomes a programmatic requirement, canister designs should be developed that would include modifications to reduce the time, cost, and complexity of filling operations.

### **References for Section 9**

AREVA (AREVA Federal Services LLC) 2013. *Task Order 14: Transfer of Used Nuclear Fuel Stored in Non-Disposable Canisters*. RPT-3009487-000. U.S. Department of Energy, Nuclear Fuel Storage and Transportation Planning Project. September, 2013.

BSC (Bechtel-SAIC Company) 2003. *The Potential of Using Commercial Dual Purpose Canisters for Direct Disposal*. TDR-CRW-SE-000030 Rev. 0. U.S. Department of Energy, Office of Civilian Radioactive Waste Management. Las Vegas, NV.

CBI (CB&I Federal Services LLC) 2013 . *Task Order 14: Transfer of Used Nuclear Fuel Stored in Non-Disposable Canisters*. U.S. Department of Energy, Nuclear Fuel Storage and Transportation Planning Project. September, 2013.

Chopra, O.K., D. Diercks, D. Ma, V.N. Chah, S.-W. Tam, R.R. Fabian, Z. Han and Y.Y. Liu 2013. *Managing Aging Effects on Dry Cask Storage Systems for Extended Long-Term Storage and Transportation of Used Fuel – Rev 1*. FCRD-UFD-2013-000294. ANL-13/15. U.S. Department of Energy, Office of Used Nuclear Fuel Disposition. September, 2013.

Cogar, J.A. 1996. *Technical Document Preparation Plan for Waste Package Filler Material Testing Report*. BBA000000-01717-2500-00007 Rev. 0. U.S. Department of Energy, Office of Civilian Radioactive Waste Management. Las Vegas, NV.

CRWMS M&O (Civilian Radioactive Waste Management System Management & Operating Contractor) 1999. *License Application Design Selection Feature Report: Additives and Fillers*. B00000000 01717 2200 00212 Rev. 01 (Draft). U.S. Department of Energy, Office of Civilian Radioactive Waste Management. Las Vegas, NV.

Forsberg, C.W., R.B. Pope, R.C. Ashline, M.D. DeHart, K.W. Childs and J.S. Tang 1995. *DUSCOBS – A Depleted-Uranium Silicate Backfill for Transport, Storage, and Disposal of Spent Nuclear Fuel*. ORNL/TM-13045. Oak Ridge National Laboratory, Oak Ridge, TN.

Forsberg, C.W., R.B. Pope, R.C. Ashline, M.D. DeHart, K.W. Childs and J.S. Tang 1996. “Depleted-Uranium-Silicate Backfill of Spent-Fuel Waste Packages for Repository Containment and Criticality Control.” In: High Level Radioactive Waste Management, Proceedings of the Seventh Annual International Conference. April 29–May 3, 1996. Las Vegas, NV. pp. 366–368.

Forsberg, C.W. 1997. *Description of the Canadian Waste Particulate-Fill Waste Package (WP) System for Spent Nuclear Fuel and Its Applicability to Light Water Reactor SNF WPs with Depleted Uranium Oxide Fill*. ORNL/TM-13502. Oak Ridge National Laboratory, Oak Ridge, TN.

Forsberg, C.W. 2000a. “Effect of Depleted-Uranium Dioxide Particulate Fill on Spent-Nuclear-Fuel Waste Packages.” *Nuclear Technology*. V.131, pp. 337-353.

Forsberg, C.W. 2000b. “Depleted Uranium Dioxide as SNF Waste Package Fill: A Disposal Option.” SPECTRUM 2000, International Conference on Nuclear and Hazardous Waste Management.

Forsberg, C.W., S.N. Storch and K.W. Childs 2001. “Depleted-Uranium Dioxide as SNF Waste Package Particulate Fill: Engineering Properties,” In: High Level Radioactive Waste Management, Proceedings of the Ninth Annual International Conference. April 29–May 3, 2001. Las Vegas, NV.

Forsberg, C.W. 2002. “Repository Applications for Depleted Uranium (DU) (Potential Use of the Entire DU Inventory).” Presented at DU Uses R&D Program Review. Oak Ridge National Laboratory, Oak Ridge, TN.

Hardin, E.L., D.J. Clayton, R.L. Howard, J.M. Scaglione, E. Pierce, K. Banerjee, M.D. Voegelé, H.R. Greenberg, J. Wen, T.A. Buscheck, J.T. Carter, T. Severynse and W.M. Nutt 2013. *Preliminary Report on Dual-Purpose Canister Disposal Alternatives (FY13)*. FCRD-UFD-2013-000171 Rev. 1. U.S. Department of Energy, Office of Used Nuclear Fuel Disposition. December, 2013.

IAEA (International Atomic Energy Agency) 2000. *Multi-Purpose Container Technologies for Spent Fuel Management*. IAEA-TECDOC-1192. Vienna, Austria. December, 2000.

Jubin, R., K. Banerjee and T. Severynse 2014. *Potential Dual-Purpose Canister (DPC) Filler Materials*. FCRD-UFD-2014-000521 Rev. 0. U.S. Department of Energy, Office of Used Nuclear Fuel Disposition. July, 2014.

Maheras, S.J., R.E. Best, S.B. Ross, E.A. Lahi and D.J. Richmond 2012. *A Preliminary Evaluation of Using Fill Materials to Stabilize Used Nuclear Fuel During Storage and Transportation*. FCRD-UFD-2012-000243. U.S. Department of Energy, Office of Used Nuclear Fuel Disposition. August, 2012.

ORNL (Oak Ridge National Laboratory) 2011. *SCALE: A Comprehensive Modeling and Simulation Suite for Nuclear Safety Analysis and Design*. ORNL/TM-2005/39 V.6.1. Radiation Safety Information Computational Center at Oak Ridge National Laboratory, Oak Ridge, TN.

Oversby, V.M. and L.O. Werme 1995. “Canister Filling Materials – Design Requirements and Evaluation of Candidate Materials.” In: *Proceedings Scientific Basis for Nuclear Waste Management XVIII*, Materials Research Society Symposium. October 23–27, 1994. V.353, pp. 743-750.

Pope, R.B., C.W. Forsberg, R.C. Ashline, M.D. DeHart, K.W. Childs and J.S. Tang 1996. “Benefits/Impacts of Utilizing Depleted Uranium Silicate Glass as Backfill for Spent Fuel Waste Packages.” In: *High Level Radioactive Waste Management, Proceedings of the Seventh Annual International Conference*. April 29–May 3, 1996. Las Vegas, NV. pp. 369–371

Puig, F., J. de Pablo and A. Martinez-Esparza 2008a. “Spent Fuel Canister for Geologic Repository: Inner Material Requirements and Candidates for Evaluation.” *Journal of Nuclear Materials*. V.376, pp. 181-191.

Puig, F., J. Dies, M. Savilla, J. de Pablo, J.J. Pueyo, L. Miralles and A. Martinez-Esparza 2008b. “Inner Material Requirements and Candidates Screening for Spent Fuel Disposal Canister.” In: *Proceedings Scientific Basis for Nuclear Waste Management XXXI*, Materials Research Society Symposium. September 16–21, 2007. V.1107, pp. 67-74.

Puig, F., J. Dies, M. Savilla, J. de Pablo, J.J. Pueyo, L. Miralles and A. Martinez-Esparza 2009. “Selection and Evaluation of Inner Material Candidates for Spanish High Level Radioactive Waste Containers,” In: *Proceedings of the 11th International Conference on Environmental Remediation and Radioactive Waste Management*. September 2–6, 2007. pp. 285-292.

SNL (Sandia National Laboratories) 2007. *Geochemistry Model Validation Report: Material Degradation and Release Model*. ANL-EBS-GS-000001 Rev. 2. Prepared for the U.S. Department of Energy, Las Vegas, NV.

Wallin, W.E. 1996. *Analysis of MPC Access Requirements for Addition of Filler Materials*. BB0000000-01717-0200-0010 Rev. 0. U.S. Department of Energy, Office of Civilian Radioactive Waste Management. Las Vegas, NV.

THIS PAGE INTENTIONALLY LEFT BLANK

## **10. R&D Needs for Technical Feasibility Evaluation**

The DPC disposal technical feasibility evaluation includes a task to identify and track the status of information needs, to guide work planning and provide an indication of when enough R&D has been done. The first list of R&D needs was in the original work plan (Howard et al. 2012). The list was then updated (Hardin et al. 2013a), and updated again (Howard et al. 2014). This section combines the lists from 2013 and 2014, with a brief description of each item and its status. A summary of R&D topics and their status is given in Table 10-1.

### **10.1 DPC Characteristics and Loading**

#### **10.1.1 Condition of SNF and Canisters Allows Storage, Transport and Disposal for Up to 100 years After Discharge**

The feasibility evaluation assumes up to 100 years of dry storage during which there may be degradation of DPCs and cladding material property changes (e.g., cladding embrittlement). Improved understanding of the likelihood and consequences of degradation is needed to plan steps leading to DPC direct disposal (including whether longer storage is feasible). Work in this area is being performed as part of the Storage and Transportation R&D portion of the Used Fuel Disposition Campaign. No specific activities, other than monitoring progress, are planned as part of the DPC disposal technical feasibility evaluation.

**Status:** In progress.

#### **10.1.2 Update Database on Existing DPCs**

Continue to compile and organize information on DPC construction, fuel loading, burnup characteristics of individual assemblies, control rod or poison rod loads, and licensing basis (e.g., limiting fuel type for 10 CFR 71.55 criticality analysis). This effort is ongoing as part of the Used Nuclear Fuel Storage, Transportation & Disposal Analysis Resource and Data System (UNF-ST&DARDS) (Petersen et al. 2013) development in the NFST planning project. UNF-ST&DARDS is a controlled source of technical data for various criticality and thermal analysis tools. The database is expected to be used for mapping which DPCs can be considered disposable, as a function of internal variables such as fuel type and construction, and external variables such as the disposal concept.

**Status:** In progress.

#### **10.1.3 Survey of Available Technologies for Application to DPC Disposal**

Available technologies in several areas were assessed Hardin et al. (2013a) unless otherwise specified. These technologies include:

- **Hoisting and Conveyance** – Assessment of international work on hoisting systems and transporters, with focus on transporting heavy waste packages (e.g., >100 MT with disposal overpack). Previous work established in principle, the technical feasibility of shafts, funiculars, ramps, and the associated equipment.
- **Underground Access (Shaft vs. Ramp)** – Assessment of construction and operational options for waste handling, and the potential for service life of at least 50 years.

Table 10-1. R&amp;D activities for technical feasibility evaluation, and status

| <b>10.1 DPC Characteristics and Loading</b>                                      |                                      |
|--|--------------------------------------|
| Condition of SNF and Canisters Allows Storage, Transport and Disposal for 100 yr | Status: In progress.                 |
| Update Database on Existing DPCs   | Status: In progress.                 |
| Survey of Available Technologies for Application to DPC Disposal                 | Status: Partly completed.            |
| <b>10.2 DPC Disposal Concept Development</b>                                     |                                      |
| Initial Concept Development  | Status: Planned completion in FY15.  |
| Backfill Performance   | Status: In progress.                 |
| Heating of Near-Field Host Rock to Higher Temperatures                           | Status: In progress.                 |
| Impacts from Cementitious Materials in the Repository on Performance             | Status: In progress.                 |
| High-Reliability Disposal Overpack Evaluation                                    | Status: Planned for FY15.*           |
| <b>10.3 Thermal Analysis</b>   |                                      |
| Thermal Analysis of Disposal Concepts  | Status: Planned completion in FY15.* |
| In-Package Temperature   | Status: Possible future activity.    |
| Loss of Helium Charge  | Status: Possible future activity.    |
| <b>10.4 Waste Package/DPC Chemical and Physical Environment After Breach</b>     |                                      |
| In-Package Degradation Model   | Status: Possible future activity.    |
| Specify Disposal Environments  | Status: Completed.                   |
| <b>10.5 DPC and Disposal Overpack Corrosion</b>                                  |                                      |
| Possible Overpack Materials and Compatibility with DPC Materials                 | Status: In progress.                 |
| Corrosion Test Planning  | Status: In progress.                 |
| Long-Term Corrosion Performance Testing  | Status: In progress.                 |
| Engineered Barrier Corrosion Rate Model Development for PA                       | Status: Possible future activity.    |
| <b>10.6 Postclosure Criticality Analysis</b>                                     |                                      |
| Mapping of DPC Inventory to Disposal Concepts Based on Potential for Criticality | Status: Planned completion in FY15.* |
| Criticality Probability and Consequence Screening Analysis Approach              | Status: Completed.                   |
| Nuclear Reactivity Sensitivity Analysis  | Status: Partly completed.            |
| Neutronics Model Validation  | Status: Possible future activity.    |
| Criticality Consequence Modeling and Implementation in PA                        | Status: Possible future activity.    |
| <b>10.7 Analysis of Key Features, Events and Processes</b>                       |                                      |
| Brine Migration in Salt  | Status: In progress.                 |
| Potential for Gas Generation and Importance for DPC-Based Repositories           | Status: Possible future activity.    |
| Waste Package Vertical Movement in Salt  | Status: In progress.                 |
| Other FEPs Influenced by Package Size, Heat Output, and Quantity of Waste        | Status: In progress.                 |
| <b>10.8 Performance Assessment for DPC Direct Disposal</b>                       |                                      |
| Performance Allocations  | Status: Completed.                   |
| Applicable Performance Assessment Scenarios                                      | Status: Completed.                   |
| FEP Crosswalks for Alternative DPC Disposal Concepts                             | Status: Completed.                   |
| Performance Assessment   | Status: In progress.                 |
| <b>10.9 System Logistics</b>   |                                      |
| Initial Logistics Simulation of DPC Selection and Decay Storage                  | Status: Completed.                   |
| Detailed Logistical Analyses   | Status: Completed.                   |
| DPC Disposal Cost Estimates  | Status: Planned for FY15.*           |
| <b>10.10 Canister Fillers</b>  |                                      |
| Initial Feasibility Study  | Status: Completed.                   |
| <b>10.11 Preclosure Operations and Safety</b>                                    |                                      |
| Loading Horizontal and Vertical DPCs into Disposal Overpacks                     | Status: Possible future activity.    |
| Preclosure Safety Assessment for Direct Disposal of DPCs                         | Status: Possible future activity.    |
| Stability of Underground Excavations   | Status: Completed.                   |
| <b>10.12 Decision Support</b>  |                                      |
| DPC Direct Disposal Decision Platform  | Status: Possible future activity.    |
| <b>10.13 Closeout</b>  |                                      |
| Develop Technology Readiness Information for Disposal Concepts                   | Status: Possible future activity.    |
| Information Needs for Site Evaluation and Selection                              | Status: Possible future activity.    |
| Comparative Evaluation of DPC Disposal in Specific Geologic Settings             | Status: Possible future activity.    |

\* Subject to availability of funding.

- **DPC Packaging** – Alternative concepts for DPC disposal overpacks, and the functions that could be assigned to them, for small and large packages, and a broad range of disposal environments (Hardin 2013a).
- **Excavation and Ground Support** – Large DPCs will require large openings, so excavation and construction may be important costs, and maintenance could be important for repository operation (see Section 3).
- **Heat Removal** – Mechanisms for heat removal during repository operations include conduction in the host rock, natural convection, and forced ventilation. Larger waste packages (greater than 4-PWR size) will need repository ventilation to allow emplacement and panel closure within the assumed time frame (150 years; Hardin and Howard 2013).
- **Closure** – For open modes, permanent closure will involve plugging, sealing, and backfilling of repository openings (unless the host medium is unsaturated). Many such operations would be conducted remotely in radiological environments (Hardin et al. 2013a).
- **Other Technologies** – Repository engineering has developed worldwide over the past several decades. Newer, advanced techniques for mining and drilling are becoming available (Section 2).

**Status:** Partly completed.

## 10.2 DPC Disposal Concept Development

### 10.2.1 Initial Concept Development

Information from U.S. and international sources was assembled to develop a comprehensive set of alternatives for direct disposal of DPCs. Each alternative disposal concept consists of a waste stream, geologic setting, and high-level concept of operations. Descriptions were provided in the form of narrative, tables, and/or schematic figures (Hardin and Voegelé 2013; Hardin et al. 2013a). A planned activity will evaluate vault-type underground systems for retrievable dry storage and eventual disposal.

**Status:** Partly completed, with completion planned in FY15.

### 10.2.2 Backfill Performance

Thermally driven processes could be active at temperatures greater than 100°C, in media such as clay-based backfill which have internationally accepted temperature limits at or below 100°C (Hardin et al. 2013a,b). R&D on the evolution of these materials will likely involve multiple technical disciplines, and laboratory investigations, simulation, and field-scale validation. Backfill temperature tolerance of 150°C could facilitate thermal management, and some disposal concepts could reach peak temperatures of 200°C. This objective will be addressed in the future by other areas of the UFD R&D program, as appropriate, and no specific activities are planned in this work package beyond monitoring progress.

**Status:** In progress.

### **10.2.3 Heating of Near-Field Host Rock to Higher Temperatures**

DPC disposal in clay/shale media could be facilitated if the peak temperature target for the near-field host rock were increased to greater than 100°C (Hardin, et. al. 2013a). The extent would be limited to the immediate vicinity of each waste package, with cooler conditions throughout the host rock and between packages. Preliminary work on this R&D need is presented in Section 6. Further work on this topic will be addressed in the future by other areas of the UFD R&D program, as appropriate, and no specific activities are planned in this work package beyond monitoring progress.

**Status:** In progress.

### **10.2.4 Impacts from Cementitious Materials in the Repository on Performance**

A repository for all projected U.S. spent fuel could involve 300 km or more of tunnels, especially in clay/shale media. Somewhat less tunneling would be needed for crystalline media because of higher thermal conductivity. With tunneling on this scale, economical materials such as concrete or shotcrete are desirable for construction and ground support. Possible impacts on long-term waste isolation performance need to be understood for development of these disposal concepts to proceed. Further work on this topic will be addressed in the future by other areas of the UFD R&D program, as appropriate, and no specific activities are planned in this work package beyond monitoring progress.

**Status:** In progress.

### **10.2.5 High-Reliability Disposal Overpack Evaluation**

The probability of early failure for engineered items such as the disposal overpack, that is assumed in performance assessment and in screening of features, events and processes (FEPs), has historically been on the order of  $10^{-5}$  per item (SNL 2007). This leads to the possibility that events such as waste package criticality could be initiated by waste package flooding associated with early failure. Verification and sensitivity analysis of the historical analysis is planned, to evaluate the prospects for improving overpack early failure performance by means of additional inspection and/or redundancy.

**Status:** Planned for FY15.

## **10.3 Thermal Analysis**

### **10.3.1 Thermal Analysis of Disposal Concepts**

Heat transfer by conduction, thermal radiation, and ventilation has been analyzed for alternative DPC disposal concepts. Generic (non-site specific) estimates were developed for minimum fuel age at emplacement, and/or maximum thermal power at repository closure, for different types of fuel and waste package sizes (Hardin and Voegelé 2013; Hardin et al. 2013a,b).

Larger dry storage canisters (up to 37 PWR or 89 BWR assemblies) are currently being loaded at some installations. Other plants may adopt these larger systems in the future, and SNF burnup is projected to increase (to approximately 60 GW-d/MTU; see Section 3). Analysis of these larger, potentially hotter configurations is planned.

**Status:** Partly completed, with completion planned in FY15.

### **10.3.2 In-Package Temperature**

In-package temperatures will likely be less than temperature limits for fuel and other components (e.g., 350°C to limit cladding creep) because of the temperature margin possible if the package surface is limited to 200°C or cooler. A significant temperature differential between fuel cladding and the waste package surface, or between the upper and lower surfaces of the package, would need to be accounted for in evaluation of thermal management.

**Status:** Possible future activity.

### **10.3.3 Loss of Helium Charge**

Loss of helium from the canister (e.g., leakage through stress corrosion cracks) would degrade internal heat transfer. Heat output may have decayed significantly if and when such leaks form. Also, while leaks will vent the pressure down to atmospheric, exchange with air could take much longer. Analysis is needed to determine the need for a helium charge during repository operations and after disposal.

**Status:** Possible future activity.

## **10.4 Waste Package/DPC Chemical and Physical Environment After Breach**

### **10.4.1 In-Package Degradation Model**

Develop conceptual and numerical models of the evolution of the disposal overpack and the DPC contained within, after initial breach. An in-package model for physical and chemical degradation is needed to support performance assessments and DPC criticality evaluations. Outputs could include pH, ionic strength, redox conditions, and other information to support degradation rates and DPC internal configuration. This R&D need parallels similar needs in Disposal Research, and will be considered as a joint effort in planning for future fiscal years.

**Status:** Possible future activity.

### **10.4.2 Specify Disposal Environments**

Evaluate geologic settings for characteristics important to chemical degradation of materials comprising existing DPCs and possible disposal overpacks. Establish a generic range of chemical conditions based on published data for potential host formations (Section 8). This work is intended to be used as a guide for selecting laboratory chemical conditions for corrosion testing. The occurrence of chloride salinity in sedimentary and crystalline media other than evaporite beds, which is of interest for criticality analysis, is evaluated in Section 7.

**Status:** Completed.

## **10.5 DPC and Disposal Overpack Corrosion**

### **10.5.1 Possible Overpack Materials and Compatibility with DPC Materials**

Identify possible overpack materials for use in chemical environments, and estimate corrosion rates from literature data (Section 8). Future work will evaluate the physical and chemical compatibility of these materials with DPC materials, and the potential impacts from degraded waste package materials (i.e., corrosion products) on the disposal environment. Further work on this topic will be addressed in the future by other areas of the UFD R&D program, as appropriate, and no specific activities are planned in this work package beyond monitoring progress.

**Status:** In progress.

### **10.5.2 Corrosion Test Planning**

Using the corrosion environments discussed above, and the literature review of corrosion data for DPC materials and prospective overpack materials, develop an experimental plan for corrosion testing. A preliminary scoping-type test plan will be completed in September, 2014. Further work on this objective will be addressed in the future by other areas of the UFD R&D program, as appropriate, and no specific activities are planned in this work package beyond monitoring progress.

**Status:** In progress.

### **10.5.3 Long-Term Corrosion Performance Testing**

Pursuant to the reviews and the preliminary test plan, institute a program of corrosion testing to acquire rate data specifically for modeling DPC direct disposal in performance assessment. The testing program will generate information that could also be used in evaluation of standardized, multi-purpose canisters (storage-transportation-disposal), or in disposal overpacks for such canisters. Further work on this objective will be addressed in the future by the UFD R&D program, as appropriate, and no specific activities are planned in this work package beyond monitoring progress.

**Status:** In progress.

### **10.5.4 Engineered Barrier Corrosion Rate Model Development for PA**

Once an experimental plan for corrosion testing is developed, a PA component model will be developed for use in system assessments, to establish the importance of corrosion in different disposal concepts. The model will serve as a guide for selecting test environments, determining test durations, post-test examination, etc.

**Status:** Possible future activity.

## **10.6 Postclosure Criticality Analysis**

These R&D needs relate specifically to analysis of the potential for criticality to occur in degraded DPCs after disposal, breach and flooding by ground water. Criticality consequence analysis is included for possible future use in a “layered” argument for use if the probability of a criticality event exceeds the regulatory exclusion threshold. Also included are measures to re-work existing DPCs to mitigate the potential for criticality (e.g., by filling with inert material to displace ground water).

### **10.6.1 Mapping of DPC Inventory to Disposal Concepts Based on Potential for Postclosure Criticality**

This activity seeks to exploit uncredited reactivity margin by maximizing the use of canister-specific data on construction, fuel loading, and as-loaded assembly burnup. The activity to collect such data is described above (Section 10.1.2). Additional analysis is planned in FY15, supporting a map of which existing DPCs could be subcritical when flooded and degraded by fresh water, that is reasonably current with new data from the GC-859 survey of nuclear utilities.

**Status:** Partly completed, with completion planned in FY15.

### **10.6.2 Criticality Probability and Consequence Screening Analysis Approach**

Develop an analysis framework for postclosure criticality risk from DPC direct disposal (Scaglione et al. 2014). Emphasize low-consequence screening to accommodate portions of the existing, heterogeneous DPC inventory.

**Status:** Completed.

### **10.6.3 Nuclear Reactivity Sensitivity Analysis**

Identify and prioritize parameters in the reactivity analysis that have the greatest impact on criticality, to identify opportunities for reducing conservatism. Develop bounding approaches where possible to cover the range of possible disposal environments. An FY14 report describes bounding analysis of DPC criticality in chloride brines, and also evaluates neutron absorption by other elements found in ground water. Additional analyses of this type are planned in FY15, that will focus on flooding with fresh water.

**Status:** Partly completed.

### **10.6.4 Neutronics Model Validation**

Evaluate use of enhanced burnup credit validation techniques to reduce computational model bias and uncertainty. Validation of burnup credit analysis methodology is particularly important for BWR fuel. Note that ISG-8 Rev 3 is specific to PWR fuel and similar guidance permitting burnup credit for BWR fuel in storage and transport has not been developed. The regulatory standard review plans for dry cask storage and transport of UNF do not allow credit for BWR fuel burnup or credit for fixed burnable absorbers. In addition, some attributes relied upon to reduce reactivity (e.g., chloride in ground water, moderator displacement effects of corrosion products) will require appropriately designed experiments to establish computational biases and uncertainties, and for validation of degraded configurations.

**Status:** Possible future activity.

### **10.6.5 Criticality Consequence Modeling and Implementation in Performance Assessment**

This activity has two parts, supporting the consequence analysis described by Scaglione et al. (2014): 1) model the consequences of intermittent criticality on thermally driven processes in the repository, and associated changes in radionuclide inventory; and 2) determine modified settings for PA model parameters to represent criticality impact on dose.

**Status:** Possible future activity.

## **10.7 Analysis of Key Features, Events and Processes**

This set of activities will provide supporting analysis for key FEPs. The assessments will consider generic disposal media and will involve collaboration with the team performing PA model development. The items listed below are known to be potentially important based on U.S. and international experience, and there is also the possibility that other potentially discriminating FEPs may be identified.

### **10.7.1 Brine Migration in Salt**

The potential for brine migration toward heat sources in salt under gradients of stress and temperature has been identified (Hansen and Leigh 2011). Brine could corrode the disposal

overpack, producing corrosion products and hydrogen gas. After cooling and reconsolidation, driving forces for brine migration toward waste packages are greatly reduced. This presents the possibility of a bounding analysis for total brine inflow under nominal (undisturbed) conditions, which could then be accommodated in the disposal overpack design. Brine migration is being considered in the planning of laboratory and field investigations in salt. No specific activities are planned in this work package beyond monitoring progress.

**Status:** In progress.

### **10.7.2 Potential for Gas Generation and Importance for DPC-Based Repositories**

Hydrogen from corrosion of the overpack, canister, or spent fuel, in reducing chemical environments, is potentially the most important source of gas generation. For some disposal concepts gas pressure could affect radionuclide transport by creating pathways or producing a pressure gradient. Assessment of gas generation effects could impact the selection of overpack materials and other system details. Effects from gas generation are not currently being directly investigated in the UFD program, but international efforts in this area have been underway for several years. No specific activities are planned in this work package beyond monitoring progress.

**Status:** Possible future activity.

### **10.7.3 Waste Package Vertical Movement in Salt**

Recent analysis has shown that vertical movement (sinking) of heavy waste packages in salt may not be significant (Clayton et al. 2013). However, the Munson-Dawson constitutive model used for that analysis, and most other constitutive models currently used in salt creep analysis, are not conditioned on low-stress, low strain-rate laboratory test data that would be appropriate for evaluating slow vertical movement of waste packages (e.g., 1 meter per 10,000 yr; see Section 7). This effort will implement an appropriate test program to corroborate the European results and provide new data for salt from the U.S.; 2) to investigate the effects of moisture; and 3) to probe the mechanism by testing under confining stress.

**Status:** In progress.

### **10.7.4 Other FEPs Influenced by Package Size, Heat Output, and Quantity of Waste**

Other FEPs that could discriminate the performance of larger, hotter DPC-based waste packaging, compared to alternative purpose-designed packaging of the same waste in the same geologic setting, were identified by Hardin et al. (2013c). In particular, they identified FEPs controlling whether radionuclide transport is advection or diffusion dominated, and thermally driven irreversible changes to near-field and EBS materials. A related analysis showed that human intrusion could dominate total system releases in sedimentary formations where undisturbed performance (without human intrusion) could provide virtually complete isolation. Performance assessment will be one of the primary tools used to quantify DPC direct disposal, and it is ongoing in the UFD R&D program. No specific activities are planned here other than monitoring progress.

**Status:** In progress.

## **10.8 Performance Assessment for DPC Direct Disposal**

### **10.8.1 Performance Allocations**

The term performance allocation refers to the parts of the safety case for each disposal concept where the influence of key system elements on waste isolation performance is determined. For example, the type of overpack, or whether to use one, may be an important performance allocation decision. Other performance allocations may identify different safety strategies for various waste types, or various radionuclide constituents. The underlying idea of performance allocation is that sufficient waste isolation performance can be achieved without using every available technology or design feature, thus controlling the cost and complexity of disposal alternatives. A preliminary performance allocation (safety strategies) for DPC direct disposal was developed by Hardin et al. (2013c).

**Status:** Completed.

### **10.8.2 Applicable Performance Assessment Scenarios**

Quantitative demonstration that alternative DPC disposal concepts will achieve regulatory performance objectives, will be based on PA. A prerequisite for performance assessment is to establish which scenarios (e.g., nominal, disturbed, and human intrusion) should be included in the total system analysis. For each scenario, different sets of features, events, and processes would be included in the PA. The initial definition of scenarios for alternative DPC disposal concepts is documented in Hardin et al. (2013c).

**Status:** Completed.

### **10.8.3 FEP Crosswalks for Alternative DPC Disposal Concepts**

The FEP crosswalk shows which FEPs are potentially important to performance for different concepts, which are likely to be included or excluded from performance assessment, and how the FEPs will be analyzed. It shows how generic FEPs (Freeze et al. 2011) could be dispositioned to evaluate postclosure performance for alternative disposal concepts and scenarios (Hardin et al. 2013c).

**Status:** Completed.

### **10.8.4 Performance Assessment**

Performance assessment will be used to evaluate the postclosure safety of DPC direct disposal, by comparing performance to alternatives involving disposal of the same SNF in purpose-designed canisters, in the same host media. Component models will be developed with fidelity sufficient for meaningful safety comparisons. These are expected to include models for: 1) overpack, canister, basket and spent fuel degradation; 2) the effects of heat; 3) radionuclide mobility; and 4) groundwater and radionuclide transport through degraded waste packages. Performance assessment will eventually be a primary tool for evaluating DPC direct disposal, and it is ongoing in the UFD R&D program. No specific activities are planned here other than monitoring progress.

**Status:** In progress.

## **10.9 System Logistics**

### **10.9.1 Initial Logistics Simulation of DPC Selection and Decay Storage**

In FY12 the Transportation-Logistic-Simulation (TSL-CALVIN) tool was developed and validated (Nutt et al. 2012). This tool generates projections of the types and quantities of DPCs that will be loaded, DPC thermal decay, DPC transport to a repository, and emplacement underground. The initial study simulated the schedule of repository operations, constrained mainly by the duration of DPC decay storage needed until emplacement thermal power limits are met (Hardin et al. 2013a).

**Status:** Completed.

### **10.9.2 Detailed Logistical Analyses**

Detailed analysis using TSL-CALVIN was used to evaluate impacts on the timing of future DPC disposal, from 1) introduction of standardized, multi-purpose (storage-transport-disposal) canisters; 2) timing of repository opening (i.e., 2048 or sooner or later); and 3) measures such as selection criteria which could decrease fuel age (out-of-reactor) at emplacement. The results are summarized in Section 3.

**Status:** Completed.

### **10.9.3 DPC Disposal Cost Estimates**

Improved cost data for DPC direct disposal are needed to represent DPC disposal alternatives, in system architecture and standardized canister studies. The available disposal cost estimates are presently limited to reference disposal concepts which did not include DPC direct disposal (Hardin et al. 2012).

**Status:** Planned for FY15.

## **10.10 Canister Fillers**

### **10.10.1 Initial Feasibility Study**

Fillers have been studied previously as a remedy for transportation damage to canistered fuel, and could also be an option for postclosure criticality control in existing DPCs. They would be applied by removing the covers welded over the dewatering ports, and injecting or pumping a substance that has desired properties. The initial feasibility study with recommendations for filler materials and filling methods, is presented in Section 9. The study also includes recommendations for follow-on R&D activities.

**Status:** Completed.

## **10.11 Preclosure Operations and Safety**

These R&D needs are driven by the additional size and weight of DPC-based waste packages. Some topics which were previously put in this category (Hardin et al. 2013a, Section 10) such as package handling and shielding, are within the state of the practice of spent fuel management so they require no R&D and are not called out here.

### **10.11.1 Loading Horizontal and Vertical DPCs into Disposal Overpacks**

Assess the availability of engineering solutions for loading horizontal DPCs into disposal overpacks, then sealing the overpacks. These operations are typically done with the vessels in

upright (vertical) orientation. Also, confirm that existing vertical DPCs can be loaded into overpacks for horizontal transport and disposal. These engineering details were identified as important in an earlier study (BSC 2003).

**Status:** Possible future activity.

### **10.11.2 Preclosure Safety Assessment for Direct Disposal of DPCs**

Waste packages and the operations required for handling and emplacement will be required to meet preclosure safety requirements (e.g., 10CFR63.111). Event sequences could be influenced by the size and weight of the waste package, particularly when installed in a shield, and the number of repeated operations. Events that could affect the safety of DPC handling and transport include impacts, rockfall, drops, collision, tip-over, transporter runaway, loss of power during handling or transport, and fire. Conduct a scoping study of preclosure safety for DPC direct disposal concepts, following current U.S. regulations (mainly 10CFR63). Compare results to safety analysis for international programs that incorporate similar facilities (shaft hoists, transporters, etc.).

**Status:** Possible future activity.

### **10.11.3 Stability of Underground Excavations**

Direct disposal of DPCs could require 300 km of emplacement drifts which would be designed to remain open with little or no maintenance for at least 50 years (Hardin et al. 2013a, Section 4). Analyze excavation and construction methods, and long-term opening stability of underground openings, in shale and other argillaceous rock types. Review selected rail and highway tunnels, and other excavations and their ground support systems. A study on excavation/construction methods in clay/shale media is summarized in Section 2.

**Status:** Completed.

## **10.12 Decision Support**

### **10.12.1 DPC Direct Disposal Decision Platform**

Identify possible future decisions that the results from this feasibility evaluation are intended to inform, such as down-selection among disposal concepts and media, standardized canister design, changes to DPC designs (e.g., for disposability), system-level decisions on whether to store SNF as bare fuel or in dry storage casks, etc. Explore possible time lines for implementation of DPC direct disposal within the broader context of an evolving fuel management system. Identify R&D needs that are likely to be important to implementation decisions, and which could require significant resources (budget, schedule).

**Status:** Possible future activity.

## **10.13 Closeout**

### **10.13.1 Develop Technology Readiness Information for Disposal Concepts**

Analyze and decompose the alternative DPC direct disposal concepts into constituent technologies and components for which the current state of knowledge, and the maturity of available technologies, can be assessed. Perform that assessment using accepted technology readiness level estimation methods.

**Status:** Possible future activity.

### 10.13.2 Information Needs for Site Evaluation and Selection

Identify important information that would be needed to implement each of the alternative DPC disposal concepts, in the site screening and selection phases of repository development (following the steps in the UFD R&D Roadmap; Nutt 2011). Identify variations in the type or quantity of site-specific information needed, across the disposal alternatives considered.

**Status:** Possible future activity.

### 10.13.3 Comparative Evaluation of DPC Disposal in Specific Geologic Settings

Perform a comparative, generic evaluation of technical feasibility and implementation risk, for alternative DPC direct disposal concepts. Explicitly address the original objectives of safety (preclosure and postclosure), engineering feasibility, thermal management, and criticality control (Hardin et al. 2013a). Consider key FEPs and critical issues that may need further analysis (additional work, much of it site-specific, would likely be required for any disposal alternative).

**Status:** Possible future activity.

### References for Section 10

BSC (Bechtel-SAIC Company) 2003. *The Potential of using Commercial Dual Purpose Canisters for Direct Disposal*. TDR-CRW-SE-000030, Rev 0. Bechtel SAIC Company, Las Vegas, NV.

Clayton, D.R., M.J. Martinez and E.L. Hardin 2013. *Potential Vertical Movement of Large Heat-Generating Waste Packages in Salt*. Sandia National Laboratories, Albuquerque, NM. SAND2013-3596.

Hansen, F.D. and C.D. Leigh 2011. *Salt Disposal of Heat-Generating Nuclear Waste*. SAND2011-0161. Sandia National Laboratories, Albuquerque, NM.

Hardin, E., T. Hadgu, D. Clayton, R. Howard, H. Greenberg, J. Blink, M. Sharma, M. Sutton, J. Carter, M. Dupont and P. Rodwell 2012. *Repository Reference Disposal Concepts and Thermal Management Analysis*. FCRD-USED-2012-000219 Rev. 2. U.S. Department of Energy, Office of Used Nuclear Fuel Disposition. November, 2012.

Hardin, E. 2013. *Spent Fuel Canister Disposability Baseline Report*. FCRD-UFD-2013-000330 Rev. 0. U.S. Department of Energy, Office of Used Nuclear Fuel Disposition. December, 2013.

Hardin, E. and R. Howard 2013. *Assumptions for Evaluating Feasibility of Direct Geologic Disposal of Existing Dual Purpose Canisters*. FCRD-UFD-2012-000352 Rev. 1. U.S. Department of Energy, Office of Used Nuclear Fuel Disposition. November, 2013.

Hardin, E., D. Clayton., R. Howard, J. Scaglione, E. Pierce, K. Banerjee, M. Voegelé, J. Wen, T. Buscheck, J. Carter, and T. Severynse 2013a. *Preliminary Report on Dual-Purpose Canister Disposal Alternatives (FY13) Revision 1*. FCRD-USED-2013-000171 Rev. 1. U.S. Department of Energy, Office of Used Fuel Disposition. November 2013.

Hardin, E., D. Clayton, M. Martinez, G. Nieder-Westermann, R. Howard, H. Greenberg, J. Blink and T. Buscheck 2013b. *Collaborative Report on Disposal Concepts*. FCRD-UFD-2013-000170 Rev. 0. U.S. Department of Energy, Office of Used Nuclear Fuel Disposition. September, 2013.

Hardin, E., C. Bryan and M. Voegelé 2013c. *Features, Events and Processes and Performance Assessment Scenarios for Alternative Dual-Purpose Canister Disposal Concepts*. FCRD-UFD-2013-000172 Rev. 0. U.S. Department of Energy, Used Fuel Disposition Campaign. July, 2013.

Howard R., J. Scaglione, J. Wagner, E. Hardin and W. Nutt 2012. *Implementation Plan for the Development and Licensing of Standardized Transportation, Aging, and Disposal Canisters and the Feasibility of Direct Disposal of Dual Purpose Canisters*. FCRD-UFD-2012-000106 Rev. 0. U.S. Department of Energy, Office of Used Nuclear Fuel Disposition.

Howard, R., J. Scaglione, E. Pierce and B. van den Akker and E. Hardin 2014. *Feasibility Evaluation for Direct Disposal of Dual Purpose Canisters: Study Plan*. FCRD-UFD-2014-000518. U.S. Department of Energy, Office of Used Fuel Disposition. April, 2014.

Nutt, W.M. 2011. *Used Fuel Disposition Campaign Disposal Research and Development Roadmap*. U.S. Department of Energy, Used Fuel Nuclear Disposition Campaign. FCRD-UFD-2011-000065 Rev. 0. March, 2011.

Nutt, M., E. Morris, F. Puig, Kalinina and S. Gillespie 2012. *Transportation Storage Logistics Model – CALVIN (TSL-CALVIN)*. FCRD-NFST-2012-000424. U.S. Department of Energy, Nuclear Fuel Storage and Transportation Planning Project. October, 2012.

Scaglione, J.M., A.A. Alsead, C.R. Bryan, E.L. Hardin and R.L. Howard 2014. *Criticality Analysis Process for Direct Disposal of Dual Purpose Canisters*. Oak Ridge National Laboratory, Oak Ridge, TN. ORNL/LTR-2014/80. March, 2014.

SNL (Sandia National Laboratories) 2007. *Analysis of Mechanisms for Early Waste Package/Drip Shield Failure*. ANL-EBS-MD-000076 Rev. 0. Prepared for the U.S. Department of Energy, Las Vegas, NV.

THIS PAGE INTENTIONALLY LEFT BLANK

## 11. Summary of FY14 Investigations

The goals of DPC direct disposal are unchanged from those set forth at the start of the technical feasibility evaluation: safety of workers and the public, thermal management, postclosure criticality control, and engineering feasibility. R&D activities in FY14 addressed all of these goals as discussed in Sections 2 through 9 of this report. The assumptions used in the study are mostly unchanged from those developed in 2012, with clarification of regulatory and statutory details, and recognition of the DOE strategy for used fuel management (DOE 2013).

Results reported here continue to support the FY13 conclusion, that direct disposal of DPCs is technically feasible, at least for some DPCs, and for some disposal concepts (geologic host media). Much of the work performed has reached a point where site-specific information would be needed for further resolution (e.g., host rock thermal conductivity and temperature tolerance, opening stability, ground water composition, disposal environment). Several activities in FY14 have focused on clay/shale media because of potential complications resulting from low thermal conductivity, limited temperature tolerance, and the need to construct ~300 km of emplacement drifts that remain stable for at least 50 years.

The following paragraphs summarize the results from this year's R&D activities:

### **Excavation and Construction in Clay/Shale Media**

Technologies for rapid excavation and integrated liner installation have significantly advanced in the past 20 years. Tunnel boring machines are the clear choice for large-scale excavation. The first TBM excavations are now approaching 50 year life, including those constructed in clay or shale media. Open-type TBMs are a good choice because pressurized-face TBMs are not designed to handle hydrostatic pressures at repository depth (300 m or greater). Use of open-type TBMs requires that the host formation have sufficient strength for the excavation face to be self-supporting to allow drilling ahead and grouting in squeezing ground or water inflow conditions, and to facilitate TBM maintenance. One way to ensure sufficient strength is to reduce the repository depth in soft formations (e.g., 300 m depth in the Pierre Shale instead of 800 m as envisioned for the Opalinus Clay).

The fastest construction appears to be possible using TBMs with a single-pass liner made of pre-fabricated concrete segments. Backfilling or grouting of the liner is typically used to assure mechanical coupling with the rock, and to seal out ground water. Major projects have been constructed with pre-fabricated segmented liner systems, and also with cast-in-place concrete liners. Cost comparisons show that differences in project management and financing may be larger cost factors than the choice of liner systems.

Reliance on concrete liners for repository emplacement drifts could require careful attention to plugging and sealing, because the liner or the space behind it could have greater permeability to ground water than the intact rock, or than the engineered backfill installed at closure. The liner may need to be replaced by a plug at regular intervals along the drifts, to impede axial flow after the repository is closed. Installation of such plugs or seals could be done during construction, prior to waste emplacement.

Costs for large-scale excavation and construction in clay/shale media vary widely but can probably be limited to \$10,000 per linear meter, which is similar to major projects and previous estimates for repository construction.

## **System-Level Logistics Modeling**

Logistical simulations were conducted using the TSL-CALVIN simulator to better understand the relationship between the needed DPC decay storage time for disposal, and future changes in the SNF management system in the U.S. such as repository opening date, and transition to loading smaller multi-purpose canisters. The study is described in Appendix C.

Whereas previous logistics studies were limited to the cooling time needed for DPC-based waste packages to be emplaced in a repository, FY14 studies looked at the impact of a system-wide transition to small, standardized MPCs. They also considered impacts from the repository accepting waste for disposal early (2036) and late (2060) in addition to the planned date (2048). The study uses metrics of maximum storage capacity, decay storage time prior to emplacement, and fuel age at emplacement.

The greatest benefit from implementing MPCs, with respect to shortening the required cooling time for all SNF including that in DPCs, requires a small MPC canister combined with the earliest repository start date. The small MPC canister can achieve any emplacement power limit sooner, while an early repository start date means earlier transition from DPCs to MPCs. As time passes without a transition to MPCs, more of the total SNF inventory will be in DPCs so the potential value of a transition to MPCs will decline.

Depending on whether and when MPCs are implemented, and on the repository emplacement thermal power limit, the range of projected repository closing dates varies by approximately 100 years, from calendar 2067 to 2162. This is comparable to the period of time over which SNF will be discharged in the U.S. (approximately 90 years from 1965 to 2055, based on projections for existing nuclear plants). Disposal solutions that are tightly constrained by emplacement power limits, requiring long periods of decay storage, reflect the long duration of SNF production. More flexible solutions that require less decay storage, particularly for younger, higher burnup fuel, can be closed significantly sooner.

The projected statistics of SNF age at emplacement are of interest to evaluate the potential risk from future changes in fuel or DPC condition that limit storage time (and could lead to re-packaging). The minimum fuel age at emplacement is obtained in the model by re-packaging all DPCs into smaller canisters, thus drastically decreasing the required surface decay storage time for disposal. If the industry transitions from DPCs to smaller MPCs without re-packaging, then the fuel age at emplacement could be comparable to re-packaging if the emplacement power limit is high enough (e.g., 10 kW or greater) so that DPCs could be emplaced sooner. For the lower 6 kW power limit two changes would be needed: both a transition to MPCs, and an early repository start, to achieve fuel age at emplacement that is comparable to the re-packaging case at the same power limit.

## **Criticality Investigations**

A new set of calculations evaluates DPC criticality when flooded with ground water containing a range of neutron absorbing elements, at different concentrations. The neutronic configuration has no basket or neutron absorbers, only fuel rods spaced equidistant in a hexagonal array. The elements evaluated include naturally occurring B, Li, and Cl, as well as many other elements commonly found in ground water. Of these, chlorine is the only one that could contribute significant neutron absorption, at chloride concentrations likely to occur in a repository. The chloride content of seawater may be enough to ensure subcriticality of some DPCs, while more

concentrated, saturated salt brines could ensure subcriticality for all DPCs (fresh fuel at 4% enrichment, or at least 10 GW-d/MTU burnup with 5% enrichment). This result could be useful for DPC disposal in salt.

Criticality analyses are also presented for actual, as-loaded DPCs when flooded with fresh water, for two canister degradation scenarios: loss-of-absorber and complete basket degradation. Five types of DPCs, presently located at five respective dry storage sites, are analyzed. For four of these the loss-of-absorber scenario is analyzed, but not the basket degradation scenario because the baskets are made from stainless steel which can corrode but will maintain fuel separation for much longer than other basket materials used in DPCs. For the fifth DPC type (sampled at Site C) both scenarios are analyzed.

The licensing basis for existing DPCs involves criticality analysis for the event of flooding associated with a transportation accident. Fuel characteristics assumed for that analysis may be conservative compared to fuel that is actually loaded. The difference is uncredited reactivity margin, mainly associated with enrichment, burnup, and loading positions for assemblies in as-loaded DPCs.

Of the 179 DPCs analyzed all would exceed the subcritical limit ( $k_{eff} > 0.98$  is used for this report) when flooded, with loss of neutron absorbers, if loaded with the design-basis fuel used for licensing. Using as-loaded fuel characteristics and burnup credit (28 nuclides) only 23 of the 179 would exceed the subcritical limit for the loss-of-absorber scenario, unless the chlorine concentration of flooding ground water is at least 13,500 ppm (seawater is 19,400 ppm chloride). For the Site C DPCs, 18 of the 20 DPCs would exceed the subcritical limit with the basket degradation scenario, unless the chlorine concentration is at least 32,500 ppm. These results may be typical of early-generation DPC designs, but more recent (“burnup credit”) designs could have less uncredited margin with as-loaded fuel characteristics.

### **Survey of Ground Water Compositions**

High-chloride waters occur at depth in both crystalline rock and shale media under certain geologic conditions. Pore waters with chloride concentration greater than the equivalent of 2 molal NaCl, sufficient to significantly reduce the likelihood of criticality in many flooded DPCs, are common in geologically ancient crystalline basement formations at depths of greater than 500 m. These saline waters primarily originated as marine brines infiltrated from overlying sediments, and have evolved through a long history of water-rock interactions. The origin of highly saline waters in shale generally involves more complex processes. Shales with chloride concentrations greater than the equivalent of 2 molal NaCl are found in context with bedded salt deposits or as marine shales in which waters are concentrated from evaporation or water-rock interaction.

In both crystalline and sedimentary environments, highly saline waters tend to be old and stagnant as a result of density differences and low rock permeabilities that inhibit mixing with more dilute waters. The correlation with age suggests that high-chloride waters may not be common in geologically young granites, or those in tectonically active settings with more connectivity between shallow and deep waters. Pore water in soft clays is likely to resemble a recent depositional environment (e.g., seawater). More lithified, high-chloride shales have been documented in the Michigan Basin and they probably occur in the Appalachian and Williston Basins, although the extent is not well documented. By analogy, high-chloride shales could be expected in the Permian Basin, but no data have been identified to support this conjecture.

### **Thermally-Driven Coupled Processes in Clay/Shale Media**

Disposal of DPC-based waste packages in argillaceous sedimentary rock has been proposed, but with thermal management challenges because of the relatively low thermal conductivity and limited temperature tolerance of clay/shale media. Peak temperature limits of 100°C or lower for argillaceous materials have been selected by international programs (see Section 6), but a limit above 100°C could help to limit the duration of surface decay storage or repository ventilation needed for DPC-based waste packages. The effects of locally higher temperatures on repository performance need to be evaluated (in addition to the effects at lower temperatures). This report describes a modeling approach that couples the TOUGH2 and FLAC3D codes to represent thermally driven THM processes, as a demonstration of the types of models needed. The models developed are based on properties of the well-studied Opalinus Clay, but are essentially generic. More complicated constitutive models are available and could be appropriate, but they tend to involve more parameters for which site-specific laboratory and field investigations would be needed. For example, creep is not modeled consistent with observations in the Opalinus Clay, however, creep may be important in other clay/shale media (Section 2).

TOUGH2 is used to evaluate the desaturation of argillaceous host rock as a result of heating, particularly during preclosure ventilation. The model was formulated with a highly permeable drift liner for a bounding-type calculation of moisture loss. A comparison of calculated temperatures with analytical solutions shows similar results, indicating that changes in thermal conductivity with water saturation in the host rock and backfill have minimal effect. Repository ventilation leads to a desaturated zone in the host rock, ranging from just a few meters up to tens of meters. Longer ventilation duration, greater host rock permeability, and the existence of a DRZ tend to increase the extent of the desaturated zone.

A more realistic 2D THM model is used to examine the THM behavior in backfill and host rock. The model represents in-drift emplacement on the floor, with a thick concrete liner and invert. Like the TH model, a bentonite backfill is installed at repository closure. The model shows that the concrete liner and host rock at the top of drift could undergo more desaturation than at the bottom. After backfill installation, resaturation (moisture migrating from the far field) takes place over a period of approximately 200 to 300 years. Transient increases in stress are calculated in the host rock and backfill due to thermally and mechanically induced increases in pore pressure, and thermal expansion of the solid framework. With installation of a thick concrete liner and swelling-clay backfill, stability is predicted for emplacement drift openings at a depth of 500 m, using this approach with properties similar to the Opalinus Clay. The models used in this work are 2D and therefore tend to underestimate peak temperatures, and associated desaturation and stress changes near the waste packages. Regions between waste packages are known to be cooler, with peak temperatures potentially much less than 100°C.

### **Potential for Vertical Movement of Waste Packages in a Salt Repository**

Vertical movement (sinking) of heavy DPC-based waste packages in salt has been identified as a potentially important process in salt repository performance. Extensive sinking (e.g., more than 1 m per 10<sup>4</sup> years) could move waste packages out of the host unit especially in bedded salt, where they could be exposed to different strata and possible ground water flux. Creep constitutive laws for salt that have been used for decades do not predict significant waste package sinking. However, recent creep tests on salt cores at low stress and low strain rates

similar to what could be produced by a sinking waste package, show the potential for creep that is not predicted by those creep laws.

If the low-stress creep rate is attenuated by confining stress, then existing creep models hold after reconsolidation of salt around the repository, and sinking of DPC-based packages could be insignificant. On the other hand, if LS-LSR creep occurs at confined as well as unconfined conditions, then waste packages could sink at velocities of 1 m per  $10^4$  years or greater. A semi-mechanistic modeling approach based on pressure solution, is proposed to supplement existing constitutive models. Confining pressure closes grain boundary voids, increases the size of grain-grain contacts, and slows down diffusive transport and thus the creep rate. Additional testing is needed to better understand low-stress, low strain-rate creep behavior over a wider range of loading conditions in different salt media, and to confirm the role of moisture.

### **DPC Materials and Corrosion Environments**

Review of corrosion literature for relevant repository environments shows that stainless steel corrosion may be slow enough to sustain DPC basket structural integrity for a performance period of 10,000 years, especially in reducing conditions. Uncertainties include basket component design, disposal environment conditions, the in-package chemical environment, and localized effects from radiolysis. Published data also show that prospective disposal overpack materials exist for most disposal environments, including both corrosion allowance and corrosion resistant materials. Whereas the behavior of corrosion allowance materials is understood for a wide range of corrosion environments, demonstrating corrosion resistance could be more technically challenging and require environment-specific testing.

Not all DPCs have stainless steel basket structures, as noted for the Site C canisters analyzed in Section 4. To investigate further, a preliminary screening is presented of the existing inventory of DPCs and other types of canisters, according to the type of closure, whether they can be readily transported, and what types of materials are used in basket construction. DPCs and other types of canisters were grouped according to whether they: 1) are licensed for transport; 2) have basket structural component materials that are susceptible to degradation on long-term exposure to ground water; and 3) are bolted casks. The results show that approximately 2/3 of the overall inventory of storage casks and canisters are considered transportable with basket structural components made from stainless steel, while 6% are transportable but with non-stainless components. The remaining 25% consists of storage-only canisters and bolted casks. The fraction of BWR assemblies in transportable canisters with stainless steel basket components is greater than the fraction of PWR assemblies. These screening results are based on assumptions, in particular that stainless steel construction denotes disposability, and that even thin stainless-steel components (e.g., guide sleeves, Figure 8-5) have sufficient thickness to sustain structural integrity.

### **Potential DPC Filler Materials**

The most promising fill materials for use in DPCs to control postclosure criticality are: 1) low-melting-point metals such as Pb-Sn, Sn-Ag-Cu or Sn-Zn; and 2) small solid particles such as glass beads, including glass beads that contain DU or UO<sub>2</sub>. In the case of low-melting-point metals, provisions would be needed to pre-heat the entire DPC and its contents to temperatures of 225 to 250°C to ensure that the liquid flows to all parts of the container without solidifying.

Two potential filling methods are possible: 1) using the drain and vent ports accessed by removing the welded covers; and 2) removal of the entire lid from each DPC. The first approach would use both ports to optimize filler delivery. For solid particulate fillers some provision for vibrating the entire DPC may be needed, as demonstrated from previous R&D by Atomic Energy of Canada, Limited. The second approach would involve cutting open the canisters using a method such as lathing (skiving). Depending on the approach chosen, a separate hot cell facility could be needed for receipt, opening, filling, closure and testing. In any case, containment will be required to control potential radiological releases when DPCs are opened and during filling and subsequent closure operations.

Criticality analysis shows that a filler material, irrespective of whether it is a neutron absorber or simply displaces water as a moderator, should occupy most if not all of the DPC free volume. Also, the eventual corrosion product of a filler material and its effect on reactivity should be considered in filler selection.

### **R&D Needs for Technical Feasibility Evaluation**

Section 10 of this report contains an annotated a list of 41 R&D topics, consolidated from lists that were developed in FY13 and FY14. The current status of these is summarized in Tables 10-1 and 11-1. Completed activities are described here and in the FY13 summary report (Hardin et al. 2013). Partly completed activities are defined as those which depend on UNF data collection from the nuclear utilities (e.g., GC-859 survey in FY15). Activities planned for FY15 (subject to availability of funding) are described in Section 10. The in-progress activities are potentially relevant to DPC direct disposal, but are conducted in other areas of the UFD R&D program, so that no further activities are planned in the DPC direct disposal feasibility evaluation beyond monitoring progress. Some important examples of in-progress activities that relate to DPC direct disposal are: corrosion testing, performance assessment, temperature tolerance of clay-based backfill and host media, impact of cementitious materials in the repository, thermally driven coupled processes, and brine migration in salt.

Possible future activities include additional thermal analyses that consider heat transfer within DPCs, analysis of gas generation effects with DPC-based packages, criticality model validation and sensitivity analysis, engineered material corrosion modeling, and preclosure safety analysis of waste package conveyance and emplacement systems. The most important gaps in technical information that could be addressed by future activities include validation of criticality modeling tools (particularly boiling water reactor fuel), and DPC basket corrosion modeling (stainless steel).

Table 11-1. Summary of R&amp;D activity status

| <b>R&amp;D Activity Category</b>   | <b>Count</b> |
|--|--------------|
| <b>Completed (FY13 and FY14)</b>   | <b>9</b>     |
| <b>Partly Completed (FY13 and FY14)</b>  | <b>2</b>     |
| <b>Planned for FY15</b>  | <b>5</b>     |
| <b>In Progress (ongoing in other work packages)</b>  | <b>12</b>    |
| <b>Working Total</b>   | <b>28</b>    |
| <b>Possible Future Activities</b>  | <b>13</b>    |
| <i>Thermal Analysis (in-package)</i>   | <i>2</i>     |
| <i>Key FEPs (gas generation)</i>   | <i>1</i>     |
| <i>Postclosure Criticality (validation)</i>  | <i>2</i>     |
| <i>DPC and Overpack Material Degradation Modeling (in-package degradation, basket longevity)</i> | <i>2</i>     |
| <i>Preclosure Safety (conveyance and emplacement)</i>  | <i>2</i>     |
| <i>Closeout and Decision Support</i>   | <i>4</i>     |
| <b>Total Identified (consolidated count)</b>   | <b>41</b>    |

### References for Section 11

Hardin, E., D. Clayton., R. Howard, J. Scaglione, E. Pierce, K. Banerjee, M. Voegele, J. Wen, T. Buscheck , J. Carter, and T. Severynse 2013. *Preliminary Report on Dual-Purpose Canister Disposal Alternatives (FY13)* Revision 1 . FCRD-USED-2013-000171 Rev. 1. U.S. Department of Energy, Office of Used Nuclear Fuel Disposition. November 2013.

THIS PAGE INTENTIONALLY LEFT BLANK

## **Appendix A. Trip Report: Symposium on Rock Mechanics and Rock Engineering of Geological Repositories in Opalinus Clay and Similar Claystones**

This trip report was filed by the author after attending the symposium on February 14, 2014, in Zurich, Switzerland. Presentations and additional information are available at <http://www.egt-schweiz.ch/index.php?id=symposium&L=2>. This 1-day symposium was principally organized by Prof. Dr. Simon L w of the Swiss Federal Institute of Technology (ETH). The stated purpose was to help the Swiss repository implementing agency (NAGRA) determine if enough is known about claystone mechanics for it to recommend that the siting process proceed past Stage 2 (a process defined in the established Swiss siting protocol). There was extensive discussion of rock conditions at the Mont Terri URL, which is situated roughly 300 m below the surface (depth of potential repository sites could be 800 m or more).

The symposium was conducted in three parts: 1) laboratory and *in situ* experiments, and models; 2) underground construction experience; and 3) proposed repository layouts and construction methods. The first part was presented by professors from academia, while underground construction experience was presented by investigators from Mont Terri and by Swiss tunneling engineers, and repository design information was discussed by staff from government agencies and R&D institutions. All presentations described below were specific to the Opalinus clay unless noted otherwise.

### **A.1 Laboratory and In Situ Experiments, and Models**

Florian Amman (ETH) described the rock mechanics challenges as anisotropy, sensitivity to moisture, describing brittle and nonlinear behaviors, time dependent deformations (consolidation, creep, swelling), and the effects of suction. In soil mechanics the solids are typically considered to be incompressible, while in clay/shale media they must be considered compressible. Simple mechanical tests (e.g., unconfined compressive strength, UCS) are not so simple when saturation is required, to represent *in situ* conditions and to produce consistent and comparable data. The soils testing literature contains useful guidelines for saturation methods and time required. Effective formation properties are calculated from undrained tests at *in situ* saturation. Note that Opalinus strength is greatest when suction is approximately -70 MPa which corresponds to a liquid saturation of roughly 50% or less. Describing transversely isotropic elasticity with pore pressure coupling requires seven constants including Skempton parameters that couple pore pressure with normal stress parallel and perpendicular.

Heinz Konietzky (Technical University – Bergakademie Freiberg) described modeling of rock structures using Voronoi bodies (UDEC code from Itasca Consulting Group) or rigid spheres (PFC code from Itasca). A variety of bulk deformation and fracture mechanics mechanism can be represented. The Opalinus was described as particles of clay, silt and carbonate, adhered by constitutive particle bonds.

The Mont Terri excavation sequence, confirmed by experimental measurements, consists of excavation, unloading, pore pressure decrease near the opening for several months, leading to changes in loading. Both tensile and shear cracks are observed at the drift wall. Pore pressure increase may be steep during early time after excavation.

Silvio Giger (NAGRA) stated that using size-based geotechnical classification, the Opalinus would have a low clay fraction (<20%) and would be a siltstone. Using mineralogy the Opalinus is 40% to 70% clay, with the remainder quartz/feldspar, and carbonate. Porosity of the Opalinus

may not be correlated to current burial depth. The UCS is 10 to 25 MPa perpendicular to bedding, and 4 to 7 MPa at 30° to bedding. Tensile strength decreases as saturation increases (consistent with the effect of suction). The protocol for UCS testing calls for undrained, with up to 2 weeks consolidation under pressure before testing. The compressive strength testing strain rate is  $10^{-6} \text{ sec}^{-1}$ . Creep or liquefaction testing is done with deviatoric stress up to 60 MPa and mean stress up to 30 MPa.

Frederic Pellet (University of Lyon, France) described microstructural and petrophysical evaluations to predict dilation and cracking in shales, which may be time-dependent, forming over 100's of years. He claimed that clay/shale behavior needs to be modeled as creep, where the strain rate tensor varies as the ratio of deviatoric to equivalent stress. Implementation of creep flow potential using the von Mises definition of equivalent stress (and by analogy, the Tresca definition) is generally suited for isotropic media, and a more complete implementation is needed for transversely isotropic media. If creep is important then the EDZ could continue to evolve as the rock flows and loads are transferred further away, or into the liner. Fracture closure and sealing in the near-field host rock might not occur. The COX argillite has been tested at  $10^{-6}$  and  $10^{-8} \text{ sec}^{-1}$  strain rates. Transgranular cracks were observed at higher strain rates, intergranular cracks at lower ones. The fundamental mechanism of plastic deformation and cracking appears to be dislocation. For the COX argillite at Bure, the UCS is 27 to 29 MPa, Young's modulus is 5 to 6 GPa, and porosity is 15.5%.

For the argillite at Tournemiere, UCS is 35 to 38 MPa, Young's modulus is 21 to 27 GPa, and porosity is 9%. Desiccation cracks are prevalent on all vertical surfaces exposed to air, with spacing of ~20 cm. In the winter these cracks open to apertures of ~2 mm, while in summer they close fully. Horizontal and vertical cracks behave similarly. Displacements are observed for relative Humidity (RH) fluctuations greater than ~15% and periods greater than ~6 hr. These displacements appear to be reversible.

Finally, Pellet instigated a spirited discussion by claiming that because there is "almost no free water" in argillites, that there is "almost no pore pressure" so that the effective stress concept does not apply and coupling to framework stress is not important. He said that Biot poroelasticity is not applicable because there are "few Hertzian contacts" (Hertzian contacts can be stiff). Also, he said that suction would effectively be minimal because of "cavitation" (ubiquitous voids).

## **A.2 Underground Construction Experience**

Derek Martin (University of Alberta) lectured on rock mechanics in claystones and similar media. Clay/shale media can be classified on UCS (0.3 to 30 MPa following the ISRM classification scheme). They are often overconsolidated reflecting previously greater burial depth. Strength is a function of water content, and these media have little or no true cohesion so the effect of water retention (suction) matters. Stress drivers include  $\frac{\sigma_1}{UCS}$  and  $(\sigma_1 - \sigma_3)$ .

The bulk rock exhibits some swelling on unloading, and squeezing if over-stressed. At Mont Terri these responses were investigated in the ED-B test and the Mine-By Experiment (the second at the site). Convergence (diameter closure) was found to be 0.1% to 0.2% in the "ED-B," and 1% to 1.5% in the Mine-By. The former test was driven perpendicular to the strike of bedding (which dips at ~40°), and latter was parallel. (For comparison, convergence in the Boom Clay is >2.5%, and 1% to 2% at Bure.) Slip on bedding was not observed at Mont Terri.

Pore pressure increased ~1 MPa at the advancing face, and decreased 2 to 3 MPa where unloaded. Pore pressure effects were observed at up to 3 diameters from the drift centerline.

Eduardo Alonso (Technical University of Catalonia) discussed the effects from transient deformation (not creep) on permeability. He referred to the HG-A test at Mont Terri, and the associated reports, for information on permeability of the EDZ. Most flow occurs along fractures or other preferential pathways, so permeability depends on the evolution of discontinuities, dilation, etc. The Barcelona Basic Model (BBM) is a reasonable constitutive model for the matrix, with addition of anisotropy. Ubiquitous fractures can be used to represent discontinuities that open due to excavation. Fracture permeability is represented using the cubic law, while unsaturated properties can be represented using a Leverett scaling approach. Initial porosity is heterogeneous in model grids, and is assigned randomly. Unfortunately, the constitutive model with these features will have more than 20 parameters. Any state-of-the-art thermal-hydrological-mechanical (THM) code can be used, but Code\_Bright has generated some reasonable agreement with field test (HG-A) results. Permeability develops along stress paths, or regions of the rock mass that are similarly stressed. Important uncertainties remain, for example, the density of discontinuities and their properties. The aperture-porosity and aperture-permeability relationships can increase numerical effort, and more linear formulations would be helpful.

Next Paul Bossart (Swisstopo, Mont Terri Project Director) described the excavation, construction, and ground support engineering experiences at Mont Terri. Excavation methods that have been tried include: drill-and-blast, roadheader, hydraulic hammer, raise boring, and steel-toothed auger. The drill-and-blast method produced the greatest overbreak and extent of excavation damage. The roadheader is the method of choice because of low cost, no water needed, limited spalling or overbreak, limited EDZ, and workable dust control. For dust control, two suction fans are used with filters.

The Mont Terri tunnels are designed for R&D, with a lifetime on the order of 20 years, with only local repairs needed. Immediately after excavation a thin layer (5 cm) of shotcrete is applied to prevent hydration or slaking. All shotcrete is formulated for early strength and low pH (balanced portlandite, excess soluble silica, and super-plasticizer). Wire mesh (e.g., coarse “welded wire fabric”) is then installed with short bolts. Long rock bolts may then be installed for larger openings, or where dictated by performance requirements (e.g., minimize maintenance, maximize service life). Rock bolt length is typically 1× to 1.5× opening diameter, and they are installed using a full 270° pattern. Bolts may be metal or fiberglass, and may use point anchors or full grouting. Alternatively, steel sets may be installed with “distortion zones” at the springlines.

After a delay of several months to allow convergence, a final layer of shotcrete is applied (15 cm). As much as 5% convergence has been observed where stress is concentrated by nearby excavations (e.g., the alcove from which the “FE” test drift was constructed; ). The floor is shotcreted all the way to the ribs, and the surface is worked to provide a running surface for vehicles and water flow. Drift convergence will continue until the floor is shotcreted. At Mont Terri, a few percent of the total drift length has been impacted by shotcrete slabbing on the ribs, which occurs in these locations with a frequency of 10 to 20 years. Renovation consists of removal of loose shotcrete and rock using a hydraulic hammer, replacement of wire mesh, and application of new shotcrete.

Rock damage at Mont Terri is dominated by bedding-induced breakouts. Stress induced breakouts are uncommon (at 250 to 400 m burial depth). Some of the drifts aligned parallel to the strike of bedding have experienced shear zone failure, with large-block (e.g., 1 to 2 m thick) movements detected using borehole extensometers. The EDZ at Mont Terri typically exhibits “plumose hackles” (Martin and Lanyon 2001) and the mechanism may be related to pore pressure excursions. Hydraulic conductivity of the EDZ at Mont Terri is on the order of  $10^{-8}$  m/sec, and gradual reduction is observed (“sealing”). For a deeper repository in the Opalinus (e.g., up to 800 m) the intensity and spatial extent of the EDZ would be significantly greater.

Walter Steiner (B+S AG, a tunnel engineering firm) described tunneling in the Swiss Jura. Early-modern tunneling methods in Switzerland were distinguished by use of movable excavation shields to stabilize rock before liner installation. The earliest methods used drill-and-blast with a shield, and a segmented liner (e.g., pre-cast concrete or cast-iron). For example, the Baregg tunnel (A1 motorway, tubes 1 and 2) was constructed by drill-and-blast with a horseshoe-shaped shield, and completed in 1970. Non-circular shields were found to be unworkable because they have a tendency to roll and cannot be readily corrected or steered. In 1970 the Heitersberg rail tunnel was constructed using a circular, open Robbins TBM (10.8 m diameter). Ground support consisted of an outer liner of shotcrete sprayed by a robot attached to the TBM, with wire mesh and rock bolts, and steel supports where needed (24%). Completed in 1985, the Gubrist highway tunnel (tubes 1 and 2) was excavated using a similar arrangement and the same shield, and the liner was mated with the shield to improve the stability of the interval between them. Another early highway tunnel, the Rosenberg tunnel, was excavated using a shield with four road headers.

Soft-rock tunneling in Switzerland advanced after the 1970’s, accelerated by extensive tunnel construction for the A16 and other motorway routes. The Mont Russelin highway tunnel completed in 1998 is 3.5 km long, with more than 300 m of maximum overburden. The Bözberg twin tubes (A3 motorway) were completed in 1994, and are 4.3 km long with more than 200 m maximum overburden. The Adler rail tunnel was completed in 2000, is 5.2 km long, and was excavated to a diameter of 12.5 m (then a record). The Bure highway tunnel was completed in 2011, is 3.1 km long, and has a diameter of 12.6 m. The Mont Terri highway tunnel was completed in 1998, is 4 km long, and replaced the tunnel now used to access the URL.

Tunneling Opalinus Clay has achieved best results with single-shield TBMs, avoiding the problems associated with conventional methods such as drill-and-blast. The tunnel should have circular cross section, and a continuous segmented liner installed immediately to prevent swelling. Stability problems close to the face may be encountered, especially in fault zones, and where there is strong water inflow. Rock instability in the crown can be mitigated by installing deformable filler material (e.g., pea gravel) behind the liner, while support can be increased by injecting grout into the filler (30% to 50%). With application of these methods since the 1970’s, advance rates have improved from ~10 m/day to ~30 m/day, with larger excavated opening diameters.

### **A.3 Proposed Repository Layouts and Construction Methods**

Oliver Heidbach (GFZ Potsdam) lectured on the state of *in situ* stress in northern Switzerland. The interpretation approach used is to model crustal deformability in 3D, then apply displacement (velocity) boundary conditions (e.g., -9 m/yr NW-SE). The stress state at any location consists of constant (e.g., gravitational), seismic (cyclic), and man-made components

(excavation). Stick-slip friction on faults is an important factor. In general, the anticipated stress state in the Opalinus at repository depth will be nearly transversely isotropic with the maximum principal stress oriented vertically ( $\sigma_1 = \sigma_v$ ), and the horizontal stresses equal ( $\sigma_2 = \sigma_3 = \sigma_H$ ) and less than the vertical stress ( $\sigma_H / \sigma_v \cong 0.8$ ).

Wulf Schubert (Technical University – Graz) gave a short presentation on repository design for rock and stress conditions. Openings should be perpendicular to foliation (including the strike of bedding) if possible to improve stability, limit displacements, and minimize the EDZ. Dipping strata are more difficult to design for than horizontal. The overall goal should be non-interference of repository drifts, through separation. If this is not achieved, stress redistribution in the rock mass may span multiple drifts, unloading some pillars and over-loading others.

Phillipe Nater (Pöyry Schweiz AG) presented an approach to repository underground design in the Opalinus and similar media. His introduction identified four excavations from which experience can be drawn: the Mont Terri URL, the historic Grenchenberg tunnel, excavations at the Konrad repository, and the Bure URL. The Grenchenberg single-track rail tunnel was completed in 1916 with a length of 8.6 km. It traverses the Opalinus claystone at approximately 700 m below the ground surface. The geology is strongly folded, and the Opalinus occurs five times with total exposure of 416 m. Rock conditions in the Opalinus were reported as good, and dry (unlike water inflow zones encountered elsewhere), but support requirements were relatively high. The lining consists of vaulted masonry up to 60 cm thick, and the invert was constructed as an arch with similar thickness. The tunnel has been abandoned. There are many tunnels through the Opalinus in Switzerland, and this one may be unique because of its age.

Repository drift sizes in claystone could range from 8 m<sup>2</sup> to 67 m<sup>2</sup> face area (for emplacement of a single HLW canister surrounded by backfill, up to a “vault” for intermediate-level and low-level waste (ILW/LLW)). Spans from 3.2 m to 8 m can be expected. For openings excavated with a roadheader, the lining system would consist of immediate application of wire mesh and shotcrete, with yielding elements as needed (as for support of access tunnels in the Jura clay at Konrad). Immediate application is necessary to support construction operations, and to prevent damage from swelling or desiccation. Excavation and ground support should be designed to minimize the accumulation of voids in the EDZ. After deformation is allowed to occur, a final cover would consist of more shotcrete, applied over more wire mesh and steel sets where needed. Thicknesses would be increased wherever extra support is needed (e.g., greater burial depth, higher stress, larger spans, and/or longer service life). Rock bolts can be installed as needed.

Modeling of repository excavation performance is approached using six alternative constitutive models (representing different conditions: intact rock, fractured rock, interfaces, faults, large-scale structures, etc.). Three in-situ stress conditions are used (based on burial depth, varying the ratio of  $\sigma_v$  to  $\sigma_h$  parallel and perpendicular to the tunnel axis, with  $\sigma_v / \sigma_h \sim 1.5$ ). Properties are estimated from available information (UCS, anisotropy, orientation to bedding, etc.). “Design levels” are used representing a range of conservatism from “most probable” through “ultimate” (unexpected conditions, beyond experience, or extended service life). Creep is not an issue for most applications because HLW disposal openings would be closed within ~5 yr, while ILW/LLW vaults would be closed in 20 to 30 yr. Only for service openings with operational lifetimes of 80 yr or longer, would creep be a design issue.

A final presentation was given by Gilles Armand (ANDRA) on rock mechanics of the COX argillite at the Bure URL, and consequences for the Cigéo repository design. The French

repository is required to facilitate retrieval for at least 100 years, which means operational areas must remain stable for up to 150 years.

Emplacement openings for HLW will be long, horizontal borings excavated using a remotely operated mini-boring machine, and lined with continuous steel casing. Vault-type openings for ILW/LLW will be 9 to 11 m in diameter and up to 400 m long. Several support options have been identified for excavated openings, namely: 1) soft, with 3-m rock bolts and 8 cm of fiber-reinforced shotcrete; 2) medium, as above with additional 27 cm of cast-in-place non-reinforced concrete; and 3) maximum, with 3-m rock bolts and 45 cm of fiber-reinforced concrete applied in four layers.

Reported *in situ* stress conditions at the site are different from the Swiss Jura, with  $\sigma_H/\sigma_v \sim 1.3$ , and  $\sigma_v \cong \sigma_h$ . Observations in the URL show that for tunnels oriented parallel to  $\sigma_H$ , shear fractures are associated with inward block movement in the pillars. For openings parallel to  $\sigma_h$ , fractures in the roof and invert dip toward and away from the face, respectively. The favored orientation for stability of HLW borings is parallel to  $\sigma_H$ . All casings and liners need to be backfilled to accommodate anisotropic deformation.

Creep is defined as time dependent deformation with no change in pore pressure and no change in mean stress. Similar long-term deformation rates are observed at Mol, Bure, and Mont Terri suggesting a common mechanism. Data from Mont Terri *in situ* tests suggests this mechanism could be gradual pore pressure dissipation.

#### **Reference for Appendix A**

Martin, D.C. and G.W. Lanyon 2002. *EDZ in clay-shale: Mont Terri Rock Laboratory*. Mont Terri Project Technical Report TR 2001-01. Swisstopo.

## **Appendix B. Peer Review Plan and Approvals**

A peer review of this report was conducted in accordance with *Fuel Cycle Technologies – Quality Assurance Program Document, Revision 2 (12/20/12)*. A peer review plan was prepared and approved, and a facsimile is appended below (3 pages). The Fuel Cycle Technologies (FCT) document cover sheet was used as the record of the peer review, and two signed copies of this form (one for each reviewer) are also appended below (2 pages total).

### **Peer Review Plan - Deliverable: M2FT-14SN0816031 (QRL 3)**

**Document Title:** *Investigations of Dual-Purpose Canister Direct Disposal Feasibility (FY14) (15Aug2014)*

**Purpose of Review:** Peer reviews shall include identification of the following: 1) work to be reviewed; 2) scope of the peer review; 3) size and required capabilities of the peer review team (there shall be at least two members on each peer review team); and 4) expected method and reporting schedule.

### ***Comments specific to this document:***

*The work to be reviewed was performed in the Dual Purpose Canisters-SNL work package in FY14, and documented in: Investigations of Dual-Purpose Canister Direct Disposal Feasibility (FY14) (FCRD-UFD-2014-000069 Rev. 0). The scope of peer review will include all information and analyses described in that report. The peer review team will consist of two members: Bret van den Akker, technical staff with ORNL, and Patrick Brady, Senior Scientist and Fellow at Sandia National Laboratories. Qualifications of these members are discussed below. The peer review will be conducted by email and teleconference, starting with distribution of the report and review instructions, followed by a review period, submittal of comments, a teleconference to discuss comments with the authors, report revision, reviewer concurrence, and issuance of FCRD-UFD-2014-000069 Rev. 0 in final form.*

### **Scope of Peer Review:**

The scope of Peer Review shall include the following considerations as they apply to the work being reviewed:

1. Determine the reasonableness of the assumptions and validity of inputs that were used as the basis for the research and analyses.
2. Verify the appropriateness of the methods and implementing documents used to complete the work.
3. Determine if the software applications (e.g., simulation, or computer model) used to complete the work under review are appropriate and adequate.
4. Determine the accuracy of the calculations and final documentation.
5. Determine the reasonableness and validity of the conclusions.
6. Verify that the conclusions are clearly stated such that misinterpretation is minimized. Identify any different conclusions that can be drawn from the results presented.
7. Verify that any uncertainty in the results is clearly and adequately discussed.

Additional criteria may be defined by the team and shall be defined in the review criteria documentation.

**Comments:**

*The above list of considerations reflects that no experimental work was performed. The document to be reviewed is an interim report, to be issued part-way through a multi-year study of DPC disposal technical feasibility. The review should emphasize whether the work reported so far is complete in its approach and thorough in its identification of technical issues. Comments that involve work scope may be responded to by incorporating recommendations that they be addressed by future work.*

**Qualification Requirements for Peer Reviewers:**

Peer reviews shall be conducted by individuals who have independence from the work under review. Independence means that the individual was not involved as a participant, supervisor, or advisor in the work under review and is, to the extent practical, free from other conflicts of interest.

The number of reviewer(s) is commensurate with the complexity of the work to be reviewed, its importance to program objectives, the number of technical disciplines involved, and the degree to which the subject issue is considered controversial by stakeholders and differing viewpoints are strongly held within the applicable technical and scientific community concerning issues under review. The supervisor, manager, or NTD of the performer of the work shall select peer reviewer(s) based on the complexity of the work being reviewed. Peer reviewers are individuals who meet at least one of the following criteria as judged by the responsible manager:

- Have adequate academic education in the same technical discipline in which the work is performed or in a closely related field, or have adequate work experience and technical activity in a related discipline.
- Have demonstrated evidence of proposing and solving engineering, experimental, or theoretical problems that are recognized as valid by the community of technical peers.
- Have contributed to the body of knowledge within a technical discipline such as publishing research results in the proceedings of scientific meetings or in professional journals.

The supervisor, manager, or NTD of the performer of work being peer reviewed must verify that peer reviewer(s) are qualified in accordance with the requirements herein. FCT MOs may require approval of peer reviewers, which should be called out in applicable work packages or otherwise formally requested.

**Comments:**

*The reviewers were not involved as participants, supervisors, or advisors in the work reviewed, with one exception, and to our knowledge, are free from other conflicts of interest. The exception is that Dr. van den Akker contributed to the workplan revision in FY14, and is listed as an author. Thus, he was involved with scoping the work but not its execution.*

*Selection of two reviewers is commensurate with the complexity, importance, technical disciplines, and stakeholder interest in the subject matter, so long as the reviewers have broad knowledge and experience in the back end of the nuclear fuel cycle in the U.S., as these reviewers do.*

*knowledge and experience in the back end of the nuclear fuel cycle in the U.S., as these reviewers do.*

*Both reviewers have credentials in relevant disciplines: Dr. Patrick V. Brady is a Senior Scientist at Sandia National Laboratories, with more than 20 years experience in a broad range of geoscientific areas important to radioactive waste management. He has a Ph.D. in Geochemistry from Northwestern University. Dr. Bret P. van den Akker is currently technical staff in the Used Nuclear Fuel Systems group at Oak Ridge National Laboratory. He has a Ph.D. in Nuclear Engineering from the University of California, Berkeley, and an extensive record of relevant R&D activities.*

*Both reviewers have in-depth experience in proposing and solving relevant problems in nuclear waste disposal and fuel cycle technology. Accordingly, they both meet all three of the criteria listed above.*

**Documenting Peer Reviews:**

The peer review will be documented using the current version of the FCT document cover sheet, to show signature approval by both peer reviewers.



8/4/14

---

Ernest Hardin, Work Package Manager

Date



08/04/2014

---

Robert MacKinnon, Responsible Manager (SNL)

Date

THIS PAGE INTENTIONALLY LEFT BLANK

## Appendix C. System-Level Logistical Calculations for DPC Direct Disposal

The purpose of this study is to understand how the timing of DPC direct disposal could be affected by cooling time, a future transition to loading multi-purpose canisters (MPCs) at the nuclear plants instead of DPCs, and the repository opening date. It follows a preliminary study (Nutt 2013; Hardin et al. 2013) that projected future DPC loading, and the timing of DPC cooling to reach repository emplacement power limits. This study adds: 1) the possibility of future transition to MPCs; 2) sensitivity to repository opening date; 3) a wider range of emplacement power limits; and 4) analysis of fuel age at emplacement (age from reactor discharge). Whereas direct disposal of DPCs has possible benefits such as reducing cost and complexity of the SNF management system, this analysis explores how long it could take, and the associated profile of SNF age at emplacement.

The definition for MPC used here is the same as that used internationally: a sealed canister intended for storage, transport, and disposal. The MPC definition should not be confused with specific DPC designs that the vendors have described as MPCs (i.e., NAC-MPC, MPC-05, MPC-06, MPC-24, MPC-26, MPC-32, MPC-68, MPC-HB, etc., discussed in Sections 4, 8 and 9). This MPC definition is generic and not based on any aspect of the storage-transport-aging-disposal (STAD) canister design under development (Howard et al. 2014).

The principal tool of these studies is the TSL-CALVIN simulator (Nutt et al. 2012). The tool is a push-type process simulator that represents reactor discharge, cooling, dry storage, transportation, and conditions for disposal of fuel from all U.S. nuclear power plants. It includes a set of information tables that describe the types and circumstances of SNF at each plant.

The total commercial SNF inventory considered in the analysis is ~139,000 MTHM, projected to be produced through shutdown of the last reactor in 2055.

**Summary of Previous Study** – The previous study showed that with an emplacement power limit of 10 kW per waste package (needed for the salt disposal concept), that emplacement of all DPCs could be substantially completed by 2130, and that this could be accomplished with a maximum repository throughput of 1,700 MTHM per year. Higher power limits (e.g., 12 kW) were examined and found to accelerate emplacement and increase the possible throughput, as expected. Lower power limits were found to have the opposite effects.

Some of the key assumptions made in the previous study were:

- Life extensions (+20 years) for all existing reactors, with gradually increasing burnup and enrichment, limited to 5% enrichment (Carter et al. 2011).
- No new reactor “builds.”
- DPC types currently in use at each power plan will continue to be used through decommissioning of its reactors, such that all commercial SNF will eventually be sealed into DPCs.
- Repository opening in 2048, consistent with the current system strategy (DOE 2013).
- Storage and transportation thermal power limits for DPCs are all greater than emplacement power limits, i.e., SNF can be shipped to a repository whenever cool enough for disposal.
- Five emplacement thermal power limit values were considered: 4, 6, 8, 10, and 12 kW.

- Two levels of waste management system throughput were considered: 3,000 and 4,500 MTHM per year. The 3,000 MTHM per year level was the greatest throughput anticipated for the proposed repository in volcanic tuff (DOE 2008), while the 4,500 MTHM per year level is high enough to examine cases for which the disposal schedule is constrained by facility throughput.

The time required to cool DPCs for disposal was compared to re-packaging strategies which would use smaller canisters, and could therefore meet thermal limits sooner, and support higher repository throughput. A repository that opens in 2048 and has throughput of 3,000 or 4,500 MTHM per year, could complete disposal by 2095 and 2080, respectively. The previous study estimated additional cost from storing DPCs, and compared it in general terms to the costs of re-packaging. The study did not account for additional costs from disposing of smaller canisters (more waste packages, more handling operations, etc.).

**Current Study** – The current study focuses on the timing of SNF cooling, and also on the age of SNF at disposal, for the previous “DPCs-only” scenario and also a second scenario called “DPCs+MPCs.” The choices are explained as follows:

- **Packaging Scenarios** – The new scenario assumes that all operating power plants will begin loading MPCs at 5 years before repository opening. A simple schedule estimate shows that if MPC canister design begins at the earliest time when repository requirements are known, that the canister design could be licensed and implemented about 5 years before the conclusion of repository licensing.
- **MPC Canister Capacity** – A small MPC with capacity for 4 PWR fuel assemblies or 9 BWR assemblies is selected to ensure that cooling time for MPCs is minimal in the analysis.
- **Repository Opening Date** – Emplacement starting dates of 2036, 2048, and 2060 were selected to span a plausible range of repository development schedules that spans the 2048 date in the DOE strategy (DOE 2013).
- **Emplacement Power Limits** – Thermal power limits of 6, 10 and 18 kW were selected. The 6 kW limit would be for open emplacement in crystalline or argillaceous rock, with the expectation that the repository would be ventilated for an additional 50 to 100 years to allowing cooling to approximately 2 to 4 kW at closure (depending on fuel burnup). Previous studies showed that the host rock peak temperature limits could be met, and a backfill peak temperature limit (e.g., 150°C) could also be met at this power level (Hardin et al. 2012, 2013). The 10 kW limit is an approximate limit for packages of any size emplaced in salt assuming 200°C peak salt temperature limit. The 18 kW limit was imposed in previous analyses (DOE 2008).

The alternative cases for analysis are summarized in Table C-1. Other parameter settings controlling the production of SNF, loading of DPCs, the order of fuel selected for storage, where fuel is stored, and so on, were the same as in previous studies (Nutt 2013; Hardin et al. 2013). Importantly, these studies have assumed that all DPCs and storage-only canisters are transportable and disposable, which simplifies the logistics model. There are currently at least 26 designs for dry storage systems, and not all have been licensed for transport (a summary of existing dry storage systems of all types, for commercial SNF, is provided in Table 8-4).

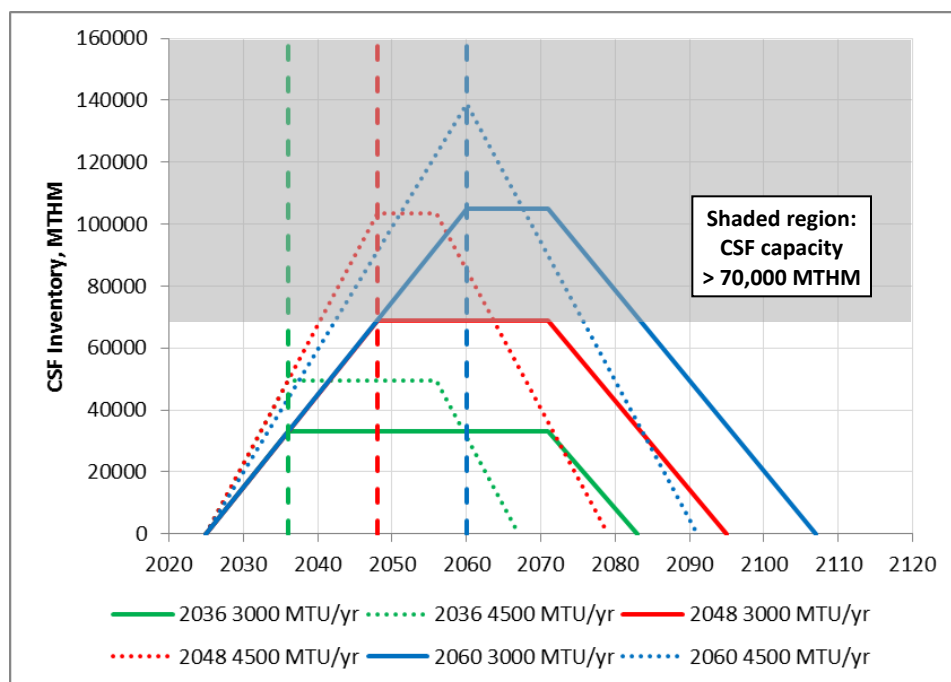
The ranges summarized in Table C-1 are intended to identify trends in disposal timing and fuel age at emplacement, as influenced by thermal limits, transition to smaller MPCs, and uncertainty in the timing of repository development. Fuel age at emplacement is potentially important if dry storage duration limits are imposed on existing DPCs due to canister aging or fuel condition. Note that these are hypothetical cases that project future decisions and events for exploratory simulations only.

**Re-Packaging Reference Case** – The timing of disposal for the alternative cases (Table C-1) is compared to a notional reference re-packaging case. The re-packaging reference case is based on schedule constraints only. By selecting the throughput of re-packaging and repository systems, and the repository start date, a simple schedule of SNF disposal is generated. The same result can be generated with TSL-CALVIN by setting facility throughput limits and relaxing all other constraints such as thermal power limits. The amount of fuel in dry storage at a CSF is shown in Figure C-1. Note that the time from repository opening until all SNF is transported to the repository is 47 years for throughput of 3,000 MTHM per year and 31 years for 4,500 MTHM per year.

Table C-1. Summary of alternative cases used for logistical analysis

| Alternative                 | Repository Start Date | Thermal Emplacement Power Limit (kW) | Fuel Loading Scenario |
|-----------------------------|-----------------------|--------------------------------------|-----------------------|
| Alternative 1               | 2036                  | 6                                    | DPCs-only             |
| Alternative 2               |                       |                                      | DPCs+MPCs             |
| Alternative 3               |                       | 10                                   | DPCs-only             |
| Alternative 4               |                       |                                      | DPCs+MPCs             |
| Alternative 5 <sup>A</sup>  |                       | 18                                   | DPCs-only             |
| Alternative 6 <sup>A</sup>  |                       |                                      | DPCs+MPCs             |
| Alternative 7               | 2048                  | 6                                    | DPCs-only             |
| Alternative 8               |                       |                                      | DPCs+MPCs             |
| Alternative 9               |                       | 10                                   | DPCs-only             |
| Alternative 10              |                       |                                      | DPCs+MPCs             |
| Alternative 11 <sup>A</sup> |                       | 18                                   | DPCs-only             |
| Alternative 12 <sup>A</sup> |                       |                                      | DPCs+MPCs             |
| Alternative 13 <sup>A</sup> | 2060                  | 6                                    | DPCs-only             |
| Alternative 14 <sup>A</sup> |                       |                                      | DPCs+MPCs             |
| Alternative 15 <sup>A</sup> |                       | 10                                   | DPCs-only             |
| Alternative 16 <sup>A</sup> |                       |                                      | DPCs+MPCs             |
| Alternative 17 <sup>A</sup> |                       | 18                                   | DPCs-only             |
| Alternative 18 <sup>A</sup> |                       |                                      | DPCs+MPCs             |

<sup>A</sup> Results presented by Kalinina (2014). Results for other cases are plotted in this appendix.



Notes:

1. The vertical dashed lines show the alternative repository start dates assumed for analysis.
2. The slope of the 2060/4,500 MTU/yr curve prior to 2060, reflects reduction of the average throughput rate to accomplish transfer of nearly all SNF to a CSF by the time a repository opens.

Figure C-1. Reference re-packaging case for ranges of throughput and repository start date, showing history of CSF inventory

## C.1 Results of Logistical Simulations

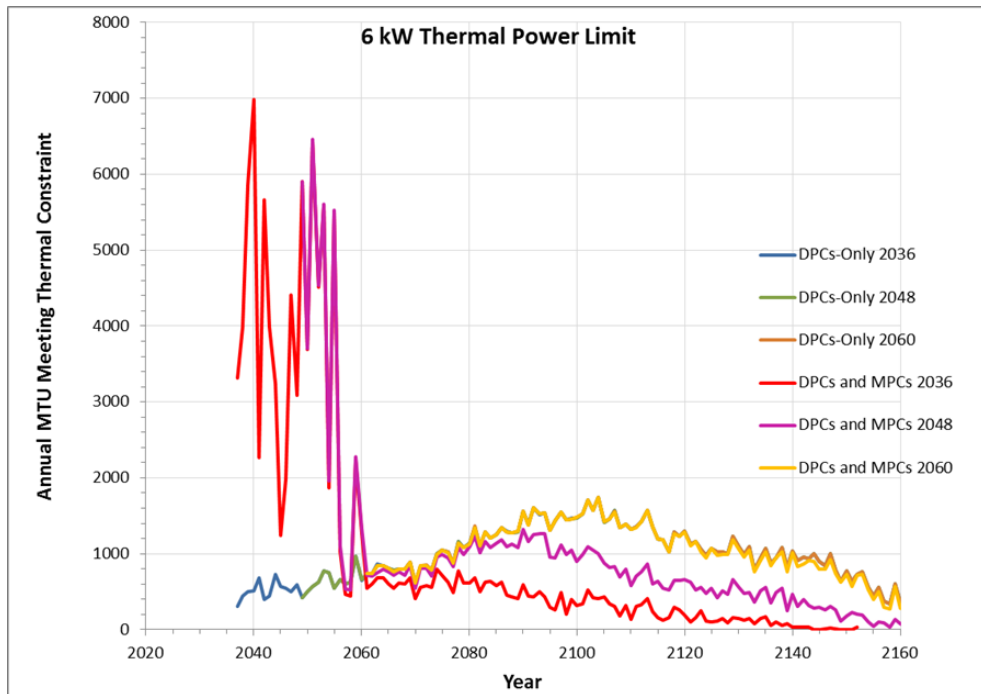
This section presents analysis for eight cases as indicated in Table C-1, corresponding to the 2036 and 2048 repository start dates, and the 6 kW and 10 kW emplacement power limits. The other cases are presented by Kalinina (2014). The timing of SNF cooling to meet emplacement power limits, and the impact of repository throughput, are discussed below. These cases are compared to the re-packaging reference case in Section C.2. Fuel age at emplacement is discussed in Section C.3.

**Timing of DPCs and MPCs Meeting Emplacement Power Limits** – The annual and cumulative amounts of SNF in DPCs, or in DPCs and small MPCs, that meet the repository emplacement thermal power limits are shown in Figures C-2 and C-3 for the 6 kW and 10 kW power limits, respectively, and for repository start dates of 2036, 2048 and 2060. Dashed vertical lines show when the reference re-packaging cases are completed. Note that SNF that cools enough for emplacement prior to the repository start date, is not shown in the time series but is shown on the cumulative plots.

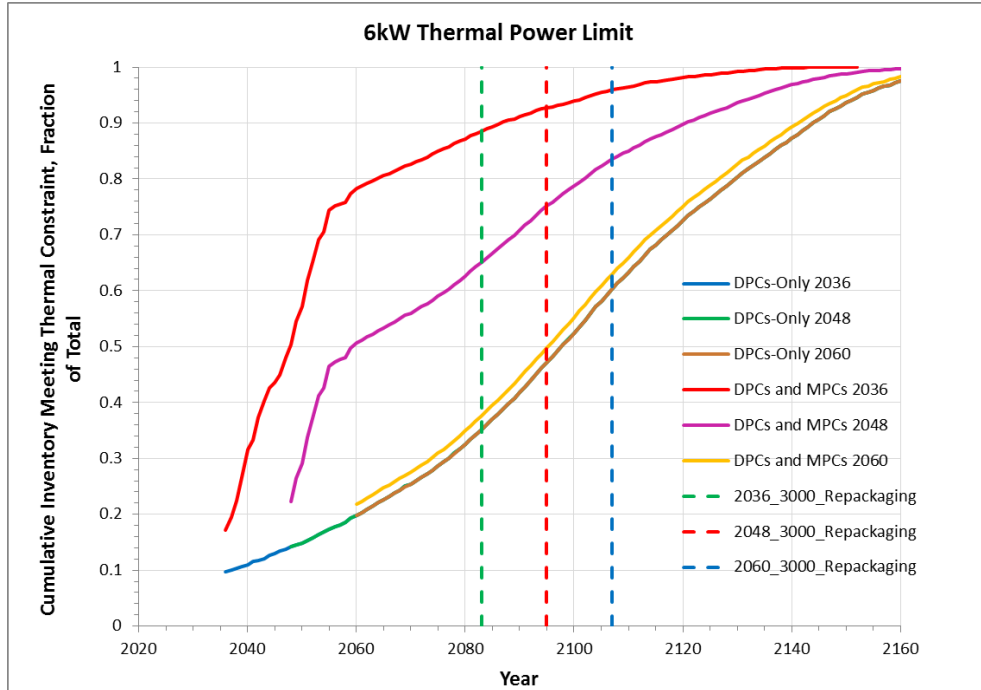
Figures C-2 and C-3 demonstrate that aging controls how soon SNF can be emplaced in a repository, for the lower emplacement power limits. Ignoring outlier waste packages (projected to have highest burnup) 98% of the total inventory in DPCs-only, can be emplaced by 2162 for the 6 kW limit and by 2112 for the 10 kW limit.

The inventory of SNF in DPCs that is cool enough for emplacement is not sensitive to the repository start date. However, the repository start date does control when emplacement is completed because of throughput constraints, compared to the reference re-packaging case. For example, if the repository start date is 2036 and the emplacement power limit is 6 kW, by the time the re-packaging is complete (2083) only 36% of the total SNF inventory in DPCs-only would be cool enough to be emplaced.

For the DPCs+MPCs scenario, the availability of SNF cool enough to emplace is significantly affected by when the MPCs are implemented (5 years before the repository start date). If the repository start date is 2036 and MPCs are implemented in 2031, cooling in the smaller MPCs accelerates the possible schedule for emplacement. The acceleration decreases with later transition to MPCs, because more SNF is loaded into DPCs, and that fuel has higher burnup than early loaded DPCs. The most significant acceleration results with the smallest (6 kW) thermal power limit.

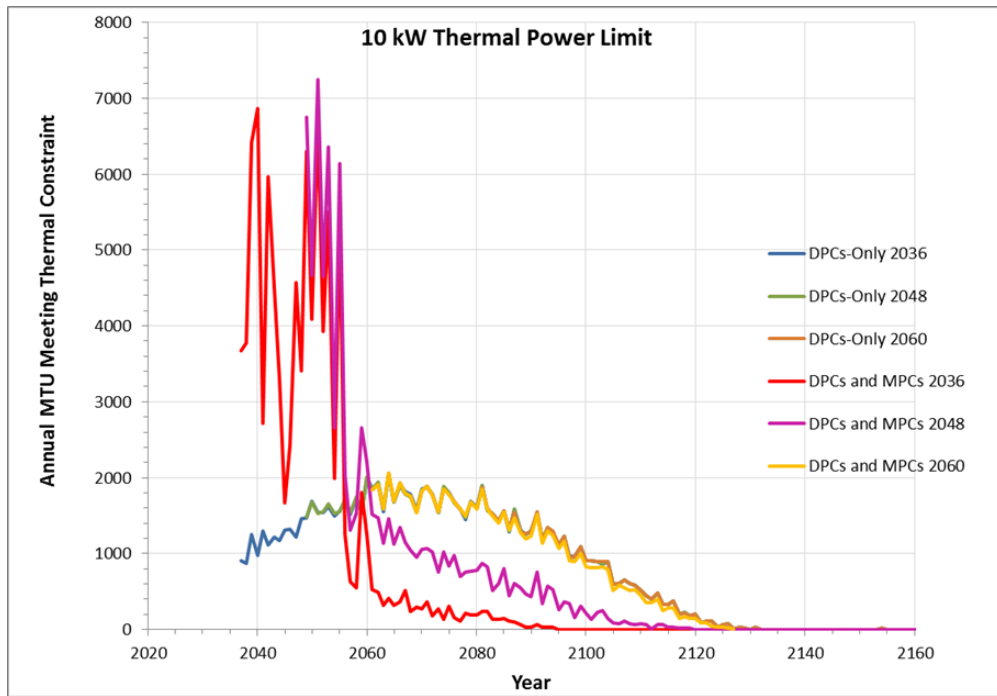


(a) Annual (in the year that the power limit is reached)

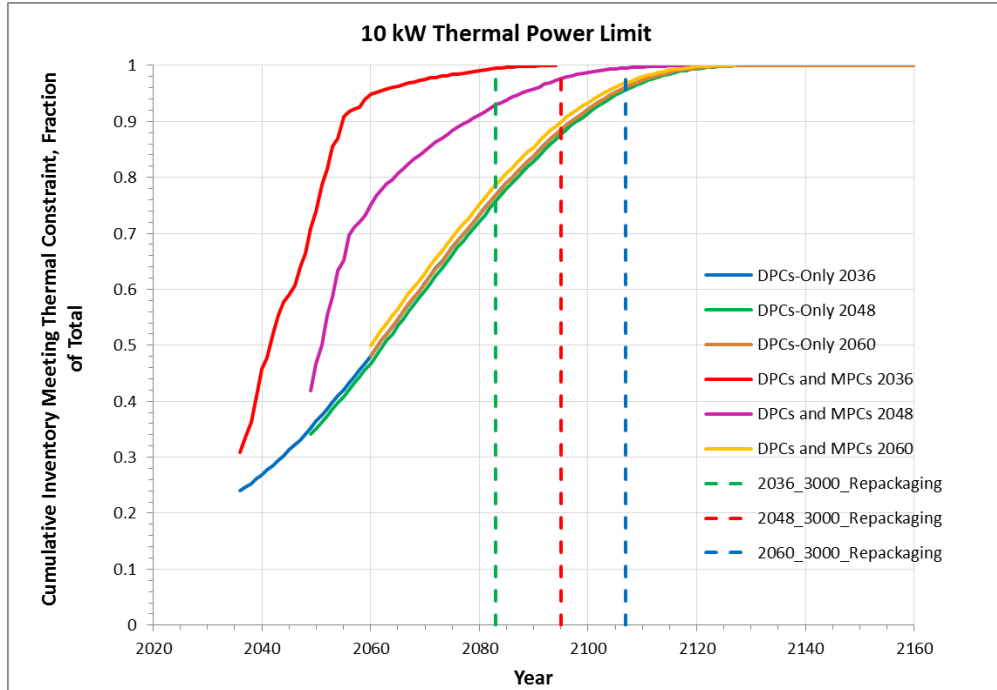


(b) Cumulative

Figure C-2. SNF inventory that has cooled to a 6 kW emplacement power limit



(a) Annual (in the year that the power limit is reached)

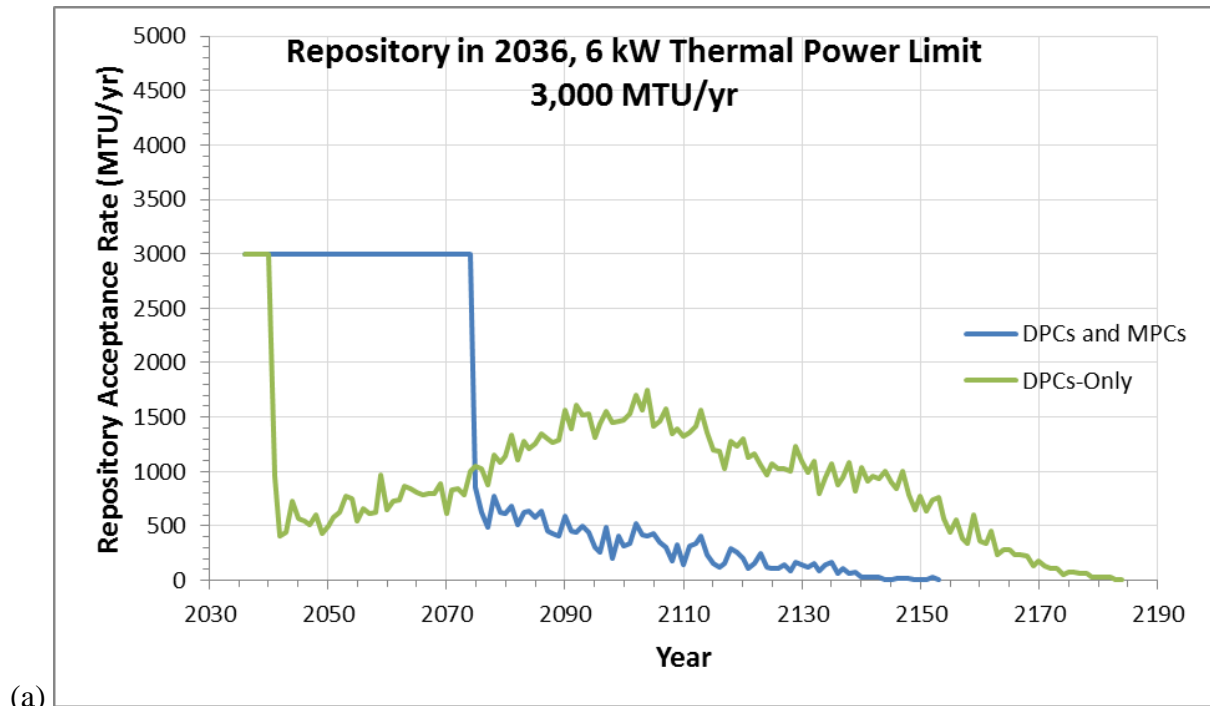


(b) Cumulative

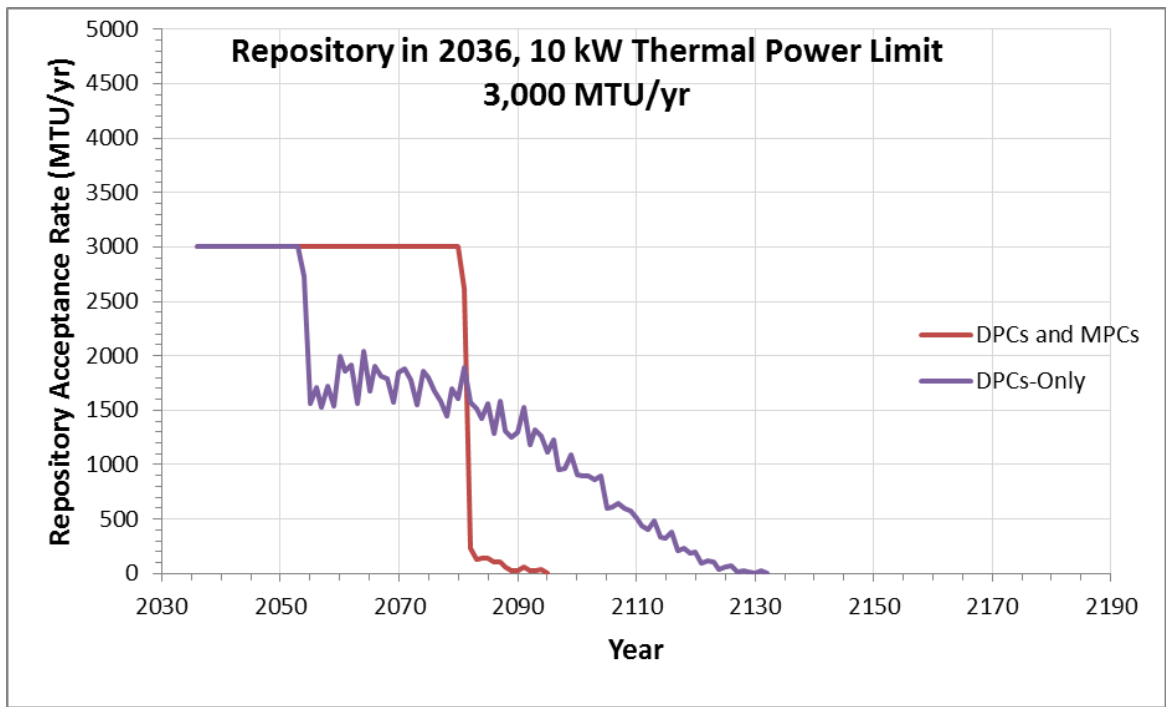
Figure C-3. SNF inventory that has cooled to a 10 kW emplacement power limit

**Results for Maximum Throughput Rate of 3,000 MTHM per Year** – Repository throughput constrained by emplacement power limits, and imposing a maximum repository throughput rate of 3,000 MTHM per year, is shown in Figures C-4 and C-5 for repository start in 2036 and 2048.

Throughput for the cases with emplacement power limits of 6 kW and 10 kW is impacted by the repository start date and the fuel loading scenario. Implementing small MPCs with the planned repository start in 2036 and 2048 could allow for maintaining the maximum repository throughput longer. However, the maximum throughput (3,000 MTHM/yr) can be sustained throughout much of the repository operational period, only for the higher power limit (10 kW). This means that for lower power limits (e.g., 6 kW) repository facilities could be designed for lower throughput, consistent with cooling requirements.

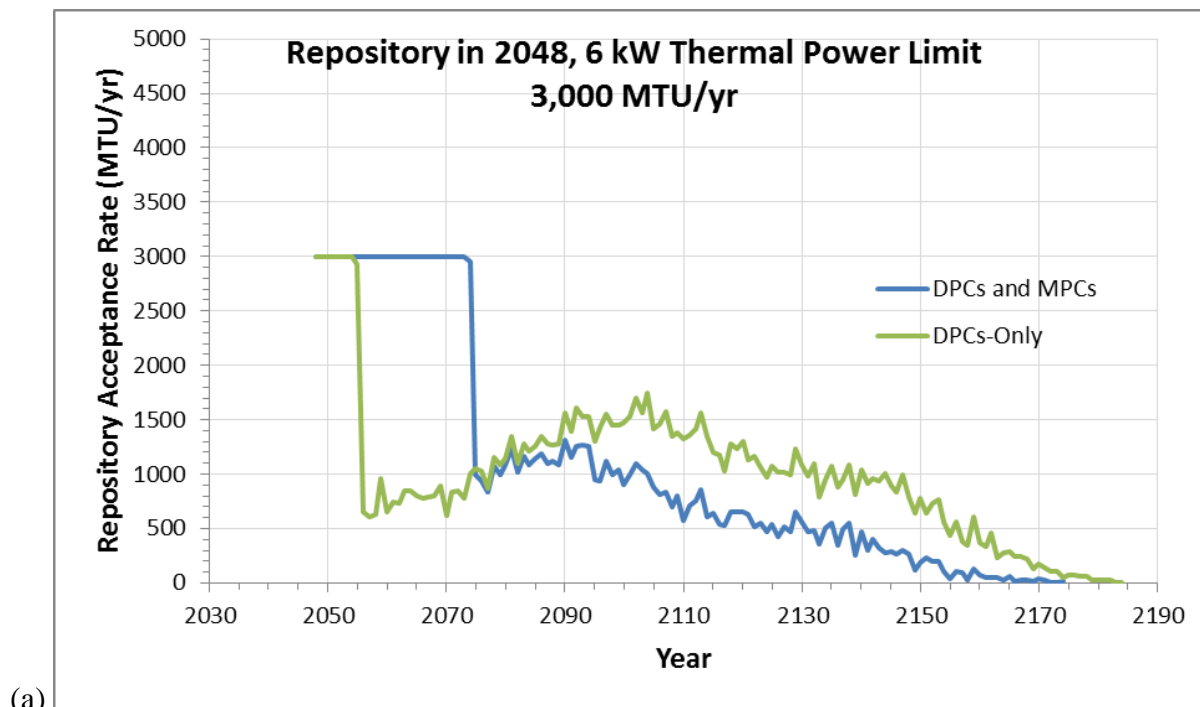


(a)

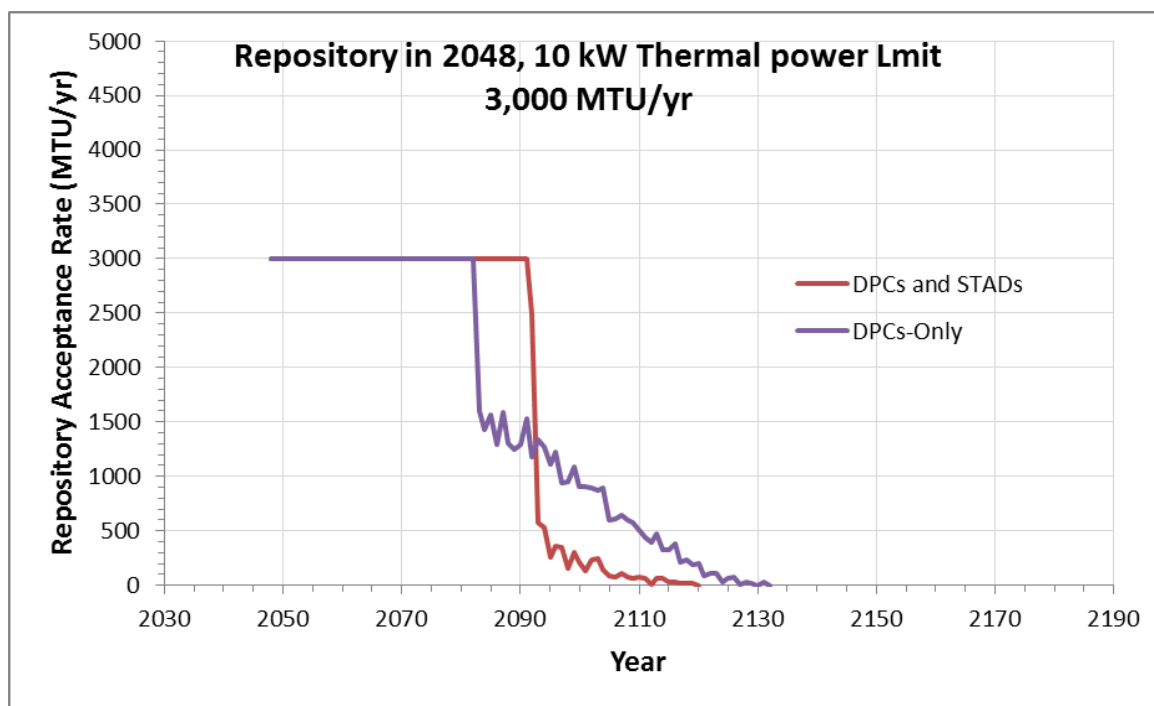


(b)

Figure C-4. Repository throughput with (a) 6 kW, and (b) 10 kW emplacement power limits, maximum throughput of 3,000 MTHM per year and repository start date of 2036



(a)

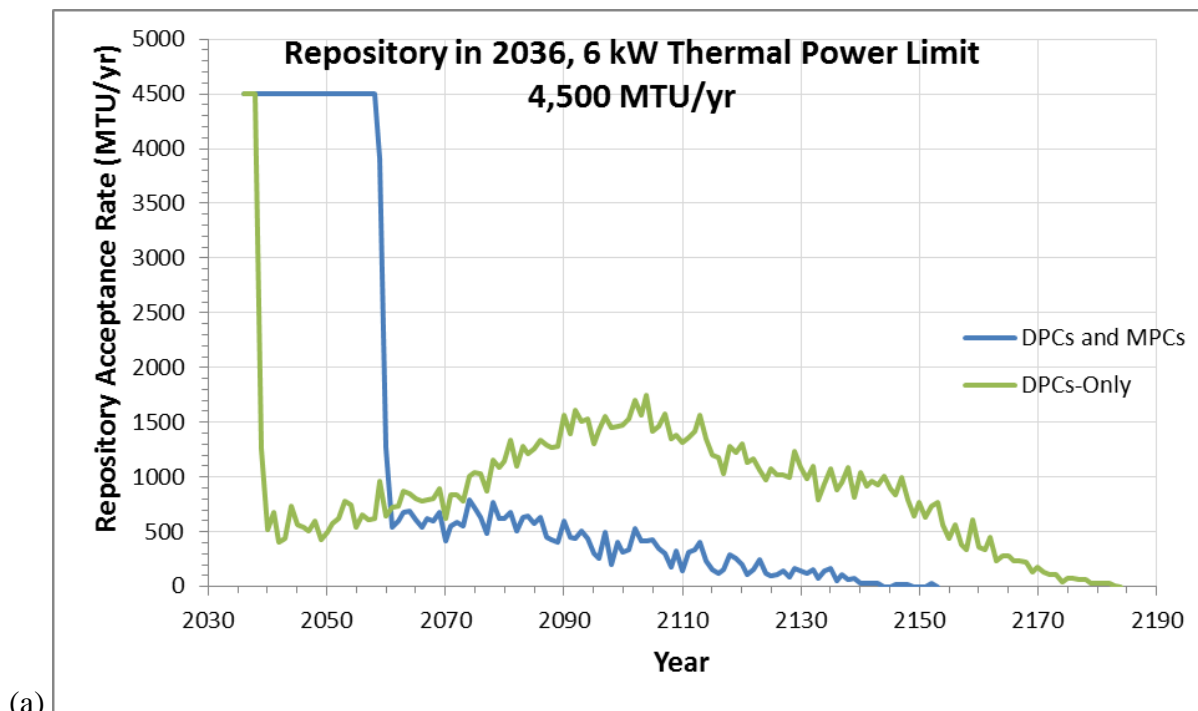


(b)

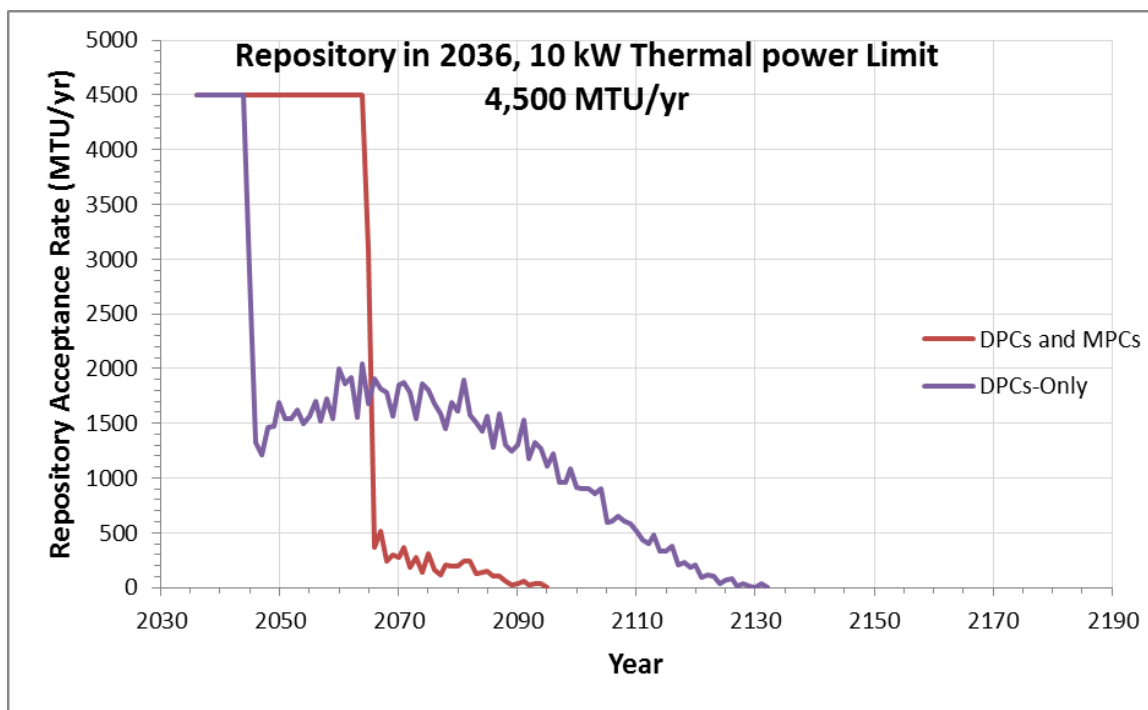
Figure C-5. Repository throughput with (a) 6 kW and (b) 10 kW emplacement power limits, maximum throughput of 3,000 MTHM per year and repository start date of 2048

**Results for Maximum Throughput Rate of 4,500 MTHM per Year** – Repository throughput constrained by emplacement power limits, and imposing a maximum throughput of 4,500 MTHM per year, is shown in Figures C-6 and C-7, for repository start in 2036 and 2048.

Cases with the 6 kW and 10 kW emplacement power limits are impacted by the repository start date and the transition to MPCs. Implementing small MPCs with the planned repository start in 2036 and 2048 allows for maintaining maximum repository throughput longer than for the DPCs-only cases. However, for most of the repository operational period the maximum throughput of 4,500 MTHM/yr cannot be sustained because of the need for cooling (Figures C-6 and C-7). This means that repository facilities could be designed for lower throughput consistent with cooling time, and that disposal timing is not significantly constrained by repository throughput at either the 3,000 or 4,500 MTHM/yr levels.



(a)



(b)

Figure C-6. Repository throughput with (a) 6 kW and (b) 10 kW emplacement power limits, maximum throughput of 4,500 MTHM per year and repository start date of 2036

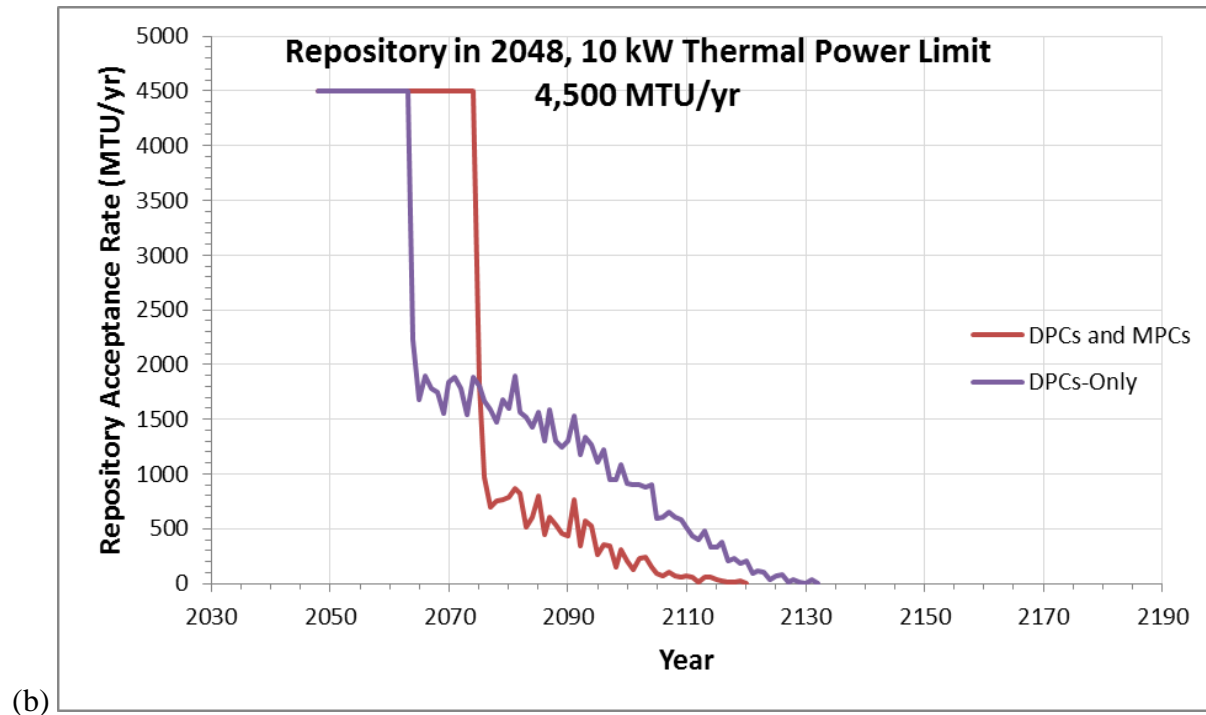
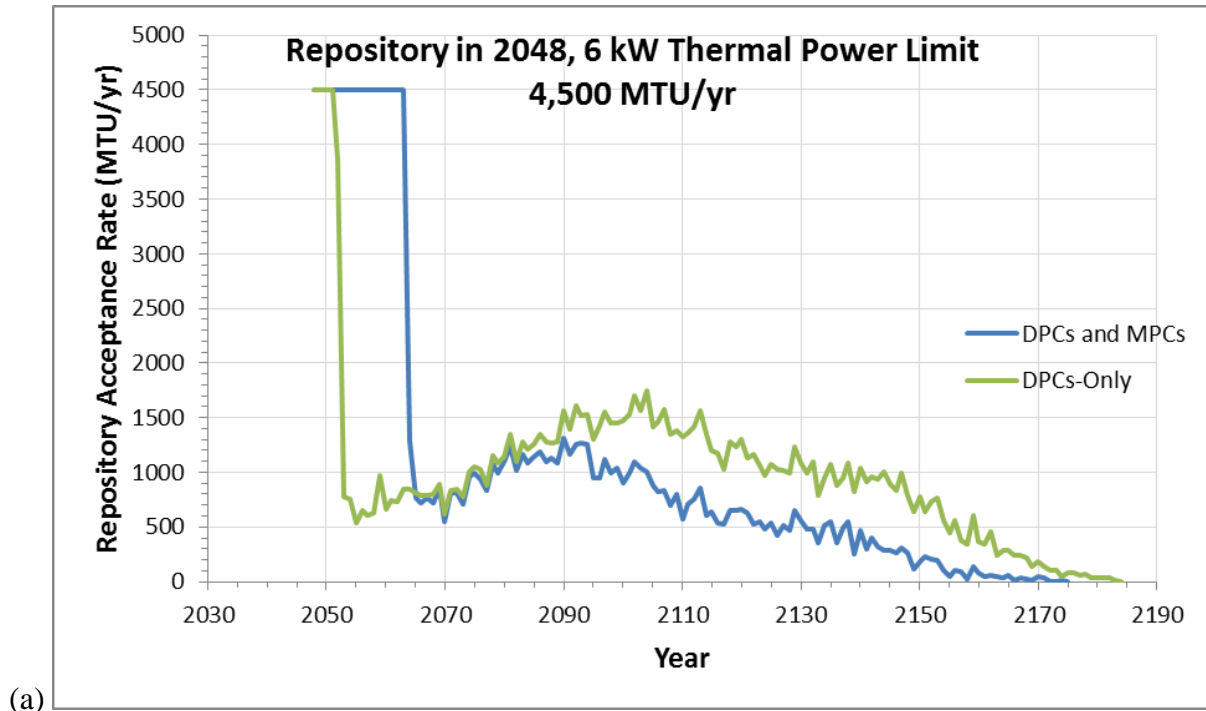


Figure C-7. Repository throughput with (a) 6 kW and (b) 10 kW emplacement power limits, maximum throughput of 4,500 MTHM per year and repository start date of 2048

## C.2 Comparison with Re-Packaging

This comparison estimates the additional storage, in terms of duration and capacity, that would be needed at a CSF to accommodate DPC direct disposal represented either with the DPCs-only or the DPCs+MPCs cases listed in Table C-1. The comparisons are possible using the TSL-CALVIN software.

As discussed previously the maximum CSF capacity in the reference re-packaging scenario is a function of the repository start date and throughput for the fuel management system including the CSF and repository (Figure C-1). Recall that in the reference re-packaging scenario the time from the repository start date to the end of CSF operations is either 31 years (4,500 MTHM per year) or 47 years (3,000 MTHM per year). The additional CSF capacity and operation time for the alternative cases is calculated relative to these reference cases.

For the tabulation in Table C-2, the last year of CSF operation (and emplacement operations at a repository) is considered to be the year in which 98% of the total inventory is emplaced. This accommodates outliers in the burnup projections from TSL-CALVIN. It also acknowledges that the remaining 2% (2,775 MTHM) is younger, hotter fuel that is loaded late in the life-cycle for the last operating power plants. Such fuel could be loaded in de-rated canisters, i.e., fewer assemblies per canister, to meet repository emplacement power limits.

The results from these cases are summarized in Table C-2. Only three alternative cases require additional CSF capacity compared to the corresponding re-packaging reference cases. These are the 6 kW power limit with repository start in 2036 and 2048, and the 10 kW power limit with repository start in 2036. The additional CSF capacity that would be needed for DPC direct disposal, relative to the reference re-packaging case, is in the range 11,000 to 70,000 MTHM. By introducing small MPCs the need for additional CSF capacity is eliminated for all cases.

Additional time for decay storage to meet repository emplacement power limits, would be needed for all cases with the 6 kW limit. The additional time ranges from 55 to 95 years for the DPCs-only cases, and the transition to small MPCs would decrease the range to 36 to 69 years. Additional time would also be needed with the 10 kW power limit for DPCs-only cases, ranging from 5 to 45 years; and transition to small MPCs decreases this range to 0 to 19 years. Introducing small MPCs nearly eliminates any additional decay storage time for the 10 kW cases when the system throughput is 3,000 MTHM per year.

Table C-2. Summary of CSF peak storage inventory and CSF operating times for the 18 alternative cases

| Repository Start Date   | Thermal Limit, kW | Fuel Loading Scenario | Maximum CSF Storage at Fixed Repository Throughput, MTHM |                     | Last Year of CSF Operation | Additional CSF Capacity at Fixed Repository Throughput, MTHM |                     | Additional Duration of CSF Operation at Fixed Repository Throughput, yr |                     | Age at Emplacement for 3,000 MTHM per year Repository Throughput, yr |         |
|-------------------------|-------------------|-----------------------|--|---------------------|----------------------------|--|---------------------|---|---------------------|--|---------|
|                         |                   |                       | 3,000 MTHM per year                                      | 4,500 MTHM per year | 3,000/4,500 MTHM per year  | 3,000 MTHM per year  | 4,500 MTHM per year | 3,000 MTHM per year   | 4,500 MTHM per year | Average  | Maximum |
| <b>2036</b>             | 6                 | DPCs-only             | 102,701  | 114,804             | 2162/2178                  | 69,701   | 65,304              | 79  | 95                  | 79   | 146     |
|                         | 6                 | DPCs+MPCs             | 33,000   | 49,500              | 2119/2135                  | 0  | 0                   | 36  | 52                  | 46   | 128     |
|                         | 10                | DPCs-only             | 53,245   | 80,444              | 2112/2128                  | 20,245   | 30,944              | 29  | 45                  | 55   | 90      |
|                         | 10                | DPCs+MPCs             | 33,000   | 49,500              | 2083/2067                  | 0  | 0                   | 0   | 6                   | 46   | 82      |
|                         | 18 <sup>A</sup>   | DPCs-only             | 33,000   | 49,500              | 2083/2067                  | 0  | 0                   | 0   | 7                   | 51   | 82      |
|                         | 18 <sup>A</sup>   | DPCs+MPCs             | 33,000   | 49,500              | 2083/2067                  | 0  | 0                   | 0   | 0                   | 49   | 81      |
|                         | <b>NA</b>         | <b>Re-packaging</b>   | <b>33,000</b>  | <b>49,500</b>       | <b>2083/2067</b>           |  |                     |   |                     |  |         |
| <b>2048</b>             | 6                 | DPCs-only             | 102,701  | 114,807             | 2162/2178                  | 33,701   | 11,307              | 67  | 83                  | 84   | 146     |
|                         | 6                 | DPCs+MPCs             | 69,000   | 102,735             | 2145/2161                  | 0  | 0                   | 50  | 66                  | 62   | 140     |
|                         | 10                | DPCs-only             | 69,000   | 103,500             | 2112/2128                  | 0  | 0                   | 17  | 33                  | 63   | 90      |
|                         | 10                | DPCs+MPCs             | 69,000   | 103,500             | 2095/2111                  | 0  | 0                   | 0   | 16                  | 58   | 90      |
|                         | 18 <sup>A</sup>   | DPCs-only             | 69,000   | 103,500             | 2095/2079                  | 0  | 0                   | 0   | 0                   | 61   | 85      |
|                         | 18 <sup>A</sup>   | DPCs+MPCs             | 69,000   | 103,500             | 2095/2079                  | 0  | 0                   | 0   | 0                   | 59   | 85      |
|                         | <b>NA</b>         | <b>Re-packaging</b>   | <b>69,000</b>  | <b>103,500</b>      | <b>2095/2079</b>           |  |                     |   |                     |  |         |
| <b>2060<sup>A</sup></b> | 6 <sup>A</sup>    | DPCs-only             | 105,000  | 134,235             | 2162/2178                  | 0  | 0                   | 55  | 71                  | 88   | 146     |
|                         | 6 <sup>A</sup>    | DPCs+MPCs             | 105,000  | 134,235             | 2160/2176                  | 0  | 0                   | 53  | 69                  | 86   | 146     |
|                         | 10 <sup>A</sup>   | DPCs-only             | 105,000  | 134,235             | 2112/2128                  | 0  | 0                   | 5   | 21                  | 73   | 97      |
|                         | 10 <sup>A</sup>   | DPCs+MPCs             | 105,000  | 134,235             | 2110/2126                  | 0  | 0                   | 3   | 19                  | 73   | 97      |
|                         | 18 <sup>A</sup>   | DPCs-only             | 105,000  | 134,233             | 2107/2091                  | 0  | 0                   | 0   | 0                   | 72   | 97      |
|                         | 18 <sup>A</sup>   | DPCs+MPCs             | 105,000  | 134,235             | 2107/2091                  | 0  | 0                   | 0   | 0                   | 72   | 97      |
|                         | <b>NA</b>         | <b>Re-packaging</b>   | <b>105,000</b>   | <b>138,735</b>      | <b>2107/2091</b>           |  |                     |   |                     |  |         |

<sup>A</sup>Based on results presented by Kalinina (2014).

THIS PAGE INTENTIONALLY LEFT BLANK

### C.3 Fuel Age at Emplacement

SNF dry storage installations in the US have been licensed for 20 years, with the possibility of extension to a total of 60 years as defined in NUREG-1927 (NRC 2011). Regulatory approval for storing SNF more than 60 years would require licensing changes and is therefore more uncertain than the current framework. Limitations on dry storage duration could arise from technical issues associated with condition of the canisters or the fuel. Simulation results described above (Table C-2) show that fuel age at emplacement could exceed 60 years, especially for higher burnup fuel, or if the repository start is delayed. Accordingly, fuel age at emplacement could affect the feasibility of DPC direct disposal. This analysis evaluates fuel age at disposal to identify age profiles for the overall inventory that could be achievable under thermal, logistical, and other constraints. This section presents analysis for eight cases as indicated in Table C-1, corresponding to the 2036 and 2048 repository start dates, and the 6 kW and 10 kW emplacement power limits. The other cases are presented by Kalinina (2014).

Fuel age at emplacement is tabulated from TSL-CALVIN results for all 18 alternative cases (Table C-1) using a system throughput of 3,000 MTHM per year. Distributions of fuel age at emplacement are shown in Figures C-8 through C-10 for repository start in 2036, and in Figures C-11 through C-13 for repository start in 2048. The average (based on tonnage) and maximum ages at emplacement for the different DPC alternatives are included in Table C-2. The main purpose of Figures C-8 to C-13 is to show the impact from introducing small MPCs on fuel age at emplacement. MPCs can help to achieve younger fuel age at emplacement, but not if the repository start is delayed beyond 2048. Fuel age at emplacement could be significantly less with the 2036 repository start. The maximum fuel age at emplacement will always be greater than 60 years even if MPCs are implemented early, and may greatly exceed 100 years if emplacement thermal power limits are low (6 kW results in Table C-2).

There are very small differences between the DPCs-only and DPCs+MPCs cases, where the emplacement power limit is greater than 10 kW or the repository is delayed. Stated differently, these results show that the advantages of MPC canister implementation may depend to some extent on timely repository implementation.

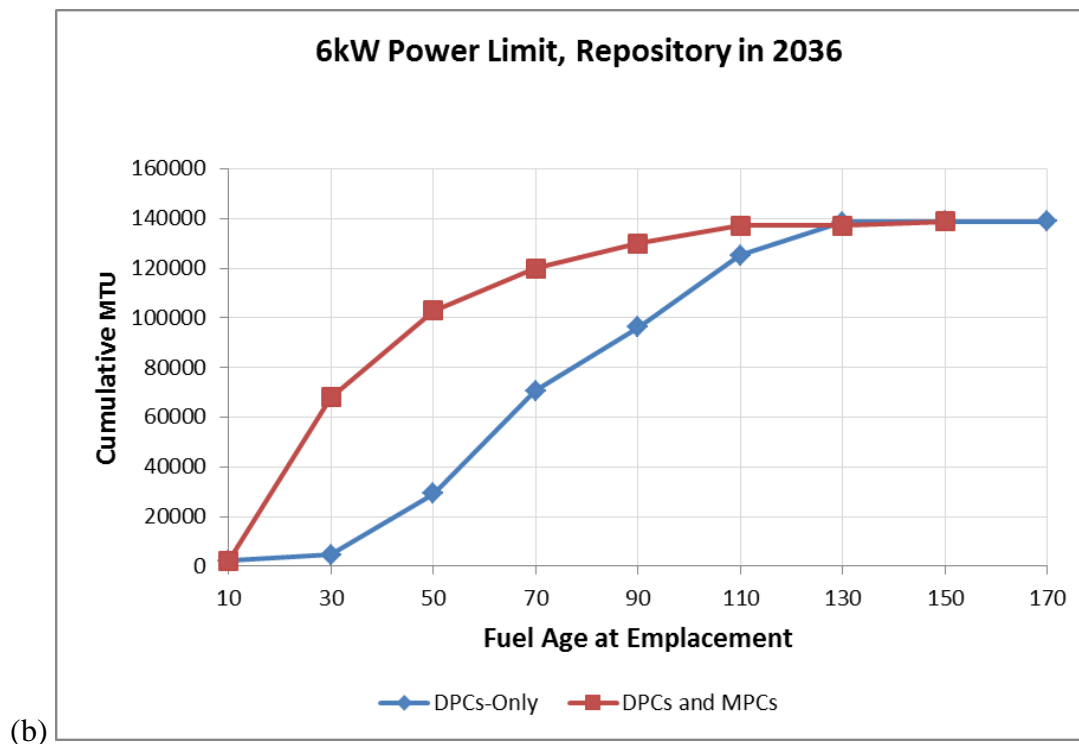
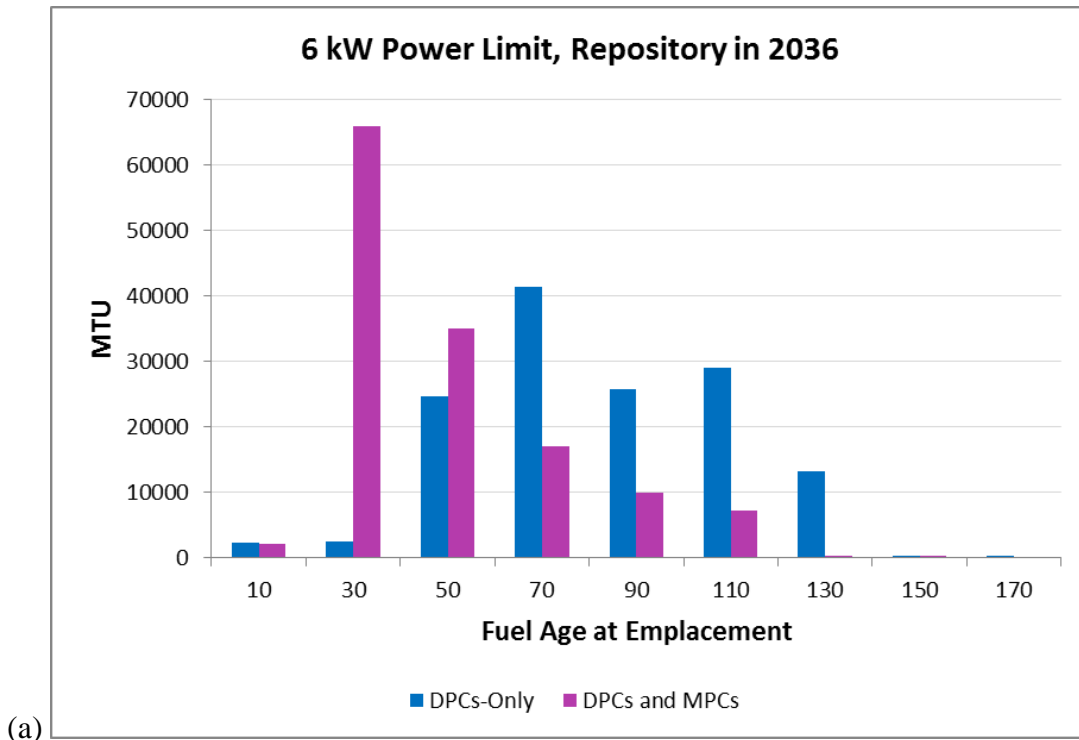


Figure C-8. Inventory age at emplacement (a) and cumulative inventory as a function of age at emplacement (b) with a 6 kW emplacement limit and 2036 repository start date

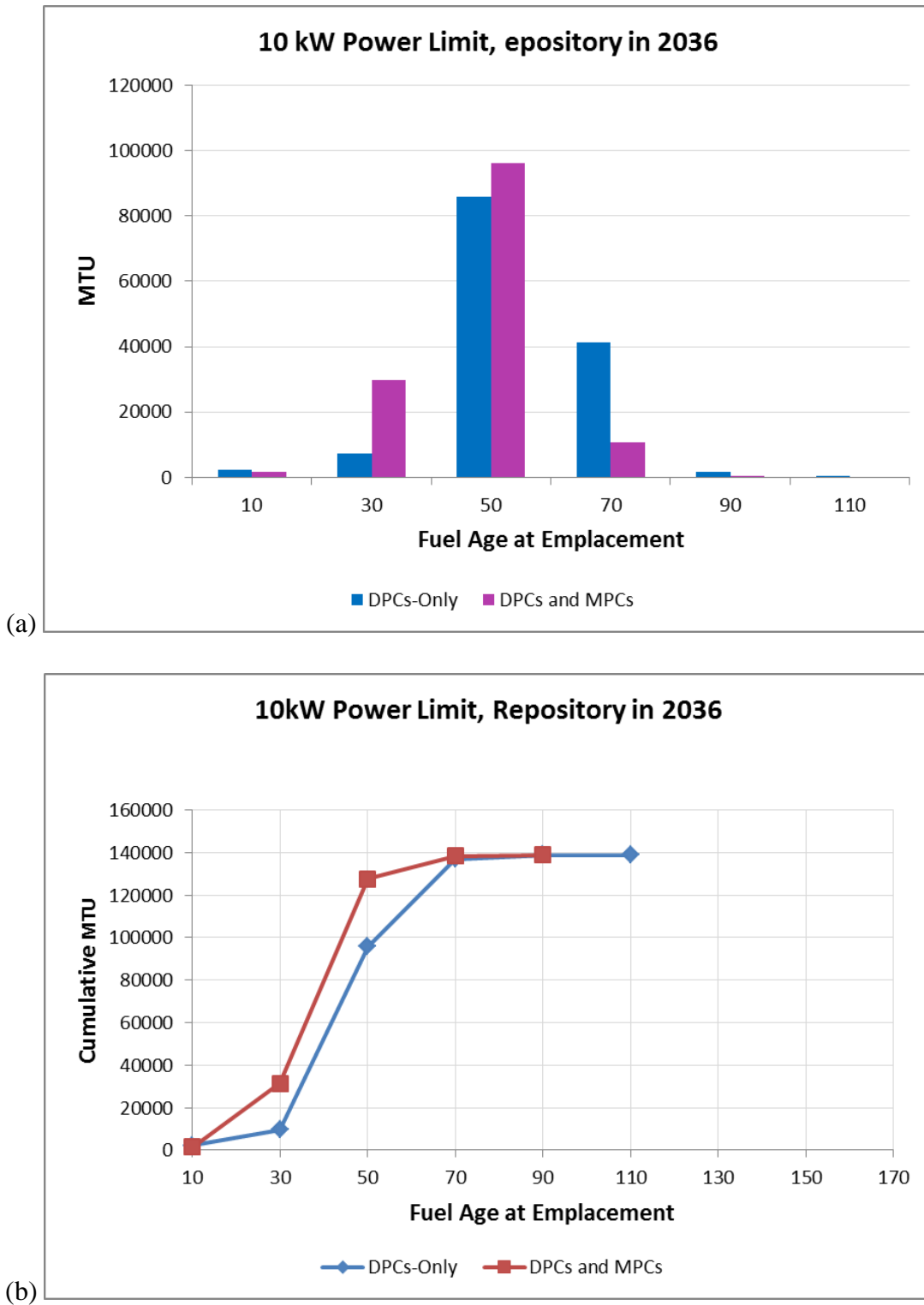


Figure C-9. Inventory age at emplacement (a) and cumulative inventory as a function of age at emplacement (b) with a 10 kW emplacement limit and 2036 repository start date

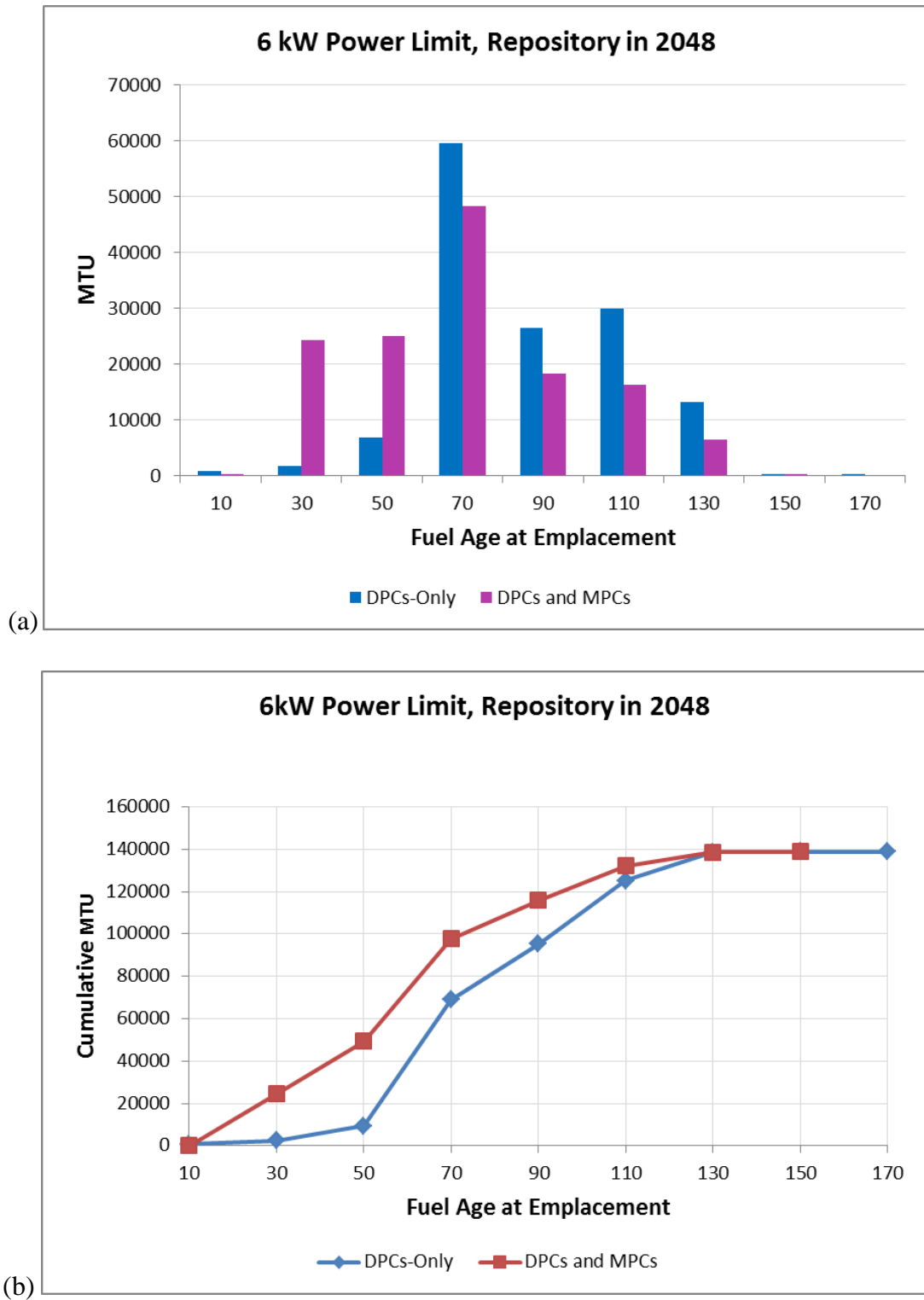


Figure C-10. Inventory age at emplacement (a) and cumulative inventory as a function of age at emplacement (b) with a 6 kW emplacement limit and 2048 repository start date

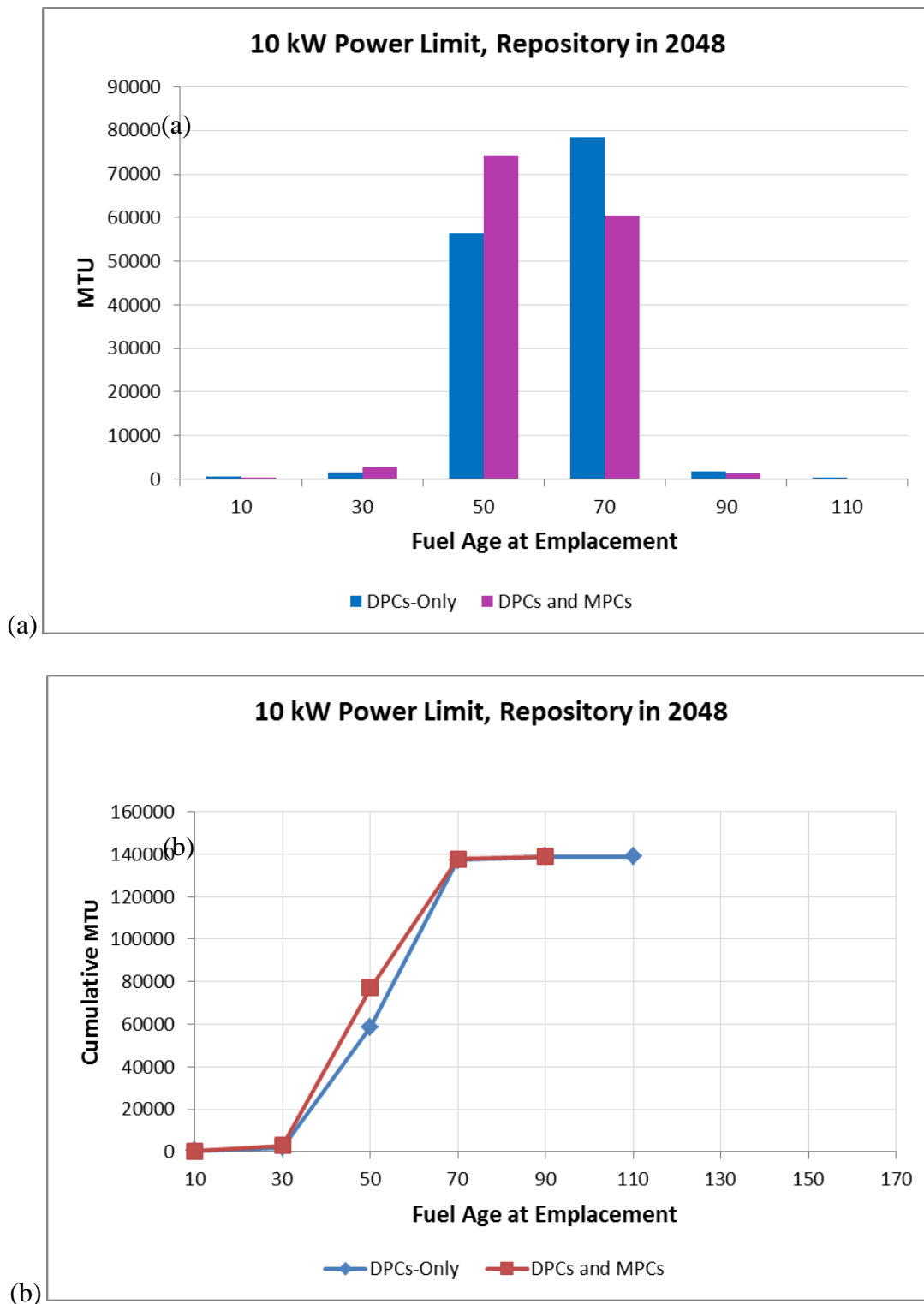


Figure C-11. Inventory age at emplacement (a) and cumulative inventory as a function of age at emplacement (b) with a 10 kW emplacement limit and 2048 repository start date

TSL-CALVIN simulates fuel burnup and enrichment using the concept of batches, where a batch is the smallest logistical unit of fuel that is assigned the same burnup and enrichment and that consists of assemblies discharged on the same date and at the same reactor site. The age at emplacement for each fuel batch, for the DPCs-only case with a 10 kW emplacement limit and repository start in 2036, is shown in Figure C-12. The plot shows that the age range becomes smaller with time, and that fuel age at emplacement tends to increase with time because of higher burnup. The calculation for the corresponding DPCs+MPCs case has a similar trend but a significantly smaller spread in time. Also, the impact from introducing MPCs becomes noticeable around 2060. From that time on, the age of the fuel at emplacement continues to increase for DPCs and decrease for MPCs.

**Summary of Fuel Age at Emplacement** – Summaries of the simulated average SNF age at emplacement, as a function of the emplacement power limit and the repository start date, are shown in Figure C-13 for the DPCs-only and DPCs+MPCs scenarios. Average age at emplacement increases linearly with the repository start date for both scenarios, and the results are practically the same for the higher emplacement power limits.

Implementing smaller MPCs allows for reducing the average SNF age at emplacement for the 6 kW and to some extent the 10 kW cases, with repository start dates in 2036 and 2048. The average age at emplacement for higher power limits, and for a repository start date delayed much beyond 2048, is not significantly affected by implementing smaller MPCs, because most SNF would be disposed of direct in DPCs in these cases (see additional results in Kalinina 2014).

The greatest benefit to fuel age at emplacement from implementing smaller MPCs is observed for the lowest emplacement power limit (6 kW) and the earliest repository start date (2036). This alternative was further examined to evaluate the differences in fuel age (Figure C-14) and burnup (Figure C-15) between the inventory in DPCs and the inventory in MPCs. For this case, 40% of the inventory is emplaced in DPCs and 60% is emplaced in MPCs. The majority of fuel in MPCs is 30 years old or younger, while most of the fuel in DPCs is 50 years old or older. The burnup of fuel in MPCs is mostly 45 GW-d/MTU or greater, while that in DPCs is mostly 35 to 45 GW-d/MTU or lower.

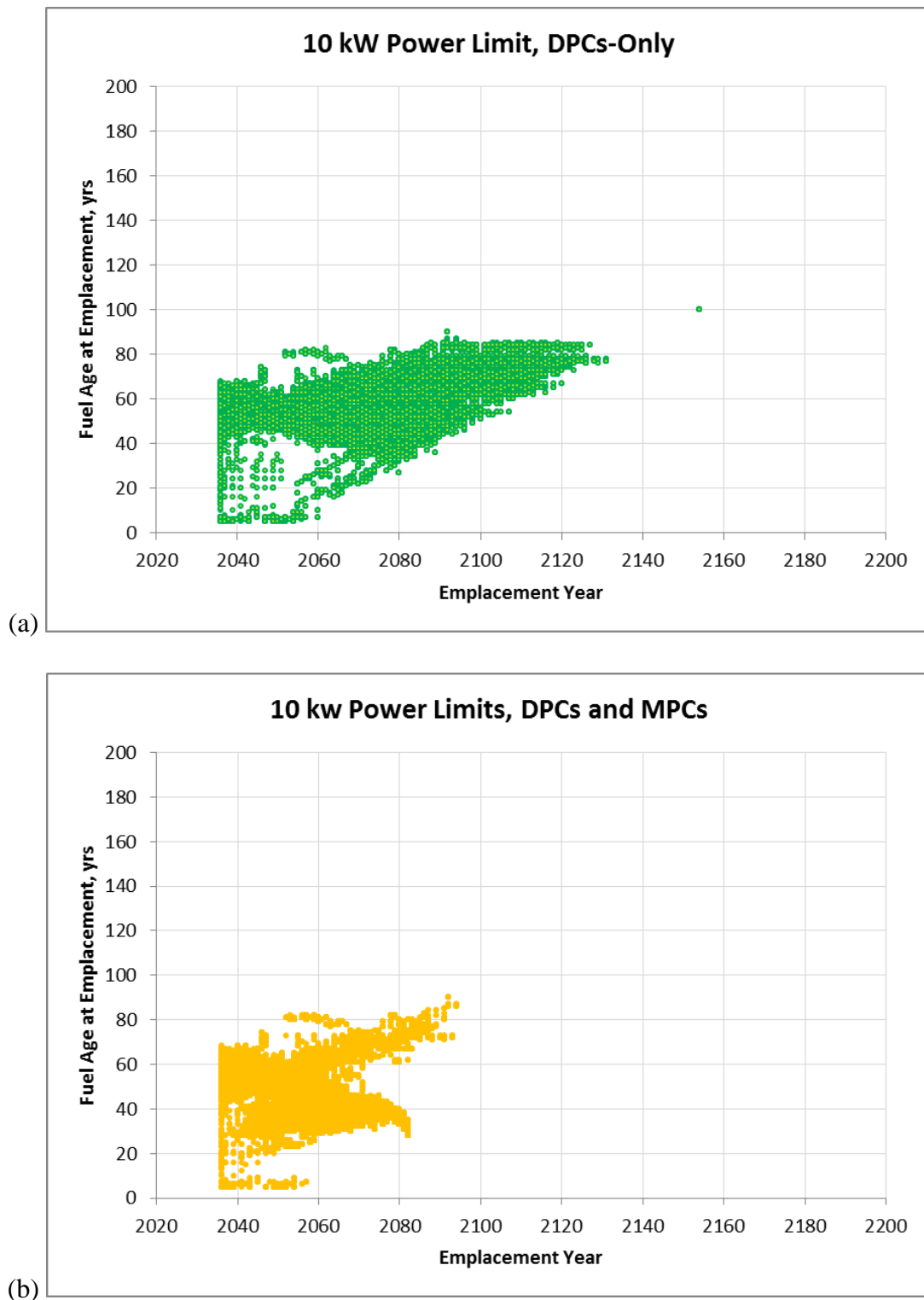


Figure C-12. Fuel age at emplacement with a 10 kW emplacement limit and 2036 repository start date: (a) DPCs-only, and (b) DPCs with transition to MPCs in 2031

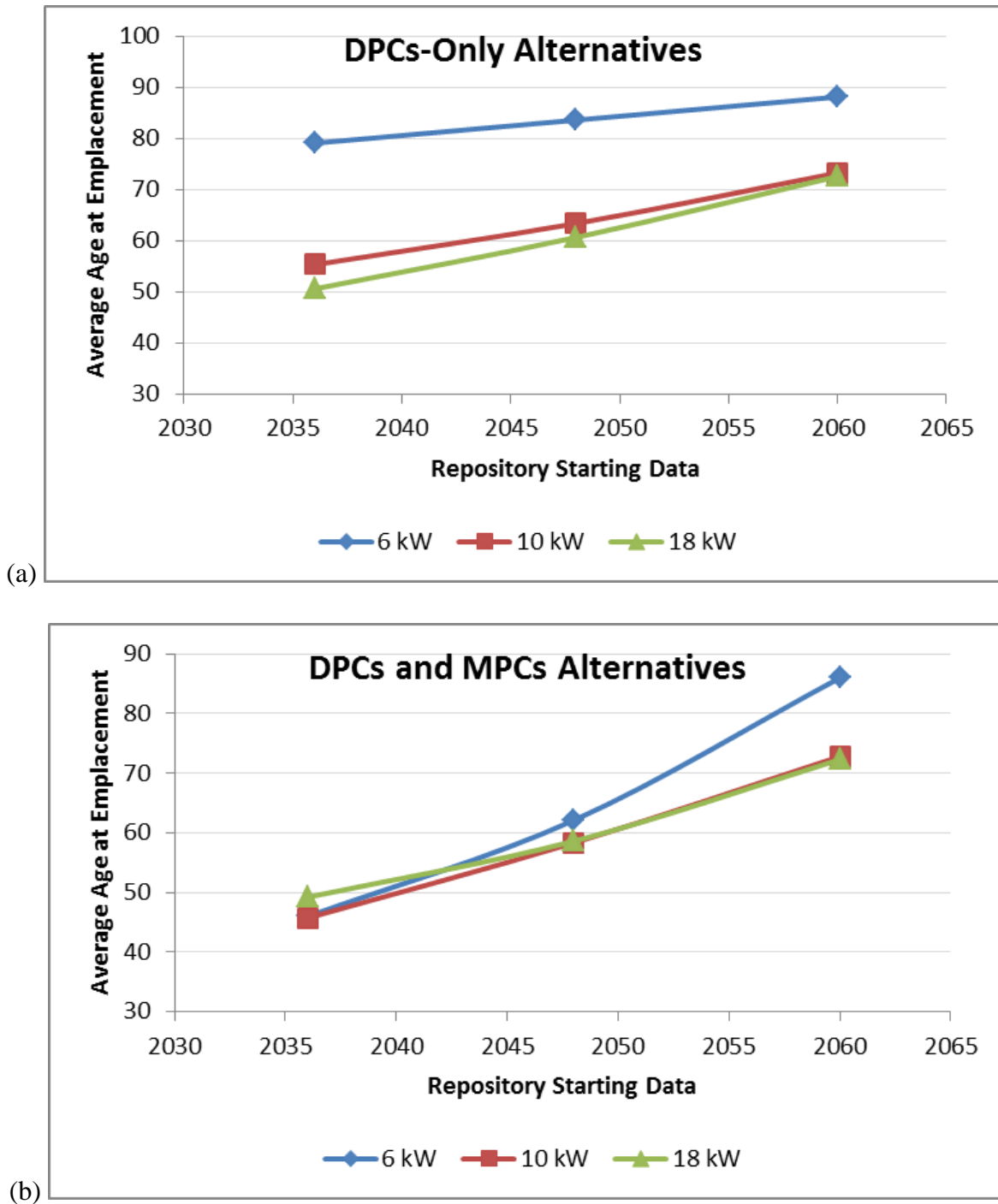


Figure C-13. Average age at emplacement as a function of repository start date and emplacement thermal power limit: (a) DPCs-only and (b) DPCs with transition to MPCs at 5 years before the repository start date

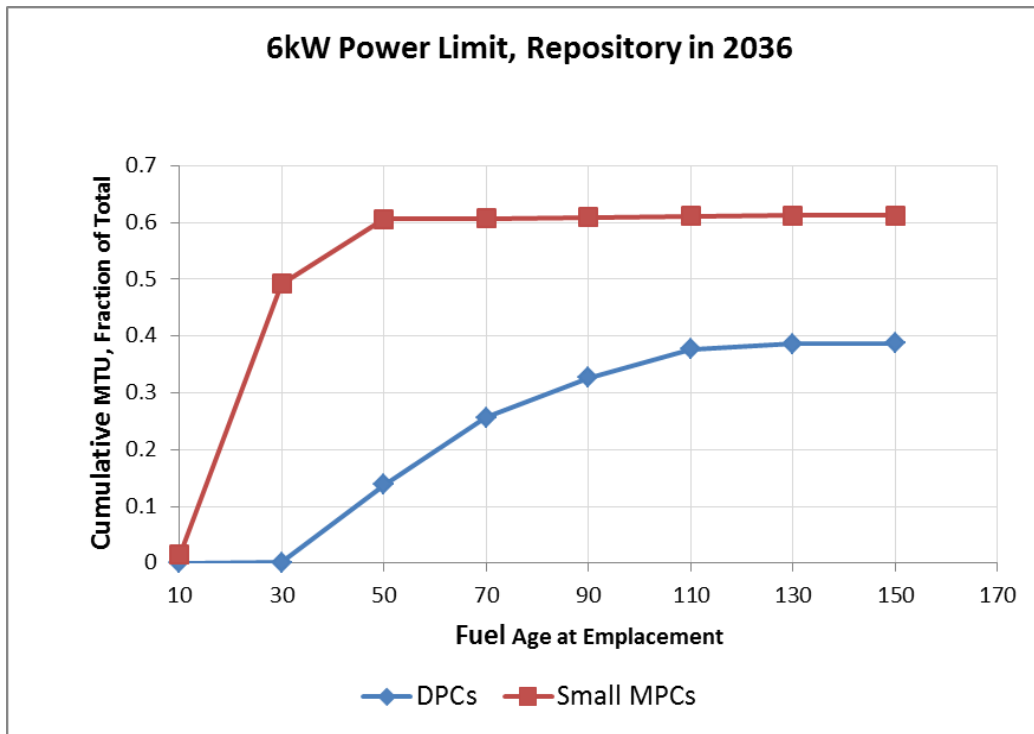
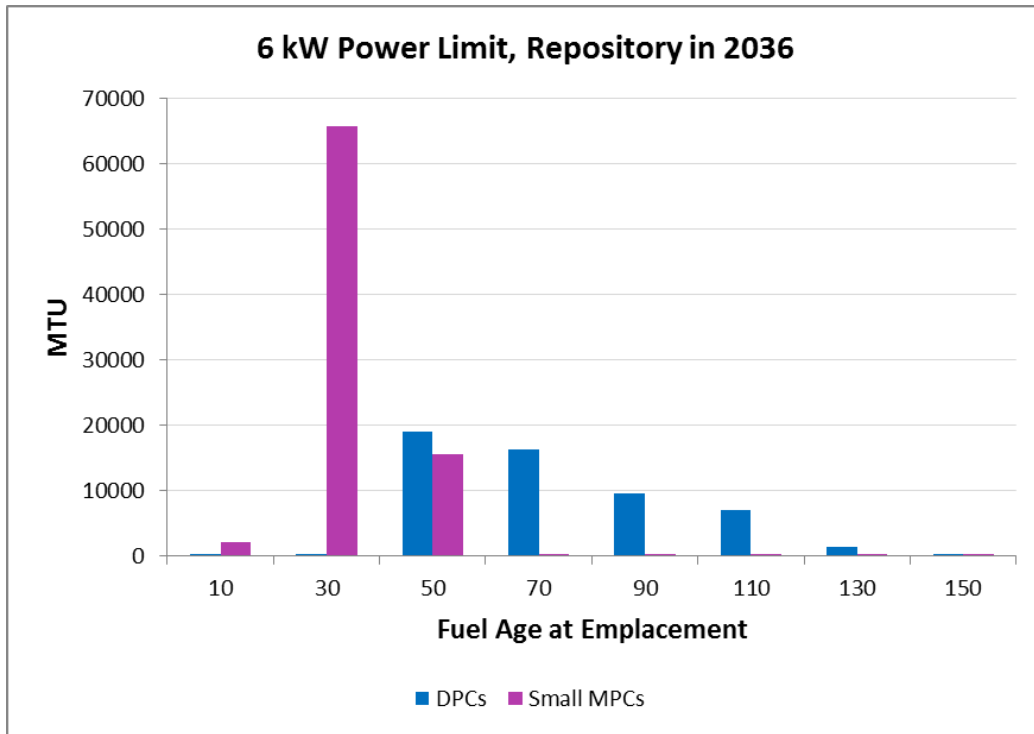


Figure C-14. Age of fuel at emplacement in DPCs and MPCs, with the 6 kW power limit and repository start in 2036, expressed as histograms (upper) and cumulative distributions (lower)

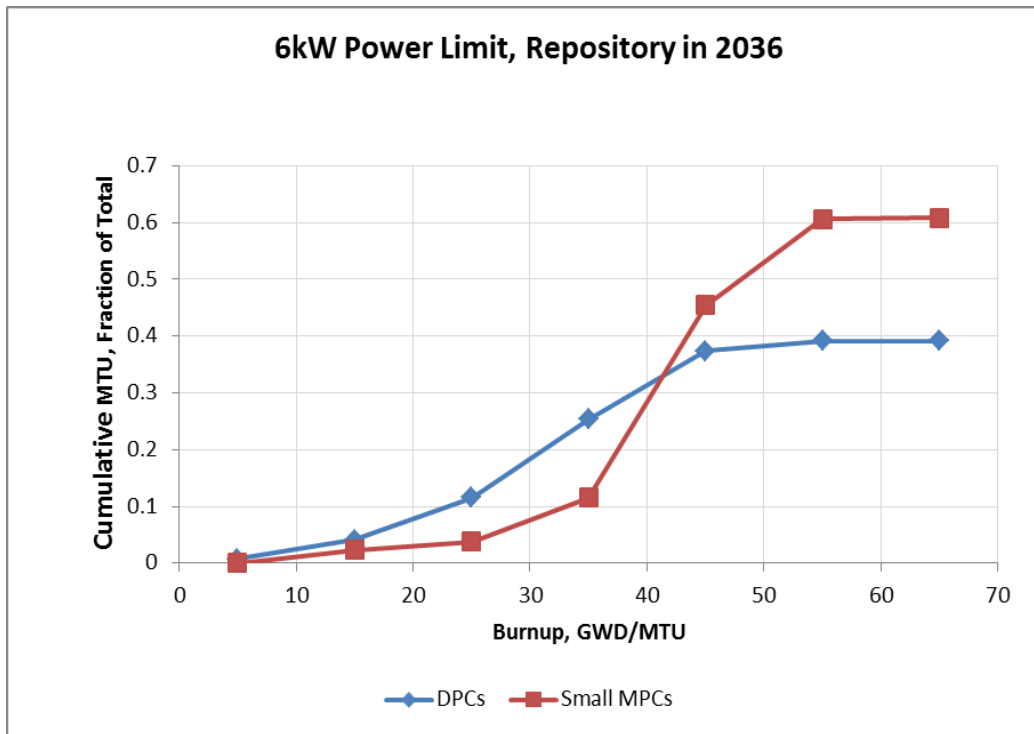
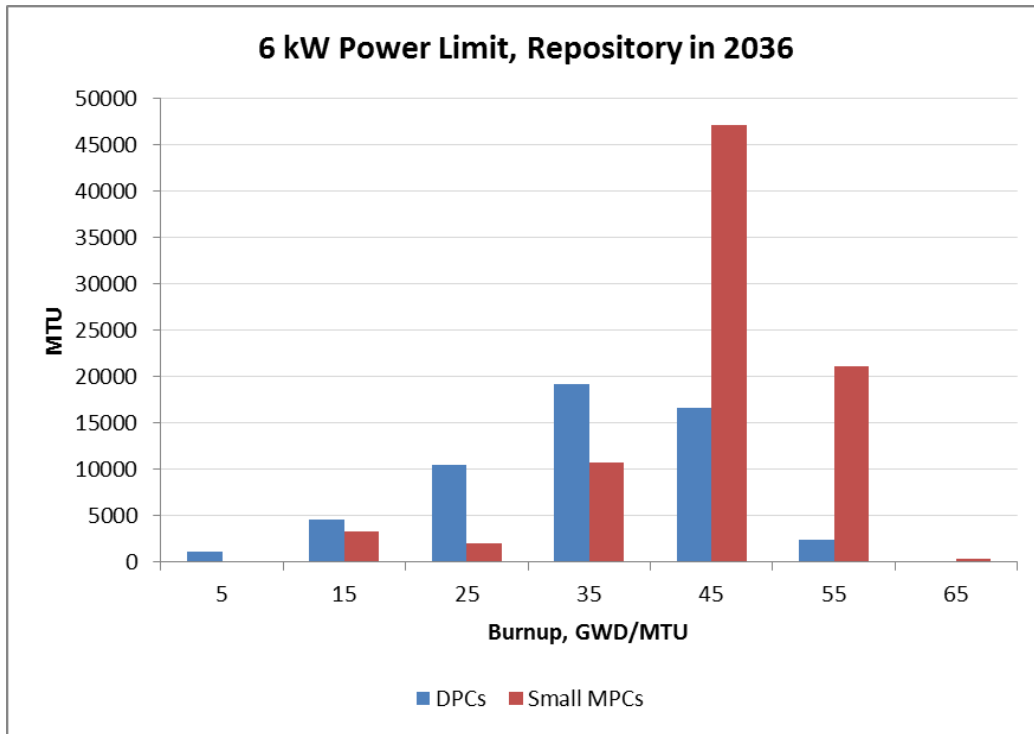


Figure C-15. Burnup of fuel in DPCs and MPCs, expressed as histograms (upper) and cumulative distributions (lower) for the 6 kW power limit and repository start in 2036

## C.4 Summary

This study evaluated how DPC direct disposal could be affected by: 1) cooling to achieve emplacement power limits; and 2) future transition to loading SNF in smaller MPCs at nuclear power plants. Cases were run for a range of power limits, and a range of repository start dates. Transition to loading MPCs was set to happen 5 years before the repository start date. Products of this evaluation include the projected history of waste emplacement (repository throughput), and the profile of SNF age at emplacement in the repository (age from reactor discharge). Logistical simulations were performed using the TSL-CALVIN simulator (Nutt et al. 2012), supplementing previous results (Nutt 2013; Hardin et al. 2013).

**Cooling of DPCs and MPCs to Emplacement Power Limits** – The greatest benefit from implementing MPCs, on cooling time needed for disposal, is associated with the smallest power limit and the earliest repository start date. The 6 kW case with repository start in 2036 shows that relatively few DPCs could meet the thermal limit by 2036, so the implementation of smaller MPCs starting in 2031 could have a greater impact. A similar impact is calculated for the 2048 repository start date, and for the alternative cases (Table C-1) with a 10 kW power limit and both 2036 and 2048 repository start dates.

For a repository start date of 2060, transition to MPCs would make little difference in cooling time regardless of the emplacement thermal power limit (Kalinina 2014). This is because most of the SNF would be in DPCs. Similarly, for higher emplacement power limits there would be little or no additional cooling time required (compared to corresponding DPCs+MPCs cases) regardless of repository start date, if the limit is high enough.

**Additional Storage Facility Capacity and Duration of Storage Operations** – Compared to the reference re-packaging cases (Table C-1) in which all SNF was re-packaged prior to disposal, the only cases requiring additional storage capacity would be the DPCs-only cases. This is true for cases with the 6 kW and 10 kW emplacement power limits, and with repository start in 2036 and to a lesser degree in 2048. By contrast, DPCs+MPCs cases would not require additional storage, regardless of the repository start date or throughput as compared to the reference re-packaging case.

Compared to the reference re-packaging cases, alternatives with the highest power limit (18 kW; Kalinina 2014) would require little or no additional storage time regardless of the repository start date, the fuel loading scenario, or repository throughput limits. Alternatives with the 10 kW power limit could require some additional cooling time even if MPCs are implemented. Alternatives with the 6 kW power limit would require the most additional emplacement time, ranging from 36 to 95 years.

The earliest date at which repository operations could conclude (2067) occurred in the cases with the 18 kW thermal limit, a repository start date of 2036, and maximum repository throughput of 4,500 MTHM per year (Kalinina 2014). Similar performance was simulated with the 10 kW power limit, but for the DPCs+MPCs cases. The latest date at which repository operations could conclude (2162) occurred in the three cases with the 6 kW thermal limit and the use of DPCs-only, regardless of the repository start date.

**Fuel Age at Emplacement** – The greatest average age of fuel (by tonnage) at emplacement is 88 years for 6 kW power limit, disposal of SNF in DPCs-only, and a delayed repository start date (2060; Kalinina 2014). The lowest average age of fuel at emplacement is 46 years for the 6 kW

power limit, repository start date of 2036, and transition to MPCs. Transition to MPCs could decrease the average age of fuel at emplacement significantly, for lower emplacement power limits (6 kW) and early repository start (2036 and 2048). The reduction in fuel age at emplacement from MPC canister implementation becomes small as the emplacement power limit increases or the repository start date is delayed.

The greatest maximum age of fuel at emplacement (~140 years) is projected to occur with: 1) a low emplacement power limit (6 kW) and disposal of SNF in DPCs-only, regardless of the repository start date; and 2) a higher power limit (10 kW), transition to MPCs (2055), and a delayed repository start (2060; Kalinina 2014). The youngest maximum age of fuel at emplacement (~80 years) would occur with a higher power limit (10 kW), early repository start (2036), and transition to MPCs. As with the average age discussed above, the reduction in maximum fuel age at emplacement from transition to MPCs becomes small as the emplacement power limit increases or the repository start date is delayed.

In general, the role of MPCs would be to store younger, higher burnup fuel. For the case with a 6 kW thermal limit and repository start in 2036, 60% of the inventory would be loaded in MPCs, and the majority could be 30 years old or younger at emplacement in a repository. The portion of SNF disposed of directly in DPCs would be at least 50 years old at emplacement, even with the early repository start date. Burnup of fuel in MPCs would be mostly 45 GW-d/MTU or greater, while that in DPCs would be mostly less than 45 GW-d/MTU.

This analysis shows how all of the 18 kW cases (Kalinina 2014) and 10 kW cases with implementation of smaller MPCs, are comparable to the corresponding re-packaging cases, albeit with some additional time required for the 10 kW cases. For the 6 kW cases, implementing smaller MPCs would make them more comparable to the corresponding re-packaging cases if the repository starts in 2036 or 2048.

It is important to note that while fuel storage, transportation and packaging costs are calculated by TSL-CALVIN, that disposal costs are not estimated and may dominate the overall fuel management system cost. Hence, only the metrics of storage capacity, storage/emplacement time, and fuel age at emplacement are used in this study.

### References for Appendix C

Carter, J., A. Luptak, J. Gastelum, C. Stockman and A. Miller 2012. *Fuel Cycle Potential Waste Inventory for Disposition*. FCR&D-USED-2010-000031 Rev. 5. U.S. Department of Energy, Office of Used Nuclear Fuel Disposition. July, 2012.

DOE (U.S. Department of Energy) 2008. *Yucca Mountain Repository License Application for Construction Authorization*. DOE/RW-0573. Washington, D.C.: U.S. Department of Energy.

DOE (U.S. Department of Energy) 2013. *Strategy for the Management and Disposal of Used Nuclear Fuel and High-Level Radioactive Waste*. January, 2013.

Hardin E.L, D.J. Clayton, R.L. Howard, J.M. Scaglione, E. Pierce, K. Banerjee, M.D. Voegelé, H.R. Greenberg, J. Wen, T.A. Buscheck, J.T. Carter, T. Severynse and W.M. Nutt 2013. *Preliminary Report on Dual-Purpose Canister Disposal Alternatives*. FCRD-UFD-2013-000171 Rev. 1. U.S. Department of Energy, Office of Used Nuclear Fuel Disposition. December, 2013.

Howard, R., J. Scaglione, E. Pierce and B. van den Akker and E. Hardin 2014. *Feasibility Evaluation for Direct Disposal of Dual Purpose Canisters: Study Plan*. FCRD-UFD-2014-000518. U.S. Department of Energy, Office of Used Nuclear Fuel Disposition. April, 2014.

Kalinina, E. 2014. *System-Level Logistics for Dual Purpose Canister Disposal*. FCRD-UFD-2014-000517. U.S. Department of Energy, Office of Used Nuclear Fuel Disposition. June, 2014.

NRC (U.S. Nuclear Regulatory Commission) 2011. *Standard Review Plan for Renewal of Spent Fuel Dry Cask Storage System Licenses and Certificates of Compliance — Final Report*. NUREG-1927. March, 2011.

Nutt, M. 2013. *Preliminary System Analysis of Direct Dual Purpose Canister Disposal*. FCRD-NFST-2013-00000. U.S. Department of Energy, Nuclear Fuel Storage and Transportation Planning Project. June, 2013.

Nutt, M., E. Morris, F. Puig, Kalinina and S. Gillespie 2012. *Transportation Storage Logistics Model – CALVIN (TSL-CALVIN)*. FCRD-NFST-2012-000424. U.S. Department of Energy, Nuclear Fuel Storage and Transportation Planning Project. October, 2012.

THIS PAGE INTENTIONALLY LEFT BLANK